

**Dissecting the role of genes involved in proteostasis  
maintenance and Wnt signaling in the pseudoexfoliation  
pathogenesis**

*By*

**BUSHRA HAYAT**

**Enrolment No. LIFE11201404001**

**NATIONAL INSTITUTE OF SCIENCE EDUCATION AND RESEARCH,  
BHUBANESWAR**

*A thesis submitted to the*

*Board of Studies in Life Sciences*

*In partial fulfillment of requirements*

*for the Degree of*

**DOCTOR OF PHILOSOPHY**

*of*

**HOMI BHABHA NATIONAL INSTITUTE**

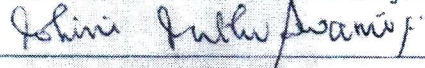
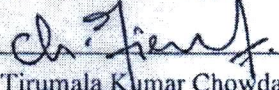


**February, 2020**

# Homi Bhabha National Institute

## Recommendations of the Viva Voce Committee

As members of the Viva Voce Committee, we certify that we have read the dissertation prepared by Ms. Bushra Hayat entitled "Dissecting the role of genes involved in proteostasis maintenance and Wnt signaling in pseudoexfoliation pathogenesis" and recommend that it may be accepted as fulfilling the thesis requirement for the award of Degree of Doctor of Philosophy.

 Chairman - Dr. Chandan Goswami	05/06/2020 Date:
 Guide / Convener - Dr. Debasmita Pankaj Alone	05/06/2020 Date:
 Examiner - Dr. Rohini Muthuswami	05/06/2020 Date:
 Member 1- Dr. Asima Bhattacharyya	5.6.2020 Date:
 Member 2- Dr. Tirumala Kumar Chowdary	05/06/2020 Date:
 Member 3- Prof. Jagdishwar Dandapat	Date: 05.06.2020

Final approval and acceptance of this thesis is contingent upon the candidate's submission of the final copies of the thesis to HBNI.

I/We hereby certify that I/we have read this thesis prepared under my/our direction and recommend that it may be accepted as fulfilling the thesis requirement.

Date: 05/06/2020

Place: NISER, Jatni

  
Dr. Debasmita P. Alone  
(Thesis Supervisor) 05/06/2020

## **STATEMENT BY AUTHOR**

This dissertation has been submitted in partial fulfilment of requirements for an advanced degree at Homi Bhabha National Institute (HBNI) and is deposited in the library to be made available to borrowers under rules of the HBNI.

Brief quotations from this dissertation are allowable without any special permission, provided that accurate acknowledgement of source is made. Requests for permission for extended quotation from or reproduction of this manuscript in whole or in part may be granted by the Competent Authority of HBNI when in his or her judgment the proposed use of the material is in the interests of the scholarship. In all other instances, however, permission must be obtained from the author.

*Bushra Hayat*  
**Bushra Hayat**

## **DECLARATION**

I, hereby declare that the investigation presented in the thesis has been carried out by me. The work is original and has not been submitted earlier as a whole or in part for a degree/diploma at this or any other Institution / University.

*Bushra Hayat*  
**Bushra Hayat**

## List of Publications arising from the thesis

### Publications in refereed journal:

#### a. Published:

1. **Bushra Hayat**, Biswajit Padhy, Pranjya Paramita Mohanty, Debasmita Pankaj Alone. Altered unfolded protein response and proteasome impairment in pseudoexfoliation pathogenesis. **Experimental Eye Research**. 181 (2019) 197-207.
2. **Bushra Hayat**, Ramani Shyam Kapuganti, Biswajit Padhy, Pranjya Paramita Mohanty, Debasmita Pankaj Alone. Epigenetic Silencing of Heat Shock Protein 70 through DNA hypermethylation in pseudoexfoliation syndrome and glaucoma. (**Journal of Human Genetics**, accepted for publication).

#### b. Manuscript under preparation:

1. **Bushra Hayat**, Biswajit Padhy, Pranjya Paramita Mohanty, Debasmita Pankaj Alone. Increased expression of the Wnt antagonist Dickkopf-1 in pseudoexfoliation syndrome and glaucoma.
2. **Bushra Hayat**<sup>\*</sup>, Senjit Ram Behera<sup>\*</sup>, Pranjya Paramita Mohanty, Debasmita Pankaj Alone. A novel variant of *CACNA1A*, rs4926246 is genetically associated with pseudoexfoliation glaucoma.

(\*equally contributed)

### Conference proceedings:

- a. **Bushra Hayat**, Biswajit Padhy, Rohit Mendke, Pranjya P. Mohanty, Debasmita P. Alone ER-UPR genes uncovered in the physiopathology of Pseudoexfoliation. Conference: ISHG meeting and international symposium, IISc, Bengaluru, 3rd-5th March, 2017, Page- 169.
- b. **Bushra Hayat**, Pranjya P. Mohanty, Debasmita P. Alone Insights into proteostasis impairment during progression of pseudoexfoliation glaucoma. Conference: EMBL Conference "Mammalian Genetics and Genomics: From Molecular Mechanisms to Translational Applications" EMBL, Heidelberg, Germany, 24th-28th October, 2017, Page- 118.

*Bushra Hayat*  
Bushra Hayat

## **DEDICATION**

*“This thesis is dedicated to my Abbi and Mummy for their dua, love and endless support and also to my siblings for their relentless motivation and encouragement.”*

## **ACKNOWLEDGEMENTS**

*I owe my heartfelt thanks to Almighty Allah for being the source of my strength throughout this PhD program.*

*I extend my profound gratitude to my mentor and supervisor, **Dr. Debasmita P. Alone**, whose invaluable support, encouragement and motivation helped me in completing my doctoral work. Her perfectionism, punctuality, enthusiasm, and freedom of conscience made me what I am today. I am glad; she has been always optimistic about my work and never discouraged me even after getting negative results. I thank her for being patient with me.*

*I express my deepest gratitude to the thesis examiners, **Prof. Rajiv Mohan, Dr. Rohini Muthuswami** and **Prof. Sreenivasulu Kurukuti** for critically assessing the thesis and improving through their constructive comments.*

*I would also like to thank **Dr. Sudhakar Panda**, Director NISER, for providing the necessary laboratory amenities and instrumentation facilities to carry out this work. I thank **NISER, DAE** for granting the fellowship during my PhD tenure.*

*I have sincere gratitude towards my Doctoral committee members, **Dr. Chandan Goswami, Dr. Asima Bhattacharyya, Dr. Tirumala K. Chowdary** and **Dr. Jagneswar Dandapat** for providing critical and useful suggestions that immensely improved my thesis. I also owe my deepest gratitude to our collaborator, **Dr. Pranjya P. Mohanty**, Sri Sri Borda hospital and the study participants for their consents and providing the necessary samples to accomplish my objectives.*

*I sincerely thank my labmates for their friendship, motivation and endless support throughout the process. I will always appreciate all that they have done, especially my senior, **Dr. Biswajit** for amplifying my PhD journey from experiments to papers. I owe deepest gratitude to my incredible junior, **Ramani** for helping me with work, hours of manuscript/thesis editing, for her relentless support and always being there whenever needed. I also thank my senior **Dr. Gargi** for her motivation and co-operation, **Maynak** for his suggestions and critical comments which helped me improve. I also thank my present and past labmates, **Senjit, Biswa, Late Vinay, Lipsa, Sushree, Sushmita, Bhagyashree, Dibya, Rajesh** and special thanks to **Pragnya** for collecting samples sincerely and maintaining the record book.*

*Staying away from home and not feeling homesick was only possible because of an exceptional friend **Somdatta**, who was a supporting pillar during the crucial phases of my PhD and for being there for me throughout the entire doctorate program.*

*I also thank my friends and batchmates, **Himani, Shashank, Dinesh, Sanjai, and Pragyesh** who always made a dull day bright.*

*For imbibing the knowledge and excitement to pursue a career in science, I am forever indebted to all my teachers from school, graduation and post-graduation.*

*It is unimaginable to have completed this thesis without the support of my loving parents, **Abbi and Mummy** who never ceased to believe in me. I am also blessed to have such motivating siblings as **Farha, Tahseen, Sanam, Rahmat and Misbah** for their encouragement and for having unrelenting faith in me to achieve this honor.*

*Last but not the least, my deep and sincere gratitude to my spouse, **Tabish, Papa and Ammi** for their endearing love and support and also heartfelt thanks to my brother-in-law's, **Syed Burhan and Dr. Nadeem** for their kind help in my PhD journey.*

**Bushra Hayat**

# CONTENTS

<b>Summary.....</b>	<b>I</b>
<b>List of Tables.....</b>	<b>III</b>
<b>List of Figures.....</b>	<b>IV</b>
<b>List of Abbreviations.....</b>	<b>VIII</b>
<b>1.0 A comprehensive overview about pseudoexfoliation.....</b>	<b>1</b>
1.1 Introduction.....	2
1.2 Historical aspects and terminology.....	3
1.3 PEX and epidemiology.....	4
1.4 PEX pathogenesis.....	5
1.4.1 Genetic players as predisposing risk factors of PEX.....	8
1.4.2 Environmental factors as risk factors for PEX development.....	12
1.5 Molecular pathways involved in the pathomechanism of pseudoexfoliation.....	13
1.6 Possible theories explaining pathogenic concept of PEX.....	16
1.7 Recent advances.....	18
1.8 Lacunae in the field of pseudoexfoliation.....	18
<b>2.0 Dissecting the role of heat shock proteins in the pathogenesis of pseudoexfoliation.....</b>	<b>20</b>
2.1 Introduction.....	21
2.1.1 Cellular stress response: Cytosolic-UPR.....	22
2.1.2 Heat shock proteins and pseudoexfoliation.....	24
2.1.3 Heat shock protein family A member 1A (HSPA1A).....	25
2.1.4 Heat Shock Protein 90 Alpha Family Class A Member 1 (HSP90AA1).....	26
2.2 Materials and Methods.....	27
2.2.1 Study subject recruitment and selection.....	27
2.2.2 DNA extraction.....	28
2.2.3 Bisulfite treatment and bisulfite-specific PCR.....	29
2.2.4 Bisulfite and Sanger's sequencing.....	31

2.2.5 RNA extraction.....	33
2.2.6 cDNA synthesis.....	33
2.2.7 Quantitative real time PCR.....	34
2.2.8 Protein extraction.....	34
2.2.9 Protein estimation.....	35
2.2.10 Western blotting.....	35
2.2.11 <i>In vitro</i> DNA methylation.....	36
2.2.12 Luciferase assay.....	37
2.2.13 <i>In silico</i> analysis.....	38
2.2.14 Cell Culture and Demethylation Treatment.....	38
2.2.15 Statistical analysis.....	38
2.3 Results.....	39
2.3.1 Decreased mRNA and protein expression of HSP70 in pseudoexfoliation syndrome but not in pseudoexfoliation glaucoma.....	40
2.3.2 <i>In silico</i> methylation analysis of the human HSPA1A gene.....	41
2.3.3 Hypermethylated CpG sites are identified in the exon of the <i>HSP70</i> gene but not in its promoter region.....	42
2.3.4 PEXS affected lens capsule has an increased expression of DNMT3A in comparison to control.....	47
2.3.5 DNA methylation in an exon region has a major regulatory activity.....	49
2.3.6 5-aza-dC induces DNA demethylation at exonic region III and restores the expression of HSP70.....	57
2.3.7 Increased expression of HSP70 regulator in PEXS affected lens capsule tissue.....	59
2.4 Discussion.....	61
2.5 Conclusion.....	64

### **3.0 To investigate the role of endoplasmic reticulum-unfolded protein response**

<b>(ER-UPR) and ubiquitin proteasome system (UPS) in PEX pathogenesis</b> .....	66
3.1 Introduction.....	67
3.1.1 ER stress signaling: ER-UPR.....	68
3.1.2 Ubiquitin proteasome system (UPS).....	70
3.2 Materials and Methods.....	72
3.2.1 Study Subjects Recruitment and selection.....	72
3.2.2 RNA Extraction, cDNA synthesis and Quantitative Real-time PCR.....	72
3.2.3 RT <sup>2</sup> Profiler PCR array.....	74
3.2.4 Immunofluorescence analysis.....	76
3.2.5 Protein extraction and Western Blotting.....	77
3.2.6 Proteasome-Glo <sup>TM</sup> assay Systems.....	77
3.2.7 Terminal deoxynucleotidyl transferase dUTP nick end labeling (TUNEL) assay.....	78
3.2.8 Statistical analysis.....	79
3.3 Results.....	79
3.3.1 Increased expression of ER-UPR genes in anterior eye tissues of Pseudoexfoliation syndrome and glaucoma.....	80
3.3.2 Validation of increased expression of deregulated genes in lens capsule and conjunctiva of PEX affected tissues.....	85
3.3.3 Validation of increased expression of differentially regulated genes in the PEX affected tissue.....	87
3.3.4 Increased expression of UBB and reduced expression of proteasome subunits.....	91
3.3.5 Decreased proteasome activity and increased ubiquitinated proteins in the lens capsule of PEXS individuals.....	94
3.3.6 Increased apoptotic cell death in lens capsule of PEXS and PEXG subject.....	97
3.4 Discussion.....	98
3.4.1 Altered expression of genes involved in the ER-UPR in anterior eye tissues of PEX patients.....	99

3.4.2 Impaired UPS in PEX affected tissues .....	100
3.4.3 Increased apoptosis in the PEX individuals .....	102
3.4.4 Activation of ER-UPR and inhibition of UPS .....	102
3.5 Conclusion .....	104
<b>4.0 Enhanced expression of the Wnt antagonist Dickkopf-1 in pseudoexfoliation syndrome and glaucoma .....</b>	<b>105</b>
4.1 Introduction .....	106
4.1.1 Dickkopf-1, a potent antagonist of Wnt signaling .....	106
4.1.2 DKK1 as a potential risk factor in Pseudoexfoliation .....	107
4.2 Materials and Methods .....	109
4.2.1 Demographic and clinical characteristics of subjects .....	109
4.2.2 Enzyme-linked immunosorbent assay (ELISA) .....	109
4.2.3 Quantitative Real time-PCR (qRT-PCR) .....	111
4.2.4 Immunostaining and immunofluorescence .....	112
4.2.5 Immunoblotting .....	113
4.2.6 Statistical analysis .....	113
4.3 Results .....	113
4.3.1 Increased mRNA expression of DKK1 in lens capsule and conjunctiva of PEX affected tissues .....	114
4.3.2 Differential accumulation of DKK1 protein in anterior eye segment of PEX individuals .....	115
4.3.3 Immunofluorescence analysis of DKK1 in lens capsule of study subjects .....	117
4.3.4 Differential expression of genes involved in canonical and non-canonical Wnt pathways in lens capsule of PEX affected subjects and control .....	119
4.3.5 Increased circulating level of DKK1 in plasma of pseudoexfoliation patients .....	122
4.3.6 Potential of the circulating DKK1 levels to become a biomarker for detection	

of PEXS and PEXG.....	124
4.4 Discussion.....	125
4.5 Conclusion.....	129
<b>5.0 CACNA1A as a probable risk factor in the pathogenesis</b>	
<b>of PEX.....</b>	<b>130</b>
5.1 Introduction.....	131
5.1.1 CACNA1A is a P/Q type voltage-sensitive calcium channel.....	131
5.1.2 Role of CACNA1A in various neurodegenerative disorders.....	133
5.1.3 Potential role of CACNA1A as a risk factor in PEX progression.....	134
5.2 Materials and Methods.....	136
5.2.1 Study subjects.....	136
5.2.2 DNA extraction, PCR, elution and sequencing.....	136
5.2.3 TaqMan SNP Genotyping Assay.....	137
5.2.4 Quantitative Real-Time PCR.....	138
5.2.5 Cell culture.....	138
5.2.6 Dual Luciferase Reporter Assay.....	138
5.2.7 CRISPR/Cas9 constructs preparation and genome editing.....	139
5.2.8 Statistical Analysis.....	140
5.3 Results.....	140
5.3.1 Genotypic association of risk variant SNP rs4926244 with pseudoexfoliation in Indian population.....	140
5.3.2 Reverse transcript expression analysis of CACNA1A in lens capsule of PEX affected patients.....	142
5.3.3 Influence of rs4926244 locus on CACNA1A gene regulation.....	145
5.3.4 <i>In vivo</i> effect of rs4926244 on CACNA1A gene expression.....	146
5.3.5 Genetic association of rs4926246, a tag SNP of r4926244 with pseudoexfoliation glaucoma.....	147
5.4 Discussion.....	152

5.5 Conclusion.....	154
<b>6.0 Discussion.....</b>	<b>156</b>
6.1 HSP70 in the pathogenesis of Pseudoexfoliation.....	157
6.1.1 Aberrant epigenetic alterations of HSP70 in PEXS .....	157
6.2 Dysregulated expression of genes involved in ER-UPR pathway.....	158
6.2.1 Impaired proteasome and increased apoptotic cell death in the lens capsule of PEX affected subjects .....	158
6.3 Elevated expression of DKK1, a potent Wnt antagonist in the anterior eye tissues of PEX.....	159
6.4 Genetic variants in CACNA1A as a risk factor in PEX pathogenesis .....	160
6.5 Conclusion.....	161
6.6 Key findings from the study.....	162
6.7 Methods standardized during the course of this project in the laboratory.....	163
6.8 Future Prospective.....	164
<b>7.0 References.....</b>	<b>165</b>

## List of Tables

Table 1.1 A detailed list of proteins involved in constituting PEX material with their functions.....	6
Table 2.1 List of oligos used in the study.....	30
Table 2.2 Predicted transcription factor binding sites in the HSP70 amplicon encompassing CpG region III.....	53
Table 3.1 List of oligos used in the study.....	73
Table 3.2 List of UPR genes used for designing custom RT <sup>2</sup> profiler PCR array.....	75
Table 3.3 List of the UPR genes with their functions and involvement in neurodegenerative diseases.....	80
Table 3.4 List of UPR related genes altered in lens capsule of PEXS and PEXG patients with respect to control.....	81
Table 3.5 Demographics of study subjects included for PCR array in LC tissues of PEXS and PEXG.....	83
Table 3.6 List of UPR related genes altered in conjunctiva of PEXS and PEXG patients with respect to control.....	84
Table 4.1 Demographics, clinical and ocular characteristics of study subjects included for ELISA in plasma samples of Control, PEXS and PEXG.....	110
Table 4.2 List of oligos used in the study.....	111
Table 5.1 Demographic of study subjects included for genotyping of CACNA1A variants.....	136
Table 5.2 List of oligos used in this study.....	137
Table 5.3 Allelic distribution of CACNA1A variant rs4926244 in PEX and control subjects.....	141
Table 5.4 Genotypic distribution of SNP rs4926244 in CACNA1A gene across PEX patients and controls.....	141
Table 5.5 Allelic distribution of CACNA1A variant rs4926246 in PEX, PEXS, PEXG and control subjects.....	149
Table 5.6 Genotype frequency of CACNA1A variant rs4926246 in PEX, PEXS, PEXG and control subjects.....	150
Table 5.7 Haplotype association of the two variants rs4926244 and rs4926246 with study subjects.....	150

## List of Figures

Figure 1.1 Image of an anterior eye segment depicting deposition of exfoliation material.....	3
Figure 1.2 Human eye anatomy elucidating PEX pathology.....	3
Figure 1.3 Prevalence of PEX.....	5
Figure 2.1 The Components of proteostasis network (PN).....	22
Figure 2.2 Diagrammatic representation of heat shock response.....	24
Figure 2.3 mRNA expression of HSP70 and HSP90 in lens capsule tissues.....	40
Figure 2.4 Western blot analysis of HSP70 and HSP90 in lens capsule tissues.....	41
Figure 2.5 DNA methylation profiles of the HSP70 gene.....	42
Figure 2.6 Methylation status of HSP70 CGIs in the lens capsule of control, PEXS and PEXG individuals.....	44
Figure 2.7 Methylation status of HSP70 CGIs in the blood of control, PEXS and PEXG individuals.....	46
Figure 2.8 mRNA and protein expression of DNMT3A and DNMT3B in lens capsule tissues.....	48
Figure 2.9 Schematic representation of regions cloned for <i>in vitro</i> methylated luciferase-based reporter gene assays.....	49
Figure 2.10 Confirmation of <i>in vitro</i> methylation assay by HpaII digestion.....	50
Figure 2.11 Functional analyses of HSP70 methylation using <i>in vitro</i> methylated luciferase-based reporter gene assays.....	51
Figure 2.12 Functional and <i>in silico</i> analyses of HSP70 methylation CpG region III using <i>in vitro</i> methylated luciferase-based reporter gene assays.....	52
Figure 2.13 Differential methylation at individual CpG sites in region III.....	56
Figure 2.14 Demethylation using 5-aza-2'-deoxycytidine increases HSP70 expression in HLE B-3 cells.....	58

Figure 2.15 Demethylation using 5-aza-2'-deoxycytidine in HLE B-3 cells.....	59
Figure 2.16 Differential expression of HSP70 regulators.....	60
Figure 2.17 A schematic representation of the findings.....	65
Figure 3.1 Schematic representation of ER-UPR signaling pathway.....	69
Figure 3.2 Schematic representation of the ubiquitin proteasome cycle.....	71
Figure 3.3 Differentially expressed genes in lens capsule of PEXS individuals (n=8) with respect to control (n=8).....	82
Figure 3.4 Differentially expressed genes in lens capsule of PEXG individuals (n=6) with respect to control (n=6).....	83
Figure 3.5 Altered expression of genes involved in the ER-UPR in conjunctiva of PEX patients.....	85
Figure 3.6 mRNA expression of <i>SYVN1</i> and <i>CANX</i> validated in lens capsule of study subjects.....	86
Figure 3.7 Validation of UPR PCR array results in conjunctiva tissues by quantitative real-time PCR.....	87
Figure 3.8 Western blot analysis of <i>SYVN1</i> in lens capsule extracts of control, PEXS and PEXG subjects.....	88
Figure 3.9 Confocal microscopy analysis showing presence of <i>SYVN1</i> in lens capsule of control, PEXS and PEXG subjects.....	89
Figure 3.10 Western blot analysis of calnexin in the tissue extract of PEX affected subjects.....	90
Figure 3.11 Confocal immunofluorescence analysis of calnexin.....	91
Figure 3.12 mRNA expression of ubiquitin genes in lens capsule of study subjects.....	92
Figure 3.13 Differential expression of proteasome subunits, <i>PSMD1</i> and <i>PMSA5</i> in the lens capsule of study subjects.....	94
Figure 3.14 Representative Immunoblot showing the presence of the 26S proteasome S4-subunit ( <i>PSMC1</i> ) in the protein extracts obtained from control, PEXS and PEXG samples.....	95

Figure 3.15 Determination of the specific chymotrypsin-like proteasomal activity in lens capsule extracts from control PEXS and PEXG.....	95
Figure 3.16 Immunoblot analyses of ubiquitinated proteins in tissue lysate of PEXS, PEXG and control.....	96
Figure 3.17 Increased apoptosis in the lens capsule of PEXS individuals.....	97
Figure 3.18 Model depicting the involvement of UPR components in PEX pathogenesis.....	103
Figure 4.1 DKK1 mRNA expression in lens capsule and conjunctiva of PEX affected tissues and non PEX controls.....	115
Figure 4.2 Immunoblotting analysis to detect DKK1 protein level in PEX affected subjects versus control.....	117
Figure 4.3 Immunofluorescence image of control, PEXS and PEXG stained for DKK1.....	118
Figure 4.4 mRNA expression of Wnt pathway genes in lens capsule of PEX affected tissues and non PEX controls.....	120
Figure 4.5. Western blot analysis of Wnt pathway genes in lens capsule lysate of study subjects.....	122
Figure 4.6 ELISA of the DKK1 in plasma samples of PEX and control.....	123
Figure 4.7 Diagnostic outcomes for plasma DKK1 in the diagnosis of PEX.....	125
Figure 4.8 Clusterin-dependent induction of DKK1 in PEX.....	129
Figure 5.1 The gene structure of <i>CACNA1A</i> .....	131
Figure 5.2 Diagrammatic representation of the voltage gated calcium channel and its subunits.....	132
Figure 5.3 Schematic representation of calcium channel disruption in neurodegenerative disorders.....	133
Figure 5.4 Schematic illustration for proposed role of <i>CACNA1A</i> in PEX pathogenesis.....	135
Figure 5.5 <i>CACNA1A</i> mRNA expression change in PEX affected subjects compared to control.....	143
Figure 5.6 rs4926244 genotype-based <i>CACNA1A</i> mRNA expression correlation.....	144

Figure 5.7 Allelic effect on luciferase activity in HEK293 and HLE B-3 cells.....	146
Figure 5.8 <i>In vivo</i> effect of rs4926244 locus on CACNA1A expression.....	147
Figure 5.9 LD block of rs4926244 and rs4926246.....	148
Figure 5.10 rs4926246 genotype wise comparison of <i>CACNA1A</i> mRNA expression.....	152
Figure 6.1 Factors contributing to pseudoexfoliation pathogenesis.....	162

# **CHAPTER 6**

## *Discussion*

## 6.0 Discussion

Proteopathies are a group of human diseases that arise due to non-native or abnormal conformational changes in the proteins. Destabilizing mutations and stress are major causes of these changes, which cause the misfolded proteins to aggregate and form intra- or extra-cellular deposits.<sup>397</sup> The cellular proteostasis network, which consists of molecular chaperones, ubiquitin-proteasomal pathway (UPP), and autophagy keeps the protein misfolding and toxic accumulation under check by breaking down the proteins into polypeptide chains.<sup>243,245,246,398</sup> When this proteostasis network is impaired, the unwanted and misfolded proteins accumulate as aggregates in various parts of the body. Therefore, in neurodegenerative disorders, such as Alzheimer's disease (AD)<sup>399</sup>, Parkinson's disease (PD)<sup>400</sup>, Prion disease, and polyglutamine diseases<sup>243,247</sup>, impaired proteostasis and aberrant accumulation of misfolded proteins in different parts of the body is noted. Pseudoexfoliation is an age-related proteinopathy characterized by aggregation of extracellular matrix (ECM) material in both ocular and extra-ocular tissues, which suggests that aberrant ECM synthesis or impaired degradation may contribute to disease pathogenesis.<sup>401</sup> Interestingly, clinical features observed in PEX individuals, such as deposition of fibrillar materials, age associated severity and neurodegeneration also resemble other age-related neurodegenerative disorders. Apart from an impaired proteostasis network, altered Wnt signaling has also been reported to be involved in ECM deposition.<sup>16,17</sup> At genetic level, numerous genes have been associated as risk factors with PEX. Recently, polymorphism in *CACNA1A* has been genetically associated with PEX though the functional studies remain unknown.<sup>9,318</sup> The current study highlights the role of proteostasis components, Wnt signaling genes and calcium channel subunit, *CACNA1A* in PEX pathology.

### 6.1 HSP70 in the pathogenesis of pseudoexfoliation

Stress induced HSP70 is the most conserved cytosolic chaperone. HSP70 is expressed as a response to a range of stress stimuli, including reactive oxygen species and DNA damage, and plays a key role in maintaining cell integrity and viability.<sup>205,206</sup> Transcriptional activation of HSP70 is dependent on the binding of heat shock factors on heat shock element of *HSP70* gene.<sup>402</sup> However, in current study both the mRNA and protein expression of HSP70 were significantly downregulated in lens capsule of PEXS patients despite the upregulation of its transcriptional regulators, PARP1 and HSF1. Decreased expression of HSP70 has been reported previously in the retina of R6/2, R6/1 and R7E spinocerebral ataxia type 7 (SCA7) mice which was attributed to an impairment at the level of gene expression or protein turnover<sup>403,404</sup> Another study has reported chromatin modification that prevents binding of heat shock regulators on HSP70 thereby reducing its expression.<sup>222,405</sup> We suspected the role of epigenetic modification in modulating the level of HSP70 expression.

### **6.1.1 Aberrant epigenetic alterations of HSP70 in PEXS**

Epigenetic aberrations have been linked with many eye diseases, including glaucoma,<sup>11</sup> age-related macular degeneration (ARMD),<sup>12</sup> uveal melanoma,<sup>406</sup> cataract,<sup>407</sup> and diabetic retinopathy<sup>408</sup> but reports on epigenetic modifications in PEX are scarce. In the study presented here, we revealed for the first time that CpG island in the exon of Hsp70 is hypermethylated in lens capsule of PEXS patients, resulting in a substantial reduction in the level of HSP70 expression. We also observed elevated expression of *de novo* methyltransferase DNMT3A in PEXS eyes, implicating that HSP70 expression is regulated in methylation dependent manner and it may be preferentially methylated by DNMT3A. Further, treating lens epithelial cells with 5-aza-dC, a demethylating agent, restored this downregulation effect of DNA hypermethylation.

Thus, the hypermethylation of the HSP70 coincides with its diminished expression suggesting that these methylation events could contribute to PEX risk or pathogenesis.

## **6.2 Dysregulated expression of genes involved in ER-UPR pathway**

Excessive production and accumulation of fibrillar materials in PEX is an indicative of proteostasis imbalance. We examined the expression status of a set of crucial UPR genes in PEX affected anterior eye tissues through Custom RT<sup>2</sup> profiler PCR arrays. Increased ER stress markers *SYVN1*, *EIF2AK*, *DNAJB11*, *CASP12*, *HSPA5*, *HSPD1* and *CANX* were identified in the lens capsule of PEX individuals compared to age-matched controls, of which relative expression of synoviolin1 (*SYVN1*), an E3 ligase protein, and calnexin, an ER localized chaperone was markedly increased and showed significant upregulation in the lens capsule of PEX subjects as compared with controls. Further assessment of *SYVN1* using immunohistochemistry and western blot exhibited an increased expression in the lens capsule of PEXS and PEXG affected tissues while *CANX* was seen to be upregulated only in lens capsule of PEXG individuals which implicates activation of UPR genes in diseased individuals. Hence, activation of UPR is taken as an indicator that ER function is disturbed in PEX pathological process under investigation. Though earlier studies have documented evidence for perturbation in cytoprotective mechanisms including cellular stress response, and antioxidant defense in anterior segment tissue of PEX eyes.<sup>199</sup> we revealed a new set of candidate genes involved in PEX pathogenesis in our study.

### **6.2.1 Impaired proteasome and increased apoptotic cell death in the lens capsule of PEX affected subjects**

Additionally, we found significant amount of ubiquitinated proteins in cases than in controls suggesting that reduced protein degradation may lead to overall accumulation of aberrant proteins with age in lens capsule of PEXS affected subjects. Subsequently, we found decreased

expression of two key proteasome subunits, PSMD1 and PMSA5 which is in concordance with a significant decrease of the chymotrypsin-like proteasome activity in the lens capsule of PEXS individuals in comparison to age-matched control. This confirmed a dysfunctional proteasomal system, which could indicate failed retro-translocation of misfolded ER proteins and a hampered ERAD mechanism in PEXS individuals. Besides impaired UPS, the role of autophagy impairment in the pathogenesis of PEXS has been recently examined by Andrew Want et al. showing that Tenon's cells from PEXS patients exhibited impaired relocation of lysosomes to the perinuclear area upon induction of autophagy and also had a reduced rate of autophagosome clearance.<sup>158</sup> When proteasome activity is inhibited, elevated ER stress can lead to the activation of apoptosis pathways including the activation of caspase-12 (CASP12) and DDIT3.<sup>267,281</sup> PEX individuals showed higher levels of ER-stress markers (including CASP12), which implies that they may also be more sensitive to apoptosis. In agreement with this hypothesis, PEXS subjects showed increased number of apoptotic cell death in the lens capsule of PEXS and PEXG which in turn might mediate ER-stress mediated cell death. Altogether, our study suggests reduced protein degradation and proteasome activity resulting in increased apoptosis in the PEX affected tissues might lead to proteostasis impairment which consequent into fibrillar protein deposition in the extracellular space.

### **6.3 Elevated expression of DKK1, a potent Wnt antagonist in the anterior eye tissues of PEX**

In Alzheimer's disease, increased clusterin led to induction of Dickkopf-1 (DKK1)<sup>344</sup> which tempted us to hypothesize that increased DKK1 expression might be induced by increased clusterin in PEX which further triggers non-canonical Wnt signaling cascade. Our findings in the current report demonstrate a comprehensive expression profile of DKK1 in the anterior eye

segment of PEX subjects which showed pronounced increase at both mRNA and protein levels in anterior eye tissues of PEXS and PEXG individuals compared to non-PEX control. The secreted glycoprotein DKK1, an antagonist of the Wnt signaling pathway, has been implicated in many neurodegenerative diseases such as Alzheimer's disease.<sup>409</sup> A very recent attempt was made to create a mouse model by transient expression of Wnt5a in the mouse anterior eye segment via Adenovirus-mediated gene expression which recapitulates certain ocular manifestations of human PEXS suggesting a possible involvement of dysregulated Wnt signaling in its pathophysiology.<sup>369</sup> Furthermore, our study revealed an enhanced circulating level of DKK1 is associated with PEX susceptibility. In addition to DKK1, Wnt5a, and ROCK responsible for non-canonical Wnt signal transduction also showed an increased expression in PEXS affected cases compared to that of control in our analysis.

#### **6.4 Genetic variants in CACNA1A as a risk factor in PEX pathogenesis**

Recently, Aung et al. discovered genetic association between an intronic variant, rs4926244 in the gene, Calcium voltage-gated channel subunit- $\alpha$ 1A (CACNA1A).<sup>9</sup> Genotypic association of rs4926244 was found with PEXS in a case-control study with 196 cases and 275 control in an Indian population with the frequency of risk genotype 'TT' being significantly higher in PEXS individuals. Genotype-specific expression analysis revealed significant increase in expression of CACNA1A by the risk genotype 'TT'. On further functional analysis, we found a significant difference in luciferase expression between control empty vector and constructs with either allele at rs4926244 in HEK293 cells, though we did not find allele specific regulatory activity, which suggest a regulatory effect of the genomic region surrounding the variants rather than the SNP itself.

We speculated a presence of unknown causal variants in *CACNA1A* that could contribute to the genetic risk of PEX. This led us to genotype an intronic variant, rs4926246 which was in strong LD with rs4926244. rs4926246 showed a significant association with PEXG individuals with the 'T' allele conferring a risk effect of 1.5. This study confirmed a novel association of the variant, rs4926246 in *CACNA1A* with PEXG individuals indicating a genetic contribution of *CACNA1A* in PEX pathogenesis in Indian population.

## **6.5 Conclusion**

Overall findings from the present study reveal a decreased expression of cytosolic chaperone, HSP70 which corresponds to the *de novo* DNA hypermethylation in its first exon. We further reported dysregulation in ER related stress marker implicating an impaired UPR pathway in individuals affected with PEX. Our study is the first to demonstrate that the plasma level of DKK1 is significantly elevated in patients with PEX compared with control subjects, subsequently its increased expression has been observed in affected tissue that provides a novel insight into disease pathogenesis. We also conducted a case-control study to identify putative risk variants in *CACNA1A* gene, coding for a subunit of a Calcium channel essential for pre- and postsynaptic signaling. Genotypic association of rs4926244 in *CACNA1A* gene substantiates its role as risk factor for pseudoexfoliation (PEX) syndrome in Indian cohort. We also found a novel variant of *CACNA1A*, rs4926246 to be genetically associated with PEXG in our study population. In summation, this study provides insight into perturbed cytoprotective mechanisms and regulatory roles of candidate genes in PEX pathogenesis.

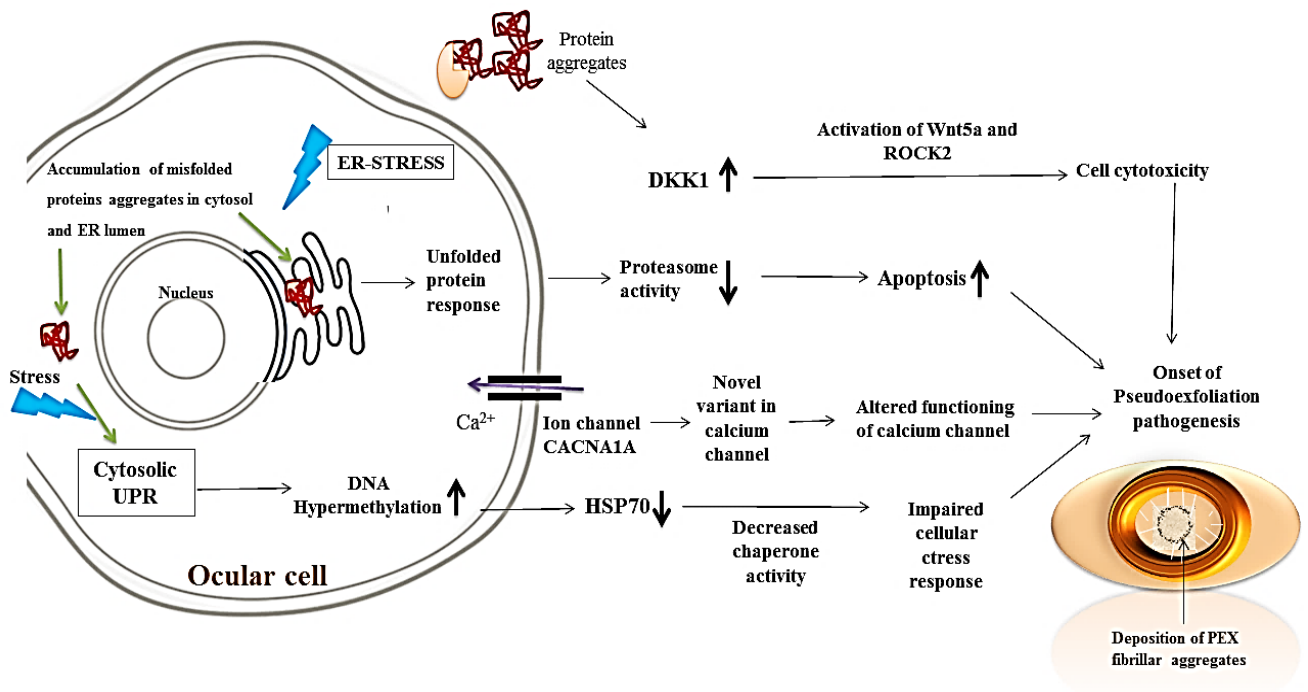


**Figure 6.1 Factors contributing to pseudoexfoliation pathogenesis.** The present study unraveled the role of components involved in maintenance of proteostasis network, Wnt signaling and calcium channel that might be derailed during PEX pathogenesis. Presence of fibrillar aggregates in PEX indicates impaired proteostasis, which activates a signaling cascade to restore protein homeostasis. We demonstrate increased DNA hypermethylation leading to decreased expression of HSP70, a stress-response chaperone in PEXS affected lens capsule tissues. Following this we found increased expression of endoplasmic reticulum related stress markers indicating unfolded protein response activation in lens capsule of PEX individuals. Reduced proteasome activity and proteasome subunit expression were also observed in PEX subjects implying impaired proteasome function which ultimately led to cell death in lens capsules. In addition, increased expression of Wnt antagonist, DKK1 in the anterior eye tissue suggests increased cytotoxicity. We also found reduced CACNA1A expression on deletion of locus surrounding rs4926244 region suggesting altered functioning of calcium channel. These findings provide evidence that proteostasis imbalance contribute significantly to abnormal XFM formation and aggregation.

## 6.6 Key findings from the study

- HSP70, major cytosolic chaperone is significantly downregulated in the lens capsule of PEXS individuals than in PEXG individuals compared to control.

- Reduced HSP70 expression corresponds to DNA hypermethylation of CpG island of *HSP70* gene.
- Hypermethylation of the exon of *HSP70* gene has a functional regulatory effect implicated in the transcriptional regulation.
- Treatment with a DNMT inhibitor, 5-aza-deoxycytidine (5-Aza DC) restored HSP70 expression in HLE B-3 cell line.
- Increased expression of ER-stress markers, Synoviolin1 and Calnexin, suggests UPR activation in PEX.
- Reduced chymotrypsin-like proteasome activity and decreased proteasome subunits (PSMD1 and PSMA5) expression indicate impaired proteasome function.
- Cells in the lens capsules of PEXS and PEXG individuals showed higher apoptotic rate.
- DKK1 expression was found to be significantly upregulated in the anterior eye tissues of PEXS and PEXG subjects than in those of control individuals.
- This is the first study to demonstrate circulating level of DKK1 in the plasma of PEX affected subjects.
- CACNA1A major susceptibility variant, rs4926244 is associated with PEXS at genotypic level.
- A novel variant, rs4926246 in CACNA1A is found to be significantly associated with PEXG in our study population.

## **6.7 Methods standardized during the course of this project in the laboratory**

- Bisulfite sequencing for checking DNA methylation
- Protein extraction from lens capsule to check protein level via immunoblotting
- *In vitro* methylation and demethylation assay to validate methylation status of gene

- TUNEL assay to check apoptotic activity in eye tissue
- Proteasome-Glo<sup>TM</sup> based assay to check proteasome activity in tissue lysates
- Sandwich ELISA assay to look for prognostic marker in plasma of affected subjects

### **6.8 Future Prospective**

- Additional elaborate studies need to be carried out to focus on the effect of locus specific DNA methylation on the role of transcription factors regulating the expression of *HSP70*.
- To determine the role of specific histone modifications in HSP70 regulation.
- Detailed role of genes, SYVN1 and CANX in the progression of PEX warrants further research.
- *In vitro* experiments such as TCF/LEF reporter assay need to be performed to determine whether DKK1 is involved in the beta-catenin dependent or independent pathway.
- Further studies are needed to find more regulatory SNPs within the *CACNA1A* gene in association with PEX.
- Functional effects of *CACNA1A* associated polymorphisms with PEX need to be explored.

## SUMMARY

Pseudoexfoliation (PEX; OMIM: 177650) is an age-dependent systemic disorder, clinically manifested by the gradual deposition of whitish fibrillar proteinaceous materials known as exfoliative material (XFM) in the ocular and non-ocular tissues. Deposition of these fibrils in ocular tissues leads to an increased intraocular pressure (IOP) which subsequently results in the death of optic nerve head cells (ONH) and gradually contributes to blindness. Early syndrome form of PEX is referred as pseudoexfoliation syndrome (PEXS) and later severe stage is known as pseudoexfoliation glaucoma (PEXG). This study primarily focuses on exploring the components involved in maintenance of proteostasis network that might be derailed during PEX pathogenesis. The key findings from the present study are summarized as follows and depicted in

### **Figure A:**

- Heat shock protein 70 (HSP70), a major cytosolic chaperone was found to be significantly downregulated in the lens capsule of PEXS individuals compared to controls indicating an impaired cytoprotective mechanisms in pseudoexfoliation.
- Aberrant DNA hypermethylation of the exonic CpG island of *HSP70* correlates to its reduced expression in PEX patients. *In vitro* assays showed that hypermethylation of the exon of *HSP70* gene has a functional regulatory effect implicated in its transcriptional regulation.
- Inhibition of DNA methyltransferases by a DNMT inhibitor, 5-aza-deoxycytidine (5-Aza-dC) restored HSP70 expression in Human lens epithelial cells (HLE B-3).
- Increased expression of endoplasmic-reticulum stress markers in lens capsule of PEX subjects was observed indicating the activation of unfolded protein response in disease condition.

- Impaired proteasome activity as reflected by reduced expression of proteasome subunits and increased accumulation of ubiquitinated proteins in PEX patients could contribute to accumulation of PEX aggregates.
- Increased apoptosis was observed in the lens capsules of PEXS and PEXG which could be due to the impaired proteostasis in PEX individuals.
- Increased expression of the Wnt antagonist, DKK-1 in the plasma as well as in the anterior eye tissues of PEXS and PEXG subjects than in those of control individuals provides a novel insight into disease progression.
- The variant rs4926246, a tag SNP of rs4926244 showed significant novel genetic association with PEXG individuals as a risk factor.

In a nutshell, our findings from this study demonstrate alterations in cytoprotective mechanisms (**Figure A**) and provide an insight into the regulatory role of candidate genes in PEX pathogenesis.

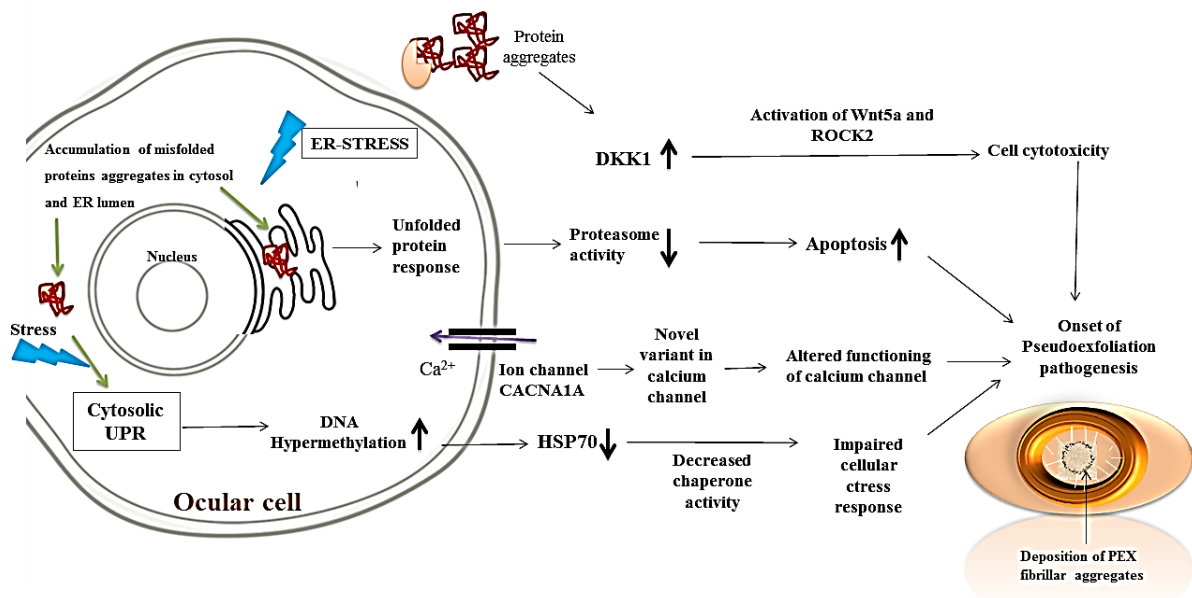


**Figure A:** Schematic representation of the key findings in alteration of cytoprotective pathways involved in PEX pathology explored in this study.

# **CHAPTER 1**

*A Comprehensive Overview about  
Pseudoexfoliation*

## 1.0 A comprehensive overview about pseudoexfoliation

### 1.1 Introduction

Pseudoexfoliation (PEX; MIM: 177650) is a complex, age-related proteinopathy, clinically manifested by the gradual deposition of abnormal fibrillar exfoliative materials (XFM) in ocular and non-ocular tissues.<sup>1</sup> PEX starts with XFM deposits and with time, it leads to extensive aggregation of fibrillar materials in the outflow pathways of aqueous humor that lead to increased intraocular pressure (IOP), optic neuropathy and subsequent development of secondary open-angle glaucoma, known as pseudoexfoliation glaucoma (PEXG), which represents 20-60% of open-angle glaucoma.<sup>19-21</sup> The early form of PEX is referred as pseudoexfoliation syndrome (PEXS). PEXS has been frequently associated with other pathological alterations involving ocular tissues like angle closure glaucoma, lens subluxation, cataract, zonular defects and occlusion of the retinal vein.<sup>1,4,22</sup> Besides, it has also been linked with many systemic complications like cardio and cerebrovascular diseases, ocular hypertension, abdominal aortic aneurysm, and pelvic organ prolapse.<sup>5,23,32,24-31</sup>

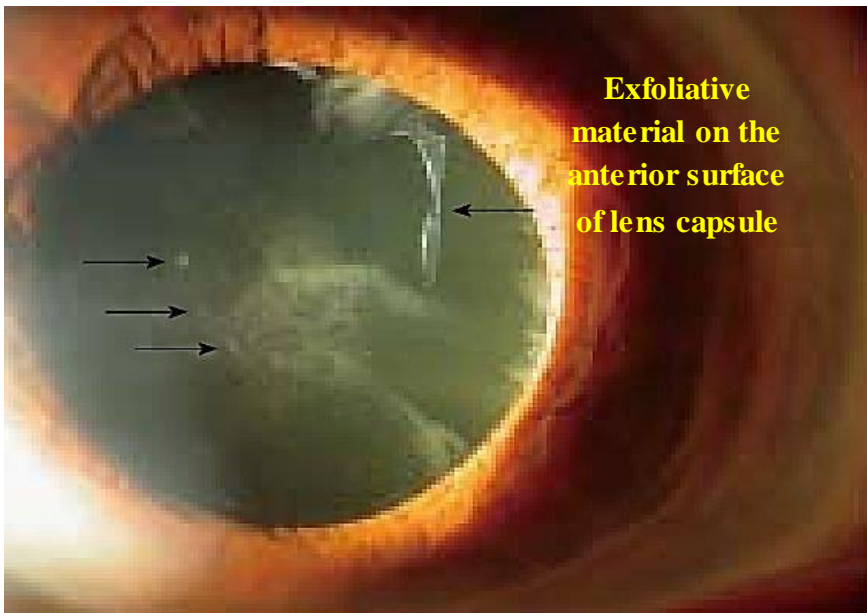


**Figure 1.1 Image of an anterior eye segment depicting deposition of exfoliation material.** This figure shows the slit lamp observation of whitish flake like deposits on the surface of lens capsule and pupillary margin of an iris. (Figure adapted from [10.4330/wjc.v6.i8.847](https://doi.org/10.4330/wjc.v6.i8.847))<sup>33</sup>

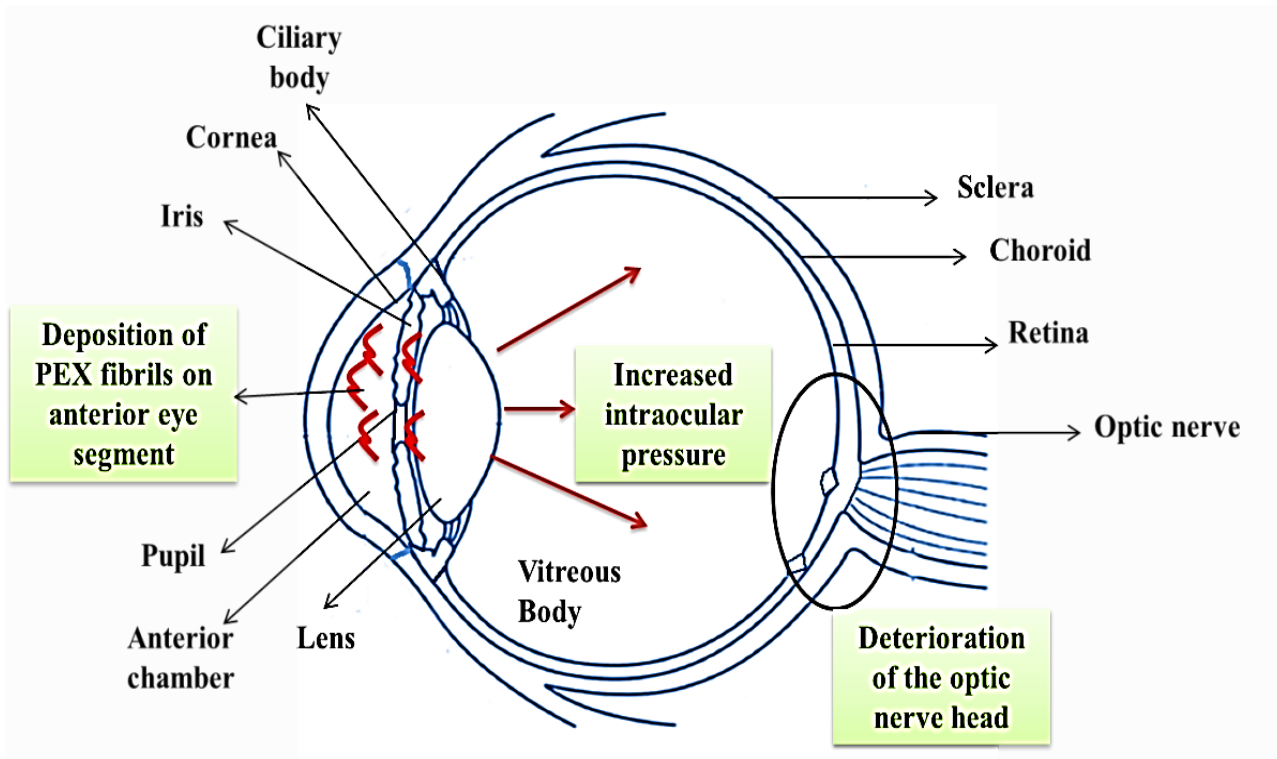


**Figure 1.2 Human eye anatomy elucidating PEX pathology.** The figure elucidates the complications and consequence of PEX deposits on the anterior eye tissue. (Outline of an eye taken from <https://www.kissclipart.com/parts-of-the-eye-clipart-human-eye-human-body-k7ln8s/>).

## 1.2 Historical aspects and terminology

Finnish ophthalmologist, Lindberg first described PEX in the year 1917, who first noticed bluish-gray specks at the iris pupillary margin in majority of patients affected with severe open-angle glaucoma.<sup>34,35</sup> Following this, Alfred Vogt (1918) termed the disease as “*capsulare glaucoma*” assuming lens capsule as the site of origin of PEX, and to be associated with glaucoma.<sup>36</sup> Later, the term pseudoexfoliation was coined by Dvorak Theobald<sup>37</sup> while exfoliation syndrome was proposed by Sunde.<sup>38</sup> Since the disease can occur in the presence or

absence of glaucoma, the term pseudoexfoliation syndrome (PEXS) is generally used for early stage while pseudoexfoliation glaucoma (PEXG) is used for a later stage of PEX.

### **1.3 PEX and Epidemiology**

PEX epidemiology is intriguing and interesting. PEX has been reported in 60 to 70 million people worldwide, although prevalence varies widely between distinct racial and ethnic groups. The reported PEX prevalence increases with age and varies from 0.2% to more than 40% in different study populations. The highest prevalence rates have been reported in Scandinavian countries- 20-25% followed by prevalence rate of 11.9% in Greece in individuals above 60 years old.<sup>39-42</sup> In other parts of the world, with zero percent prevalence in the Eskimos of Greenland<sup>43,44</sup> to lesser prevalence have been recorded in countries such as Germany (4.7%), England (4%), United States (1.8%), Australia (2.3%), and South Africa (2.8%).<sup>3,45-47</sup> In Chinese and Japanese populations, the prevalence of PEX was reported to be 0.4 and 3.4%, respectively.<sup>48,49</sup> Epidemiology studies so far showed that PEX is more prevalent in Caucasians than in Afro-Americans.<sup>50,51</sup> In Indians, prevalence of the disease range from 0.69-3.8% which then increases with age upto 8.45%.<sup>52-54</sup> PEXS is noted as a leading risk factor for glaucoma, 14.2% glaucoma in patients with PEXS has been reported by the Blue Mountain Eye study.<sup>55</sup> It is a late onset ailment whose prevalence increases considerably with increasing age.<sup>56</sup> Individuals over the age of sixty years are found to be more susceptible to PEX.

PEX prevalence has varied in terms of gender. Although many studies have showed a higher incidence in women than men, this bias was considered secondary to improved lifespan.<sup>43,57-60</sup> Further, 12-year occurrence level of PEX was correlated with older age and female sex in population based survey in Reykjavik<sup>61</sup> while few reports also show about same or increased prevalence in male cohort.<sup>49,52,62,63</sup> So far, no gender predilection has been reported for

the disease in many studies as gender association is not always reproducible.<sup>56,64-68</sup>

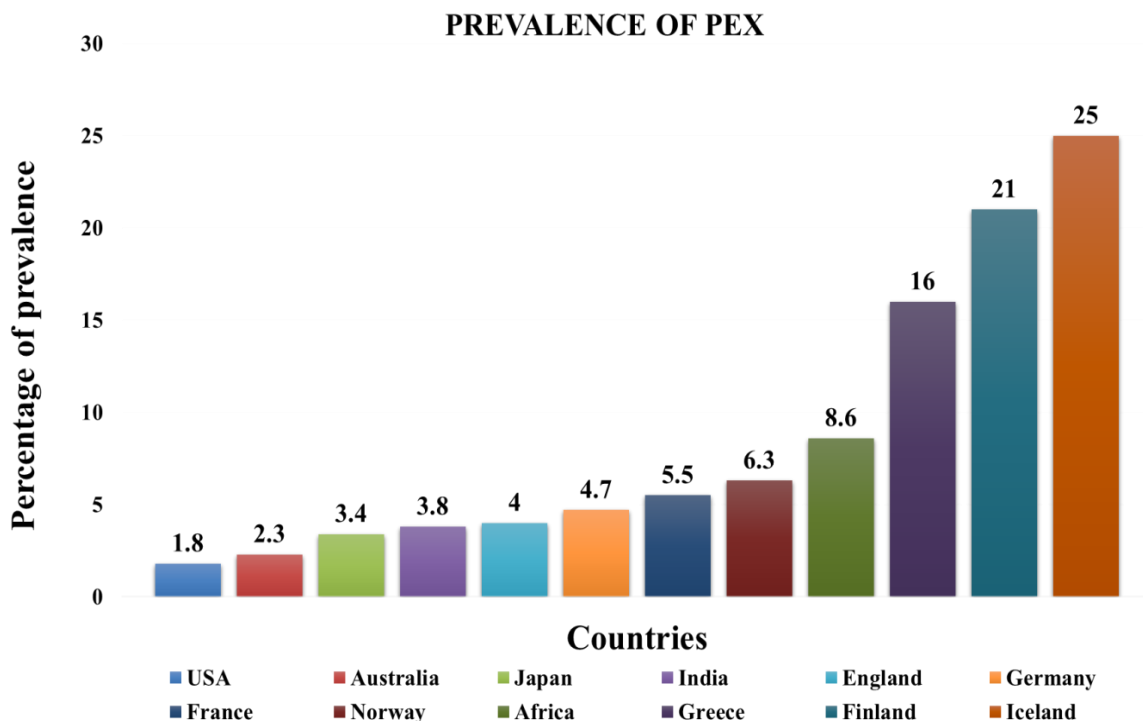


**Figure 1.3 Prevalence of PEX.** Bar graph showing PEX is reported worldwide with the highest prevalence in Icelandic population and lowest in USA.<sup>49,53,56,69-71</sup>

### 1.4 PEX pathogenesis

PEX pathological trait involves gradual deposition of abnormal fibrillar, extracellular matrix (ECM) material in the anterior ocular tissues and an elevated IOP. Proteomic and electron microscopy studies suggest fibrillar nature of PEX material (XFM) comprising of elastic fiber and basement membrane components such as elastin, laminin, fibrillin, vitronectin.<sup>56,72</sup> This implicates that PEX is a stress-inducible fibrillopathy, primarily caused by the genetic predilection and increased stress conditions that facilitate the aggregation and deposition of fibrillar material in intra and extra ocular tissues. **Table 1.1** enlists the proteins that form the constituents of PEX aggregates.

**Table 1.1 A detailed list of proteins involved in constituting PEX material with their functions.**

<u>Protein</u>	<u>Protein functions</u>	<u>Role in PEX</u>
<b>A. Components of ECM and Basement membrane</b>		
1. Fibrillin-1 ( <u>Gene ID: 2200</u> )	A glycoprotein that participates in formation of microfibrils.	Major constituents of PEX deposits. <sup>73</sup>
2. Fibulin-2 ( <u>Gene ID: 2199</u> )	Adapter protein in the extracellular matrix and interconnects elastin and fibrillin-1.	A significant part of PEX aggregates consists of fibulin-2 protein. <sup>72</sup>
3. Elastin ( <u>Gene ID: 2006</u> )	Elastin is a key ECM protein that determines the elasticity and resilience of many tissues such as skin.	Elastin is an integral component of PEX material and its deposition was found in PEX affected tissues. <sup>74</sup>
4. Fibronectin ( <u>Gene ID: 2335</u> )	Binds to ECM proteins and helps in ECM remodeling.	Constituents of PEX material, involved in the deposition of PEX aggregates <sup>75</sup>
5. Fibulin-5 ( <u>Gene ID: 10516</u> )	It functions as an ECM protein and is helpful in scaffolding and elastogenesis.	Deregulated expression of fibulin-5 was found in the lens capsules of PEXS subjects. <sup>76</sup>
6. LOXL-1 ( <u>Gene ID: 4016</u> )	Lysyl oxidase-like 1 participates in elastic fibre formation.	Involved in abnormal cross linking and promote aggregation of PEX fibrils. <sup>77,78</sup>
7. MMPs (MMP2; <u>Gene ID: 4313</u> ) and (MMP 9; <u>Gene IDs: 4318</u> )	Involved in ECM maintenance and stability.	Decreased level of MMP2 reported in aqueous humor of PEXS <sup>79</sup> and PEXG <sup>80</sup> , while MMP9 activity

		was found increased in tear samples of PEXS and reduced in tears of PEXG. <sup>81</sup>
8. Vitronectin (Gene ID: 7448)	An extracellular glycoprotein, promotes cell-adhesion by interacting with membrane protein integrin.	Presence of vitronectin protein in XFM deposits was revealed by proteomic study. <sup>72</sup>
9. Laminin (Gene ID: 284217)	A basement membrane protein, mediates cell adhesion and growth.	Promote formation and accumulation of PEX material. <sup>82</sup>
<b>B. Stress response proteins</b>		
1. Clusterin (Gene ID: 1191)	Act as a chaperone to prevent unwanted protein aggregation.	Presence of clusterin in XFM deposits, dysregulated expression of clusterin associated with PEX. <sup>8,83</sup>
2. Adenosine A3 receptors (Gene ID: 140)	Act as a regulator of IOP and aqueous humor secretion.	Increased expression of A3 receptor in PEXS eyes. <sup>84</sup>
3. GST (Gene ID: 2938)	Glutathione S Transferase, a multifunctional detoxification enzyme, provides protection from oxidative stress.	Reduced expression of GST isoenzyme, mGST was found in anterior ocular tissues of PEX patients. <sup>85</sup>
<b>C. Proteins involved in immune regulation</b>		
1. Complement factors (C1q, C3c, C4c) (Gene ID: 9370 708, 718 respectively).	Complement factors play an important part in innate immune system.	Proteomic studies also found deposition of complement factors in fibrillar deposits of PEX affected tissues. <sup>72</sup>

<p>2. LTBP-1 and LTBP-2 (Gene ID: 4051 and 4053 respectively)</p>	<p>Latent transforming growth factor b (TGF-β) binding proteins (LTBP-1 and LTBP-2)</p>	<p>Immunolabeling studies reported the presence of LTBP-1 and LTBP-2 in intra and extra ocular deposits of PEX.<sup>78</sup></p>
---	---	--

#### 1.4.1 Genetic players as predisposing risk factors of PEX

Research in the past has improved our understanding on the cumulative contribution of genetic and environmental factors that confer risk of PEX to individuals around the world. However, their precise mechanism of action remains to be understood. Like any other inherited disease, scientists have tried to identify the genetic contributor for this disease through familial linkage studies,<sup>57,86</sup> genome wide association study (GWAS)<sup>87</sup> and polymorphic markers which suggested a genetic nature of this disease.

##### a. Lysyl oxidase-like 1

Lysyl oxidase like-1 (LOXL1; Gene ID: 4016) identified as a major risk factor in PEX pathology, is a member of lysyl oxidase (LOX) family involved in elastin formation and ECM maintenance. A GWAS study by Thorleifsson et al., in 2007 reported a strong genetic association of polymorphic markers in the *LOXLI* gene located on chromosome 15 (q24.1) with PEX in Icelandic and Swedish population.<sup>87</sup>

Two of the three associated SNPs within *LOXLI* are non-synonymous, missense variants present in protein coding exon 1: rs1048661 (Arg→Leu, R141L) and rs3825942 (Gly→Asp, G153D).<sup>87</sup> The other variant, rs2165241, is present in the first intron and may be linked with *LOXLI* transcriptional regulation.<sup>88,89</sup> Many replicative studies in different populations from Australia,<sup>90</sup> China,<sup>91</sup> Japan,<sup>92</sup> India,<sup>93</sup> Korea,<sup>94</sup> Mexico,<sup>95</sup> Pakistan,<sup>96</sup> Poland,<sup>97</sup> Saudi Arabia,<sup>88</sup>

and the USA<sup>98,99</sup> have confirmed genetic association of variants in *LOXL1* with PEX, thus demarcating *LOXL1* as the major genetic player for the disease.

Later studies revealed that genetic risk conferred by *LOXL1* variants are reversed in different ethnicities. For instance, the allele “G” at both rs1048661 and rs3825942 are risk allele for PEX susceptibility in Caucasian as well as in Indian populations.<sup>90,100–103</sup> However, a replicative study conducted in Japanese and Chinese population found “T” as the risk allele at rs1048661 while “A” at rs3825942 in Black South African population, contrary to that reported in major populations.<sup>65,92,104–106</sup> Reports from Greek<sup>107</sup> and Polish population also conferred the absence of genetic association between rs1048661 with PEX.<sup>108</sup> Further, risk alleles at *LOXL1* variants have higher frequency in the control subjects and very low specificity in predicting the affected status suggesting the role of other interacting factors in predicting disease susceptibility.<sup>98</sup> Ubiquitous expression of *LOXL1* has been detected in all anterior and posterior segments of eye tissues mainly in iris, ciliary body, lens capsule, and lamina cribrosa. In anterior eye tissues (lens capsule and ciliary body), higher mRNA expression of *LOXL1* has been reported in PEXS while later stage PEXG was found with decreased expression.<sup>89</sup> While, posterior chamber of PEX affected eye tissue, like lamina cribrosa showed a consistent downregulated expression of *LOXL1*.<sup>74</sup> Immuno-histochemical (IHC) studies identified *LOXL1* as an integral component in PEX fibrils where it was found to co-localize with other matrix components such as elastin, fibrillin-1, and fibulin-4.<sup>89,109</sup> Recent study has demonstrated protective role of *LOXL1* novel variant rs7173049 that mediates upregulation of gene *STRA6* (stimulated by retinoic acid receptor 6) associated with retinoic acid signaling pathway in ocular tissues suggesting an involvement of impaired retinoid metabolism in PEX disorder.<sup>110</sup> This finding implicates a pivotal role of *LOXL1* in catalyzing the crosslinking of elastin into tropoelastin and

helps in maintaining and remodeling ECM, thus its dysregulation is associated with increased accumulation of PEX aggregates.

### **b. Clusterin**

Clusterin (CLU, Gene ID: 1191) (otherwise called as Apolipoprotein J) is a multifunctional protein involved in many extracellular processes including its role as an extracellular molecular chaperone that checks on precipitation and aggregation of misfolded proteins.<sup>111</sup> Clusterin is another potential genetic factor responsible for occurrence of PEX occurrence.<sup>112</sup> The presence of Clusterin in pseudoexfoliation deposits and its higher concentration in ocular fluid of PEXG individuals laddered into an examination for the genetic variants of Clusterin.<sup>8,72,83</sup> Further, candidate gene studies reported polymorphisms in *CLU* as risk factors for pseudoexfoliation; an intronic variant, rs2279590 and rs3087554 present in the 3' UTR were found to be significantly associated with PEX in German and Australian populations, respectively.<sup>112,113</sup> Similarly, dataset from our group also elucidated a strong association between PEX affected individuals and rs2279590 and rs3087554 in an Indian population.<sup>8</sup> We also reported an elevated level of clusterin protein in aqueous humor of PEXG individuals while the expression of *CLU* mRNA remained unchanged between cases and control, however, a significant increase in mRNA per “G” risk allele was found.<sup>8</sup> Not only we found a functional role of the intronic variant, rs2279590 in its gene expression, but this variant was also seen to regulate two distal genes, *EPHX2* (Epoxide Hydrolase 2) and *PTK2B* (protein tyrosine kinase 2 beta) that have been associated with AD.<sup>114</sup>

### **c. Contactin Associated Protein-Like 2**

Contactin associated protein-like 2 (CNTNAP2; Gene ID: 26047) encodes protein CASPR2A which is a neuronal membrane protein and helps in regulation of potassium channel.<sup>115,116</sup> It was

identified as a candidate risk factor in PEX through GWAS wherein two SNPs, rs2107856 and rs2141388 of *CNTNAP2* were associated with PEX in German population and the study reported that the TT haplotype confers a risk of 1.42 in Germans.<sup>117</sup> The other two intronic variants rs1404699 and rs7803992 were associated with PEX in Japanese population.<sup>118</sup> *CNTNAP2* is expressed ubiquitously in all ocular tissues, IHC studies have found its localization mainly in corneal epithelium, trabecular meshwork, Schlemm's canal, iris pigment and ciliary body of both PEX and control eyes.<sup>113,119</sup> *CNTNAP2* is basically involved in the maintenance of membrane stability by promoting cell-cell adhesion, cell assembly and differentiation, migration. So it is presumed that alteration in *CNTNAP2* functions might lead to abnormal matrix formation and thus suggested *CNTNAP2* as a potential candidate gene for PEX manifestation.

#### **d. Calcium voltage-gated channel subunit- $\alpha$ 1A:**

Calcium voltage-gated channel subunit-alpha 1A (*CACNA1A*; Gene ID: 773) belongs to a family of genes that codes for calcium channel (CACN). These channels mainly transport calcium ions and play an important role in contraction of muscles, release of neurotransmitters and gene regulation (Diriong et al., 1995). The *CACNA1A* gene is especially expressed in Purkinje cells in cerebellum (Nature and Westenbroek *et al.*, 1995). Mutations in this gene lead to defects in the formation of the subunit consequently leading to an imbalance in the calcium transport. Worldwide GWAS study across Japan and 17 other countries identified a novel locus in *CACNA1A* gene, encoding alpha subunit of a calcium channel and detected a significant association of the novel variant rs4926244 in *CACNA1A* with PEXS.<sup>9</sup> Earlier studies have also demonstrated the presence of calcium in the aggregates of PEX fibrils.<sup>120,121</sup> Besides, calcium also plays a protective role in stabilizing fibrillin-1 to form stable aggregates.<sup>122</sup> This may insinuate a role of calcium in forming PEX fibrils.

#### **e. Other genetic variants**

Other genetic variants that have been noted so far in PEX are present in Glutathione transferase (GST), Matrix metalloproteinases (MMP-1 and MMP-3), Homocysteine metabolism genes, Tumor necrosis factor- $\alpha$  (TNF-  $\alpha$ ), Lysosomal trafficking regulator (LYST) and Adenosine receptor A3.<sup>79,84,123,124</sup> GST is a class of enzymes that take control over xenobiotics and oxidative stress by inactivating them.<sup>78</sup> TNF- $\alpha$  is a proinflammatory cytokine involved in neurodegenerative disorders, depending on the receptor activated, TNF can act as a neuroprotectant after binding to its high affinity receptor (TNF-R2). It can also lead to cell death or neurodegeneration upon binding to its low affinity receptor (TNF R3).<sup>125,126</sup> Polymorphism in TNF- $\alpha$  SNP G-308A of rs1800629 was found to be strongly associated with PEXG in Pakistani cohort.<sup>127</sup> Association studies found the genotypes “GG” and “GA” to be strongly associated with Pakistani<sup>127</sup> and Iranian cohort<sup>128</sup> but the replicative studies did not find a significant association in Caucasian<sup>129</sup> or Turkish cohort.<sup>130</sup>

Apart from the genetic variants, environmental factors too are known to play a role in the manifestation of PEX.

#### **1.4.2 Environmental factors as risk factors for PEX development**

PEX is a complex disorder where environmental factors also contribute in its etiopathogenesis besides genetic factors. Epidemiologic studies reported that PEX is more prevalent in a region relatively with high UV exposure and in people living at higher latitude.<sup>131,132</sup> Countries with cooler climate have highest risk for PEX which may be due to the increased deposition of XFM at colder temperature and thus support the cold precipitation hypothesis.<sup>133</sup> Similarly, a case control studies have shown that those who lived at higher altitude, or are involved in outdoor occupations have increased incidence of PEX.<sup>134,135</sup> Besides geographical factors, other non-

genetic factors such as, food intake, dietary supplements, autoimmunity, infectious agents, and trauma, were also found to contribute to PEX pathogenesis, however, further research is needed to detail the exact mechanism. In a recent prospective study, higher folate intake was associated with reduced risk of developing PEX, while, no association was observed with the intake of vitamin B6 or B12.<sup>136</sup> In a similar study, high caffeine consumption is linked with greater risk of PEX.<sup>137</sup> Though it is yet unclear how it affects PEX, it has been speculated that folate intake and coffee consumption is linked with elevating homocysteine levels and altering LOXL1 activity which enhances the formation of XFM and confers an increased risk in genetically predisposed individuals.

Non-genetic risk factors also provide perspective into biochemical pathways (such as ECM turn over, oxidative and cellular stress, autophagy etc.) that functionally relate to PEX etiology. Mechanisms hampering these crucial pathways will provide a better understanding of PEX pathology. Moreover, it is unclear which anomalies promote PEX development and which are an intermediate response, thus further studies are required to understand their role in the PEX pathology.

## **1.5 Molecular pathways involved in the pathomechanism of pseudoexfoliation**

### **a. Oxidative stress**

The late-onset PEX syndrome is characterized by progressive accumulations of fibrillar aggregates. Many epidemiologic studies have investigated the function of oxidative stress in PEX development. The formation of many reactive oxygen species (ROS) including superoxide dismutase (SOD), hydrogen peroxide (H<sub>2</sub>O<sub>2</sub>) and hydroxyl radicals propagating free radicals generally induce oxidative stress.<sup>138</sup> There is growing evidence that the balance of oxidative-antioxidant is disrupted in PEX that involves the entire body. Elevated level of oxidative stress

markers, such as H<sub>2</sub>O<sub>2</sub>, nitric oxide, were reported in AH samples of PEXS patients.<sup>139</sup> At the same time, diminished levels of enzymatic activity of antioxidant enzymes (SOD and Catalase) in lens epithelium of PEX have been reported.<sup>140</sup> Other antioxidant markers such as glutathione-S-transferases (GST), catalase, ascorbate and glutathione (GSH) showed decreased activity in AH of PEX.<sup>141–143</sup> Oxidative stress also obstructs the aqueous outflow by promoting degeneration of trabecular meshwork (TM) resulting in increased IOP and subsequent development of glaucoma. The reduced level of total antioxidant capacity (TAC) and higher rate of total oxidant status were detected in blood of PEX individuals (Erdurmus et al., 2011). Moreover, 8-hydroxy-2'-deoxyguanosine (8-OHdG), a marker for DNA damage induced by oxidative stress was found to be enhanced in plasma of PEXG patients when compared with control.<sup>144</sup>

Elevated level of malondialdehyde (MDA) has been reported in serum of PEXS and PEXG and in lens epithelial cells of patients with PEXS in comparison to non-PEX patients.<sup>145–147</sup> High level of oxidative stress markers indicates that oxidative stress contributes to the development of XFM and glaucoma in PEX individuals. An overall, past and present findings show that there is an accelerated oxidative stress response with depressed antioxidant protection in eyes with PEX.<sup>148,149</sup>

#### **b. Homocysteine metabolism**

Homocysteine is a highly reactive amino acid which is derived from methionine. An elevated homocysteine level in blood leads to neurological and coronary disorders.<sup>150</sup> Methylene tetrahydrofolate reductase (MTHFR) regulates the homocysteine and folate concentration in the body. Elevated levels of homocysteine have been observed in plasma, aqueous humor and tear fluid in both PEXS and PEXG compared with controls.<sup>151–154</sup> High homocysteine level leads to

several pathological changes such as altered expression of MMP/TIMP, vascular endothelium inhibition, oxidative stress and increased DNA methylation. However, some researchers believe that lack of association of MTHFR gene polymorphism and homocysteine level with PEXS or PEXG in Caucasian population might suggest that it cannot be considered as a risk factor for PEX disease.<sup>155</sup>

### **c. TGF- $\beta$ and ECM metabolism**

Transforming growth factor beta (TGF- $\beta$ ) is a modulator of ECM formation and has been implicated in the development of PEX. In anterior eye segment, such as samples obtained from ciliary body and aqueous fluid from PEXS patients, high levels of both forms of TGF- $\beta$  (active and latent) have been observed with respect to control.<sup>156,157</sup> TGF- $\beta$  facilitates the aggregation of ECM protein by upregulating the synthesis of different components of ECM thus contributing to the production of exfoliative materials.<sup>78</sup> The mechanism underlying the increased level of TGF- $\beta$ 1 in PEXS remains unknown.

### **d. Autophagy**

Andrew Want et al., recently explored the role of autophagy dysfunction in PEXS pathology and reported that Tenon's fibroblast from PEXS subjects showed larger vacuoles filled with cellular waste followed by reduced autophagosome clearance and failure of lysosomes relocation to the perinuclear region when autophagy is induced.<sup>158</sup> Likewise, Bernstein et al. reported the defects in lysosomal and autophagosome positioning in PEXG fibroblast cells documenting autophagy dysfunction.<sup>159</sup> The increase in the ratio of autophagosome-bound LC3 (LC3-II) and LC3-II/LC3-I upon acceleration of starvation induced autophagy and the congestion of the LAMP-1-positive vesicles were found to be linked with a reduced level of autophagosome clearance from the cell.<sup>158,160</sup> Thus, it can be deduced that autophagy impairment in PEXS may contribute to the

aggregation of aberrant deposits of fibrillar protein in ocular and systemic tissues. Eventually, it is important to remember that autophagy serves as the defense mechanism to control misfolded and denatured proteins, the failure of which leads to increased apoptosis.

#### **e. Cytokines**

Cytokines play an important role in inflammation and immune regulation. Elevated expression of interleukins IL-6 and IL-8 has been reported in the anterior ocular segment of PEXS individuals but not in PEXG cases.<sup>161,162</sup> Whereas, recent study by Chono and group has reported high level of IL-8 in aqueous humor of PEXG individuals compared to controls.<sup>163</sup> In response to oxidative stress, both IL-6 and IL-8 expression increases *in vitro* which in turn induces the expression of TGF- $\beta$  and other fibrotic factors in the ECM.<sup>157</sup> This entails a role of stress induced cytokine in the development of abnormal production of ECM protein characterizing PEX pathology. In addition, increased serum and aqueous humor levels of an inflammatory marker, YKL-40 were found in PEXS patients compared to controls.<sup>164,165</sup>

### **1.6 Possible theories explaining pathogenic concept of PEX**

PEX pathology is characterized by the gradual accumulation of abnormal fibrillar material which is a consequence of increased production and decreased degradation or both of ECM proteins. Historically, many theories have been proposed regarding the disease pathogenesis.

#### **a. Basement membrane theory**

Basement membrane of different cell types has been frequently associated with XFM suggesting altered membrane metabolism.<sup>166-168</sup> IHC studies have revealed the presence of basement membrane protein epitopes such as laminin, heparin sulfate proteoglycan in aggregates of XFM.

82,120,169

#### **b. Elastic microfibril theory**

Presence of elastic microfibril components such as fibrillin, vitronectin in PEX material advocates association of exfoliative fibres with the elastic system. The lamina cribrosa of PEXS eyes also has a marked localized elastosis of the elastic fibers. The IHC analysis of various elastic element epitopes, e.g. elastin, microfibril-associated glycoprotein (MAGP-1) in XFM, further supported this model. Immunoelectron microscopy of XFM further demonstrated abnormal aggregation and accumulation of elastic microbrils in PEXS.<sup>56,73</sup>

### **c. Infectious origin**

Ringvold et al., reported PEX prevalence in both partners of married couple implicating an involvement of a contaminating particle responsible for PEX origin.<sup>170</sup> Studies of younger patients developing PEX following intraocular surgery provide additional evidence for the likelihood of an infectious agent.<sup>171-174</sup> However, due to inconclusive evidence, further studies are needed to support the theory of infectious agents contributing to PEX.

### **d. Protein sink theory**

A protein sink model has been proposed to explain the aberrant association of proteins in forming PEX materials. According to this model, soluble proteins form insoluble structure by changing their native conformation that accumulates in the form of extra or intracellular aggregates.<sup>133</sup> It has been suggested that proteins in the aqueous humor of an eye are bonded by an atypical nucleation protein forming larger complex protein aggregates which ultimately settle down from the aqueous humor and eventually deposit on the anterior surface of eye tissues.<sup>133</sup> On molecular level, LOXLI an elastin protein associated with PEX interacts with other extracellular scaffold protein fibulin-5, fibrillin-1, LTBP-1/2 which are components of XFM and form a supra complex that precipitates as microfibrillar protein complexes and form a core of large protein aggregates.<sup>74,175,176</sup>

## **1.7 Recent advances**

Recent years have seen advancement in the field of PEX. Early stage detection has been enhanced by the improvement of diagnostic criteria; clinical-histopathological correlations have helped to illustrate the mechanisms underlying the disease pathogenesis and improve clinical management of possible complications; the identification of systemic PEX deposits has defined a prevalent process that appears to be linked with increased cardio and cerebrovascular lethality. Further, modern research strategies have offered new insights into the underlying molecular mechanism involving stress-related elastosis. Study by Hauser and colleagues have identified non-coding variants in *LOXLI-ASI* (*LOXL1*- antisense RNA1) to be associated with PEXG, and recently they elucidated *LOXLI-ASI* functional role in regulating ECM homeostasis, aqueous outflow pathways that have been implicated in PEXG pathogenesis.<sup>177,178</sup> However, search for clinical biomarkers, and development of cellular and animal-based models for PEX are still underway.

## **1.8 Lacunae in the field of pseudoexfoliation**

Although PEX has been known since decades, yet researchers don't know what causes it in most cases. Despite the extensive research, the disease etiology remains elusive. Little is known about the underlying possible molecular mechanisms leading to XFM accumulation and progression. And most importantly the major question that remains yet unanswered is does a patient with pseudoexfoliation syndrome likely to develop glaucoma, as PEX material has been seen in many patients with no sign of glaucoma. The factors that promote PEXS patients to develop glaucoma are still being explored. Though many genetic variants have been associated with PEX, due to inconsistent outcomes across various populations due to incomplete penetrance and allele reversals, the exact etiology and mechanistic pathways underlying the disease pathology remain

unknown. As the disorder progresses with age, an epigenetic control over disease causation and progression is highly anticipated. Thus, the present study provides a mechanism for interplay between genetic and epigenetic effects in PEX pathophysiology.

Lack of experimental and cellular models and minimal availability of ocular tissues limit the understanding of cellular basis of PEXS/PEXG progression. Regardless of these limitations, our present study investigates the components of proteostasis network, expression of genes involved in Wnt signaling and genetic association of intronic variant in calcium channel.

To address these questions the following thesis is divided into following chapters to achieve their respective objectives.

1. Dissecting the role of heat shock proteins in pseudoexfoliation pathogenesis (**Chapter-2**).
2. To investigate the role of endoplasmic reticulum- unfolded protein response (ER-UPR) and ubiquitin proteasome system in PEX pathogenesis (**Chapter-3**).
3. Elucidating the expression of the Wnt antagonist; Dickkopf-1 in the anterior eye segment of pseudoexfoliation (**Chapter-4**).
4. CACNA1A as a probable risk factor in the pathogenesis of PEX (**Chapter-5**).

# **CHAPTER 2**

*Dissecting the role of heat shock  
proteins in the pathogenesis of  
pseudoexfoliation*

## **2.0 Dissecting the role of heat shock proteins in the pathogenesis of pseudoexfoliation**

### **2.1 Introduction**

Proteostasis network (PN) is comprised of chaperones, degradative components and signaling pathways that trigger and direct protein folding in response to cellular stress.<sup>179</sup> Some of the factors within this network, promote protein folding, some prevent or correct misfolding, while others prevent and/or redirect aggregation and some direct proteins to degradation pathways.<sup>179</sup>

With a proteotoxic insult, cell activates unfolded protein response (UPR) that prevents misfolding of proteins as well as degradation of unwanted proteins. UPR is divided into cytosolic UPR and endoplasmic reticulum-UPR (ER-UPR) depending on the site of insult. Later, degradation pathways such as ubiquitin proteasome system (UPS) and autophagy act as a defense to degrade misfolded proteins and restore protein homeostasis when the protein folding capacity is saturated. Coordinated regulation of PN components representing protein translation, folding and degradation ensure the proteome maintenance. **Figure 2.1.** illustrates the components of PN where chaperones direct protein folding, signaling pathways such as heat shock response (HSR) and UPR facilitate the function of the PN to generate and maintain functional proteins as well as pathways that select proteins for degradation e.g., UPS, endoplasmic-reticulum-associated degradation (ERAD) and autophagy. The compromised potential of UPR to remove unfolded protein aggregates is primary cause of a wide range of neurodegenerative disorders and could be a key mechanism for PEX pathogenesis. The prevalence of proteostasis impairment in the disorder of protein aggregopathy is confirmed by the existence of familial forms of neurodegeneration induced by mutation of PN components.<sup>180</sup>

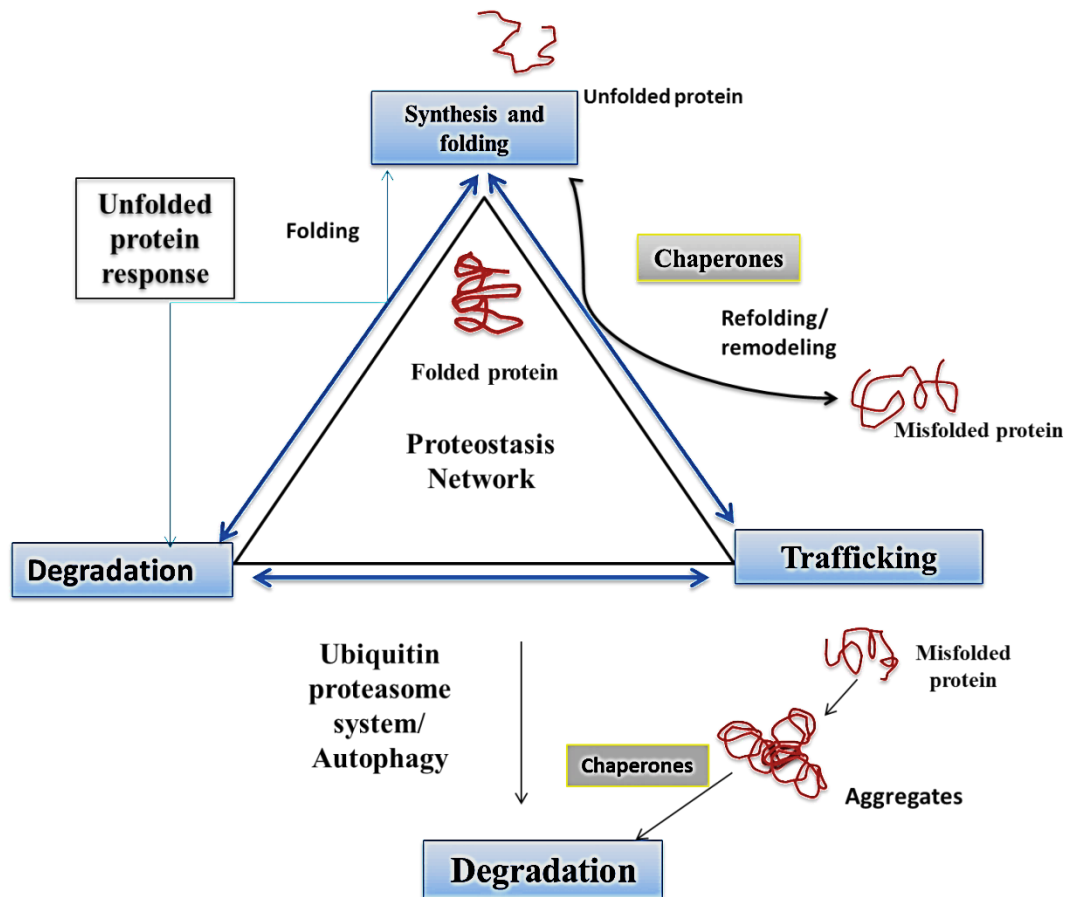


**Figure 2.1 The Components of proteostasis network (PN).** The protein homeostasis maintained by integrating major branches of the PN: (i) Protein synthesis, the folding factors responsible for the folding of newly synthesized proteins, (ii) The UPR pathways that resolve stress by inducing stress response elements, (iii) The chaperone pathways for remodeling of misfolded proteins and protein disaggregation and (iv) The pathways of protein degradation by the ubiquitin–proteasome system (UPS) and autophagy.

### 2.1.1 Cellular stress response: Cytosolic-UPR

If a cell is challenged by stress, which may lead to impairment of proteostasis, which in turn activates cellular responses, including the heat shock response (HSR). The hallmark of HSR is the activation of heat shock factors (HSFs) which leads to increased expression of heat shock proteins (HSPs), which work together to alleviate cellular stress. HSPs are a family of proteins that act as chaperones to help and stabilize proteins to achieve their native conformation.<sup>181</sup> They are classified into different groups based on their molecular weight as Hsp60, Hsp70, Hsp90, Hsp100 and the small Hsps (Hsp27 and  $\alpha$ -Crystallin).

Chaperones maintain protein homeostasis by mediating folding and refolding of proteins, and aid in protein degradation. Chaperone synthesis in response to proteotoxic stress is reliant on a group of transcription factors named HSFs, which include HSF-1, HSF-2 and HSF-4.<sup>182</sup> Of these, HSF-1 is known to be essential for regulating heat shock response (HSR) in mammalian cells.<sup>182-184</sup> Detailed mechanism of cytosolic UPR is schematically represented in **Figure 2.2** which shows: in unstressed cells, HSF-1 associates with HSP70/HSP90 complex and exists in a monomeric state<sup>185</sup> HSF1 is released from the HSP70/HSP90 complex when cells are exposed to stress, misfolded protein aggregation or other forms of physiological stress. This result in its dimerization, nuclear accumulation and extensive post-translational modification<sup>186</sup> where it binds to regulatory element called heat shock response element (HSRE) of heat shock genes including many cytosolic chaperones such as Hsp70 and proteasome subunits and induces their expression<sup>187</sup> This leads to improved protein folding, increased protein trafficking efficiency and increased degradation of proteins.<sup>188,189</sup> As the level of molecular chaperones increases, HSR ends with an auto-regulatory mechanism wherein HSF-1 binds to HSPs such as Hsp70 and Hsp90.<sup>185,190,191</sup>

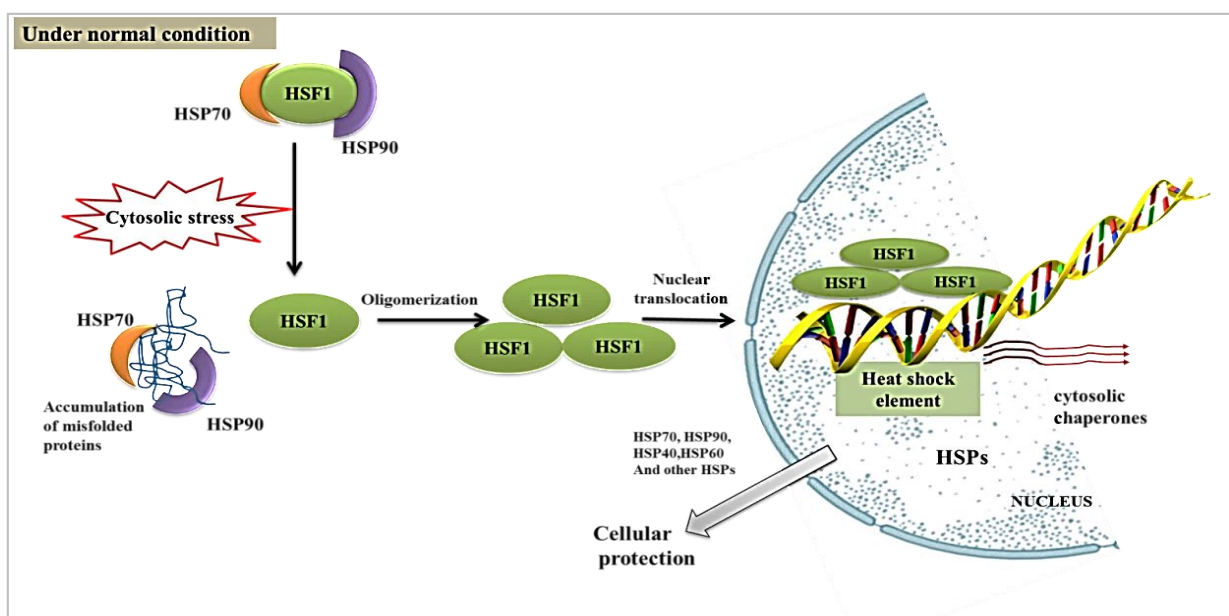


**Figure 2.2 Diagrammatic representation of heat shock response.** Under unstressed condition, HSF-1 remains in a complex with hsp70 and hsp90. When the cell is challenged with stress, HSF-1 releases from the complex, undergoes post translational modification and trimerization, translocate to nucleus. It binds to heat shock element present in promoter and activates the expression of cytosolic chaperones thus providing cellular protection.

HSPs are constitutively expressed and prevent aggregation and solubilization of proteins, thereby, acting as a crucial modulator of neurotoxicity in numerous neurodegenerative disorders like Alzheimer's disease (AD), Parkinson's disease (PD) and Huntington disease (HD). A previous study has reported that HSPs, such as Hsp90, Hsp70, and Hsp32, facilitate amyloid beta (A $\beta$ ) clearance by the induction of cytokines and increase A $\beta$  degradation by the activation of the Toll-like receptor-4 (TLR4) pathway in AD.<sup>192</sup> Hsp90 forms complex with carboxy terminus of Hsp70-interacting protein (CHIP), an ubiquitin ligase to degrade phosphorylated tau protein in AD pathology.<sup>193</sup> Evidence suggests that co-localization of polyQ-containing insoluble aggregates and molecular chaperones and their decrease in expression has been observed in several polyQ disease models.<sup>194–196</sup> Reduced levels of mutant Huntingtin (Htt) in both full-length and N-terminal forms, in cellular models was found after Hsp90 silencing, suggest that Htt is an Hsp90 client protein, and inhibition of Hsp90 promotes its degradation.<sup>197,198</sup> Thus, molecular chaperones are potential therapeutic targets for neurodegenerative diseases characterized by the accumulation and aggregation of misfolded proteins.

### **2.1.2 Heat shock proteins and pseudoexfoliation**

Impaired cellular stress has been implied in the etiology of pseudoexfoliation syndrome and glaucoma, although the exact etiopathogenesis has not yet been elucidated. Elements of the cellular stress-response heat shock proteins (HSP40 and HSP60), displayed an upregulation in PEX tissues as anticipated in response to stress conditions.<sup>199</sup> Recent study from our lab reported the significant upregulation of HSF1 mRNA expression in anterior eye tissues (lens capsule and

conjunctiva) of PEXS but not in PEXG individuals implicating proteotoxic stress in the eyes of pseudoexfoliation syndrome.<sup>114</sup> Dataset from our group provided further evidence for the dysregulation of another set of stress related genes, Synoviolin1 (SYVN1) and Calnexin (CANX) in PEX eyes and also confirmed the candidature of HSP40 and HSP60 in PEX pathogenesis.<sup>200</sup> Impaired proteasome and aberrant accumulation of misfolded proteins in PEX indicates a potential role of HSPA1A (Heat shock protein family A member 1A); the major stress inducible 70-kDa heat shock protein (Hsp70) and HSP90AA1 (Heat Shock Protein 90 Alpha Family Class A Member 1) in modulating pathogenic aggregate formation. Thus, the present study explored the role of HSP70 and HSP90 in PEXS and PEXG at mRNA and protein levels.

### **2.1.3 Heat shock protein family A member 1A (HSPA1A)**

HSPA1A is the stress-inducible heat shock 70 kDa protein. It is the most conserved chaperone, localized in cytosol as well in all cellular compartments. The HSP70 protein has two active domains involved in a wide variety of cellular functions. The amino terminal ATPase domain of HSP70 provides the energy needed for proper folding and maturation of proteins (M.P. Mayer, 2005). The other HSP70 carboxyl terminal substrate binding domain (SBD) has  $\beta$ - sandwich subdomain and a helical lid that recognizes the protein segment enriched in hydrophobic amino acids.<sup>201,202</sup> The HSP70 helical lid adopts an open conformation when bound with an ATP, and the lid closes when ATP hydrolysis occurs. ATP hydrolysis is accelerated by HSP40, which also interacts with misfolded peptides, and facilitates the recruitment of HSP70 to protein substrates. (H.H. Kampinga, et al., 2010). HSP70 also stabilizes proteins against aggregation in tandem with other heat shock proteins, and mediates the translocation of newly translated proteins in the cytosol and in organelles.<sup>203,204</sup> HSP70 can be expressed as a response to a range of stress stimuli

including reactive oxygen species, DNA damage and plays a key role in maintaining cell integrity and viability.<sup>205,206</sup> Several studies have shown in recent years that activation of the heat shock response (HSR) and in particular elevation of HSP70 levels in neurodegeneration models has a protective effect. Earlier reports showed that HSP70 reduced the amount of aggregated  $\alpha$ -synuclein *in vivo* and *in vitro*.<sup>207</sup> The lens expresses HSP70 when the normal microenvironment of the lens is stressful and it is continuously needed to deal with the stress stimuli.<sup>208,209</sup> Thus, HSP70 is a central player in protein folding and proteostasis maintenance.

#### **2.1.4 Heat Shock Protein 90 Alpha Family Class A Member 1 (HSP90AA1)**

Heat shock 90 kDa protein is the ubiquitous and abundant molecular chaperone that aids in the folding and stabilization of cellular proteins. It functions downstream to HSP70 and participates in a wide range of biological functions such as activation and inactivation of proteins depending on the cell's needs, regulation of several signaling pathways, and promoting regulation of receptors in cell death pathways.<sup>210</sup> It primarily binds and stabilizes non-native peptide and prevents them from getting accumulated.<sup>211</sup> HSP90 is a homodimer protein, each monomer comprises of N-terminal ATPase domain that promotes binding with co-chaperones, a central domain that regulates interaction with client proteins and ATP hydrolysis and a high-affinity C-terminal dimerization domain.<sup>212</sup> HSP90 expression is induced by various environmental stresses and growth factors in tumours where it participates in stabilizing and activating client proteins involved in malignant transformation.<sup>213</sup> HSP90 is considerably expressed in many human tumor cells and is a significant modulator of malignant transformation in epithelial cancers, including squamous cell carcinoma.<sup>214-216</sup> Both these HSPs, (HSP70 and HSP90) are constitutively expressed and are critical for proper protein folding and maturation, thus, preventing their aggregation and solubilization, they are important players in proteasome regulation.

The following study has been conducted to check the role of HSP70 and HSP90 in the progression of PEX. Following specific aims were addressed in this chapter:

1. Differential expression of HSP70 and HSP90 in the PEX affected ocular tissues.
2. The methylation status of HSP70 determined using DNA extracted from blood and tissue via bisulfite sequencing.
3. Status of DNA methyltransferases (DNMT3A and DNMT3B) in lens capsule tissues of individuals affected with PEX.
4. Functional analyses of HSP70 methylation using luciferase-based reporter gene assays.
5. Effect of DNA methyl transferase (DNMT) inhibitor 5 Aza-dC on HSP70 expression in HLE-B3 cells.
6. Expression of HSP regulators, HSF1 and PARP1 in PEX tissues.

## **2.2. Materials and Methods**

### **2.2.1 Study subject recruitment and selection**

This study was approved by the Institutional Human Ethics Review boards of NISER. All the participants underwent a detailed ocular examination, including slit lamp microscopy, ocular biometry and Goldman applanation tonometry and 4 mirror gonioscopy. All procedures adhered to the Declaration of Helsinki and an informed consent was taken from all subjects included in this study.

Cataract patients diagnosed with pseudoexfoliation syndrome (PEXS) or pseudoexfoliation glaucoma (PEXG) in cataract screening camps and outpatient departments were recruited for this study after obtaining informed consent. Inclusion criteria for PEXS were newly diagnosed adults >40 years with visually significant cataract, clinically evident pseudoexfoliation like material over lens or pupillary ruff with or without poor dilatation, open

or closed angles on gonioscopy, baseline IOP <21mmHg, no prior anti glaucoma treatment and with no evidence of glaucomatous optic nerve damage or visual field defects. Inclusion criteria for PEXG were newly diagnosed adults >40 years with visually significant cataract, clinically evident pseudoexfoliation like material over lens or pupillary ruff, raised IOP >21mm Hg without prior anti-glaucoma treatment, along with evidence of glaucomatous optic nerve head damage (defined as vertical cup-to-disc ratio of  $\geq 0.7$ , cup-to-disc asymmetry of more than 0.2, focal notching or rim loss, or a combination thereof and field defects corresponding to disc damage. Cataract patients without PEXS or PEXG matching the inclusion criteria were included as controls. Inclusion criteria for controls were newly diagnosed adults >40 years with visually significant cataract, no clinically evident pseudoexfoliation like material over lens or pupillary ruff, baseline IOP <21mmHg, normal disc and visual field.

Exclusion criteria involved patients with corneal or retinal pathology precluding reliable visual field and disc examination and fixation losses of >20%, false positives of >33%, false negatives of >33% in Humphrey's visual field- test. All experiments were performed with age and gender- matched participants.

### **2.2.2 DNA extraction**

QIAamp DNA Micro kit (Qiagen) was used to extract genomic DNA from the blood and lens capsule (LC) tissues. 300 $\mu$ l of whole blood or a single LC tissue was taken into a 1.5ml microcentrifuge tube. Samples were lysed by adding 180 $\mu$ l of lysis buffer (ATL) followed by the addition of 20 $\mu$ l of proteinase K and were mixed thoroughly by vortexing. For efficient lysis, blood samples were incubated at 56°C for 1hour, and tissue samples for 4 hours. Later 100 $\mu$ l buffer AL was added along with 10 $\mu$ l carrier RNA and the sample was mixed homogenously for 15 seconds, this step provides efficient lysis and optimum binding of DNA to the column

membrane. Subsequently, 50µl of ethanol (96–100%) was added and mixed thoroughly by pulse-vortexing for 15 seconds. The samples were incubated for 3 minutes at room temperature. The 1.5ml tube was centrifuged briefly to remove drops from inside the lid. The entire lysate was then transferred to the QIAamp MinElute column (in a 2ml collection tube). The column was centrifuged at 6000 x g (8000 rpm) for 1 minute. Subsequently 500µl Buffer AW1 followed by 500µl Buffer AW2 were added and centrifuged at 6000 x g (8000 rpm) for 1 min. Later the tube was centrifuged at maximum speed (20,000 x g; 14,000 rpm) for 3 minutes to dry the membrane completely. The QIAamp MinElute column was placed in a clean 1.5 ml microcentrifuge tube and 20–100µl Buffer AE was added to the center of the membrane. After 5 minutes of incubation, DNA was collected by spinning at 14000rpm.

### **2.2.3 Bisulfite treatment and bisulfite-specific PCR**

Genomic DNA (500ng) was converted using the EpiTect Bisulfite Kit (Qiagen, Inc., Frederick, MD). DNA conversion reactions were performed in a total reaction volume of 140µl, containing sodium bisulfite (85µl) that results in the deamination of unmethylated cytosine into uracil, and 15µl DNA protect buffer. The PCR tubes containing the bisulfite reactions were then placed into a thermal cycler and incubated in a repeating cycle of denaturation at 95°C, followed by incubation at 60°C for 5 hours. For the positive control, EpiTect Control DNA (Qiagen, Inc.) was used in all experiments. After the bisulfite conversion reaction was completed, the bisulfite reactions were then transferred to a clean 1.5ml microcentrifuge tubes to clean up the bisulfite converted DNA. Then 620 µl freshly prepared buffer BL with carrier RNA was added to the previously converted reaction and mixed thoroughly by vortexing and the whole mixture was then transferred into an EpiTect spin column. The spin columns were centrifuged at 15000 rpm for 1 minute. After the flow-through is discarded, 500µl Buffer BW was added to each spin

column, and centrifuged at maximum speed for 1 minute. Then 500µl Buffer BD was further added to each spin column, and incubated for 15 minutes at room temperature. Followed by centrifugation, buffer BW (500µl) was added again to each spin column and centrifuged at maximum speed for 1 minute. The spin columns were then placed into clean 1.5 ml microcentrifuge tubes and 20µl Buffer EB was dispensed onto the center of each membrane. The purified bisulfite converted DNA is eluted after centrifugation for 1 minute at 15,000 rpm.

The bisulfite-specific PCR (BSP) primers were designed using web-based MethPrimer software (<http://www.urogene-.org/methprimer/>) and the online BiSearch software (<http://bisearch.enzim.hu/>) around the CpG island (CGI) in HSP70 (**Table 2.1**) and later used for PCR amplification of bisulfite-converted DNA. The Bisulfite-specific PCR (BSP) was carried out using EpiTaq HS (Takara Bio, Shiga, Japan). Bisulfite converted DNA was mixed with PCR reagents (10mM dNTPs, 25mM MgCl<sub>2</sub>, 10X buffer, 10µM forward and reverse primer, and 1 unit of EpiTaq polymerase). Thermocycling conditions for PCR reactions include initial denaturation at 94°C for 5 minutes preceeded by 40 cycles of 30 seconds denaturation step at 95°C, 45 seconds annealing temperatures and extended for 45 seconds at 72°C and finally incubated at 72°C for 10 minutes for final extension. The amplicons were stored at -20°C until further use.

**Table 2.1. List of oligos used in the study**

No.	Gene ID	Purpose	Sequence (5'→3')	Melting T <sub>M</sub> °C
1.	<i>HSP70</i> (HSPA1A) (NM_005345.6)	qRT-PCR	F: CCACCATTGAGGAGGTAGATTAG R: CAGGAAATTGAGAACTGACAAACA	60
2.	HSP90 (HSP90AA1) (NM_001017963.3)	qRT-PCR	F: GTCGTGAAGGATCTGGTCATC R: CATCAGCAGTAGGGTCATCTTC	60

3.	PARP1 (NM_001618.4)	qRT-PCR	F: GCCGAGATCATCAGGAAGTATG R: ATTCGCCTTCACGCTCTATC	60
4.	DNMT3A (NM_022552.4)	qRT-PCR	F: TCAGTGGTGTGTGTTGAGAAG R: GTAGATGGCTTTGCGGTACA	60
5.	DNMT3B NM_006892.4	qRT-PCR	F: CCATTTCGAGTCCTGTCATTGT R: GCGACGTACTTTCCTACCTTTAT	60
6.	GAPDH NM_002046.5	qRT-PCR	F: GGTGTGAACCATGAGAAGTATGA R: GAGTCCTTCCACGATACCAAAG	60
7.	ACTB NM_001101.3	qRT-PCR	F: GCACAGAGCCTCGCCTT R: GTTGTGCGACGACGAGCG	60
8.	CpG Region 1	Bisulfite-specific PCR and sequencing	F: AAATTGGTTTATGAGGTTAGAGA R: CTTAAACCAATCAAAAACCAAATAC	52.5
9.	CpG Region 2	Bisulfite-specific PCR and sequencing	F: ATTTATAAAAGTTTAGGGGTAAG R: CAAAATAAATAATACCCAAAT	51
10.	CpG Region 3	Bisulfite-specific PCR and sequencing	F: GGGGATATTAAGGTATTTTATTTTG R: CCAACCTATTATCAAATCCTCCCA	54
11.	CpG Region 1	Luciferase assay	F: CTCCGGTACCGCCCATGAGGTCAGAGACAGTA R: CACCGCTAGCTGGGAAGGGTGTGGTCTCC	66.3
12.	CpG Region 2	Luciferase assay	F: CTCCGGTACCATAAAAAGCCCAAGGGCAAGCGGTC R: CACCCTCGAGATGATCTCCACCTTGCCGTG	61.5
13.	CpG Region 3	Luciferase assay	F: CTCCGGTACCGGGGGAGACCAAGGCATTCTACCCCG R: CACCCTCGAGCAGCCTGTTGTCAAAGTCCTCCCA	63.7

#### 2.2.4 Bisulfite and Sanger's sequencing

The amplified PCR products were subsequently electrophoresed on 1% agarose gel at 100V and 200mA and further eluted by gel elution kit (QIAquick Gel Extraction Kit, QIAGEN, Hilden) and sequenced unidirectionally using one of the previously mentioned primers (**Table 2.1**) with the help of BigDye Terminator v.3.1 cycle sequencing kit (Applied Biosystems, Austin, TX78744, USA). Briefly, eluted PCR products were quantified before setting up each sequencing PCR. For each PCR, 0.25µl of 2.5X ready reaction mix, 2µl of dilution buffer (5X), 50ng of eluted DNA template, 2µl of primer (2pmol/ µl) and nuclease free water (NFW) (MP Biomedicals, USA) were added for a 10µl total reaction volume. The thermal cycling sequencing PCR reaction was carried out for 25 cycles with each cycle having a denaturation step at 96°C

for 10 seconds, annealing at 50°C for 5 seconds, extension at 60°C for 4 minutes and kept at -20°C until further use.

After sequencing PCR, each reaction product was cleaned by using Master Mix-I (10µl nuclease free water (NFW) and 2 µl of 125mM EDTA per reaction) and Master Mix-II (2µl of 3M NaOAc pH 4.6 and 50µl of ethanol per reaction). 12µl of Master Mix-I was added to each sequencing reaction containing 10µl of PCR product and thoroughly mixed. Then 52µl of Master Mix-II was added to each reaction, mixed and incubated for 20 minutes at room temperature (RT). After incubation, the sample was centrifuged at 12000x g for 20 minutes at RT. The pellet was then washed by adding 250µl of 70% ethanol and centrifuged at 12000x g for 10 minutes at RT. After removing the supernatant, the pellet was air dried at room temperature for 1 hour and resuspended in 15µl of Hi-Di formamide. Final product was then transferred to a 96 well sequencing plate (ABI 1400, Applied Biosystems, USA), covered with septa, denatured at 95°C for 5 minutes and snap chilled on ice for 10 minutes and finally sequenced on 3130xl Genetic Analyzer. The sequencing read-out was obtained in .abi format and was analyzed using sequencing analysis software BioEdit v7.1 (Tom Hall, Ibis Biosciences, USA) software. The automated sequencer 3130xl genetic analyzer from Applied Biosystems was used for sequencing.

In the technique of bisulfite sequencing, the fragment of interest was amplified and purified from the bisulfite converted DNA followed by Sanger sequencing to obtain the methylation status of individual CpG sites within the CGI of interest. After sequencing these converted residues were read as thymine. However, methylated cytosine residues were resistant to bisulfite conversion and were read as cytosine. Subsequently, comparing the sequencing read from an untreated DNA sample to the same sample following bisulfite treatment enabled the

detection of the methylated cytosines. The BiQ Analyzer software was used for performing stringent quality control and visualizing the results.<sup>217</sup>

### **2.2.5 RNA extraction**

Total RNA was extracted from non-processed anterior eye tissues (lens capsule and conjunctiva) or human lens epithelium B-3 (HLE B-3) cells. Briefly, each tissue was removed from RNALater, and placed in a new 1.5ml centrifuge tube and were processed for extraction using RNA extraction kit (RNeasy Mini Kit, QIAGEN). 350µl RLT buffer was added in tube to lyse the tissue. After incubation with RLT buffer for 15 minutes at RT, tube was placed on ice and the sample was disrupted with the help of pipette and vortex. After total rupture of tissue, an equal volume of 70% ethanol was added to the tube. This solution (700µl) was then transferred onto the RNeasy mini column and centrifuged at 9000 x g (4°C) for 20 seconds. The 750µl RW1 buffer was added in column followed by 500µl RPE buffer and centrifuged at 9000 x g (4°C) for 20 seconds to remove contaminants from the column. Then the column was centrifuged for a dry spin at 13000 rpm for one minute at 4°C. The column was air dried for 5 minutes at RT. 15µl RNase-free water was added to elute RNA from the column and quantified. RNA quantification was done spectrophotometrically and its quality was checked by A260/A280 and A260/A230 ratios in Nanodrop 2000 (ThermoFisher Scientific, USA).

### **2.2.6 cDNA synthesis**

1µg of total RNA was converted into cDNA using a Verso cDNA synthesis Reverse Transcription Kit (AB1453A; Thermo Scientific). In a standard reaction of 20µl, 4µl of 5x cDNA synthesis buffer, 2µl dNTP mix, 1µl of Random hexamers, 1µl of RT enhancer as genome wipeout buffer and 1µl of Verso reverse transcriptase enzyme were used as provided in the kit to convert whole RNA into cDNA library. The cDNA synthesis was done at 42°C for 30 minutes in

a C100 Touch Thermal Cycler (BioRad, USA) followed by enzyme inactivation at 95°C for 2 minutes.

### **2.2.7 Quantitative real time-PCR**

Quantitative real-time RT-PCR (qRT-PCR) reaction was carried out with an RT-PCR (Applied Biosystems 7500 version 2.0). Specific primers were designed using PrimerQuest Tool (IDT) spanning the exon-exon junction (**Table 2.1**). Total 5ng of cDNA was mixed with Dynamo color flash SYBR green qPCR mix (F416XL, Thermo Scientific) in a 20µl reaction mixture in triplicate for each sample. 0.4µM each of forward and reverse primers was used for each test and endogenous control genes. Melt curve analysis helps to check the specificity of the amplified PCR product. The relative expression change in fold was calculated by Comparative Ct method ( $\Delta\Delta$ Ct method) and change in expression was represented as fold difference. The housekeeping genes, Glyceraldehyde 3-phosphate dehydrogenase (GAPDH) and beta-actin (ACTB) were used as an internal standard to normalize mRNA expression of the target genes.

### **2.2.8 Protein extraction**

Cytosolic and nuclear extract from the lens capsule and whole cell lysate from the HLE B-3 (HLE B-3) cells were isolated using NE-PER kit (Thermo Fisher Scientific). Tissue and cell pellets were placed in fresh tube and washed with 1X PBS (phosphate buffer saline), followed by centrifugation at 500 x g for 5 minutes. The supernatant was carefully discarded leaving the pellet dry and ice cold cytoplasmic extraction reagent I (CER I) was added as per the cell volume and tissue amounts. Subsequently, the tube was vortexed at high speed to fully suspend the samples and incubated on ice for 10 minutes. In an appropriate volume of CER I (depending on the cells and tissue volume, 100µl mainly for tissues), cell/tissue was homogenized and disrupted completely. While cells ruptured easily, the tissue needs to be disrupted either by vortexing or

pipetting 15 to 20 times at interval of 5 minutes. Ice cold cytoplasmic extraction reagent II (CER II) was later added to the tube after disruption and vortexed at highest setting for 5 second. The tube was incubated on ice for 1 minute followed by vortex again for 5 seconds. The tube was centrifuged at 16000 x g for 5 minutes. The supernatant (cytoplasmic extract) obtained was immediately transferred to a clean pre- chilled tube and stored at -80°C until further use.

The pellet obtained in the above step was further proceeded with for collection of nuclear extracts. The pellet was suspended in ice cold NER (nuclear extraction reagent) and vortexing for 15 seconds at maximum settings. It was placed on ice and vortex was continued for 15 seconds every 10 minutes, approximately for a total of 45 minutes. Later the tube was centrifuged at 16000 x g for 10 minutes to obtain the nuclear extract.

### **2.2.9 Protein estimation**

Proteins extracted from anterior eye tissues and HLE B-3 cells were quantitated using Bradford assay. Total protein was measured spectrophotometrically using Bradford's reagent and bovine serum albumin (BSA) as a standard. For the assay, four BSA protein standard points were used (2µg/µl, 4µg/µl, 8µg/µl, 16µg/µl) to prepare the standard curve.

### **2.2.10 Western blotting**

The protein extract was denatured by adding 5X Laemelli buffer at 95°C for 5 minutes. The denatured extract (10µg) was then resolved on an 8-12% SDS polyacrylamide gel and subsequently transferred onto a PVDF membrane (IPVH00010, Millipore-Merck). The transfer was done in semidry transfer cell (BioRad) at 15 V for 45 minutes in 1X transfer buffer (48 mM Tris-Base, 39 mM Glycine, 0.01% SDS and 20% Methanol). Monoclonal antibodies for HSP70, HSP90, DNMT3B (SC-32239, SC-13119, and SC-376043; Santa Cruz Biotechnology respectively, 1:250) and DNMT3A (PA577945; Thermo Scientific, 1:250) were used as a

primary antibody. HRP-conjugated goat anti-mouse IgG (621140680011730, Bangalore GeNei, India, 1:5000) and HRP-conjugated goat anti-rabbit IgG (621140380011730, Bangalore GeNei, India, 1:5000) were used as secondary antibody. Equal loading was verified with GAPDH antibody, (ABM22C5, Abgenex, India; 1:1000) and Lamin B1 (SC-374015, Santa Cruz Biotechnology, 1: 500). Chemiluminescence detection was performed using the Super Signal Femto Maximum Sensitivity Substrate, kit (PI34094, and Thermo Fisher Scientific) in a Fusion Solo S Chemi-Doc (Vilber Lourmat). Evolution Capt software (Vilber Lourmat fusion solo S) was used for image acquisition and densitometry analysis of the gels and blots in this study. The protein expression levels were expressed relative to endogenous control levels.

#### **2.2.11 *In vitro* DNA methylation**

The regions of interest including all three CpG islands (CGIs) were PCR amplified, and then digested using the appropriate restriction endonucleases followed by gel extraction and methylation with CpG methyltransferase (M.SssI) and S-adenosyl-methionine (SAM) (MO226M, New England Biolabs, Beverly, MA). 500ng DNA was incubated with 1 $\mu$ l M.SssI, 2 $\mu$ l SAM and 2 $\mu$ l 10x NEB buffer 2 at 37°C for 4 hours. The reaction was stopped by heating at 65°C for 20 minutes. Controls included mock methylated constructs similarly generated but omitting Ado-Met (S-adenosyl methionine). After the reaction, the DNA was purified using an extraction kit (Qiagen) and the methylation status was confirmed upon incubation with the methylation-sensitive restriction enzyme HpaII (R0171S, NEB, Beverly, MA). The methylated and mock-methylated DNA fragments were then individually ligated into the luciferase vector having the expression constructs, and successful constructs was validated by Sanger sequencing (Applied biosystem). *In vitro* methylation and ligation of insert fragments into unmethylated reporter vectors before transfection was done to avoid the methylation of backbone CpGs.

### 2.2.12 Luciferase assay

To test the functionality of DNA methylation on gene expression, a dual luciferase gene expression assay (Dual-Luciferase Reporter Assay System; Promega, Madison, WI, USA) was performed. Luciferase reporter vector pGL3 (for CpG region spanning promoter) and pGL4.23 (Promega) with a minimal promoter (for CpG region spanning the exon) were used. Region I (466 bp) comprising of a promoter region was cloned into basic pGL3 vector, and subsequently region II (329 bp) and region III (388 bp) spanning regions downstream from the TSS were cloned in pGL4.23. The insert fragment size used in the luciferase assay for cloning for regions I to III was made sure to be consistent as that of MethPrimer database; though, few additional bases were included in region I and II as it spans the transcription factor binding sites (TFBS) and DNase I hypersensitivity region we thought it would be helpful to check their regulation after methylation in respective regions. As for region I, extra bases were incorporated to cover the maximum binding sites of heat shock factor 1 (HSF1) on heat shock element (HSE). We hypothesized that methylation of CpG island in region I of HSP70 might prevent binding of HSF1 to HSE which might lead to decrease in HSP70 expression. Region I included five HSE sites, for region II, extra bases fall in DNase 1 hypersensitive sites and region III was same as mentioned in MethPrimer database.

Amplified insert fragments and vector were double digested by KpnI-HF and XhoI-HF (NEB) and subsequently cloned into the multi-cloning site (MCS) present upstream to the minimal promoter. HLE B-3 cells were seeded in a 24-well plate for transfection. At 80% confluency, cells were proceed for transient transfection with the prepared constructs along with internal control Renilla vector (pGL4.74) for normalizing transfection efficiency. A total 500 ng of each test vector with 500 ng of control vector was added together to corresponding well. After

48 hours of post transfection, cell lysates were prepared following Dual-Luciferase® Reporter Assay System (Promega). Reporter activities were measured in Varioskan® Flash Multimode reader (Thermo Scientific) as suggested by the manufacturer. Luciferase activity was presented after normalization with Renilla reporter activity. Independent experiments were performed in replicates and repeated at least three times.

### **2.2.13 *In silico* analysis**

*In silico* analyses were performed using the online database JASPAR (<http://jaspar.genereg.net/>; (Mathelier A, et al., 2016) to unravel the probable binding sites for transcription factors in the CpG sites located in region III of HSP70 gene.

### **2.2.14 Cell Culture and Demethylation Treatment**

Human lens epithelium B-3 (HLE B-3) cells were obtained from ATCC (B-3 CRL-11421, Virginia, USA), cultured in DMEM/F12 medium (11330057, Invitrogen GIBCO) supplemented with 10% inactivated FBS (16000044, Invitrogen), 1% penicillin (100U/ml) and streptomycin (0.1mg/ml) (A001, HiMedia) at 37°C and 5% CO<sub>2</sub>. At 60–70% confluency, the cells were demethylated by adding freshly prepared 1µM of 5-aza-2'-deoxycytidine (5-aza-dC) (A3656, Sigma-Aldrich) in dimethylsulfoxide (DMSO) to the culture medium changing it every 24 hours for 72 hours. Control wells were treated with equivalent volumes of vehicle (culture medium including DMSO) for nullifying nonspecific solvent effects on cells. After the end of treatment duration, the culture medium was withdrawn, and the DNA, RNA and whole cell protein extracts were isolated for bisulfite sequencing, qRT-PCR and western blotting respectively.

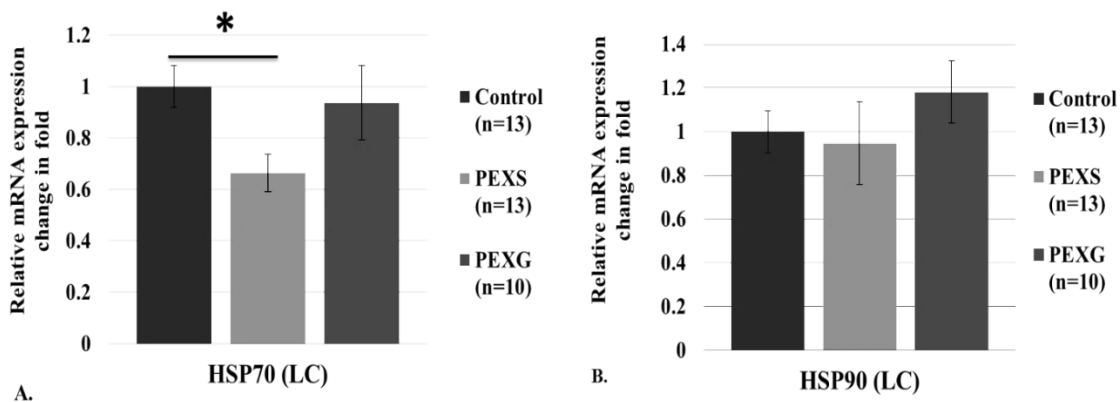
### **2.2.15 Statistical analysis**

Statistical analyses were conducted using SPSS software package (version 23.0; SPSS, Chicago, IL). All plots were presented as mean  $\pm$  SEM (standard error of mean). Data were analyzed using Student's t-test, and one-way analysis of variance (one-way ANOVA) was used for comparing more than two groups. All experiments were performed independently at least three times and with biological triplicates each time. A value of  $P < 0.05$  was considered statistically significant.

## 2.3. Results

### 2.3.1 Decreased mRNA and protein expression of HSP70 in pseudoexfoliation syndrome but not in pseudoexfoliation glaucoma

We investigated the expression of heat shock proteins, HSP70 and HSP90, which in turn are regulated by HSF1 with the hypothesis that they would be upregulated like all other reported HSPs such as HSP40 and HSP60.<sup>200,218</sup> Surprisingly, the qRT-PCR analysis showed significant downregulation of HSP70 in lens capsule of PEXS (0.66 fold;  $p=0.02$ ) while in PEXG we didn't find any significant difference (0.93 fold;  $p=0.89$ ) when compared with control (**Figure 2.3A**). On the contrary, we did not observe any significant difference in *HSP90* mRNA expression in either PEXS (0.94 fold;  $p=0.92$ ) or PEXG (1.18 fold;  $p=0.66$ ) when compared with control tissues (**Figure 2.3B**).



Study Subjects (Lens capsule)	N (Females in %)	Age (in years) Mean± SD	P-value	Gender Mean± SEM	P-value
PEXS	13 (38.4%)	71.6 ± 8.27	0.68	0.8 ± 0.13	0.12
Control	13 (61%)	69.76 ± 8.81		0.4 ± 0.16	
PEXG	10 (20%)	74.1±9.2	0.2	0.9 ± 0.10	0.18
Control	10 (50%)	67.8±7.7		0.5 ± 0.16	

C.

**Figure 2.3 mRNA expressions of HSP70 and HSP90 in lens capsule tissues.** **A.** *HSP70* mRNA expression was downregulated significantly in lens capsule of PEXS (n=13; p=0.02), while no significant difference was observed in PEXG (n=10; p=0.58) with respect to that from lens capsule of control (n=13). Data was normalized to *GAPDH*. **B.** The bar graph represents the fold change of *HSP90* mRNA in the lens capsules of control (n=13), PEXS (p=0.92; n=13) and PEXG (p=0.66; n=10) with no significant differences in either cases. **C.** Demographics of the study subjects included for qRT-PCR assay in lens capsule tissue. Bar plots represented as mean ±SEM. All data shown are representative of three or more independent experiments. \* p<0.05.

To further analyze the HSP70 protein expression, western blot analysis was performed using protein extracts from the lens capsule (**Figure 2.4A**). Comparison of the protein content by densitometry of the immunoreactivity bands revealed that the levels of HSP70 were significantly decreased in lens capsule from eyes with PEXS (0.50 fold; p=0.04) while no significant difference was observed for PEXG subjects (0.73 fold; p=0.29), with respect to control lens capsule tissues (**Figure 2.4B**). Likewise, at the protein level, immunoblotting data and densitometry analysis of HSP90 mirrored its mRNA expression data depicting no significant difference in PEXS (0.81 fold; p=0.79) and PEXG (1.05 fold; p=0.76) with respect to control (**Figure 2.4C-D**).

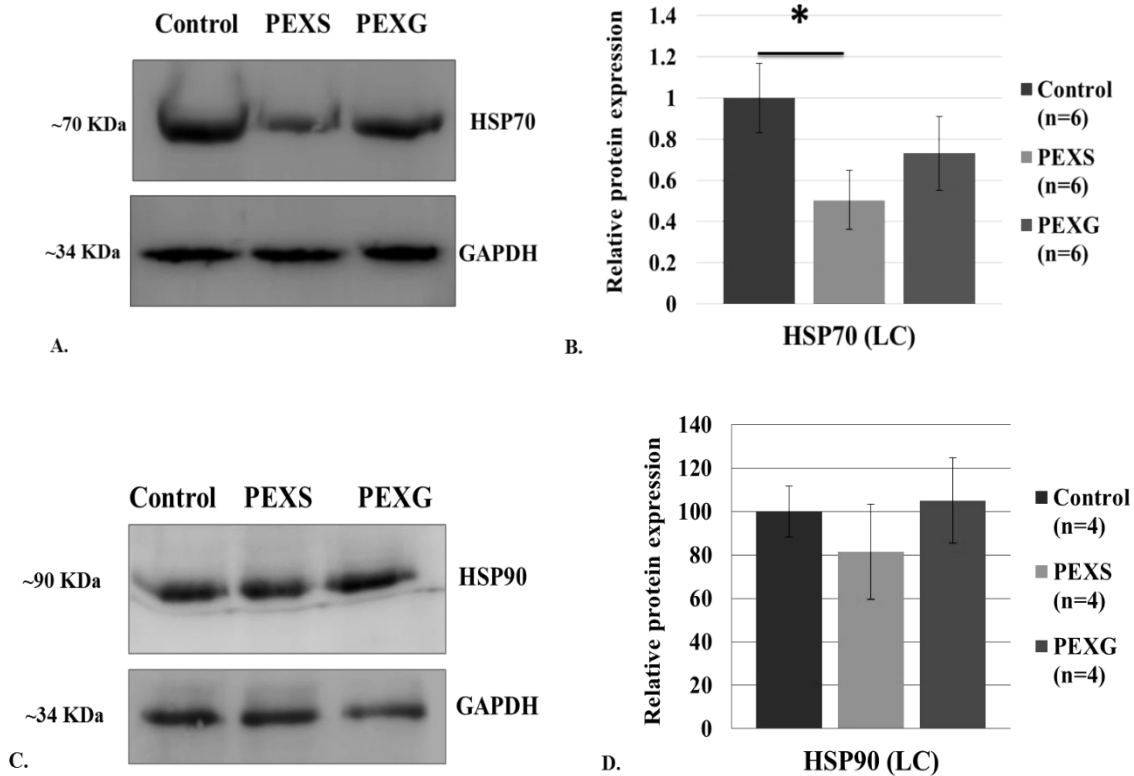


**Figure 2.4. Western blot analysis of HSP70 and HSP90 in lens capsule tissues.** **A.** Representative Immunoblot of HSP70 showed downregulation of HSP70 in PEXS ( $p=0.04$ ;  $n=6$ ) but not in PEXG ( $p=0.29$ ;  $n=6$ ) cases with respect to control tissue samples ( $n=6$ ). **B.** Quantification of the immunoblot of HSP70 expression was normalized for GAPDH and is presented as a percentage relative to control. **C and D.** Representative immunoblot and densitometry analysis showing presence and fold change of HSP90 in the lens capsule of control ( $n=4$ ), PEXS ( $p=0.79$ ;  $n=4$ ) and PEXG ( $p=0.76$ ;  $n=4$ ) subjects, depicting no significant difference. Study subjects were age and gender matched. Bar plots represented as mean  $\pm$ SEM. All data shown are representative of three or more independent experiments. \*  $p<0.05$ .

### 2.3.2 *In silico* methylation analysis of the human HSPA1A gene

ENCODE data on UCSC genome browser showed the presence of 185 CpG sites spanning the promoter region, TSS and gene body of HSP70 (**Figure 2.5**). CpG islands (CGIs) within HSP70 were identified using online software (<http://www.urogene.org/methprimer/>). Based on the threshold-based definitions of CGI (16), regions with higher level of CpG content ( $>50\%$ ),

length (>200bp) and the ratio of observed and expected presence of CpG dinucleotide (>0.6) consisting of 82 CpGs were analyzed for methylation studies.

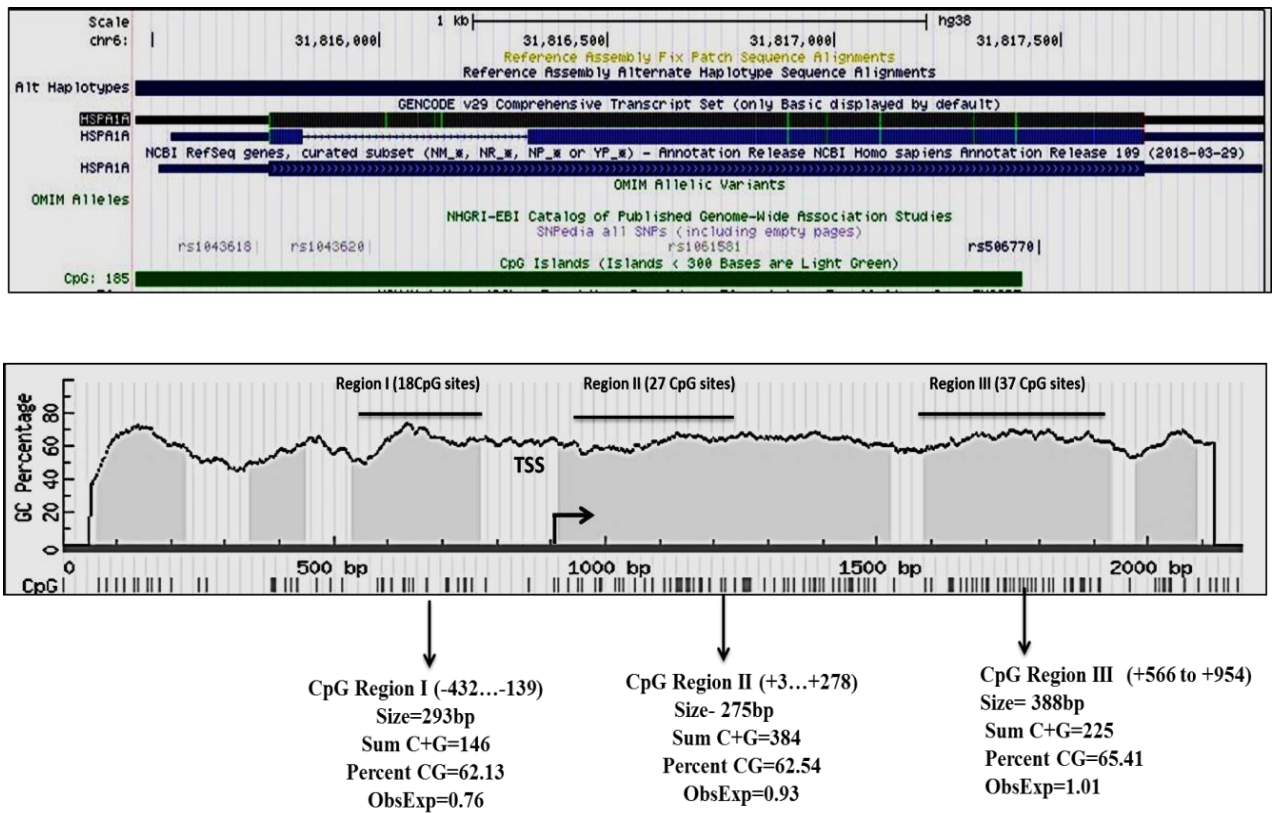


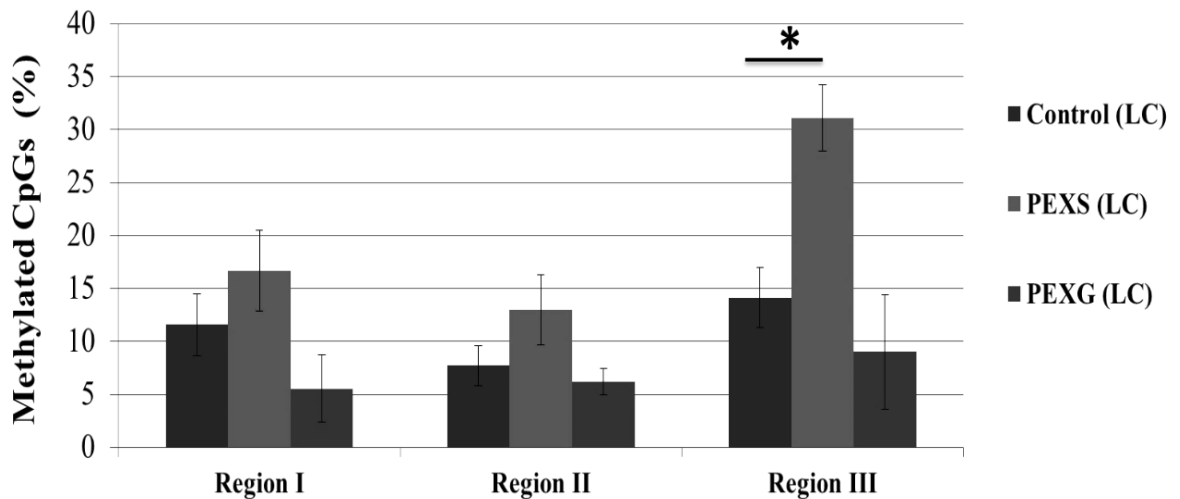
**Figure 2.5 DNA methylation profiles of the HSP70 gene.** HSP70 DNA sequence was obtained from the UCSC genome database. Online database (<http://dbtss.hgc.jp/>) was used to predict Transcription start site (TSS) of the gene. CpG island (CGIs) of HSP70 were predicted by using online software MethPrimer (<http://www.urogene.org/methprimer/>). The parameters used to examine CGI<sup>16</sup> in HSP70 were identified with CG content, CpG frequency, and length (as obtained from EMBO CGI report). Regions analyzed are represented as CpG region I, region II and region III.

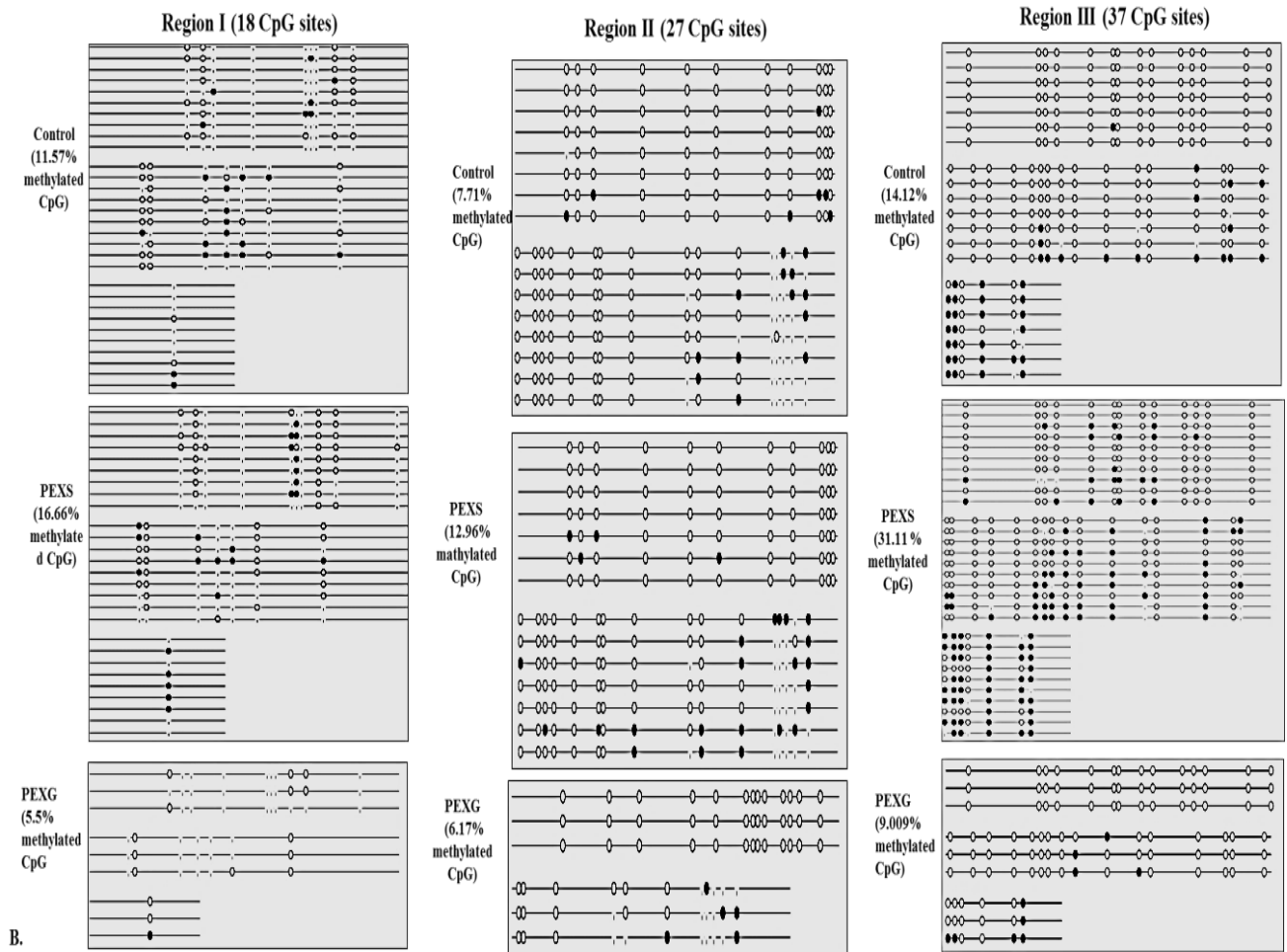
### 2.3.3 Hypermethylated CpG sites are identified in the exon of the *HSP70* gene but not in its promoter region

We hypothesized that DNA hypermethylation might be responsible for reduction in HSP70 expression, and to test the same, we assessed the DNA methylation status of *HSP70* by bisulfite sequencing. To check for any tissue-specific effect in the context of the disease, we investigated

the DNA methylation status of CGIs in the promoter (region I), near the TSS (region II) and in the exon (region III) of *HSP70* in DNA extracted from lens capsule of control, PEXS and PEXG subjects. By analyzing the bisulfite sequencing results of 12 control, 10 PEXS and 3 PEXG samples for each region, it was found that in PEXS, region III displayed hypermethylation (31.1%) in comparison with the control group (14.12%;  $p=0.02$ ;) while no significant difference was observed in PEXG individuals (9.0%;  $p=0.31$ ) in comparison with the control group (14.12%). Region I (control- 11.5%, PEXS- 16.6%;  $p=0.13$ , PEXG- 5.5%,  $p=0.21$ ) and region II (control-7.7%, PEXS-12.9%  $p=0.10$ , PEXG- 6.17%,  $p=0.45$ ) showed no significant differences (**Figure 2.6A**). A representation of methylation status in each group from DNA extracted from lens capsule is depicted in lollipop style where open circles indicate unmethylated CpG and closed circles represent methylated CpG sites as shown in **Figure 2.6**.

A.



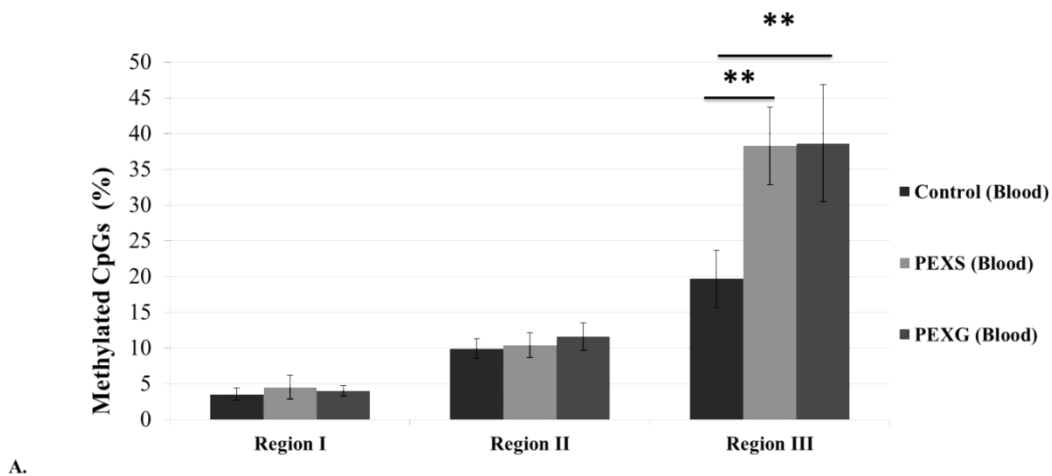


Study Subjects (Tissue DNA)	N (Females in %)	Age (in years) Mean ± SD	P-value	Gender Mean± SEM	P-value
Control	12 (33.3%)	69.83 ± 5.30		0.6 ± 0.16	
PEXS	10 (30%)	73.0 ± 9.86	0.26	0.5 ± 0.16	0.87
PEXG	3 (33.3%)	70.6 ± 9.03	0.38	0.2 ± 0.13	0.27

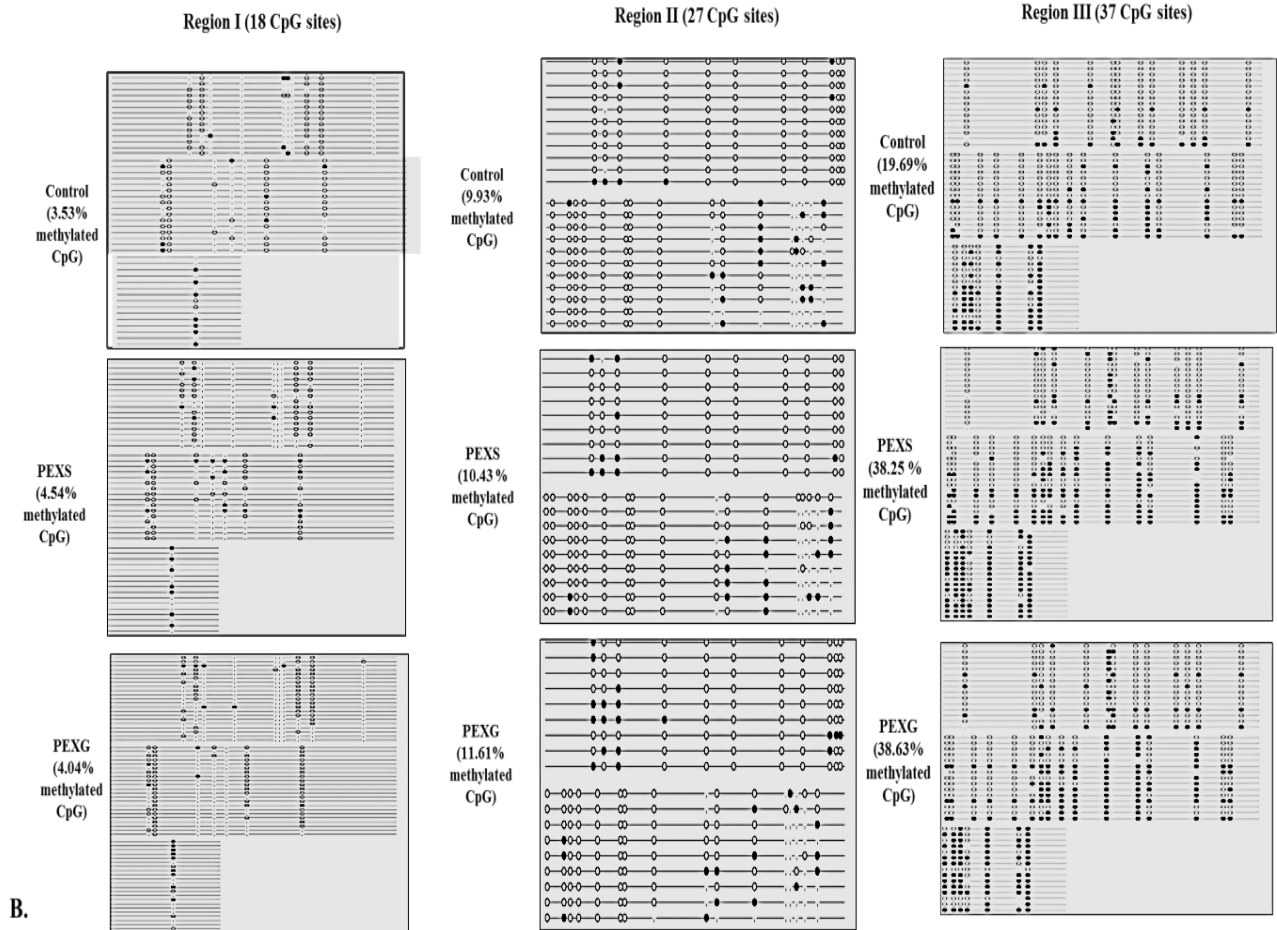
**Figure 2.6 Methylation status of HSP70 CGIs in the lens capsule of control, PEXS and PEXG individuals.** **A.** Increased methylation of the HSP70 region III in the lens capsule of PEXS ( $p=0.02$ ;  $n=10$ ) when compared with controls ( $n=12$ ) while PEXS in region I ( $p=0.13$ ;  $n=10$ ) and region II ( $p=0.10$ ;  $n=10$ ) didn't show any significant differential methylation. No significant differential methylation was observed in region I ( $p=0.21$ ;  $n=03$ ), region II ( $p=0.45$ ;  $n=03$ ) and region III ( $p=0.31$ ;  $n=03$ ) of PEXG subjects when compared with the control group ( $n=12$ ) ( $n$ =sample size; LC=lens capsule). **B.** Bisulfite sequencing illustration of three regions in lollipop style. **C.** Demographics of study subjects included for

bisulfite sequencing of the DNA extracted from the tissue (N= sample size). Bar plots represented as mean  $\pm$ SEM. All data shown are representative of three or more independent experiments. \*p<0.05.

As PEX is a systemic disease, in order to examine whether the blood of PEX patients harbor disease-related epigenetic biomarkers, we performed the bisulfite sequencing analysis of 22 DNA samples in each category extracted from the blood. **Figure 2.7** presents the methylation status for all CpG sites in the tested CGI from region I to III. It was found that the CpG sites located in region I and region II did not show differential methylation in PEXS and PEXG patients compared to control. The percentage of methylation in region I was 4.54% in PEXS (p=0.57), 4.04% in PEXG (p=0.66) and 3.5% in control subjects. Likewise, region II also displayed no significant differences in either case (PEXS-10.43%; p=0.81, PEXG-11.61%; p=0.64) versus control (9.93%) in blood DNA. We further assessed the DNA methylation in the transcribed region III. The CpGs within this exonic region displayed hypermethylation in PEXS (38.2%; p=0.008) and PEXG (38.6%; p=0.006) in comparison with the control group (19.6%). **Figure 2.7** depicts a representation of methylation status in each group from DNA extracted from blood in lollipop style where open circles indicate unmethylated CpGs and closed circles represent methylated CpGs.



A.



B.

Study Subjects (Blood DNA)	N (Females in %)	Age (in years) Mean ± SD	P-value	Gender Mean± SEM	P-value
Control	22 (45.45%)	69.09 ± 7.83		0.45 ± 0.14	
PEXS	22 (45.45%)	71.63 ± 6.71	0.18	0.45 ± 0.14	1
PEXG	22 (36.36%)	72.4 ± 6.27	0.22	0.36 ± 0.12	0.55

C.

**Figure 2.7 Methylation status of HSP70 CGIs in the blood of control, PEXS and PEXG individuals.**  
**A.** Methylation analysis in a region I comprising of 18 CpGs showed no significant differences in PEXS ( $p=0.57$ ;  $n=22$ ) and PEXG ( $p=0.66$ ;  $n=22$ ) patients with respect to controls ( $n=22$ ). Likewise, in region II comprising of 27 CpGs no significant differences were observed in PEXS ( $p=0.81$ ;  $n=22$ ) and PEXG ( $p=0.64$ ;  $n=22$ ) when compared with control samples ( $n=22$ ), while region III comprising of 37 CpG sites showed significantly increased methylation in PEXS ( $p=0.008$ ;  $n=22$ ) and PEXG ( $p=0.005$ ;  $n=22$ ) patients with respect to controls in blood DNA. **B.** Lollipop style representation of the methylation status

of 3 CGIs in HSP70 in DNA from the blood of control, PEXS and PEXG samples. Open and solid circles represent unmethylated and methylated CpG sites, respectively, in all three investigated regions, n=sample size. C. Demographics of study subjects bisulfite sequenced from the DNA obtained from blood (N=sample size). Bar plots represented as mean  $\pm$ SEM. All data shown are representative of three or more independent experiments with similar results. \*\*P<0.01.

In a nutshell, the exonic region of HSP70 comprising of 37 CpG sites was inferred to be hypermethylated in lens capsule of only PEXS subjects versus control corresponding to the mRNA and protein expression data as seen in **Figure 2.3**. We found tissue-specific effect while comparing methylation status in exonic region in blood cells wherein both PEXS and PEXG groups showed hypermethylation when compared to control blood cells. On the contrary, the CpG sites of the HSP70 gene promoter and nearby TSS region were not found to be differentially methylated in either patient group compared to control.

#### **2.3.4 PEXS affected lens capsule has an increased expression of DNMT3A in comparison to control**

DNA hypermethylation is commonly associated with increased levels or altered function of DNMTs. Suspecting de novo methylation at the CGI spanning exonic region, we further checked the mRNA expression of *de novo* DNMTs, *DNMT3A* and *DNMT3B*, that mediate the transfer of a methyl group to the 5'-carbon position of the cytosine ring in a CpG sites residue in lens capsule of control, PEXS and PEXG individuals (**Figure 2.8**). Significantly increased expression of *DNMT3A* was observed in lens capsule of PEXS affected individuals at both mRNA (4.03 fold; p=0.01) and protein level (2.03 fold; p=0.04) while no significant differences were observed in PEXG cases neither at mRNA level (0.83 fold; p=0.49) nor at protein level (1.4 fold; p=0.46) with respect to controls (**Figure 2.8**). Furthermore, *DNMT3B* showed no significant differences in mRNA expression in either PEXS (0.88 fold; p=0.68) or PEXG individuals (0.84

fold;  $p=0.44$ ) when compared with control group. Likewise, no considerable differential protein level of DNMT3B was observed in either PEXS (1.00 fold;  $p=0.98$ ) or PEXG (0.92 fold;  $p=0.87$ ) subjects when compared with control group (**Figure 2.6B-D**).

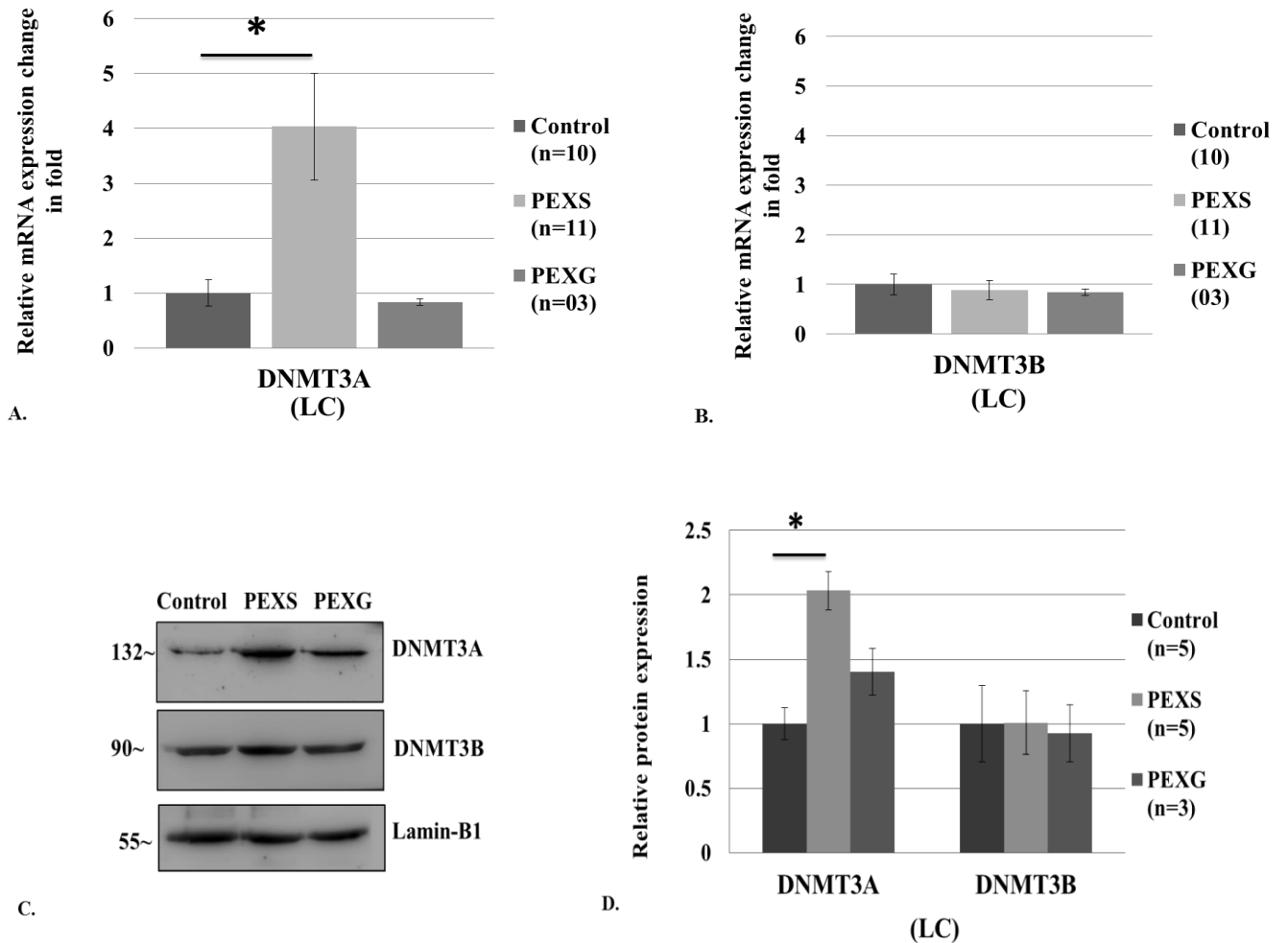


**Figure 2.8 mRNA and protein expression of DNMT3A and DNMT3B in lens capsule tissues.** **A.** Increased expression of *DNMT3A* was observed in the lens capsule of PEXS affected individuals ( $p=0.01$ ;  $n=11$ ) while no significant difference was observed in PEXG ( $p=0.49$ ;  $n=03$ ) when compared with control ( $n=10$ ). **B.** *DNMT3B* failed to show significant differential expression in either PEXS ( $p=0.68$ ;  $n=11$ ) or PEXG affected subjects ( $p=0.44$ ;  $n=03$ ) when compared with control ( $n=10$ ). **C.** Representative image of western blot showing immunoreactivity band of DNMT3A, 3B and Lamin-B1 in nuclear extract of LC samples of control, PEXS and PEXG. **D.** Densitometry graph showing quantification of band intensities normalized to loading control and relative to control subject. The relative protein level of DNMT3A is significantly increased in PEXS ( $p=0.04$ ;

n=05) while no significant difference was observed in PEXG (p=0.46; n=03) with respect to control. On the contrary, DNMT3B showed no significant differences in either affected subjects when compared with the controls (n=05), PEXS (p=0.98; n=05) and PEXG (p=0.87; n=03). Bar plots represented as mean  $\pm$ SEM. All data shown are representative of three or more independent experiments with similar results. \*p<0.05.

### 2.3.5 DNA methylation in an exon region has a major regulatory activity

*In vitro* luciferase assays were performed to validate a potential functional effect of differential methylation at the presently investigated CpG sites on HSP70 gene expression. Methylated and unmethylated insert fragments were ligated into a luciferase reporter vector followed by transient transfection into the HLE B-3 cell line to detect the effect of methylation of the three regions of HSP70 on the luciferase activity, if any. **Figure 2.9** illustrates the targeted regions amplified for luciferase reporter assay.

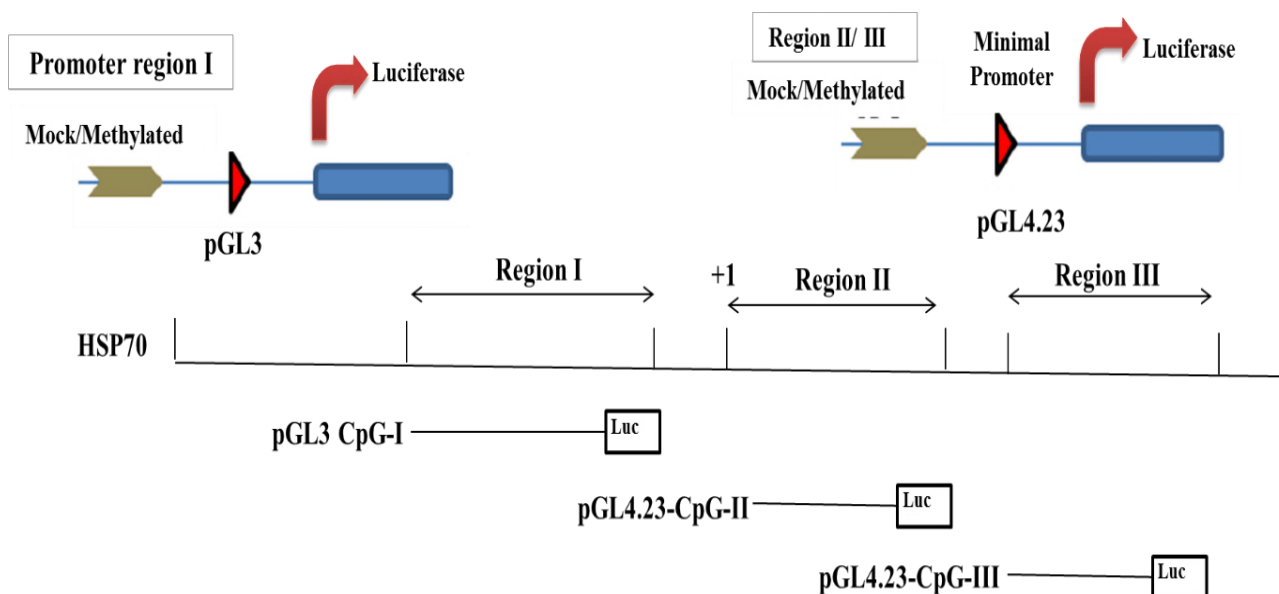


**Figure 2.9 Schematic representation of regions cloned for *in vitro* methylated luciferase-based reporter gene assays. A.** The luciferase activity of CGIs at region I, II and III of HSP70 was analyzed in HLE B-3 cell line. Targeted regions are marked with arrows.

**Figure 2.10** depicts *in vitro* methylated and unmethylated insert fragments of CpG regions cloned in luciferase vectors. Cells were co-transfected with Renilla as a transfection efficiency control, and in each experiment, the empty vector was used as a negative control.

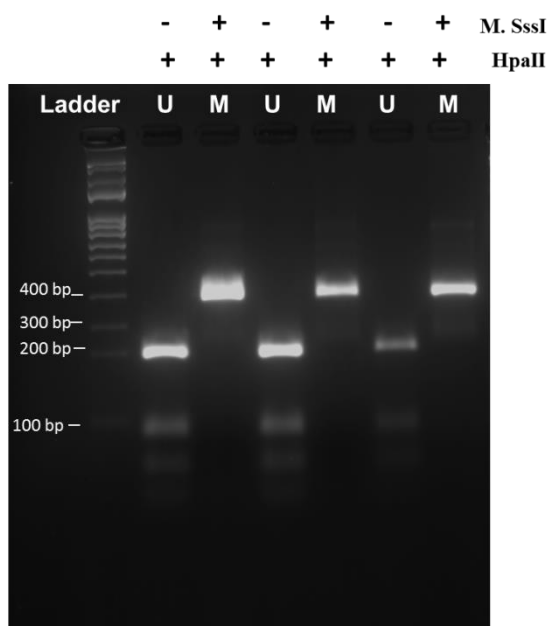


**Figure 2.10 Confirmation of *in vitro* methylation assay by HpaII digestion.** Gel image of HpaII digested *in-vitro* methylated and unmethylated insert of CpG region III. *In vitro* methylated insert showed resistance to HpaII digestion with PCR product of (388bp) while unmethylated control insert susceptible to HpaII digestion break into fragments. U= unmethylated and M= methylated, +/- indicate the presence and absence of the enzyme.

As shown in **Figure 2.11**, HLE B-3 cells transfected with unmethylated and methylated luciferase constructs of region I and II showed no significant differences in the luciferase activity ( $p=0.92$  and  $p=0.33$  respectively); while the relative luciferase activity was decreased by 60% in the methylated construct containing region III compared to the unmethylated control ( $p=0.04$ ). This finding confirms that DNA hypermethylation in the HSP70 exon is much more tightly linked to transcriptional silencing than is methylation in the upstream region.

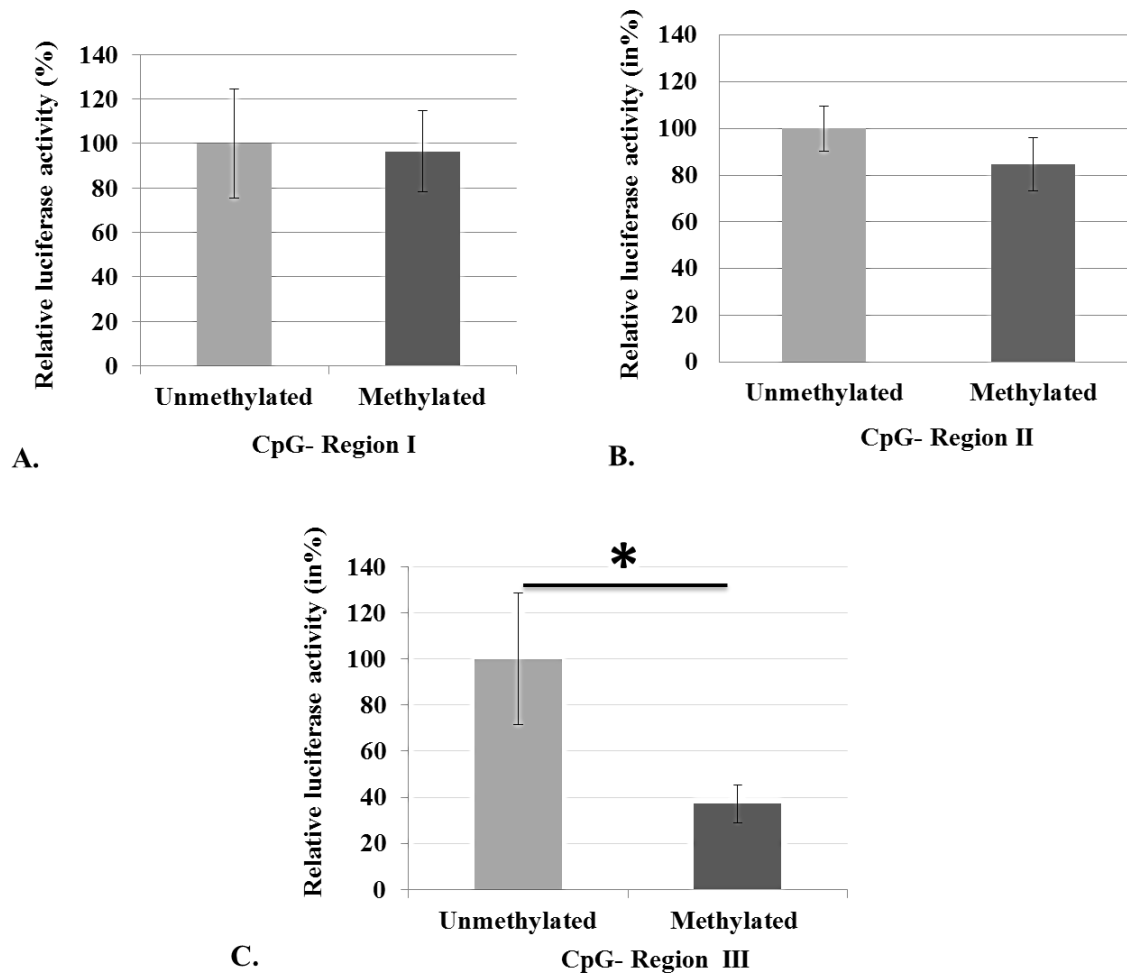
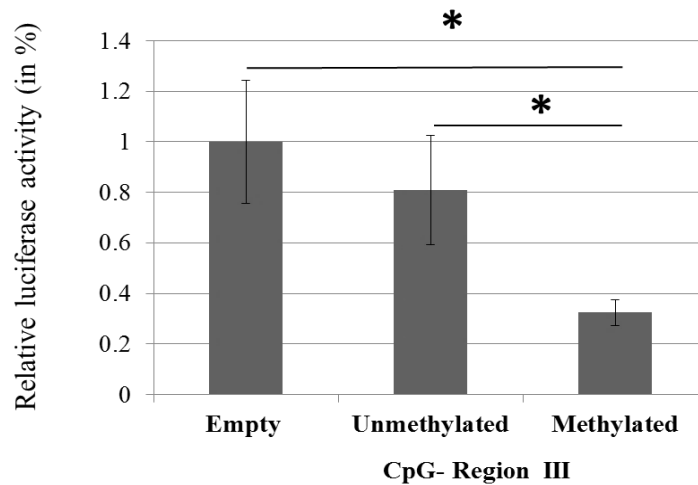


**Figure 2.11 Functional analyses of HSP70 methylation using *in vitro* methylated luciferase-based reporter gene assays.** A-C. Normalized luciferase gene expression was significantly reduced in methylated pGL4.23\_CpG-Region III vector containing CGI-III site spanning +566 to +954 compared to unmethylated vectors ( $p=0.04$ ). On the other hand, CpG region containing CGI-I (spanning from -727 to -261) and CGI-II (near the TSS from +2 to +331) did not show any significant differences ( $p=0.92$  and  $p=0.33$ , respectively) in luciferase activity. Values are the mean  $\pm$  SEM obtained from more than three independent experiments. \* $p<0.05$ .

Further we did comparison of luciferase expression between control empty vector and unmethylated region III to show whether or not this region has enhancer activity. To our surprise, on comparison the unmethylated region did not show a significant difference in reporter activity ( $p\text{-value}=0.35$ ); thus implying that by itself the exon region might not possess an

enhancer activity (**Figure 2.12A**). However, a significant difference was observed between empty vector and methylated construct as well as unmethylated and methylated region III, confirming the functional effect of hypermethylation in exonic region.

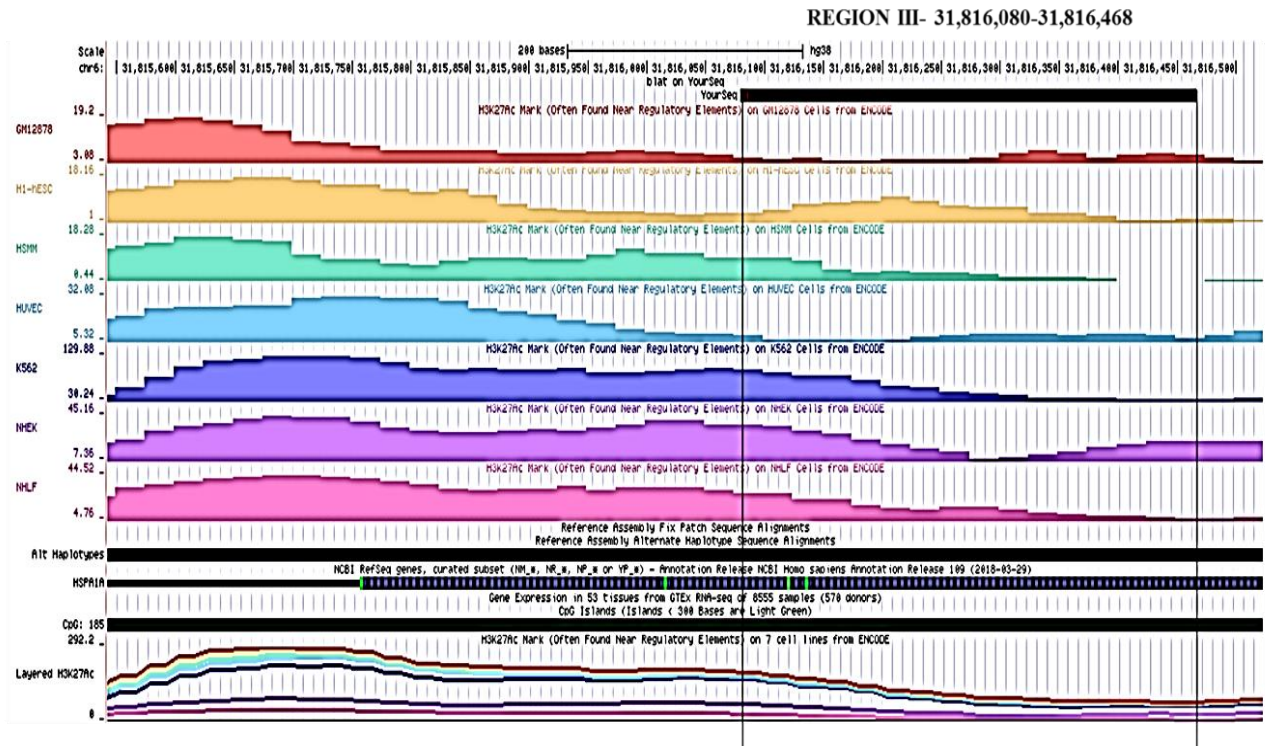


A.

**Figure 2.12A. Functional analyses of HSP70 methylation CpG region III using *in vitro* methylated luciferase-based reporter gene assays.** Normalized luciferase gene expression was significantly reduced in methylated pGL4.23\_CpG-Region III vector compared to unmethylated vectors ( $p=0.04$ ) while no difference were obtained when unmethylated region compared empty vector ( $p=0.35$ ).

On contrary to the above findings, data obtained from *in silico* analysis showed region III to be a potential enhancer. ENCODE data showed a moderate enrichment of H3K27ac in region III in different cell lines, compared to the upstream regions (**Figure 2.12B**). To some extent region III might possess an enhancer activity but we did not observe a significant differential luciferase activity with region III, a plausible reason being that the regulatory constraints which govern the transcriptional repression of the endogenous genes do not operate on the construct when introduced into the cells by transient transfection.

## Regulatory marks on HSPA1A from ENCODE



B.

**Figure 2.12 B.** We assessed the distribution of HEK27ac marks to determine the region of the gene body to be used for regulatory region. The data obtained from the Encyclopedia of DNA Elements (ENCODE; <https://genome.ucsc.edu/ENCODE/>).

*In silico* analysis also identified 22 potential binding sites for transcription factors (TFs) in the sequence spanning region III which might regulate HSP70 expression on DNA methylation (**Table 2.2**).

**Table 2.2 Predicted transcription factor binding sites in the HSP70 amplicon encompassing CpG region III.** Putative sites which showed maximum hypermethylation were predicted with these settings (90%) in sequence named hg19\_dna.

<b>Transcription Factor</b>	<b>Gene name</b>	<b>Start</b>	<b>End</b>	<b>Strand</b>	<b>Predicted site sequence</b>
MAFK	MAF bZIP transcription factor K	15	29	-1	CTTGGTCAGCACCAT
ZEB1	Zinc finger E-box-binding homeobox 1	48	56	1	GCGTACCTG
BRCA1	Breast cancer type 1 susceptibility protein	70	76	1	CCAACGC
NFIC	Nuclear factor 1 C-type	114	119	-1	CTGGCG
En1	engrailed homeobox 1	147	157	-1	ACGTTGAGCCC
HIF1A::ARNT	hypoxia inducible factor 1 subunit alpha	152	159	1	CAACGTGC
Arnt	aryl hydrocarbon receptor nuclear translocator	153	158	1	AACGTG
NFE2L1::MafG	nuclear factor, erythroid 2 like 1	165	170	-1	GATGAT
THAP1	THAP domain containing 1	212	220	-1	TTGCCCGTT
MZF1_5-13	myeloid zinc finger 1_5-13	218	227	1	CAAGGGGGAG
MZF1_1-4	myeloid zinc finger 1_1-4	221	226	1	GGGGGA
HIF1A::ARNT	hypoxia inducible factor 1 subunit alpha	230	237	1	CAACGTGC
Arnt	aryl hydrocarbon receptor nuclear translocator	231	236	1	AACGTG
SP1	Sp1 transcription factor	249	259	-1	CCCCCGCCCAG
KLF5	Kruppel like factor 5	250	259	-1	CCCCGCCCA

Klf4	Kruppel like factor 4	250	259	1	TGGGCGGGGG
HIF1A::ARNT	hypoxia inducible factor 1 subunit alpha	266	273	1	CGACGTGT
NR4A2	nuclear receptor subfamily 4 group A member 2	309	316	1	AAGGCCAC
Zfx	zinc finger protein X-linked	309	322	-1	CCGGCCGTGGCCTT
MZF1_1-4	myeloid zinc finger 1_1-4	320	325	1	CGGGGA
ZEB1	Zinc finger E-box-binding homeobox 1	327	335	1	ACCCACCTG
ZNF354C	zinc finger protein 354C	327	332	1	ACCCAC

Predictions based on results generated from JASPAR database (<http://jaspar.genereg.net/>; <sup>219</sup>). ‘Start’ and ‘End’ point indicate the respective base pair in the investigated CGI.

The relevant factors identified were NFE2L1 (Nuclear factor, erythroid 2 like 1), THAP1 (THAP Domain Containing 1), KLF 5 (Kruppel like factor 5), Zfx (zinc finger protein X-linked) and HIF1A (Hypoxia inducible factor 1 subunit alpha) that spanned the CpG sites which showed maximum differential methylation with respect to control after analyzing methylation at individual CpG sites at region III (**Figure 2.13**). These factors might constitute a mechanism by which locus-specific DNA methylation regulates HSP70 expression.

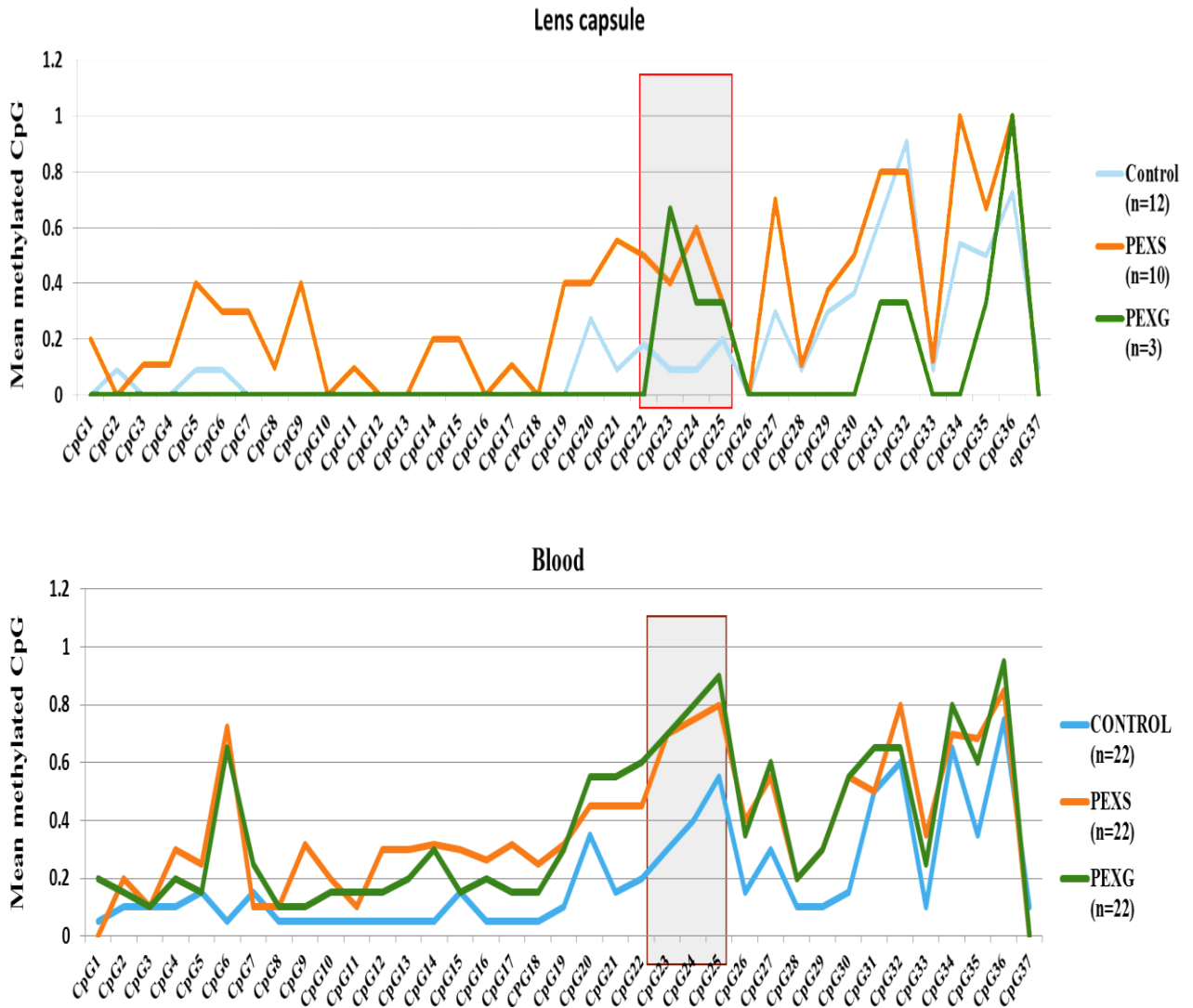
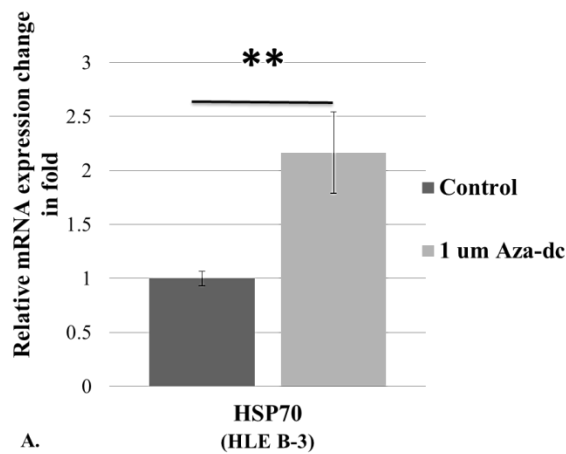


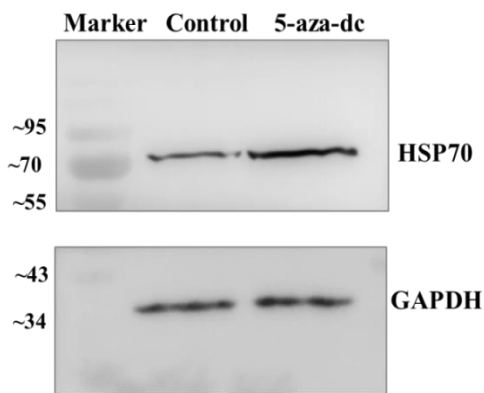
**Figure 2.13 Differential methylation at individual CpG sites in region III.** Scatter plot shows the mean percentage of methylated CpG at individual CpG in DNA obtained from blood and lens capsule of PEXS and PEXG. The CpG sites which showed significant difference between lens capsule of control and PEXS are CpG sites 9, CpG 19, CpG 21, CpG 24 and CpG 34. The CpG sites differentially methylated between tissue control and PEXG are CpG sites 23, 30 and CpG 34. The CpG sites which showed significant difference between blood PEXS, PEXG when compared with control are CpG 6, CpG 14, CpG 21, CpG 23, CpG 24, and CpG 30. Red box denotes the significantly differentially methylated CpGs common in both blood and lens capsule of control, PEXS and PEXG.

### 2.3.6 5-aza-dC induces DNA demethylation at exonic region III and restores the expression of HSP70

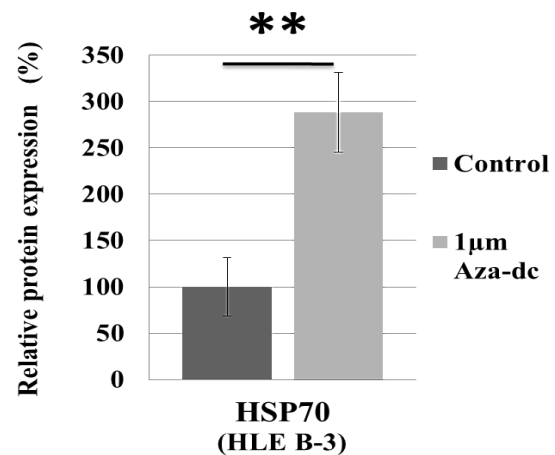
To evaluate the relationship between hypermethylation of the CGIs and downregulation of HSP70, an *in vitro* study using DNA demethylating agent; 5-aza-dC was performed. qRT-PCR was performed to assess the effect of 1 $\mu$ M 5-aza-dC on *HSP70* mRNA expression. 5-aza-dC induced DNA demethylation, significantly increased *HSP70* mRNA expression in HLE B-3 cells ( $p=0.008$ ) (**Figure 2.14A**). Western blot analysis further validated qRT-PCR results showing increased level of HSP70 after treatment (**Figure 2.14B**) and the level was significantly higher than in the untreated control ( $p=0.006$ ) (**Figure 2.14C**).



A.



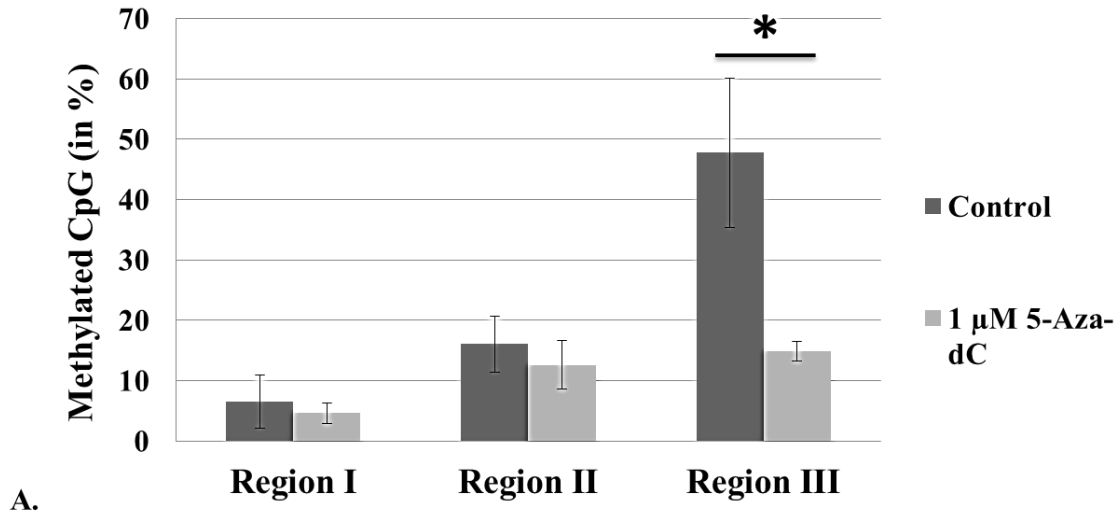
B.



C.

**Figure 2.14 Demethylation using 5-aza-2'-deoxycytidine increases HSP70 expression in HLE B-3 cells.** **A.** qRT-PCR and **B.** western blot analysis show that mRNA expression ( $p=0.008$ ) and protein level ( $p=0.006$ ) of HSP70 were significantly upregulated in HLE B-3 cells after treatment with 5-aza-2'-deoxycytidine at a concentration of  $1\mu\text{M}$  for 72 hours. **C.** Relative HSP70 protein level to GAPDH is presented as mean  $\pm$  SEM. All data shown are representative of more than three independent experiments with similar results.  $*p<0.05$ ;  $**p<0.01$ .

To examine if this expression restoration was linked with a change in the methylation pattern of HSP70 region III, DNA was extracted from drug-treated HLE B-3 cells and subjected to bisulfite sequencing assay. DNA obtained from 5-aza-dC treated cells showed partial demethylation of region III in HSP70 (**Figure 2.15A**) while no significant demethylation was observed for region I and region II. We further assessed the effect of 5-aza-dC on *de novo* DNMTs expression in HLE B-3 cells. Our finding depicts considerable depletion of *DNMT3A* ( $p=0.03$ ) in  $1\mu\text{M}$  5-aza-dC treated cells, while *DNMT3B* failed to show significant changes ( $p=0.31$ ) as expected (**Figure 2.15B**). The findings as mentioned above imply that the loss of HSP70 expression correlated with epigenetic modification involving DNA methylation.



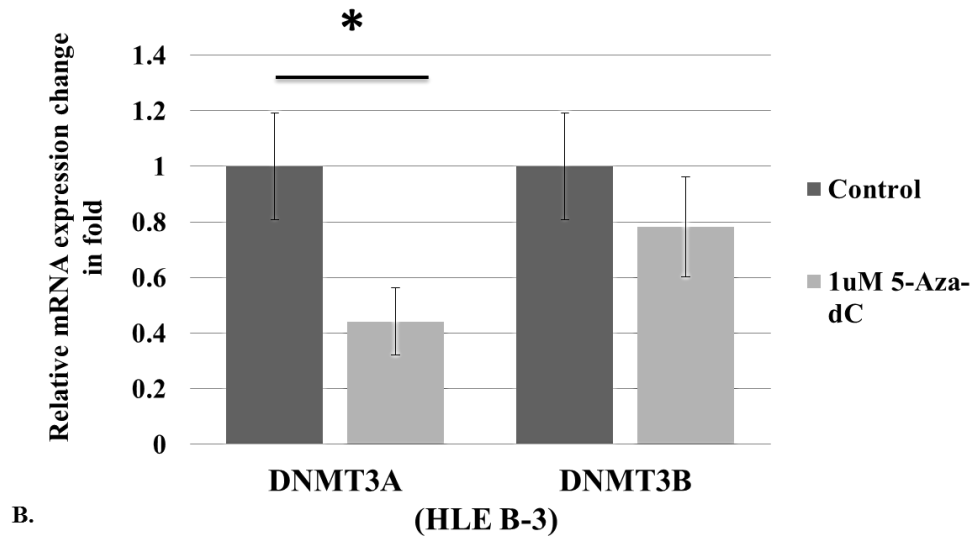


**Figure 2.15 Demethylation using 5-aza-2'-deoxycytidine in HLE B-3 cells.** A. Loss of DNA methylation at region III in HLE B-3 cells treated with demethylating agent 5-aza-dC ( $p=0.04$ ) while region I and region II didn't show significant demethylation ( $p=0.70$  and  $p=0.49$  respectively). B. Effect of 5-azadC on *DNMT3A* and *DNMT3B* mRNA expression, where *DNMT3A* showed significant reduction ( $p=0.03$ ) while *DNMT3B* failed to show considerable differences ( $p=0.31$ ) in treated HLE B-3 cells. All data shown are representative of more than three independent experiments with similar results. \* $P<0.05$ .

### 2.3.7 Increased expression of HSP70 regulator in PEXS affected lens capsule tissue

The lower induction of HSP70 expression led us to check the expression of its regulator. Recent data set from our group showed HSF1 mRNA is highly expressed in lens capsule in PEXS but not in PEXG in comparison to control.<sup>114</sup> We speculated that there might be a less accessibility of HSF1 binding to the HSE elements on HSP70 promoter and this binding might be inhibited or restricted due to less receptive chromatin landscape. As it is reported that the binding of HSF1 leads to nucleosome displacement which is regulated by the enzymatic activity of PARP1 (Poly (ADP-ribose) polymerase-1). Henceforth, we checked the protein level of HSF1 and mRNA expression of PARP1 in LC tissue. We found significantly increased expression of PARP1 in LC of PEXS affected individual ( $p=0.04$ ;  $n=10$ ) and elevated level of HSF1 in LC extract of PEXS, however by densitometry analysis, we did not find significant increased HSF1

immunoreactivity in whole tissue lysate of PEXS and PEXG individuals with the present sample size (n=2) (**Figure 2.16**). Further studies are underway to investigate the biological consequences of PARP1 activation and its effect on the heat shock response.

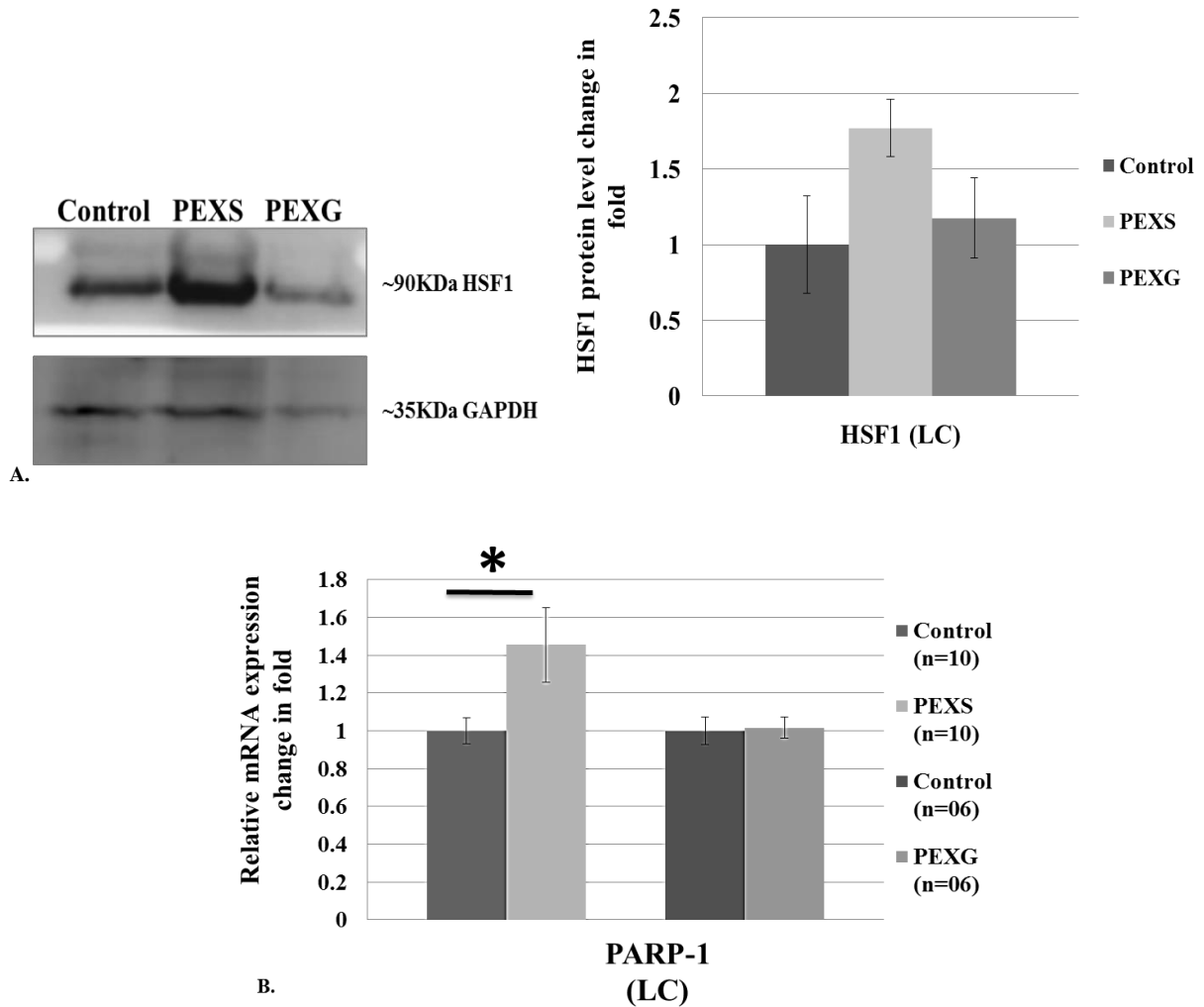


**Figure 2.16 Differential expression of HSP70 regulators** **A.** Immunoblotting and densitometry plot of HSF1 showing elevated level of HSF1 in LC extract of PEXS subjects though failed to reach significance due to small sample size (p=0.25; n=2). While, PEXG didn't showed considerable differences (p=0.71; n=2) when compared with controls. **B.** mRNA expression of PARP1 showed increased expression in PEXS individuals (1.5 fold) and no differential change in PEXG individuals (1.02 fold) when compared with control.

## 2.4 Discussion

The prevalent observation of abnormal fibrillar aggregates in pseudoexfoliation suggests dysregulation of chaperone activity. Zenkel and co-workers had reported the increased expression of stress-inducible chaperone proteins such as HSP40 and HSP60 in iris and ciliary tissues of PEXS patients.<sup>199</sup> In accordance with their findings, dataset from our group has also reported deregulated expression of clusterin (CLU), heat shock factor 1 (HSF1), HSPD1 (Heat shock 60kDa protein 1), DNAJB1 (DnaJ (Hsp40) homolog, subfamily B, member 1) and DNAJB11 (DnaJ (Hsp40) homolog, subfamily B, member 11) in lens capsule of PEXS individuals.<sup>8,114,200</sup> These findings implicate an essential role of chaperone proteins in curbing the effects of proteotoxic stress observed in PEX disease pathogenesis. In the present study, we examined the expression of HSP70 and HSP90, which are critical elements of cellular defense against misfolded proteins and are activated in various stress conditions. Our findings showed a decreased expression of HSP70 in PEXS lens capsule at both transcript and protein levels. However, in the lens capsule of PEXG subjects, no significant differences were observed at either mRNA or protein level. Conversely, the difference in expression of HSP90 was not statistically significant in either PEXS affected cases or PEXG cases when compared with non-PEX controls. Downregulation of cytosolic chaperone, HSP70 emphasizes the notion that PEX pathogenesis entails reduced cytoprotective mechanisms. Stress-inducible HSP70 is a ubiquitous molecular chaperone, involved in protein translocation across membranes, assembly of monomeric proteins to larger macromolecular complexes, and ubiquitination of protein aggregates and alterations in its function have been linked with numerous age-related neurodegenerative diseases.<sup>220,221</sup> In concert with our current finding, a diminution of HSP70 in the Y79 retinoblastoma cell line was reported where the loss of stress responsiveness was linked with a lack of promoter occupancy.<sup>222</sup>

DNA modifications can regulate gene expression at transcriptional level. One such modification mechanism is CGI methylation.<sup>223</sup> DNA methylation is the only epigenetic modification that directly affects the DNA and is generally linked with transcriptional silencing of genes without altering the DNA sequence. It is mainly confined to cytosine in a CpG context, which occurs in clutches throughout the genome known as CpG islands.<sup>224</sup> Majority of CpG islands are positioned in either the genes promoters or first exon.<sup>225</sup> To understand the mechanism underlying the declined expression of HSP70, we assessed the CpG methylation level in the region constituting 1 kb upstream and downstream of TSS of HSP70 in blood and lens capsule (LC) of study subjects.

Bisulfite sequencing analysis revealed DNA hypermethylation of CpGs in the exonic region (region III) of HSP70 but not at its upstream promoter and TSS region, in both blood and lens capsule of PEXS patients, resulting in a substantial reduction in the level of HSP70 expression. While we found hypermethylation in only region III in blood of PEXS and PEXG subjects, no significant differential methylation was observed in the lens capsule of PEXG when compared to control. The probable explanation for the differential methylation in the blood and lens capsule tissue of affected patients could be cell-type-specific methylation following tissue-specific functions.<sup>223</sup> CpG hypermethylation is a characteristic of mammalian genes that have assumed an inaccessible and inert state of transcription. Previously, in cataract lenses, differential DNA methylation has been reported to regulate the gene expression of  $\alpha$ A-crystallin (CRYAA) and KEAP1 genes.<sup>226,227</sup> Hongfei and co-workers had reported hypermethylation of the CGI in the LOXL1 (lysyl oxidase-like 1) promoter region in lens capsule of PEXS patients suggesting that promoter hypermethylation reduces the gene expression.<sup>228</sup> The methylation of CGIs is mainly catalyzed by DNMTs that transfer methyl groups to cytosine residues. DNMT3A

and DNMT3B function as de novo DNA methyltransferases that effectively methylate hemimethylated or unmethylated DNA and perform a major role in normal embryonic development and disease.<sup>229</sup> In our study, we observed an elevated expression of DNMT3A, which is ubiquitously expressed and is mostly associated with heterochromatin, in PEXS eyes but no differential expression of DNMT3B was observed in either PEXS or PEXG affected subjects. The present study identified an inverse association between HSP70 expression and CGI methylation in PEXS affected subjects.

Further, *in vitro* methylated reporter assays showed that methylation of CpGs in the exon (region III) has a regulatory effect on gene expression while that of CpG region containing promoter sequences (region I) and nearby TSS (region II) does not. This implies DNA methylation affects the affinity of TFs for their binding sites. Notably, the binding of numerous TFs to CpG region III encompassing CpG sites was found. One of the relevant transcription factors binding to the differentially methylated CpG sites is NFE2L1 that binds to the cis-acting enhancer, antioxidant response element (ARE) and regulates the expression of genes involved in oxidative stress.<sup>230</sup> Besides, it also recruits coactivators such as p300/CBP associated factor ([P/CAF], where CBP means cAMP response-element-binding protein) that creates a chromatin environment favoring transcription.<sup>231</sup> Another known transcriptional activator, KLF5 promotes transcriptional activation by interacting with chromatin regulators and epigenetic mediators such as CBP/p300.<sup>232,233</sup> HIF1A binds to the enhancer erythropoietin (EPO), a critical event in the hypoxic activation of EPO transcription.<sup>234</sup>

Epigenetic silencing by DNA methylation is reversible, unlike gene inactivation by deletion and mutation. This propelled us to investigate the expression and methylation status of HSP70 in HLE B-3 cells before and after treatment with a DNA demethylating agent, 5-aza-dC

which is a deoxycytidine analog and induces depletion of DNMTs including DNMT1 (DNA methyltransferase 1) one of the critical enzymes present in human lens epithelial cells and *de novo* methyltransferase (DNMT3A) and mediates the restoration of hypermethylated gene.<sup>235,236</sup> 5-Aza-dC does not act on the genomic DNA randomly but somehow keeps the constitutively methylated regions “shielded” from its demethylating effect.<sup>237</sup> It has been commonly employed to induce gene expression and cellular differentiation.<sup>238,239</sup> Treatment of HLE B-3 cells with 5-aza-dC restored HSP70 expression and also induced demethylation in region III confirming that the transcriptional repression of HSP70 was caused by DNA methylation. Besides, a significant reduction in the expression of DNMT3A in 5-aza-dC treated HLE B-3 cells demonstrates that HSP70 expression might be regulated in a methylation-dependent manner and that DNMT3A preferentially methylates HSP70.

Other than epigenetic regulators we also detected an increased expression of PARP1 and HSF1 level despite the lower induction of HSP70 which suggest the role of factors other than HSP regulators in transcriptional regulation of HSP70.

In this study, we did not investigate the role of transcription factors or the pathways that affect DNA methylation. Additional elaborate studies are being carried out to focus on the effect of locus-specific DNA methylation on the role of transcription factors regulating the expression of HSP70. Nevertheless, our findings provide the very first evidence that the methylation of CpG sites in the exonic region is associated with transcriptional regulation of HSP70 in PEX.

## **2.5 Conclusion**

In conclusion, we report here the first evidence of a decrease in the most conserved cytosolic chaperone, HSP70 in lens capsules of PEXS patients. On the basis of our findings we proposed a model which demonstrates that the reduction in HSP70 expression results in impaired cellular

stress defense, which could be one of the contributing factors in causing pseudoexfoliation syndrome (**Figure 2.17**). Bisulfite sequencing analyses, demethylation studies, transfection experiments and in vitro methylated reporter assays altogether revealed the prominent role of *de novo* exon methylation in HSP70 regulation. Although traditionally transcriptional repression is associated with promoter methylation, we found that HSP70 downregulation in PEX is due to methylation in its exon region. The hypermethylation of HSP70 coincides with its diminished expression, thus, suggesting that these methylation events contribute to PEX pathogenesis. This study is useful for a deeper understanding of the pathogenesis of PEX, and it can be used to identify novel opportunities for the prevention of and therapy for the disease in future.

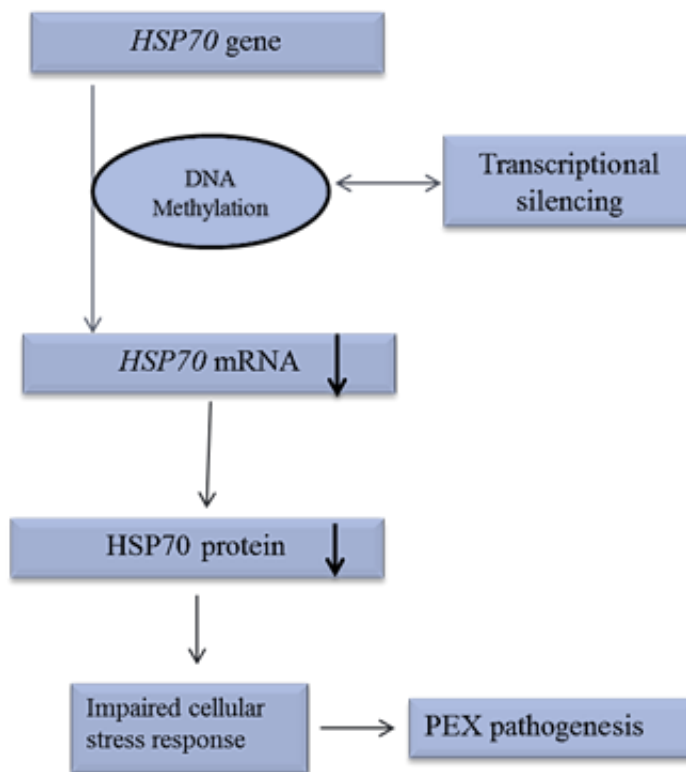


**Figure 2.17 A schematic representation of the findings.** This flowchart demonstrates that when there is a lower induction of HSP70 due to DNA hypermethylation, it results in its repressed expression which promotes proteopathy, and impaired cellular stress response which leads to aggregation of PEX fibrils and contributes to PEX pathogenesis.

# **CHAPTER -3**

*To investigate the role of endoplasmic reticulum-unfolded protein response (ER-UPR) and ubiquitin proteasome system (UPS) in PEX pathogenesis*

### **3.0 To investigate the role of endoplasmic reticulum-unfolded protein response (ER-UPR) and ubiquitin proteasome system (UPS) in PEX pathogenesis**

#### **3.1 Introduction**

Endoplasmic reticulum (ER) function is highly sensitive to stresses that reduce its folding capacity, which triggers misfolded proteins accumulation and aggregation in the ER lumen. These factors promote the unfolded protein response (UPR) activation and restore ER function. In addition, misfolded proteins are retro-translocated to the cytosol, where they are ubiquitinated and degraded by the proteasome machinery via the ER-associated degradation (ERAD) pathway.<sup>240-242</sup> Protein misfolding is alleviated by the protein quality control system, which comprises of the chaperones and intracellular degradation pathways such as ubiquitin-proteasomal system (UPS) and autophagy.<sup>221,243</sup> These mechanisms, are often referred to as the cellular proteostasis network (PN) that prevent the aggregation of aberrant and misfolded proteins by breaking down the proteins into polypeptide chains.<sup>244-246</sup> Any impairment of the PN system causes proteins to accumulate and promotes severe neurodegenerative disorders, such as AD, PD and prion or polyQ diseases.<sup>243,247</sup> Hallmarks of PEX include aggregation of microfibrils on the anterior eye tissues surface, which contribute to worldwide glaucoma. Elevated production and accumulation of fibrillar materials in PEX could be an implication of dysregulated proteostasis network. ER-associated stress and aberrant misfolded protein have been linked with range of eye diseases such as cataract, glaucoma, retinal inflammation and diabetic retinopathy.<sup>248,249</sup> Zenkel and co-workers have provided evidence for perturbation in cytoprotective mechanisms including cellular stress response, and antioxidant defense in anterior segment tissue of PEX eyes.<sup>199</sup> Similarly, we and others have previously reported a significant increase of an extracellular chaperone, Clusterin in the aqueous humor of PEXG individuals.<sup>8,250</sup>

We additionally detailed an upregulation in the mRNA levels of heat shock factor-1 (HSF1) in the anterior eye tissues (lens capsule and conjunctiva) of PEXS subjects, suggesting an increased proteotoxic stress.<sup>114</sup> Increased HSF1 protein expression has been confirmed in lens capsule of PEXS individuals in comparison with control by Western blot analysis in Chapter 2 (Figure 2.16, page No. 60). In order to provide further evidence of the key players in the protein quality control machinery under normal and PEX conditions we went ahead to unravel the role of genes involved in UPR and UPS in the anterior eye tissues obtained from PEX patients and non-PEX controls. Identifying the involvement of impaired proteostasis network in PEX development will broaden the current understanding of its complex pathophysiology.

### **3.1.1 ER stress signaling: ER-UPR**

ER triggers the stress response signaling pathways collectively called ER-UPR (endoplasmic reticulum- unfolded protein response) to cope with the accumulation of unfolded or misfolded proteins. ER-UPR is regulated through signaling cascade by three sensor proteins; inositol-requiring enzyme 1 $\alpha$  (IRE1 $\alpha$ ), activating transcription factor 6 (ATF6) and Protein kinase-like endoplasmic-reticulum kinase (PERK) (**Figure 1**). All three sensors relieve ER stress and restore protein homeostasis by attenuating protein translation, upregulating the expression of chaperones that facilitate protein folding, and by clearing the abnormally folded proteins by autophagy and ER-associated degradation (ERAD) pathway. However, in case of overwhelming burden UPR promotes cell death.<sup>251</sup> Activated stress sensor, IRE-1 $\alpha$ ; an endonuclease, cuts out a specific region from X-box binding protein 1 (XBP1) mRNA which is then translated into the XBP1 protein.<sup>252,253</sup> XBP1 acts as a transcription factor that binds to ER stress response elements (ERSE) of UPR stress genes including glucose regulated proteins (GRP) and upregulates their expression required for combating ER stress.<sup>254</sup> Activated PERK, on the other hand,

phosphorylates elongation factor 2 $\alpha$  (eIF2 $\alpha$ ) and blocks overall translation in the cell.<sup>255</sup> Further, ATF6 after being cleaved by proteases is translocated to nucleus where it activates the transcription of several ER stress genes like CCAAT-enhancer-binding homologous protein (CHOP), protein disulfide isomerase (PDI) and GRP proteins.<sup>256</sup> PDI maintains native structure of ER proteins while CHOP acts as a pro-apoptotic protein and plays a major role in ER stress-induced apoptosis.

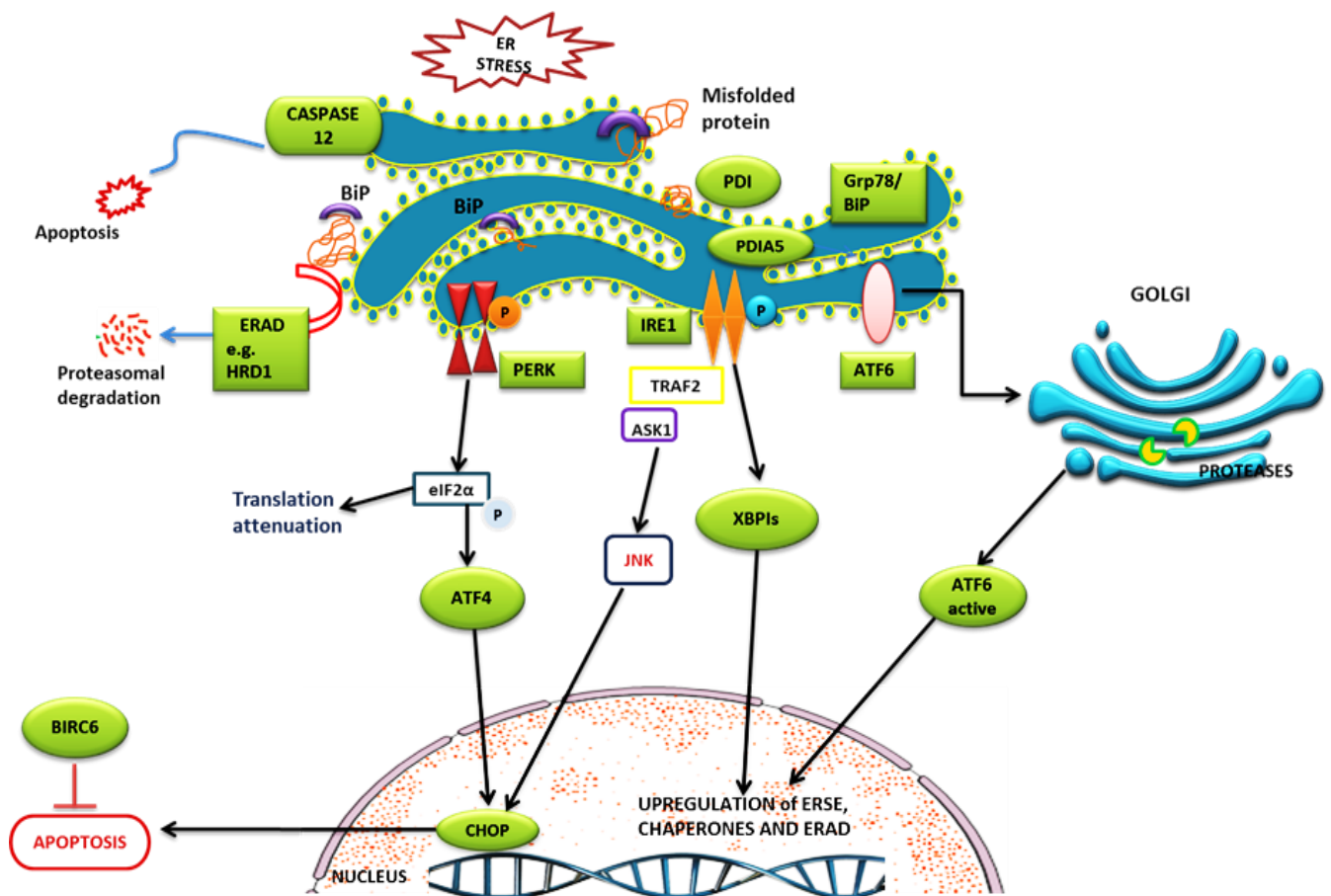


**Figure 3.1 Schematic representation of ER-UPR signaling pathway.** The UPR is mediated by activation of three UPR sensors that include inositol-requiring enzyme 1 (IRE1), protein kinase RNA-like ER kinase (PERK) and activating transcription factor 6 (ATF6). These three sensors are regulated by one master regulator, GRP78/BIP. Upon accumulation of misfolded proteins, the UPR is activated, GRP78/BiP dissociates from ATF6, PERK and IRE1 and bind to misfolded proteins. GRP78 upon dissociation from PERK and IRE1 causes its oligomerization, auto phosphorylation and activation of

these proteins. After being activated, PERK phosphorylates the eukaryotic initiation factor 2 $\alpha$  (eIF2 $\alpha$ ) resulting in termination of global protein synthesis, while IRE1 activates XBP1 protein that functions as transcription factor after translocated to the nucleus activates genes coding for chaperones involved in the folding of proteins and processing reactions. ATF6 translocate to the Golgi where it is split by proteases to form the active ATF6 transcription factor that induces expression of CHOP, thereby resolving the stress and reinstating the ER homeostasis by the UPR. Baculoviral inhibitor of apoptosis repeat containing 6 (BIRC6) and 3-hydroxy-3-methylglutaryl reductase degradation 1 (HRD1) act as anti-apoptotic factor and induce proteasomal degradation of pro-apoptotic proteins thereby reducing cellular stress. In case of prolonged stress, IRE1 $\alpha$ , and PERK can activate c-JUN N-terminal kinase (JNK) which promote caspase dependent apoptosis. In addition, CHOP production in the PERK pathway and CASPASE12 also leads to apoptotic cell death.

### 3.1.2 Ubiquitin proteasome system (UPS)

The Ubiquitin proteasome system (UPS) is a major intracellular pathway for elimination of short-lived, aberrant, and misfolded proteins, via ubiquitination and protein degradation.<sup>257,258</sup> It involves the sequential action of three enzymes, ubiquitin-activating enzyme E1 which activates ubiquitin protein, E2 ubiquitin-conjugating enzyme transfer ubiquitin to lysine residue via its carboxy terminal glycine, and finally the ubiquitin ligase E3, catalyzes the covalent attachment of ubiquitin to a substrate protein.<sup>259</sup> The formation of a polyubiquitin chain after multiple rounds of ubiquitination, targets the ubiquitinated protein to the proteolytic complex 26S proteasome for protein degradation. The proteasome system comprise of two-multi subunits: catalytic core (20S) and regulatory particle (19S). The 20S core particle contains the active sites responsible for substrate degradation by the caspase-like/PGPH (peptidylglutamyl-peptide hydrolyzing), trypsin-like and chymotrypsin-like activities The proteasome unfolds substrates and drives the polypeptide chains through the inner chamber into the core particle, where they are cleaved into shorter peptides, which are rapidly processed and recycled after they are released from the barrel.<sup>260,261</sup> Aberrations in UPS have been exhibited in many

neurodegenerative diseases notably PD and AD.<sup>262-264</sup> Recently a link has also been established between PEXS pathology and autophagy dysfunction in tenon fibroblast showing reduced capacity for degradation of denatured protein.<sup>158</sup>

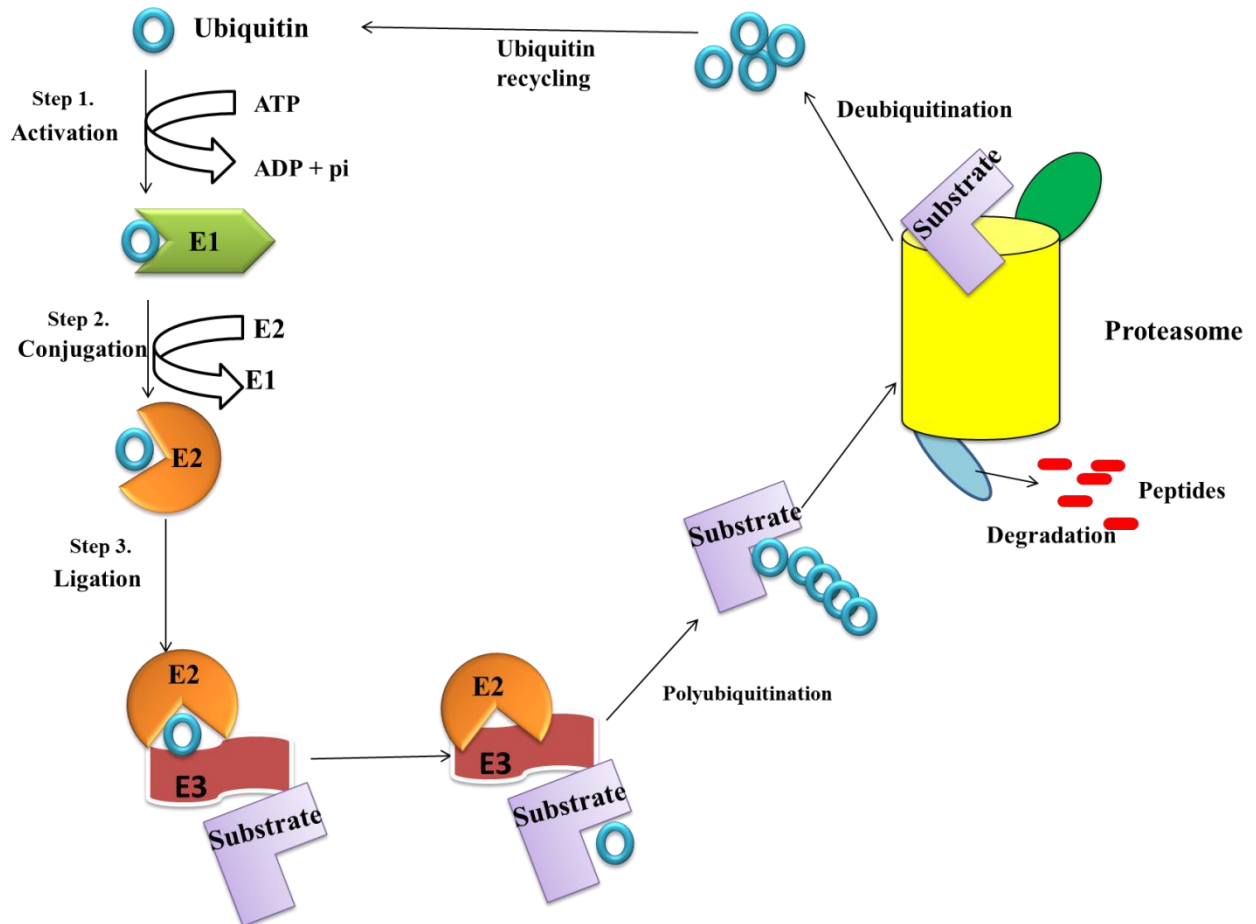


**Figure 3.2 Schematic representation of the ubiquitin proteasome cycle.** The process of ubiquitination is facilitated through the sequential action of enzymes. UPS is initiated when the free ubiquitin is activated by an E1 activating enzyme in an ATP (adenosine triphosphate) dependent process (step 1). Ubiquitin is then transferred from E1 to the conjugating enzyme-E2 (step 2); subsequently E3 ligase catalyzes the attachment of ubiquitin from the E2 to the substrate protein (step 3). Polyubiquitinated substrates are then guided to the proteasome where it is unfolded and translocated in the catalytic 20S core complex for degradation, and the free ubiquitin are released by deubiquitinases (ubiquitin recycling enzymes).

The tell-tale pathological features of PEX: late-onset and protein aggregate formation, led us to hypothesize that an impaired proteostasis might be at play, which had never been assessed. We, therefore, set forth to check alterations in the molecular events of UPR and UPS by studying the differential gene expression pattern using targeted array analysis for UPR pathway in PEX affected tissues followed by validation of positive hits in PEX affected tissues. Broader understanding of the key players of protein quality control machinery under normal and PEX conditions is crucial for developing novel strategies that target their activity.

Following specific aims were proposed under this objective:

1. To identify differentially regulated ER-UPR genes in anterior eye tissues of study subjects.
2. To validate the expression of differentially regulated gene in PEX pathology.
3. To assess the role of ubiquitin proteasome system (UPS) components in the development of PEX.
4. To check apoptotic activity in the lens capsule of PEX affected subjects.

## **3.2 Materials and Methods**

### **3.2.1 Study Subjects Recruitment and selection**

Detailed procedure for inclusion and exclusion criteria and the grouping of control and PEX affected individuals are enlisted in chapter 2 (page-28-29). Anterior eye tissues (lens capsules and conjunctiva) from PEX affected study subjects and age matched controls were collected in RNAlater stabilisation solution (Invitrogen, USA) during cataract surgery and stored at -80°C until further use.

### **3.2.2 RNA Extraction, cDNA synthesis and Quantitative Real-time PCR**

Total RNA extracted from the anterior eye tissues followed the manufacturer's protocol of RNA extraction kit (RNeasy Mini Kit, QIAGEN GmbH, Hilden). Extracted and quantified RNA was

converted into cDNA using Reverse Transcription Kit (Quantitect Reverse Transcription Kit, QIAGEN, Hilden). Transcript specific primers were designed by using PrimerQuest Tool, Integrated DNA technologies (IDT) (**Table 3.1**). qRT-PCR was performed using ABI 7500 Real time PCR (Applied Biosystems). Total 5ng of cDNA mixed with Fast Start Universal SYBR Green Mastermix (Rox) (Roche, 04913914001) was used in 20µl reaction mixture in triplicate for each sample. 0.4µM each of forward and reverse primers was used for both target and housekeeping genes. Comparative threshold cycle ( $\Delta\Delta$ Ct) method was used for normalization of target gene and change in expression was represented as fold difference.

**Table 3.1 List of oligos used in the study.**

No.	Gene	Purpose	Sequence (5'>3')
1	<i>SYVN1</i> (NM_172230)	qRT-PCR	F: CGCAACATGAACACCCTGTATC R: GCACCAGTCACCATCTCTTCT
2	<i>CANX</i> (NM_001746)	qRT-PCR	F: TATGATGGAAAGTGGGAGGTAGA R: AGGCTTGGTGTCAAACAGGA
3	<i>EIF2AK3</i> (NM_004836)	qRT-PCR	F: AGCAAACCAGAGGTATTTGGGA R: TTTCCATGCTTTCACGGTCTTG
4	<i>DDIT3</i> (NM_004083)	qRT-PCR	F: AAGTCTAAGGCACTGAGCGTATC R: CCTTCTTGAACACTCTCTCCTC
5	<i>HSPA5</i> (NM_005347)	qRT-PCR	F: GGTGCCTACCAAGAAGTCTCAG R: GTCAGGGGTCTTTCACCTTCAT
6	<i>UBB</i> (NM_018955)	qRT-PCR	F: CTGAGGGGTGGCTGTTAATTC R: TGGGGCAAATGGCTATAGTG
7	<i>UBA1</i> (NM_003334)	qRT-PCR	F: GTGGAGATCGCTAAGAACATCA R: AGGTAGAACTGGGAGGAAAGA
8	<i>UCHL1</i> (NM_004181)	qRT-PCR	F: TTCGTCTTCCCTAGGCTATTTC R: CAGCACTTTGTTTCAGCATCTC
9	<i>UBE2J1</i> (NM_016021)	qRT-PCR	F: TTCTCCTAACGGCTAATGGTC R: TGATGGCTAATAATGCTGTCCT
10	<i>PSMD1</i> (NM_002807)	qRT-PCR	F: GAAGTGGATGAGGCAGAGAAA R: TAAGCTGGGCAGGCATAAC
11	<i>PSMA5</i> (NM_002790)	qRT-PCR	F: CCACTGGTTCACCTACAATGA R: CCTGGATCTGCATCTTCTTCTC

### 3.2.3 RT<sup>2</sup> Profiler PCR array

We utilized Custom RT<sup>2</sup> Profiler PCR Arrays (CAPH13433, SABiosciences Corp., Frederick USA) to analyze gene expression and determine pathway activity with a real-time PCR experiment for each specimen (**Table 3.2**). For the present study Custom PCR array format for 19 target genes and 5 controls were designed. Custom RT<sup>2</sup> include built-in positive control elements such as housekeeping gene (HKG) for the proper normalization of the data, genomic DNA contamination (GDC) control for the detection of any DNA contamination with high sensitivity, reverse transcription control (RTC) for the quality, integrity and purity of RNA samples and positive PCR control (PPC) test the efficiency of the PCR performance and detects the pre-dispensed artificial DNA sequence and the primer set. Any impurities that affect the positive control PCR amplification also affect amplification of the gene specific products of interest.

The cDNA was synthesized in a two-step reaction using a RT<sup>2</sup> first strand kit (330404, Qiagen) in a 20µl reaction volume. Total RNA (25.0ng to 1µg) was mixed with 2µl of 5X genomic DNA elimination buffer (GE) and required water in a total reaction volume of 10µl. The reaction mixture was incubated at 42°C for 5 minutes followed by immediate chilling on ice for one minute. Subsequently reverse transcriptase (RT) cocktail was prepared constituting 4µl of 5X RT buffer (BC3), 1µl of P2 (primer and external control mix), 1µl of RE3 (RT enzyme mix 3) and 3µl water. 10µl of RT cocktail reaction was mixed with 10µl of GE elimination mixture and incubated at 42°C for 15 minutes followed by heat inactivation at 95°C for 5 minutes. The amplified cDNA was then diluted with nuclease free water to a final concentration of 2.5ng. Total 5ng of cDNA was used in a 25µl reaction for each sample mixed with SYBR Green (Roche) and aliquoted into 24x4 plate layout of an RT<sup>2</sup> Profiler PCR array containing UPR specific primer pairs. The amplification profile includes 1<sup>st</sup> step 1 cycle: 95°C for 10 minutes, 2<sup>nd</sup>

step – 40 cycles: 95°C for 15 seconds followed by 60°C for 1 minute, 3<sup>rd</sup> step (melt curve) – 95°C for 1 minute, 60°C 30 seconds, and 95°C for 30 seconds. Raw data was analyzed using the integrated web based automated software for RT<sup>2</sup> Profiler PCR Array Data Analysis version 3.5 available through SABiosciences. Raw data sets were uploaded using the PCR array data analysis template available at (<http://pcrdataanalysis.sabiosciences.com/pcr/arrayanalysis.php>). Each sample was tested for efficiency, reproducibility, and genomic DNA contamination using the controls included in the plate. All samples passed this test. Next, from the panel of five housekeeping genes, the software identified GAPDH as the most stably expressed housekeeping gene for data normalization. Comparative threshold cycle ( $\Delta\Delta$ Ct) method was employed to calculate gene expression from raw threshold cycle data using average cycle threshold value of control samples as reference. Fold changes were represented as the difference in average gene expression of control samples compared individually with PEX patient's samples.

**Table 3.2 List of UPR genes used for designing custom RT<sup>2</sup> profiler PCR array.**

Gene Symbol	Refseq	Official Full Name	RT2 Catalog Number
<i>XBPI</i>	NM_005080	X-box binding protein 1	PPH02850
<i>PDIA5</i>	NM_006810	Protein disulfide isomerase family A, member 5	PPH01725
<i>ERN1</i>	NM_001433	Endoplasmic reticulum to nucleus signaling 1	PPH12383
<i>EIF2AK3</i>	NM_004836	Eukaryotic translation initiation factor 2-alpha kinase 3	PPH10874
<i>GAPDH</i>	NM_002046	Glyceraldehyde-3-phosphate dehydrogenase	PPH00150
<i>ATF4</i>	NM_001675	Activating transcription factor 4 (tax-responsive enhancer element B67)	PPH02016
<i>ATF6</i>	NM_007348	Activating transcription factor 6	PPH20143
<i>DNAJB11</i>	NM_016306	DnaJ (Hsp40) homolog, subfamily B, member 11	PPH05920
<i>TRAF2</i>	NM_021138	TNF receptor-associated factor 2	PPH00352
<i>PPP1R15A</i>	NM_014330	Protein phosphatase 1, regulatory (inhibitor) subunit 15A	PPH02081
<i>DDIT3</i>	NM_004083	DNA-damage-inducible transcript 3	PPH00310
<i>CASP12</i>	NM_001191016	Caspase 12 (gene/pseudogene)	PPH68979
<i>HSPA5</i>	NM_005347	Heat shock 70kDa protein 5 (glucose-regulated protein, 78kDa)	PPH00158

<i>CANX</i>	NM_001746	Calnexin	PPH05937
<i>CALR</i>	NM_004343	Calreticulin	PPH02060
<i>SYVNI</i>	NM_172230	Synovial apoptosis inhibitor 1, synoviolin	PPH16893
<i>ACTB</i>	NM_001101	Actin, beta	PPH00073
<i>HSPB1</i>	NM_001540	Heat shock 27kDa protein 1	PPH00165
<i>DNAJB1</i>	NM_006145	DnaJ (Hsp40) homolog, subfamily B, member 1	PPH01207
<i>HSPD1</i>	NM_002156	Heat shock 60kDa protein 1 (chaperonin)	PPH01205
<i>CLU</i>	NM_001831	Clusterin	PPH00243
<i>HGDC</i>	SA_00105	Human Genomic DNA Contamination	PPH65835
<i>RTC</i>	SA_00104	Reverse Transcription Control	PPX63340
<i>PPC</i>	SA_00103	Positive PCR Control	PPX63339

### 3.2.4 Immunofluorescence analysis

For immunofluorescence labeling, lens capsules were obtained from subjects at the time of cataract surgery and transferred in a tube of RNAlater (Sigma) and stored at -80°C until further use. The lens capsules from PEXS, PEXG and control were utilized for immunofluorescence staining. Tissues was first washed twice in PBS after removing them from RNA later. It was then fixed in freshly prepared 4% paraformaldehyde (PFA) in 1X PBS for 20 minutes, followed by washing in 1X PBS for three times. Later tissue was permeabilized with 0.5% Triton X-100 in PBS (PBST) for 5 minutes. Blocking was done in 10% normal horse serum (NHS) in PBST for 30-45 minutes and incubated overnight at 4°C in primary polyclonal antibody at 1:250 dilutions in blocking solution. After subsequent washing in PBST, the tissue was treated with Alexa-Fluor 594 Chicken anti-rabbit IgG (A21442, Invitrogen) and Alexa-Fluor 488 Chicken anti-mouse IgG (A21200, Invitrogen) secondary antibody at 1:250 dilutions for two hours in dark at room temperature. Nuclear staining was done with DAPI (4,6-diamino-2-phenylindole; Sigma-Aldrich, 32670-5MG-F) and lens capsule was flat mounted on the slide along with ProLong Gold antifade reagent (P36934, Invitrogen). Immunofluorescence imaging was done in Olympus

FV 3000 confocal Laser scanning microscope and images were further processed in FV31S-DT. Images were quantified in ImageJ and fluorescence intensity was plotted with respect to control.

### **3.2.5 Protein extraction and Western Blotting**

Whole tissue lysate from lens capsule and conjunctiva tissue was isolated using NE-PER reagent (Thermo Fisher Scientific) as per the manufacturer's guidelines. Polyclonal antibodies for Synoviolin (SC-130889, Santa Cruz Biotechnology at 1:250 dilution), Calnexin (SC-130059, Santa Cruz Biotechnology at 1:250 dilution), Ubiquitin (BB-AB0030, Bio Bharati life sciences at 1: 500 dilution), PSMC1 (ARP56476\_P050, Aviva Systems Biology at 1: 500 dilution) were used as primary antibody and HRP-conjugated Goat anti-rabbit IgG (621140380011730, Bangalore GeNei, India), goat anti-mouse IgG-HRP (621140680011730, Bangalore GeNei, India) were used as secondary antibody at 1: 5000 dilutions. GAPDH antibody (ABM22C5, Abgenex, India, 1:500) was used as loading control. Detection was done using the chemiluminescence kit (Super Signal Femto Maximum Sensitivity Substrate, PI34094, Thermo Fisher Scientific) in a Fusion Solo S Chemi-Doc (Vilber Lourmat). Evolution Capt software (Vilber Lourmat fusion solo S) was used for image acquisition and densitometric analysis of the gels and blots in this study.

### **3.2.6 Proteasome-Glo™ assay Systems**

A commercially available indirect enzyme-based luminescent assay, the Proteasome-Glo™ system (Promega, G8621) with a substrate for chymotrypsin-like activity (Suc-LLVY-aminoluciferin) was used for the proteasome activity assay which is recommended for small amounts of tissue samples (typically 5mg). This assay kit is designed and developed to measure the proteolytic activities of the proteasome using a luminogenic substrate. In the present study removal of nonspecific background activities was determined by incubating the protein extracts

with the reversible (10 $\mu$ M of MG132, Sigma) and irreversible inhibitor (Epoxomicin, 15 $\mu$ M, Sigma). The inhibitor was suspended in dimethylsulfoxide (DMSO). The assay procedure was adapted from the study reported by Strucksberg and co-workers (Strucksberg et al., 2010). 15 $\mu$ g of protein extract was analyzed by western blot to quantify the amount of 26S proteasome S-subunit (PSMC1). Proteasome activity was calculated by subtracting the values obtained from the assays with inhibitor (background) from the total peptidase activity (no inhibitor). Subsequently, we calculated the specific proteasomal activity by normalizing the values of the luminescence signals to the values obtained from the PSMC1 immunoblot densitometry. In a 96-well plate, 50 $\mu$ l of Proteasome-Glo<sup>TM</sup> reagent containing the Ultra-Glo<sup>TM</sup> luciferase and the specific luminogenic substrate for the chymotrypsin-like activity assay was added to 50 $\mu$ l of blank, control or test sample. 15 $\mu$ g of total protein (constituting 50 $\mu$ l of extract) was used for the study. Components were mixed gently and incubated for 60 minutes at room temperature. Luminometric measurement was recorded three times with an integration time of 5 seconds using a Varioskan Flash multimode reader (Thermo Scientific).

### **3.2.7 Terminal deoxynucleotidyl transferase dUTP nick end labeling (TUNEL) assay**

To determine apoptotic activity in the lens capsule of study subjects, we performed TUNEL assay using the DeadEnd<sup>TM</sup> Fluorometric TUNEL System (G3250, Promega). The procedure includes following steps: Tissues were first fixed in a 4% freshly prepared paraformaldehyde (PFA) in PBS for 15 minutes, followed by washing twice in PBS, 5 minutes each time. Tissue was permeabilized in 0.2% Triton<sup>®</sup> X-100 in PBS for 5 minutes, preceded by addition of 100 $\mu$ l of a 20 $\mu$ g/ml Proteinase K solution for 10 minutes (this step is essential for tissue permeabilization). Tissues were then washed twice in PBS, for 5 minutes. Later, 100 $\mu$ l Equilibration Buffer was added and tissues were equilibrated at room temperature for 10

minutes. 50µl of incubation buffer comprising of 45µl equilibration buffer, 5µl of nucleotide mix and 1µl of Terminal deoxynucleotidyl Transferase (TdT) were added to the tissues and covered with plastic coverslips to ensure even distribution of the mix. Tissue was then incubated for 120 minutes at 37°C in a humidified chamber. For negative control incubation buffer without TdT enzyme was prepared. Exposure to light was avoided from this step forward. Plastic Coverslips were removed and the reaction was stopped by adding 2X SSC buffer for 15 minutes. Tissues were washed three times in PBS, at interval of 5 minutes each. It was counterstained with DAPI (Sigma) followed by mounting with antifade reagent (Invitrogen). The slides were observed using the automated fluorescence microscope (BX63, Olympus, Japan) at 200x and 600x magnification. Images were analyzed and quantitated using ImageJ software. Two to three fields were selected randomly for each group and the captured TUNEL and DAPI images were overlaid with ImageJ software. TUNEL-positive cells were labeled with both fluorescein-dUTP and DAPI. The percentage of apoptotic cells were calculated by dividing the total number of TUNEL-positive cells by the number of nuclei and multiplied by 100.

### **3.2.8 Statistical analysis**

Groupwise results were analyzed for statistical significance by Student's t-test. For comparing more than two groups One-way ANOVA was used and multiple comparisons were conducted using Bonferroni test. The statistical analyses were performed using IBM SPSS statistics V23.0 (SPSS, Inc., Chicago, IL, USA). P-value <0.05 was considered significant. Histogram data are presented as mean values ± standard error of the mean.

### **3.3 Results**

### 3.3.1 Increased expression of ER-UPR genes in anterior eye tissues of pseudoexfoliation syndrome and glaucoma.

Relative expression of nineteen genes shortlisted on the basis of their involvement in protein folding,<sup>265</sup> protein quality control,<sup>266</sup> apoptosis,<sup>267</sup> and inhibiting protein aggregation<sup>268</sup> and suspected to be involved in pseudoexfoliation was compared between PEXS, PEXG and control using lens capsules and conjunctiva as study specimens (**Table 3.3**). Transcript levels of nineteen genes were investigated via custom RT<sup>2</sup> profiler PCR array.

**Table 3.3 List of the UPR genes with their functions and involvement in neurodegenerative diseases.** (AD- Alzheimer’s Disease; PD- Parkinson’s Disease; HD- Huntington’s Disease; ALS- Amyotrophic Lateral Sclerosis; POAG- Primary Open Angle Glaucoma; PSP- Progressive Supranuclear Palsy; CJD- Creutzfeldt–Jakob Disease; SPG- Spastic Paraplegia and PEX- Pseudoexfoliation).

Sl No.	Genes	Diseases	Functions	References
1	XBP1	AD,PD &HD	Activate UPR genes	269–271
2	PDIA5	POAG	Disulphide bond rearrangement	272
3	ERN1	HD	Trigger growth arrest and apoptosis	273
4	EIF2AK3	AD, PSP	Translation inhibition	274
5	ATF4	ALS	Transcriptional activator	275
6	ATF6	PD	ER stress sensor	276
7	DNAJB11	AD	Inhibit protein aggregation	277
8	TRAF2	PD	Anti-apoptotic signal	278
9	PPP1R15A	ALS	Dephosphorylates eIF2 $\alpha$	279,280
10	DDIT3	ALS	Apoptosis	267
11	CASP12	CJD, AD	ER stress mediated apoptosis	281,282
12	HSPA5	CJD, AD, ALS	Protein transport	283,284
13	CANX	AD	Protein folding and assembly	266
14	CALR	AD	Protein quality control	285
15	SYVN1	PD	Removes unfolded proteins	286
16	HSPB1	AD	HSPs regulation	287
17	DNAJB1	Poly Q	ATPase activator activity	288
18	HSPD1	SPG	Folding and assembly	265
19	CLU	AD,PEX	Extracellular chaperone	8,112,289

Upon comparison of the relative expression of targeted genes, we observed a significant upregulation in eight genes of the nineteen genes in the lens capsule of PEXS and PEXG affected eyes; while rest genes failed to show significant differential expression (**Table 3.4**). Expression of genes such as Eukaryotic translation initiation factor 2-alpha kinase 3 (EIF2AK3) (1.47 fold), DnaJ (Hsp40) homolog, subfamily B, member 11 (DNAJB11) (1.75 fold), Caspase 12 (CASP12) (1.61 fold), Heat shock 70kDa protein Family A Member 5 (HSPA5) (1.34 fold), synoviolin 1 (SYVN1) (2.26 fold), and Heat shock 60kDa protein D1 (HSPD1) (1.69 fold) were significantly upregulated in PEXS in comparison to control tissues with  $p \leq 0.05$  (**Figure 3.3**).

**Table 3.4** List of UPR related genes altered in lens capsule of PEXS and PEXG patients with respect to control. Genes that are highlighted in bold have significant expression change in fold compared to control samples with p value <0.05.

Position	Gene Symbol	PEXS LC (n=8)		PEXG LC (n=6)	
		Fold Change	p-Value	Fold Change	p-Value
1	<i>XBPI</i>	1.452	0.114	1.357	0.265
2	<i>PDIA5</i>	1.322	0.15	1.303	0.161
3	<i>ERN1</i>	1.129	0.778	1.504	0.193
4	<b><i>EIF2AK3</i></b>	<b>1.476</b>	<b>0.013</b>	1.218	0.357
5	<i>*GAPDH</i>	1	0	1	0
6	<i>ATF4</i>	0.98	0.928	1.244	0.127
7	<i>ATF6</i>	1.388	0.051	1.325	0.284
8	<b><i>DNAJB11</i></b>	<b>1.755</b>	<b>0.03</b>	1.409	0.23
9	<i>#TRAF2</i>	26.879	0.093	11.601	0.812
10	<i>PPP1R15</i>	1.369	0.146	1.932	0.341
11	<i>DDIT3</i>	1.231	0.254	1.625	0.055
12	<b><i>CASP12</i></b>	<b>1.62</b>	<b>0.003</b>	1.324	0.148
13	<b><i>HSPA5</i></b>	<b>1.35</b>	<b>0.047</b>	0.623	0.695
14	<b><i>CANX</i></b>	1.327	0.326	<b>1.914</b>	<b>0.044</b>
15	<i>CALR</i>	1.802	0.106	1.8	0.256
16	<b><i>SYVN1</i></b>	<b>2.267</b>	<b>0.005</b>	1.864	0.129
17	<i>*ACTB</i>	1.406	0.114	1.272	0.437
18	<i>HSPB1</i>	1.343	0.152	1.202	0.427
19	<i>DNAJB1</i>	1.438	0.109	1.418	0.052
20	<b><i>HSPD1</i></b>	<b>1.692</b>	<b>0.005</b>	1.341	0.078
21	<i>CLU</i>	1.002	0.943	1.362	0.166

\* GAPDH was identified as the most stably expressed housekeeping gene for data normalization, due to extensive variability in ACTB expression.

#Due to well detection problem in 96-well plate template (Well A5, CAPH13433) TRAF2 genes were found undetermined in most subjects.

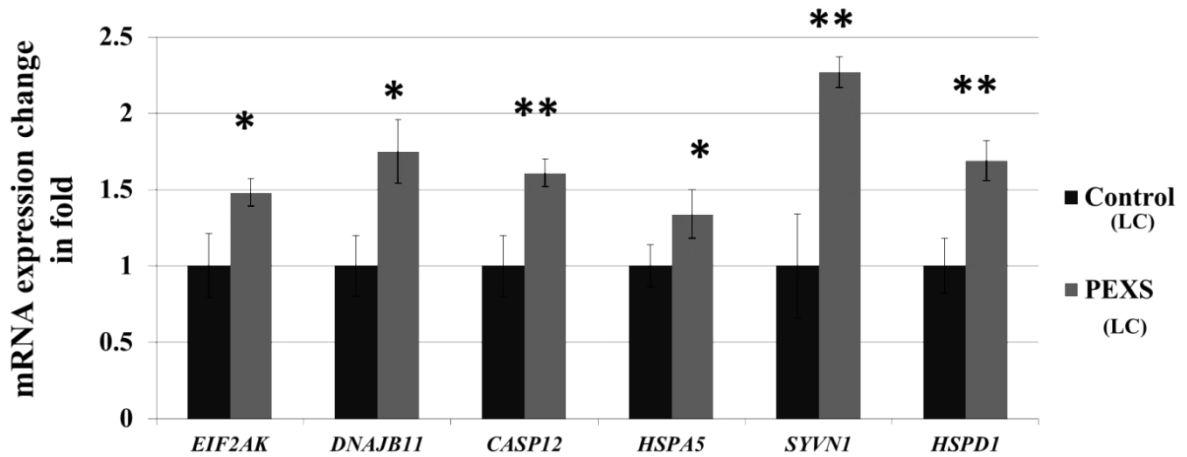


**Figure 3.3 Differentially expressed genes in lens capsule of PEXS individuals (n=8) with respect to control (n=8).** *SYVN1* showed greater than two fold changes in expression with respect to control. All genes were normalized against GAPDH from the panel of housekeeping genes. Errors bars represent standard error of mean (SEM). Sample size is denoted by ‘n’ and bar plot is represented as mean ± SEM. \*Represents P <0.05, \*\* P <0.01.

However, in lens capsules from PEXG affected individuals only calnexin (CANX) showed a significant upregulation (1.9 fold) with respect to control with  $p \leq 0.05$  (**Table 3.4**). Two new candidates, DNA-damage-inducible transcript 3 (DDIT3) (1.62 fold; P=0.05), and DNAJB1 (1.41 fold; p=0.05), showed differential expression data but did not reach statistical significance ( $p \geq 0.05$ ) (**Figure 3.4**). Demographics of the study subject used for PCR array presented in **Table 3.5**.

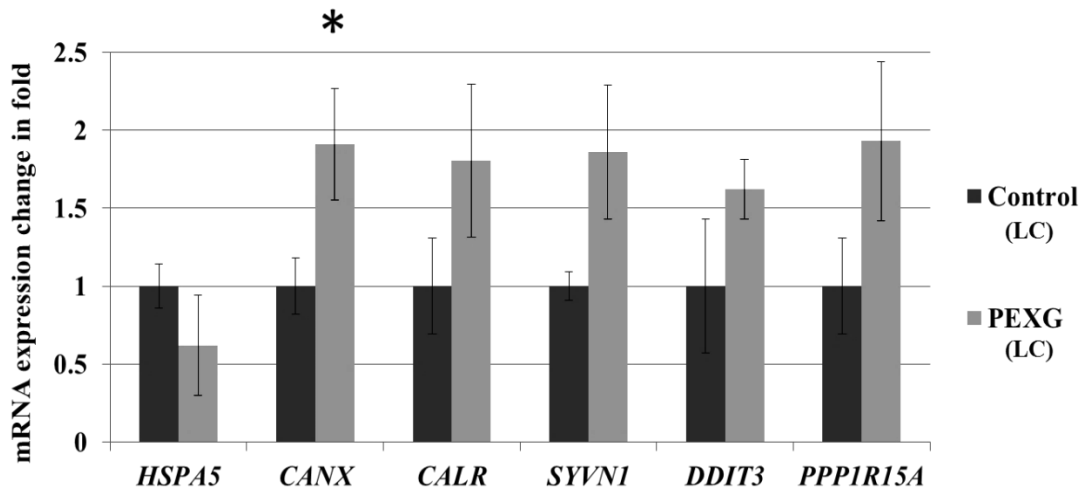


**Figure 3.4 Differentially expressed genes in lens capsule of PEXG individuals (n=6) with respect to control (n=6).** CANX showed significant and greater fold change in expression (1.91 fold; p=0.04) with respect to control. All genes were normalized against GAPDH from the panel of housekeeping genes.LC- lens capsule; n- sample size. Errors bars represent standard error of mean (SEM). Bar plot is represented as mean  $\pm$  SEM. \*Represents P <0.05, \*\* P <0.01.

**Table 3.5 Demographics of study subjects included for PCR array in LC tissues of PEXS and PEXG.** N=sample size.

Study subjects (Lens capsule)	N (Female in %)	Gender	P-value	Age (in years)	P-value
		Mean $\pm$ SEM		Mean $\pm$ SD	
PEXS	8(44%)	0.44 $\pm$ 0.17	0.83	69.11 $\pm$ 8.89	0.77
Control	8(50%)	0.5 $\pm$ 0.18		67.75 $\pm$ 9.99	
PEXG	6 (33%)	0.33 $\pm$ 0.21	0.49	67.5 $\pm$ 5.37	0.49
Control	6 (33%)	0.33 $\pm$ 0.21		69.5 $\pm$ 4.41	

On the contrary, in conjunctiva tissues though few genes showed greater fold change variation but many failed to reach significance due to large variance (**Table 3.6**). In conjunctiva tissue of PEXS subjects none of the genes showed significant expression changes in fold (**Figure 3.6**). However, a statistically significant upregulation of the X- Box binding protein 1(XBP1) (1.84 fold), DDIT3 (2.34 fold), HSPA5 (2.84 fold), and EIF2AK3 (2.45 fold) were detected in

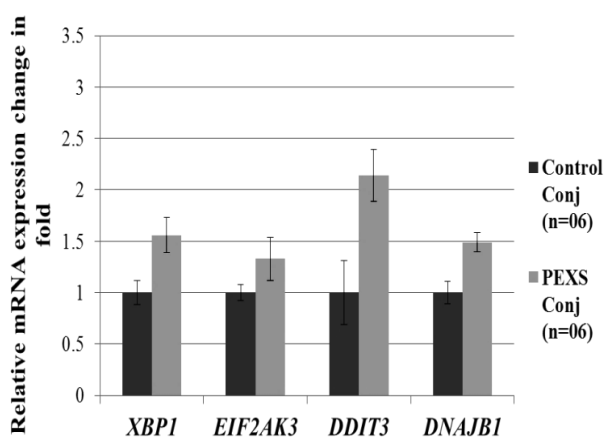
conjunctiva of PEXG individual with respect to control (**Figure 3.6**). Above all, PCR array results displayed a tissue specific differential expression pattern. Positive candidates were further validated with qRT-PCR.

**Table 3.6 List of UPR related genes altered in conjunctiva of PEXS and PEXG patients with respect to control.** Genes that are highlighted in bold showed significant change in expression compared to control samples with p value <0.05.

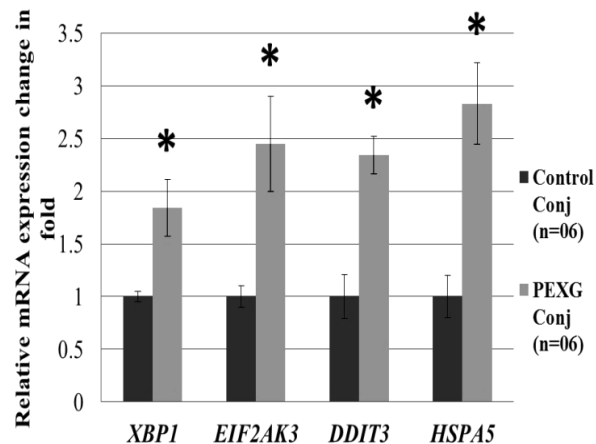
Position	Gene Symbol	PEXS conjunctiva (n=06)		PEXG conjunctiva (n=06)	
		Fold Change	p-Value	Fold Change	p-Value
1	<i><b>XBPI</b></i>	<b>1.565</b>	<b>0.43</b>	<b>1.836</b>	<b>0.045</b>
2	<i>PDIA5</i>	0.699	0.575	2.646	0.054
3	<i>ERN1</i>	0.839	0.966	2.91	0.066
4	<i><b>EIF2AK3</b></i>	<b>1.336</b>	<b>0.349</b>	<b>2.45</b>	<b>0.024</b>
5	<i>*GAPDH</i>	1	0	1	0
6	<i>ATF4</i>	1.02	0.413	1.16	0.275
7	<i>ATF6</i>	0.862	0.739	1.555	0.418
8	<i>DNAJB11</i>	0.805	0.61	1.405	0.528
9	<i>#TRAF2</i>	1.814	0.274	2.122	0.209
10	<i>PPP1R15</i>	1.153	0.384	1.427	0.261
11	<i><b>DDIT3</b></i>	<b>2.142</b>	<b>0.334</b>	<b>2.339</b>	<b>0.013</b>
12	<i>CASP12</i>	0.724	0.356	3.897	0.665
13	<i><b>HSPA5</b></i>	<b>0.841</b>	<b>0.903</b>	<b>2.835</b>	<b>0.026</b>
14	<i>CANX</i>	0.669	0.54	0.835	0.444
15	<i>CALR</i>	0.77	0.795	0.631	0.183
16	<i>SYVNI</i>	1.199	0.354	1.014	0.522
17	<i>*ACTB</i>	1.207	0.307	0.786	0.613
18	<i>HSPB1</i>	1.229	0.406	0.36	0.172
19	<i>DNAJB1</i>	1.49	0.593	1.331	0.321
20	<i>HSPD1</i>	1.326	0.431	1.24	0.247
21	<i>CLU</i>	0.704	0.302	0.388	0.336

\* GAPDH was identified as the most stably expressed housekeeping gene for data normalization, due to extensive variability in ACTB expression.

#Due to well detection problem in 96-well plate template (Well A5, CAPH13433) TRAF2 genes were found undetermined in most subjects.



A.



B.

Study subjects (Conjunctiva)	N (Female in %)	Age (in years)	P-value	Gender	P-value
		Mean $\pm$ SD		Mean $\pm$ SEM	
PEXS	6 (50%)	67.33 $\pm$ 6.21	0.95	0.50 $\pm$ 0.22	0.59
Control	6 (33%)	67.00 $\pm$ 12.47		0.33 $\pm$ 0.21	
PEXG	6 (33%)	66.33 $\pm$ 5.39	0.61	0.33 $\pm$ 0.22	0.9
Control	6 (33%)	68.16 $\pm$ 6.61		0.33 $\pm$ 0.21	

C.

**Figure 3.5 Altered expression of genes involved in the ER-UPR in conjunctiva of PEX patients.** A. Differentially expressed genes in the conjunctiva of PEXS individuals (n=06) with respect to control (n=06). B. Differentially expressed genes in lens capsule of PEXG individuals (n=06) with respect to control (n=06). All genes were normalized against GAPDH from the panel of housekeeping genes. ‘n’ denotes the sample size, conj refers to conjunctiva. Errors bars represent standard error of mean (SEM) and expression change in fold is represented as mean  $\pm$  SEM. C. Demographic of the study subjects included for PCR array of control, PEXS and PEXG in conjunctiva tissue. \*Represents P < 0.05, \*\* P < 0.01.

### 3.3.2 Validation of increased expression of deregulated genes in lens capsule and conjunctiva of PEX affected tissues

After the primary screening of the nineteen genes through RT<sup>2</sup> profiler, we independently validated the highly deregulated genes, through real-time PCR in freshly acquired lens capsule

and conjunctiva tissues from study subjects. We validated the mRNA expression of *SYVNI* and *CANX* in the lens capsule of PEXS and PEXG subjects. Similar to PCR array results, we observed a significant increase in the mRNA expression of *SYVNI* in the lens capsule of PEXS (1.57 fold) and even also in PEXG (1.73 fold) when compared with that of control (**Figure 3.6 A**). *CANX* showed upregulation in the lens capsule of PEXG subjects (2.04 fold) compared to control individuals, while no significant changes were observed for PEXS (1.19 fold) in accordance with PCR array results (**Figure 3.6 B**).

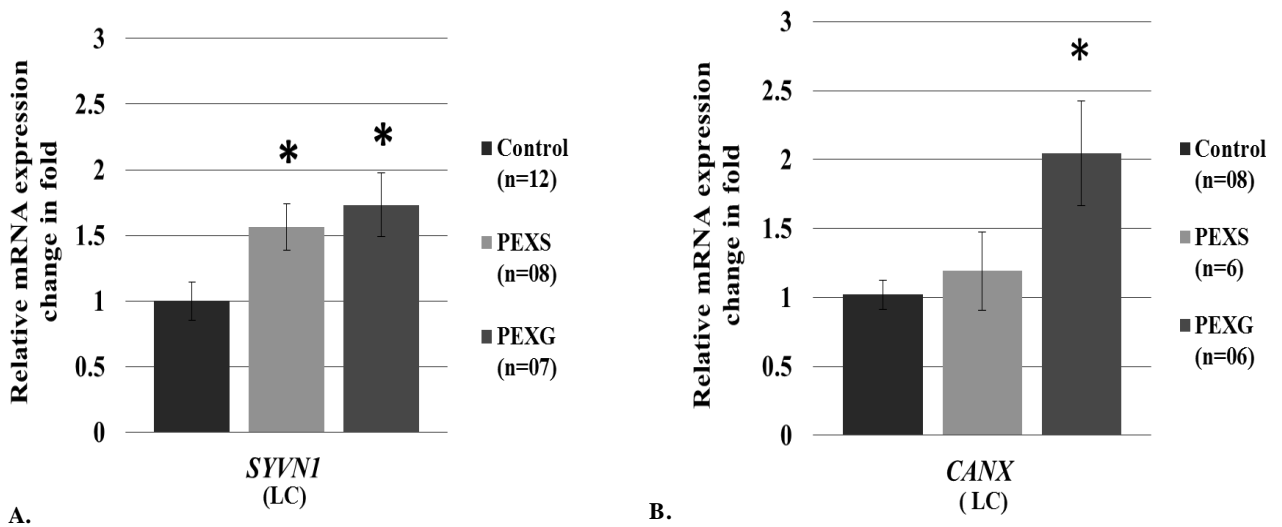


**Figure 3.6 mRNA expression of *SYVNI* and *CANX* validated in lens capsule of study subjects.** **A.** Synoviolin1 was found to be significantly upregulated with respect to control in PEXS ( $p=0.03$ ) and PEXG ( $p=0.01$ ) suggesting its involvement in PEX pathogenesis. **B.** Calnexin showed significant upregulation in PEXG (0.03), while no differential expression was observed for PEXS ( $p=0.58$ ) with respect to control in accordance with PCR array results. Age-gender matched study subjects used in the experiments. Error bar represents Mean  $\pm$  SD. \* P-value<0.05.

Subsequently, we validated the expression of highly deregulated genes obtained from PCR array in conjunctiva tissues via qRT-PCR. Similar to the PCR array results, in PEXG conjunctiva samples genes which showed differential change in expressions are EIF2AK3 (2.08 fold;  $p=0.10$ ), DDIT3 (1.74 fold;  $p=0.49$ ) and HSPA5 (1.83 fold;  $p=0.06$ ) with respect to control, but

failed to reach statistical significance on independent validation by RT-PCR due to large variance (**Figure 3.7**). Likewise, in conjunctiva of PEXS tissues none of the genes showed significant fold change. In nutshell, PCR array results suggest tissue-specific operation of different mechanisms in the onset of early and severe form of PEX.

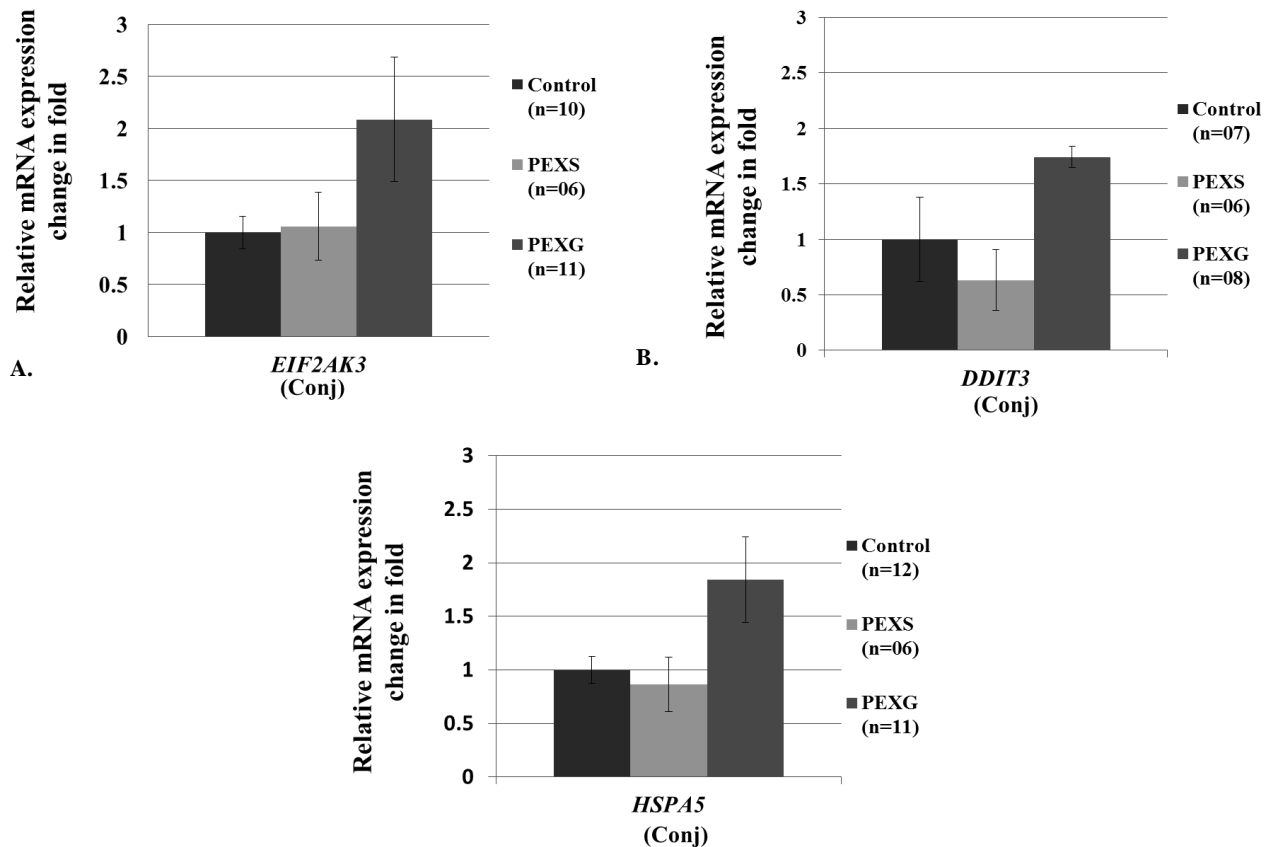


**Figure 3.7 Validation of UPR PCR array results in conjunctiva tissues by quantitative real-time PCR.** Bar graph shows the mRNA expression of *EIF2AK3* (p=0.10), *HSPA5* (p=0.06), and *DDIT3* (p=0.49) checked in conjunctiva of study subjects respectively. Due to large variance in study none of the genes showed statistical significance on validation. Age-gender matched study subjects recruited for the experiment. Error bar represents Mean  $\pm$  SD. \* P-value<0.05.

### 3.3.3 Validation of increased expression of differentially regulated genes in the PEX affected tissue

After the primary screening of the nineteen genes through RT<sup>2</sup> profiler, and independent validation of the highly deregulated genes, we found *SYVN1* and *CANX* to be consistent in their expression in lens capsule tissues. Thus, we further analyzed the protein expression and localization of synoviolin 1 that were significantly upregulated at the mRNA level in PEX lens capsule tissues, indicating impaired protective mechanisms; we performed western blot analyses using lens capsule extracts and immunohistochemistry on tissues of PEXS, PEXG and control eyes. When synoviolin 1 level was checked through western blotting, it showed substantial  $\geq$ two-fold upregulation in both PEXS (2.24 fold) and PEXG (2.45) individuals in comparison to controls (**Figure 3.8**). By densitometry analysis, we found increased synoviolin1 immunoreactivity in whole tissue lysate of PEXS and PEXG individuals.

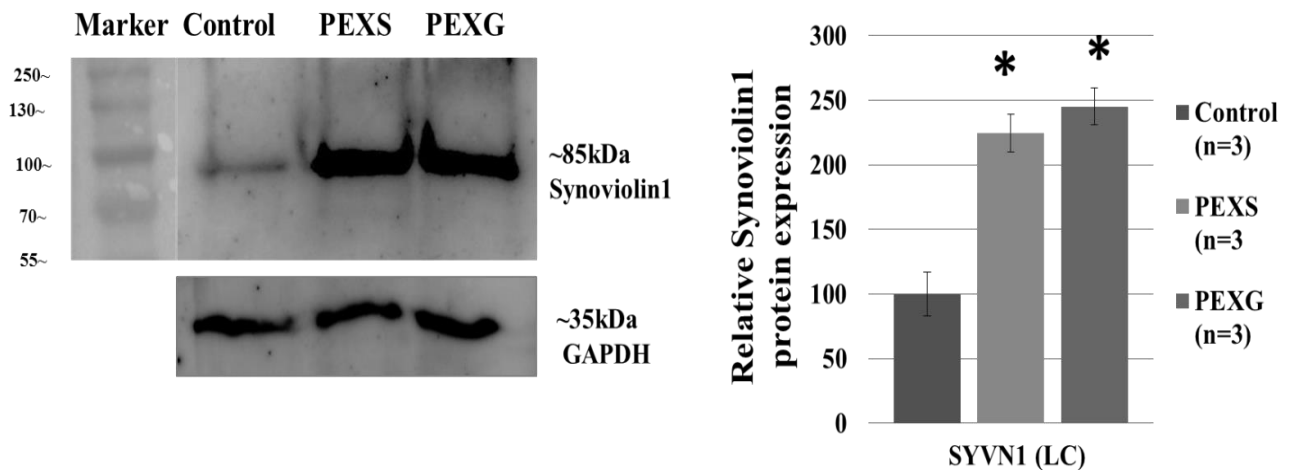


**Figure 3.8 Western blot analysis of SYVN1 in lens capsule extracts of control, PEXS and PEXG subjects.** **A.** In consistent with mRNA data synoviolin1 protein showed significant upregulation in PEXS and PEXG cases with respect to control tissue extract. **B.** Densitometry analysis of synoviolin1 protein normalized to loading control. Bar plot represented as Mean  $\pm$  SE of three independent experiments. Age-sex matched study subjects used in the experiment. Sample size denoted by ‘n’; LC- lens capsule. \* P-value<0.05.

We further validated the expression of SYVN1 through intracellular immunostaining in lens capsules. The relative fluorescence intensity of SYVN1 demonstrated a significant increase in both PEXS and PEXG individuals when compared to control subjects (**Figure 3.9**).

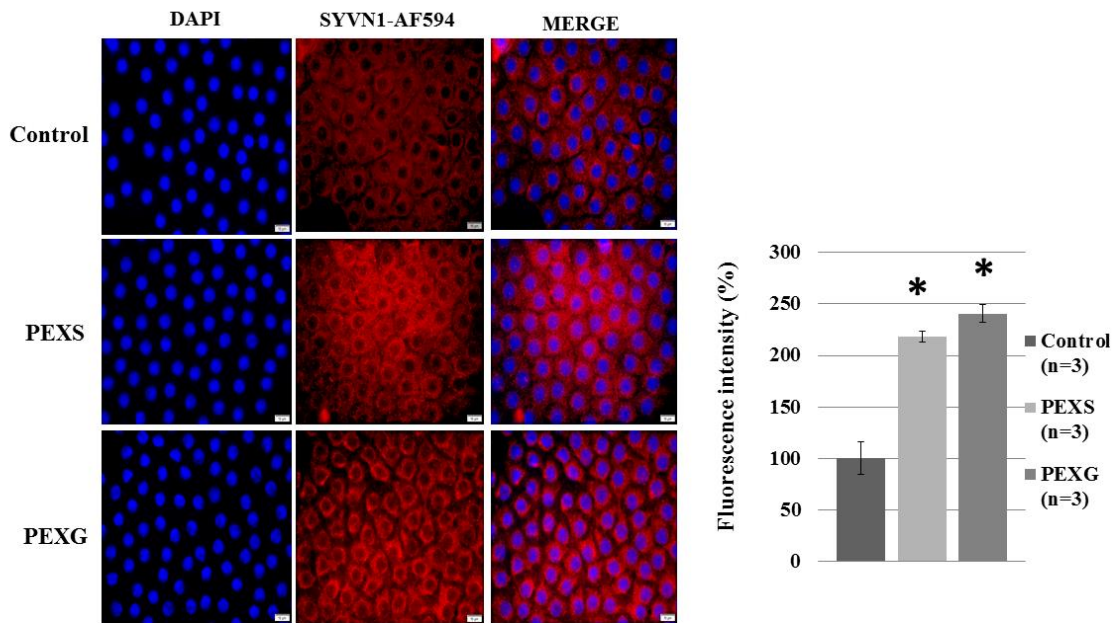


**Figure 3.9 Confocal microscopy analysis showing presence of SYVN1 in lens capsule of control, PEXS and PEXG subjects.** **A.** Increase of Synoviolin 1 immunoreactivity was observed in lens capsule of PEXS and PEXG with respect to control tissues. Nuclear staining with DAPI and SYVN1-IF detected by Alexa 594. Magnification, 60X. Scale bar 20 $\mu$ m. **B.** Synoviolin 1 immunoreactivity in lens capsules obtained from study subjects were measured using ImageJ. Field views were taken into consideration for the fluorescence quantitation of each sample. In consistent with mRNA data, the increased expression of Synoviolin 1 protein was statistically significant in PEXS and PEXG (p-0.03 and p-0.009 respectively). Bar plot represented as mean $\pm$  SE of three or more independent experiments. Age-gender matched study subjects employed for the experiments. Sample size denoted by 'n'; LC- lens capsule. \*P<0.05.

CANX also showed upregulation at protein level (2.84 fold) in the LC of PEXG subjects compared to control individuals as demonstrated by western blot analysis (**Figure 3.10**). However, we did not find any significant difference in calnexin at protein level in PEXS (1.39

fold) with respect to control. Our validation data are in consensus with the preliminary RT2 profiler data.

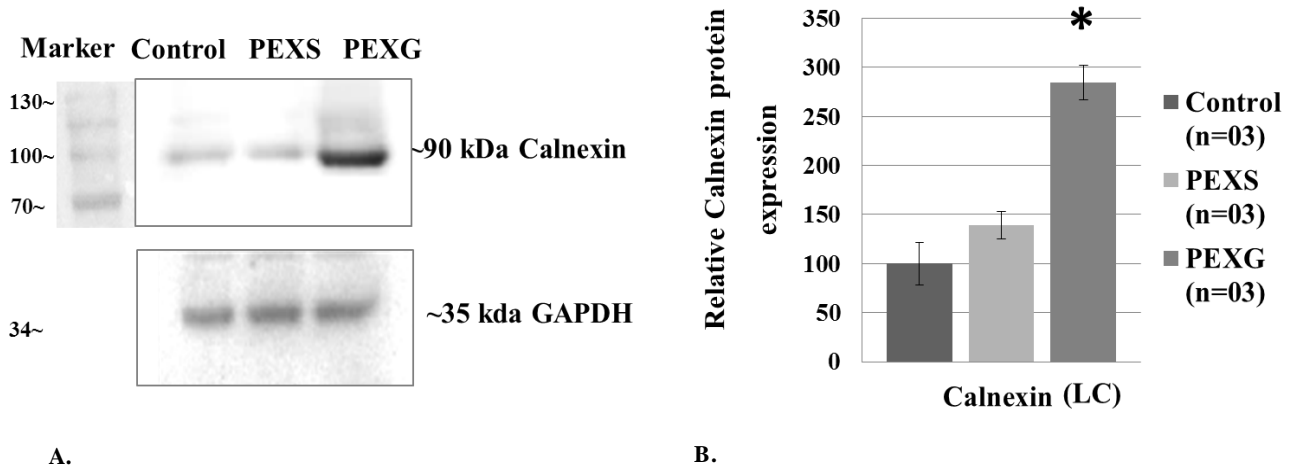


**Figure 3.10 Western blot analysis of calnexin in the tissue extract of PEX affected subjects. A.** Representative Immunoblot of CANX showed significant upregulation in PEXG ( $p=0.02$ ) but not in PEXS cases with respect to control tissue extract. **B.** Quantification of the immunoblot of CANX expression was normalized for GAPDH and is presented as percentage over control. Bar plot represented as mean  $\pm$  SE of three or more independent experiments. Study subjects for the above experiment were age-gender matched. Sample size denoted by ‘n’; LC- lens capsule; \*Represents  $P < 0.05$ .

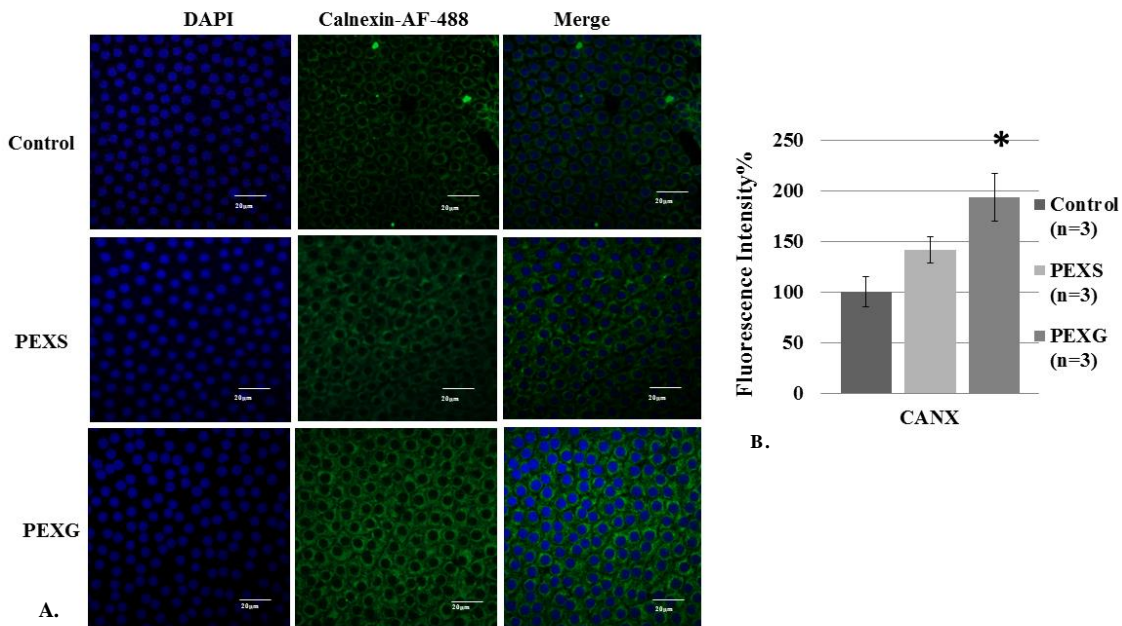


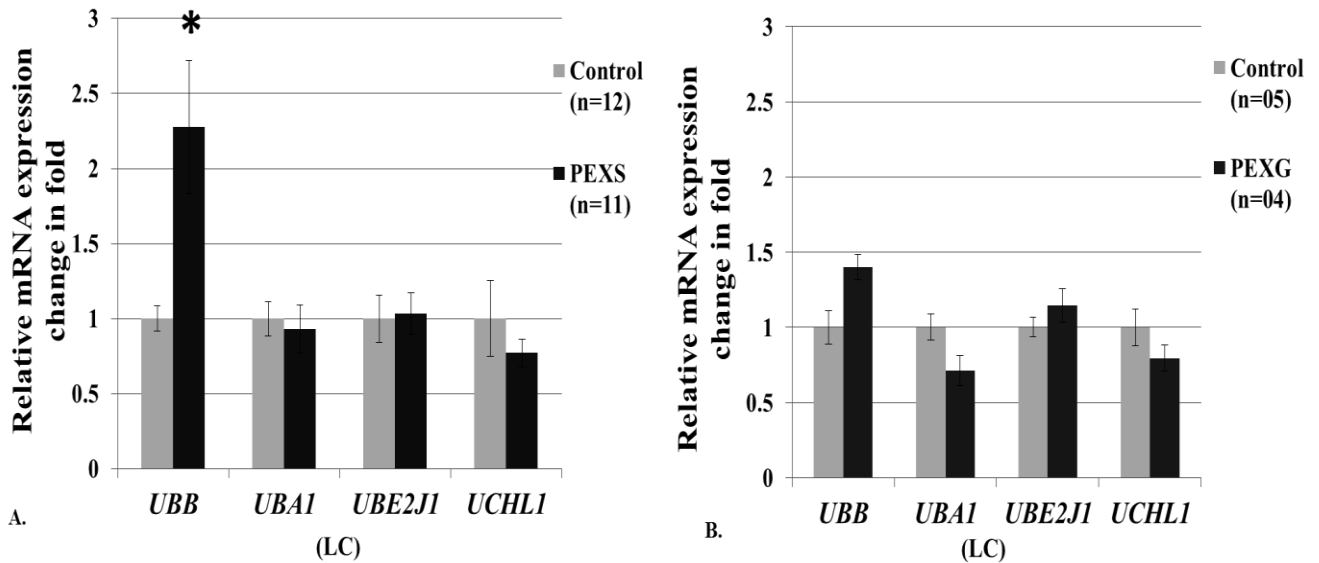
**Figure 3.11 Confocal immunofluorescence analysis of calnexin.** **A.** Increased CANX immunoreactivity was observed in lens capsule of PEXS and PEXG with respect to control tissues. Nuclear staining with DAPI and CANX-IF detected by Alexa-fluor 488. Magnification, 63X. **B.** CANX immunoreactivity in lens capsules was measured using ImageJ. 2-3 field views were taken into consideration for the fluorescence quantitation of each sample of PEXS (n=3) and PEXG (n=3) (p=0.33 and p=0.03 respectively) individuals as compared to control (n=3). Bar plot represented as mean± SE of three or more independent experiments. Age-gender matched study subjects recruited for the experiment. Sample size denoted by 'n'; LC- lens capsule; \*Represents P <0.05, \*\*P<0.01.

In case of CANX immunofluorescence (**Figure 3.11**), increased calnexin immunoreactivity was observed in PEXG with respect to control tissues. Substantiating the RNA data, the protein expression data of CANX as quantitated from immunofluorescence intensity in PEXS samples remained indifferent to the disease condition.

### **3.3.4 Increased expression of UBB and reduced expression of proteasome subunits**

To study further the role of degradative components involved in PEX pathology, we analyzed mRNA expression by performing qRT-PCR assays of four major ubiquitin genes studied for the first time in lens capsules of control, PEXS and PEXG individuals. Ubiquitin like modifier activating enzyme 1 (UBA1) participates in ubiquitination and is also linked with other neurodegenerative diseases.<sup>290</sup> Ubiquitin B (UBB) the most conserved proteins required for intracellular protein degradation, ubiquitin carboxy-terminal hydrolase L1 (UCHL1) a deubiquitinating enzyme that stabilize the monomers of ubiquitin preventing their degradation and ER-associated ubiquitin conjugating enzyme E2, J1 (UBE2J1) that participates in the clearance of misfolded membrane proteins from the ER via ERAD pathway.<sup>291</sup> We observed increased UBB mRNA expression in PEXS (2.27 fold; p=0.01) individuals with no significant differences in PEXG (1.39 fold; p=0.23) and control. While, other ubiquitin genes; UBA1 (0.93 fold; p=0.64), UBE2J1 (1.03 fold; p=0.83) and UCHL1 (0.77 fold; p=0.0.7) did not show any

significant or considerable differences in mRNA expression in either PEXS or in PEXG affected cases when compared with control (**Figure 3.12**).

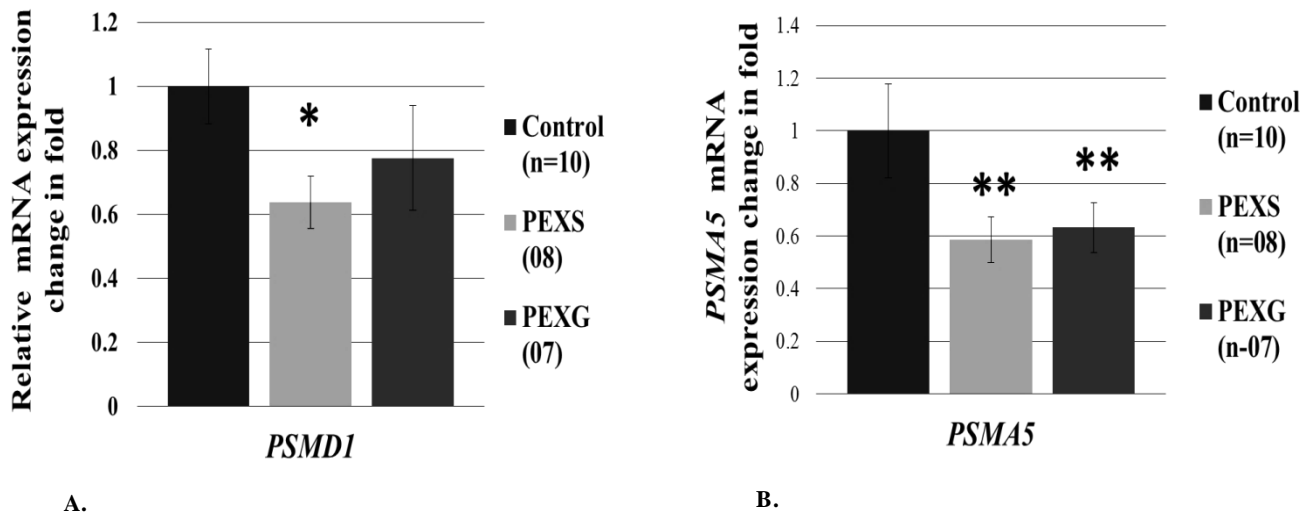


Study subjects (Lens capsule)	N (Female in %)	Gender	P-value	Age (in years)	P-value
		Mean $\pm$ SEM		mean $\pm$ SD	
PEXS	11 (23%)	0.23 $\pm$ 0.12	0.17	75.30 $\pm$ 7.21	0.28
Control	12 (57%)	0.57 $\pm$ 0.13		68.71 $\pm$ 11.59	
PEXG	4 (25%)	0.5 $\pm$ 0.25	0.68	72.66 $\pm$ 7	0.47
Control	5 (40.6%)	0.66 $\pm$ 0.33		68 $\pm$ 4	

C.

**Figure 3.12 mRNA expression of ubiquitin genes in lens capsule of study subjects.** **A.** mRNA expression of UBB, UBA1, UBE2J1 and UCHL1 in lens capsules of control and PEXS. No significant differences were observed in any of the studied genes in lens capsule of PEXS except UBB (2.27 fold;  $p=0.01$ ) versus age matched control. **B.** mRNA expression of UBB (1.23 fold;  $p=0.23$ ), UBA1 (0.79 fold;  $p=0.35$ ), UBE2J1 (1.13 fold;  $p=0.74$ ) and UCHL1 (0.86 fold;  $p=0.20$ ) in lens capsules of control and PEXG showing no significant differences. Sample size is denoted by 'n'; LC- lens capsule, bar plot is represented as mean  $\pm$  SEM. **C.** Demographics table for samples used for comparing mRNA expression of ubiquitin genes. N-sample size. \* $P<0.05$ .

To further investigate the status of proteasome degradation machinery, we analyzed the mRNA expression of two important proteasome subunits PSMD1 (26S proteasome non-ATPase regulatory subunit 1) and PSMA5 (Proteasome subunit alpha type-5). In **Figure 3.13**, PSMD1 displayed a significant downregulation in the lens capsule of PEXS eyes (0.74 fold;  $p=0.03$ ) in comparison to control samples with no significant difference observed in PEXG cases (0.90 fold;  $p=0.41$ ). Whereas, PSMA5 showed the significant reduced expression in the lens capsule of PEXS (0.60 fold;  $p=0.003$ ) and PEXG subjects (0.65 fold;  $p=0.009$ ) when compared with control.



Study Subjects (Lens capsule)	N (Female in %)	Gender	P-value	Age (in years)	P-value
		Mean± SEM		Mean± SD	
PEXS	8 (50%)	0.5 ± 0.18	0.42	69.75 ± 6.204	0.32
Control	10 (70%)	0.70 ± 0.15		65.6 ± 10.77	
PEXG	7 (42%)	0.42 ± 0.20	0.3	69.71 ± 5.05	0.31
Control	10 (70%)	0.70 ± 0.15		65.6 ± 10.77	

**Figure 3.13 Differential expression of proteasome subunits, PSMD1 and PMSA5 in the lens capsule of study subjects. A.** PSMD1 was found to be significantly downregulated in PEXS (0.74 fold;  $p=0.03$ )

with respect to control, while no significant differences observed in PEXG (0.90 fold;  $p=0.41$ ). **B.** PSMA5 showed decreased expression in both PEXS (0.60 fold;  $p=0.003$ ) and PEXG (0.65 fold;  $p=0.009$ ) with respect to controls. Decrease in proteasome subunits expression suggest decrease in proteasome activity and impaired proteasome degradation pathway Expression change in fold is represented as mean  $\pm$  SEM Sample size is denoted by 'n'; LC- lens capsule, **C.** Demographics of study subjects for samples used for comparing mRNA expression of proteasome subunits. N- sample size. Student's t-test was used to calculate statistical significance between groups. \* $P<0.05$ ; \*\* $P<0.01$ .

### 3.3.5 Decreased proteasome activity and increased ubiquitinated proteins in the lens capsule of PEXS individuals.

Anticipating an effect of the deregulation of proteasomal subunits on proteasome activity, we checked the chymotrypsin-like proteasome activity in the tissue lysate of lens capsule from study subjects using Proteasome-Glo<sup>TM</sup> Chymotrypsin-Like Assay. To determine the specific proteasomal activity, immunoblotting of 26S proteasome S4-subunit (PSMC1) was performed which correlates with the proteasomal protein content (**Figure 3.14**).

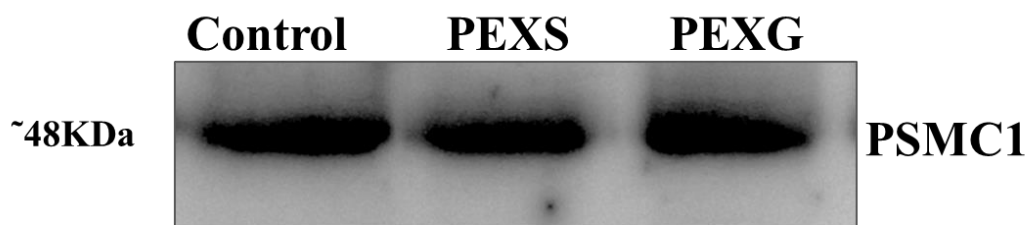
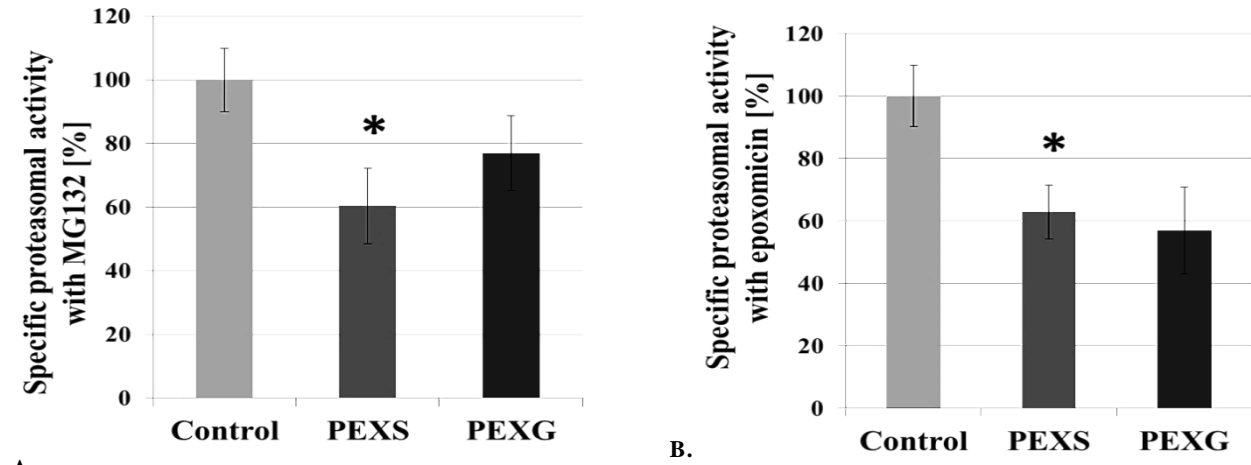


**Figure 3.14** Representative Immunoblot showing the presence of the 26S proteasome S4-subunit (PSMC1) in the protein extracts obtained from control, PEXS and PEXG samples. Quantification of all three bands was performed to calculate specific proteasomal activity.

We further examined the chymotrypsin like-proteasome activity in lens capsule extracts of PEX affected subjects. **Figure 3.15A**, illustrates a significant decrease in the specific chymotrypsin-like proteasome activity in PEXS ( $p=0.03$ ) individuals with respect to controls when reversible inhibitor MG132 was used to eliminate background activity. Likewise, in **3.15B**, proteasome

activity was found to be significantly decreased in PEXS ( $p=0.01$ ) but not in PEXG individuals ( $p=0.08$ ) using  $15\mu\text{M}$  epoxomicin, a specific and irreversible inhibitor.



Study subjects (LC protein extracts)	N (Female in %)	Age (in years)	P-value	Gender	p-value
		Mean $\pm$ SD		Mean $\pm$ SEM	
PEXS	3 (33%)	65.0 $\pm$ 5.01	0.68	0.33 $\pm$ 0.33	1
PEXG	3 (33%)	68.0 $\pm$ 10.44	0.84	0.33 $\pm$ 0.3	1
Control	3 (33%)	67.00 $\pm$ 6.08		0.33 $\pm$ 0.3	

C.

**Figure 3.15 Determination of the specific chymotrypsin-like proteasomal activity in lens capsule extracts from control PEXS and PEXG.** **A.** The mean specific chymotrypsin-like proteasomal activities in protein extracts of control, PEXS and PEXG with  $20\mu\text{M}$  reversible MG132 inhibitor. We found a significant decrease of proteasomal activity in PEXS individual with respect to control. **B.** The mean specific chymotrypsin-like proteasomal activity in protein extracts of control, PEXS and PEXG with  $15\mu\text{M}$  specific and irreversible epoxomicin inhibitor. In accordance with reversible inhibitor the PEXS subjects showed significant decrease in proteasomal activities with respect to control. The mean activities of PEXS and PEXG are given as percentages from mean activities of the control. **C.** Demographics of the study subjects included for proteasome activity assay are tabulated. Luminescence values were derived from three independent experiments, each read out three times using lens capsule extract from control, PEXS and PEXG. N refers to sample size. \* $P<0.05$ .

Decreased proteasome activity led us to check the amount of ubiquitination, where through immunoblotting we found an increased accumulation of ubiquitinated proteins in LC lysate of PEXS affected tissues that was significantly higher compared control (p=0.04) (**Figure 3.16**).

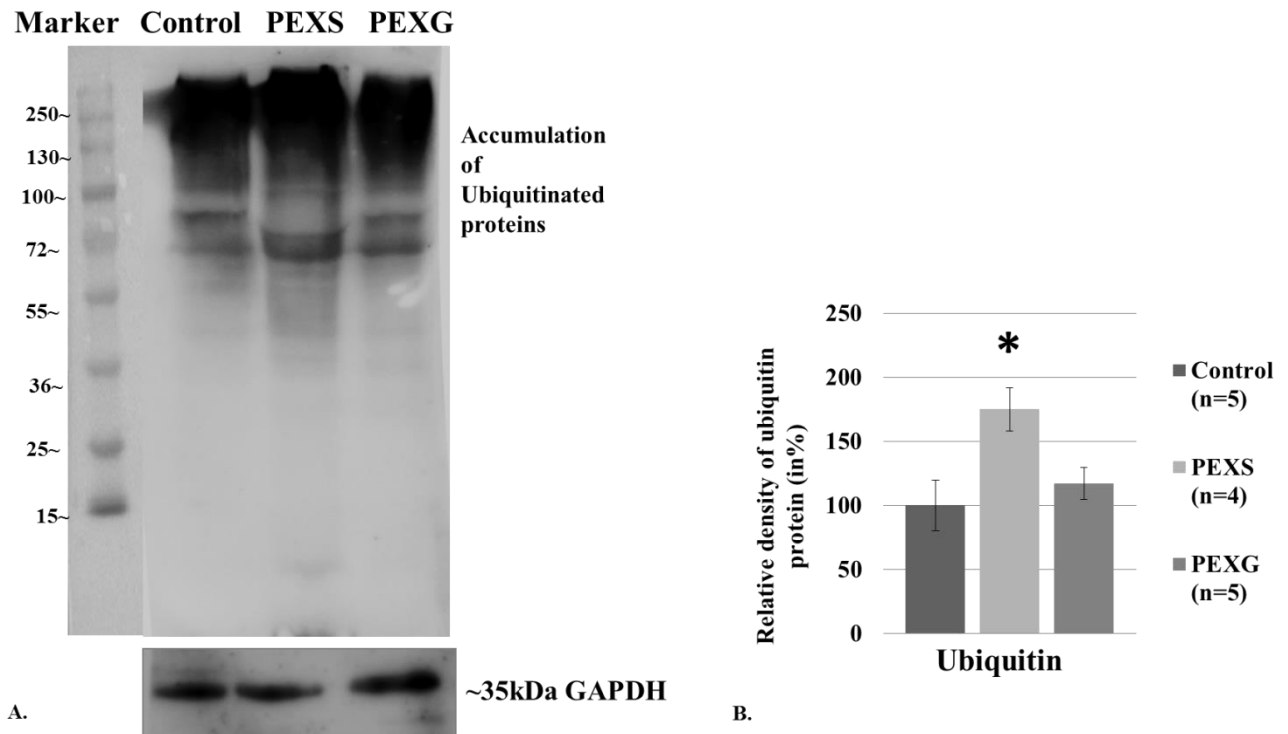


**Figure 3.16 Immunoblot analyses of ubiquitinated proteins in tissue lysate of PEXS, PEXG and control.** **A.** Western blot analysis showed PEXS had increased level of ubiquitination in a broad region of membrane proteins shown as enhanced smears. GAPDH served as the loading control. **B.** Densitometry analysis of immunoblots normalized to GAPDH. Sample size denoted by ‘n’; LC- lens capsule. **C.**

Demographics of study subjects included for immunoblotting is tabulated. N= sample size. Bar graph are expressed as the mean  $\pm$  SE of more than three independent experiments. \* $p$ <0.05.

### 3.3.6 Increased apoptotic cell death in lens capsule of PEXS and PEXG subjects

Decreased proteasome activity and increased ER stress can perturb protein homeostasis and induce apoptosis, thus, we performed TUNEL assay using lens capsule tissues of PEXS, PEXG and control individuals to check for apparent cell death when misfolded protein accumulates beyond a threshold. Immunofluorescence analysis (**Figure 3.17**) in the lens capsule of PEXS and PEXG individuals showed a significant increase in the number of TUNEL-positive cells when compared with control suggesting that an elevated ER stress and reduced level of UPS components might be responsible for increased apoptosis.

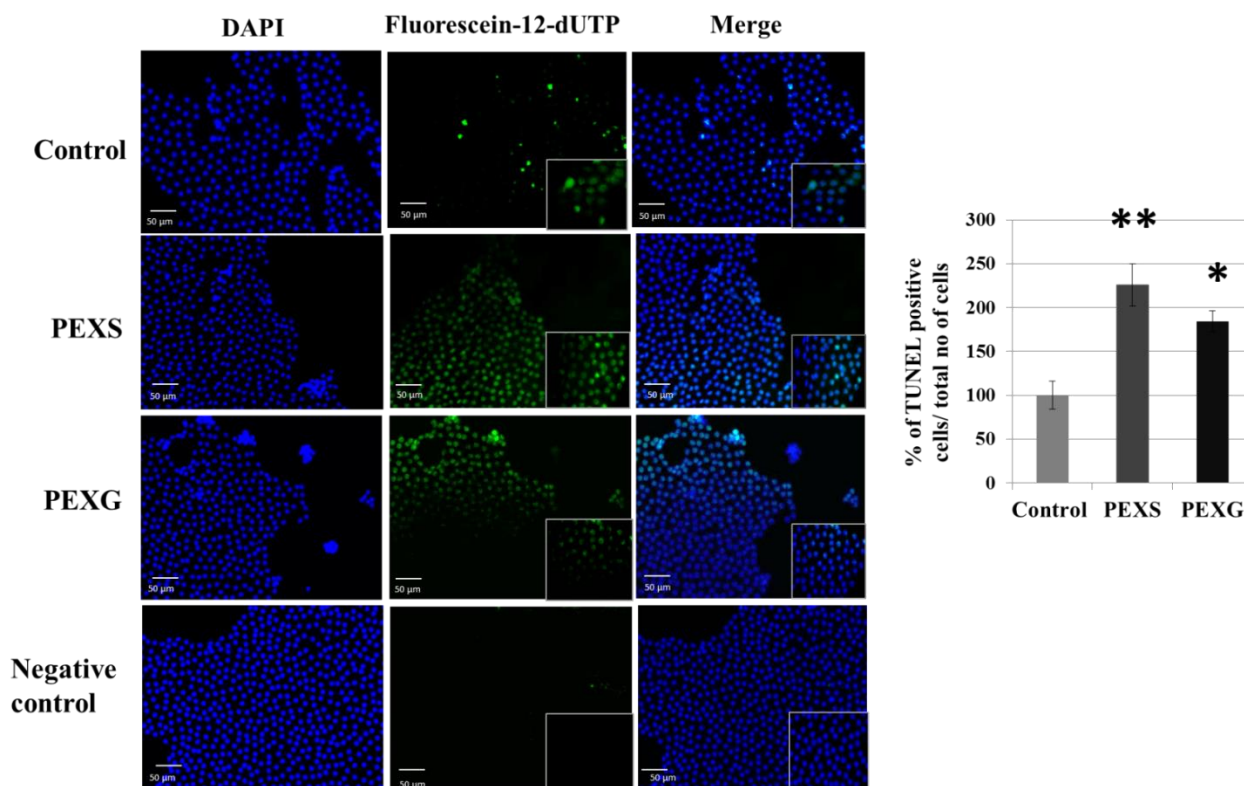


**Figure 3.17 Increased apoptosis in the lens capsule of PEXS individuals.** A. Representative immunofluorescence image of TUNEL assay in the lens capsule of control, PEXS and PEXG individuals.

All pictures were taken at 200x and 600x magnification. Scale bars, 50  $\mu$ m. White arrows show the apoptotic cells. B. Quantification of TUNEL positive cells per field is shown. PEXS (n=4) and PEXG (n=3) showed significant increase of apoptotic cells (p=0.002 and p=0.02, respectively) when compared with control tissues (n=4). For each group, 2–3 fields were randomly selected, and the captured TUNEL and DAPI images were overlaid using ImageJ software. Cells labeled with both TUNEL and DAPI were noted as TUNEL-positive. Age-gender matched study subjects were included in the experiments. Values are presented as percentage of TUNEL-positive cells/total cells per field  $\pm$  SEM. \*P <0.05, \*\*P<0.01.

### 3.4 Discussion

Proteostasis impairment is now acknowledged as one of the major underlying cause of many neurodegenerative diseases.<sup>292–295</sup> The diminution of proteome activity is considered as one of the hallmarks of age-related diseases ranging from AD to PD including PEX where genes involved in proteasome pathway i.e. UBE2A/B were reported to have reduced expression.<sup>296, 199</sup> PEX is mainly characterized by the aggregation of extracellular matrix (ECM) material in both ocular and extra-ocular tissues, which suggests that aberrant ECM synthesis or impaired degradation may contribute to disease pathogenesis.<sup>297</sup> Protein misfolding leading to deposition of fibrillar material might be the main reason behind the onset of this disease. ER dysfunction has been implicated in the formation of myocilin aggregates in patients with myocilin caused Glaucoma<sup>298</sup> and is also associated with formation of extracellular aggregates and amyloid fibers.<sup>299</sup> Several components of cellular stress response such as HSF1, superoxide dismutase, Growth arrest and DNA damage-inducible gene 153 (GADD153) were found to be dysregulated in PEX eyes.<sup>114,199</sup> Impaired regulation of cytosolic UPR genes, HSPs and HSF1 in PEX (as reported in Chapter1) made us to explore the components of ER-UPR to understand the nature of its pathogenesis.

### **3.4.1 Altered expression of genes involved in the ER-UPR in anterior eye tissues of PEX patients.**

In this chapter, we investigated the components of UPR, UPS and apoptosis in PEX affected individuals as comprehensive information on ER-associated degradation (ERAD) and UPS in connection with the ER stress in PEX is limiting. RT<sup>2</sup>-PCR array using lens capsule of PEX individuals revealed a significant increase in the expression of ER-UPR components involved in folding and assembly of proteins (DNAJB11, HSPD1, DNAJB1, HSPA5 and CANX), translation inhibition (EIF2AK3), apoptosis execution (CASP12), protein degradation and anti-apoptosis (SYVN1) in PEX affected individuals. Increased level of chaperones within the ER, such as HSPA5, CANX; an ER luminal chaperone targets the misfolded protein cargo for their degradation through ERAD pathway<sup>300-302</sup> suggests that ER-UPR first tries to alleviate the debilitated homeostasis by upregulating their expressions.<sup>303</sup> We also found an increase in EIF2AK3, a serine/threonine protein kinase that inhibits global protein synthesis, in PEXS. Study by Hoozemans and colleagues found that the EIF2AK3 (PERK) expression was increased in the AD hippocampal neurons, particularly in neurons containing granulovacuolar degeneration..<sup>268</sup> Increase in DNAJB1 and HSPD1 is also consistent with previous studies which showed an upregulation of ER-related stress proteins in PEX affected tissues.<sup>199</sup> However, we observed tissue specific expression in conjunctiva of PEXG individuals, where XBP1, EIF2AK3, DDIT3 and HSPA5 genes showed significant upregulation but on independent validation though maintained the fold difference but failed to reach significance due to large variance. Increasing the sample size could have made the data more significant but we invested the limiting samples in understanding the mechanism of proteostasis impairment in PEX pathogenesis.

Among all candidates, SYVN1 was picked as a novel UPR candidate gene with a role in PEX pathology being highly upregulated in PEXS and PEXG affected lens capsules. Synoviolin 1

also known as HRD1 (3-hydroxy-3-methylglutaryl reductase degradation protein 1), an E3 ubiquitin ligase plays a prominent role in ERAD system to maintain protein homeostasis. It suppresses ER stress induced cell death by degrading misfolded proteins through the UPS.<sup>304,305</sup> It has been observed that under ER-stress conditions, both mRNA and protein levels of synoviolin1 increases to provide cytoprotection against cell death.<sup>306</sup> Masayuki Kaneko et al., demonstrated the protective effect of HRD1 (SYVN1) overexpression against ER stress-induced apoptosis in Parkinson's disease (PD).<sup>307</sup> Therefore, upregulation of synoviolin1 in response to ER-stress via UPR signaling pathways in PEX most likely represents its cytoprotective behavior whereby, it degrades the accumulated misfolded proteins in the ER. Importantly, SYVN1 associates with cofactors to execute ERAD, but their roles and how they assemble with SYVN1 are not well understood. Further, we envisioned that tracing molecular analysis of the SYVN1 localization and function may help enhance our understanding of PEX pathogenesis.

Similar to Synoviolin1, we also observed increased Calnexin expression in lens capsule of PEXG individuals. Calnexin is an integral protein that assists in protein folding and quality control and is upregulated primarily as an intracellular defense mechanism against cellular stress.<sup>308</sup> Overexpression of Calnexin has been reported to suppress amyloid beta (A $\beta$ ) production in Alzheimer's disease.<sup>266</sup> Importantly, Calnexin is a component of the early autophagosomes pointing to its potential role in an alternative mechanism for degradation of misfolded proteins and removal of organellar membranes.<sup>309</sup> Calnexin translocate specific substrates to synoviolin1 which together with UBE2J1 (E2 ubiquitin-conjugating enzyme) target it for ubiquitination and degradation. Hence, activation of UPR is taken as an indicator that ER function is disturbed in PEX pathological process under investigation.

### **3.4.2 Impaired UPS in PEX affected tissues**

Based on the above results, we further investigated the components of UPS where we found an upregulation in one of the ubiquitin response genes, UBB in PEXS but not in PEXG samples. Although there aren't any direct reports on UBB overexpression with PEX, upregulation of ubiquitin-protein conjugates and enhanced ubiquitin conjugation activity were observed in response to oxidative stress in lens epithelial cells<sup>310</sup> whereas, reduced expression of ubiquitin-conjugating enzymes UBE2A/B in PEX eyes was reported by Zenkel and coworkers.<sup>218</sup> Elevated levels of ubiquitin protein demonstrated that the housekeeping function is overactive and/or that signaling pathways mediated by ubiquitination are chronically hyperactive. Further, our study emphasizes the likely involvement of two proteasomal subunits in PEX pathogenesis. The multisubunit protease complex, 26S proteasome, is liable for protein degradation and thus maintenance of intracellular proteostasis.<sup>311-313</sup> While PSMD1 is a subunit of 19S regulatory complex of 26S proteasome which is involved in the degradation of ubiquitinated protein that relates to various biological processes<sup>314,315</sup>; PSMA5 is an integral part of the 20S-core particle (20S-CP) and is required for adenosine triphosphatase-mediated threading of the substrate into 20S-CP.<sup>316,317</sup> We noted a decreased expression of proteasome subunits, PSMD1 in PEXS subject, while, decreased expression of PSMA5 was seen in both PEXS and PEXG individuals when compared with control. In concert with our findings, recent study demonstrated reduced expression of ubiquitously expressed proteasome maturation protein (POMP) and a transmembrane protein (TMEM136) in anterior segment structures (such as iris and ciliary body) in PEXS eyes in comparison to control eyes suggesting anomalies in the signaling of ubiquitin-proteasome pathway in affected individuals.<sup>318</sup>

We also confirmed the impairment of the UPS machinery in PEX by examining proteasome activity in lens capsule tissue via enzyme-based luminescent assay. Proteasome-

Glo<sup>TM</sup> based assay mirrored mRNA expression data showing a significant decrease of the chymotrypsin-like specific proteasomal activity in the lens capsule of PEXS individuals in comparison to age-matched control. Reduced proteasome activity is supported by increased accumulation of ubiquitinated protein levels in PEXS tissue lysates. This is consistent with the previous report from our lab and others which showed increase in the total protein level in anterior eye tissues of PEX eyes compared to control group,<sup>8,85,319</sup> substantiating the role of impaired protein degradation in over-accumulation of protein in diseased PEX individuals.

### **3.4.3 Increased apoptosis in the PEX individuals**

When proteasomal activity is inhibited, the resulting elevated ER stress leads to the activation of apoptosis pathways including the activation of caspase-12 and DDIT3.<sup>267,281</sup> PEX individuals showed increased levels of ER-stress markers Caspase 12 (CASP12), followed by increased number of TUNEL positive cells in PEXS and PEXG which emphasizes an ER-stress mediated cell death. Luthra S et al., reported CASP12 involvement in apoptosis of human retinal pigment epithelial cells.<sup>320</sup> The total antioxidant levels in PEXS and PEXG patients were significantly lower and reduced antioxidant levels may contribute to higher apoptotic lens epithelial cells (LEC) density in PEX patients compared to the control subjects.<sup>321,322</sup> Our data is consistent with a recent report demonstrating more apoptosis in the human lens epithelial cells (LECs) of PEXS population.<sup>322</sup> Consistent with the above finding, we also report for the first time increased apoptosis in the lens capsule of PEXG individuals compared to control.

### **3.4.4 Activation of ER-UPR and inhibition of UPS**

Altogether, cumulative data from our study and others in the field led us to propose a model as represented in **Figure. 3.18**. It depicts that with the increased deposition of PEX fibrils resulting in an onset of PEXS, there is an overexpression of genes involved in ER-UPR and ERAD

pathway; however, there is a decreased expression of genes involved in proteasome degradation. We suspect that there might be impairment in ERAD complex formation that results in decreased degradation. Thus, downregulated protein degradation and reduced proteasome activity in the PEXS affected tissues might lead to proteostasis impairment which consequent into fibrillar protein deposition in the extracellular space. The dysregulated UPR and UPS genes' effect has been primarily detected in PEXS subjects but not in the advance stage of PEX, i.e. PEXG; suggesting that the protective role of these genes is diminished in the later stages of the disease condition thus, augmenting severity.

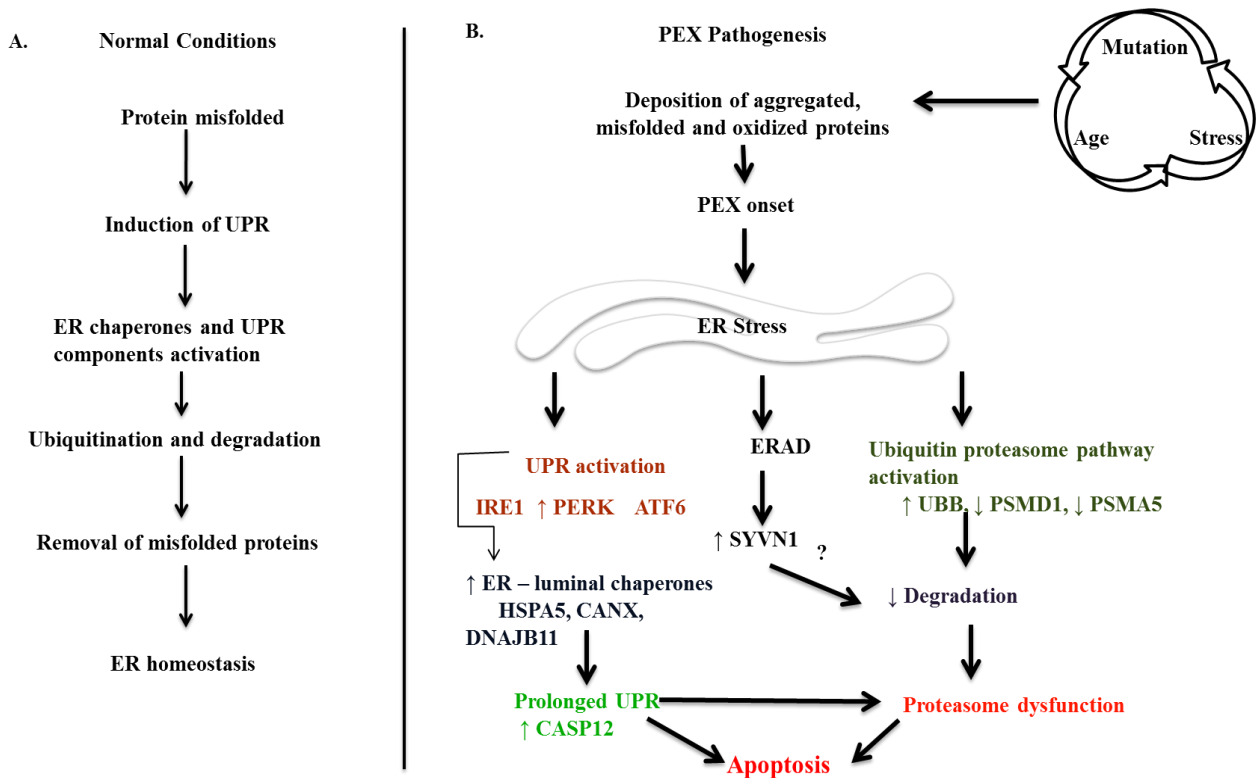


**Figure 3.18 Model depicting the involvement of UPR components in PEX pathogenesis.** A. Under normal conditions, accumulation of misfolded proteins in ER leads to upregulation of chaperones and co-factors, such as 70 kDa heat-shock protein (Hsp70)-family members (HSPA5, HSPB1, DNAJB11), calnexin and calreticulin. Misfolded substrates are targeted to the retrotranslocation machinery (the retrotranslocon) and/or to E3 ligase (SYVN1). As proteins exit the retrotranslocon, they are

polyubiquitylated by E3 ubiquitin ligases. The ubiquitinated substrate is then recognized and degraded by the 26S proteasome complex. **B.** In PEX, gradual accumulation of aberrantly folded proteins because of genetic mutations, external stresses and ageing result in ER stress. Subsequently various defense mechanisms set in, such as, UPR activation with increased expression of PERK, ER- luminal chaperones (HSPA5, CANX, DNAJB11) and ERAD protein SYVN1. However, a compromised UPS leads to inefficient degradation of misfolded proteins causing their accumulation in the lens capsule. Proteasome impairment and the resulting increased ER stress beyond a threshold cause apoptosis.

### **3.5 Conclusion**

Upregulation of several chaperones and ER stress proteins such as HSPA5, DNAJB11, HSPD1 and DNAJB1 is observed in patients with pseudoexfoliation suggesting ER stress and abnormal homeostasis as key features of PEX disease. The increased levels of ERAD components, SYVN1 and CANX and reduced expression of proteasome subunits, PSMD1 and PSMA5 and thereby, decreased proteasome activity depict imbalance in proteasome maintenance in the diseased condition which compromise the cellular pathway against stress and contribute to an accumulation of abnormal fibrillar material. Characterizing these dysregulated genes of UPR and UPS in detail in future will aid in understanding the complex network underlying the UPR pathway responsible for PEX which could eventually be used as possible targets to develop future therapeutic interventions. In conclusion, ERAD in the ER and UPS in the cytosol are tightly coupled processes essential for protein quality control and imbalance in the functioning of these processes seems to be involved in the pathogenesis of PEX.

# **CHAPTER-4**

*Enhanced expression of the Wnt  
antagonist Dickkopf-1 in  
pseudoexfoliation syndrome and  
glaucoma*

## **4.0. Enhanced expression of the Wnt antagonist Dickkopf-1 in pseudoexfoliation syndrome and glaucoma**

### **4.1. Introduction**

PEX etiology is still uncertain and tends to involve a complex multifactorial inheritance including the influence of multiple genes in conjunction with environmental factors; but one of the major pathways affected is believed to involve extracellular matrix (ECM) defects. The following chapter is focused on finding the potential pathogenic role of Dickkopf-related protein 1 (DKK1; Gene ID: 22943) protein in the progression of pseudoexfoliation. DKK1 is an important Wnt (wingless) modulator involved in cell adhesion, cell proliferation, extracellular matrix (ECM) metabolism and tumor progression.<sup>323–327</sup>

#### **4.1.1 Dickkopf-1, a potent antagonist of Wnt signaling**

DKK1 belongs to a glycoprotein Dickkopf family comprising of DKK1, DKK2, DKK3, DKK4 and a novel DKK3-related protein, termed Soggy. All DKK members contain an amino terminal signal peptide sequence and two conserved carboxy-terminal cysteine-rich domains.<sup>14,328,329</sup> The hallmark function of dickkopf protein to negatively modulate Wnt signaling is performed by DKK1/2 and 4, while DKK2 depending on the cells, sometimes activates or suppress Wnt / $\beta$ -catenin signaling.<sup>14,330</sup> DKK3 functions as a tumor suppressor and its overexpression suppress tumor cell growth.<sup>331–333</sup> DKK1 is a glycoprotein of 255-350 amino acids and expressed with an apparent molecular mass of 29–50 kDa molecular weight as shown by immunoblots from representative H1299, HEK293 (42-50KDa), and U118 cell lines.<sup>330,334,335</sup> DKK1 plays a significant role as an antagonist of the canonical Wnt signaling pathway.<sup>330,336–338</sup> It forms a ternary complex with lipoprotein receptor related-protein-5/6 (LRP5/6) and another receptor,

Kremen, inducing LRP endocytosis and subsequently inhibiting beta-catenin mediated Wnt signaling pathway.<sup>339</sup>

The secretory nature of the DKK1 protein aids in clinical investigation of diseases linked with Wnt signaling and easily diagnosed in the circulation.<sup>340</sup> Reports from earlier studies have demonstrated that altered DKK1 expression levels are associated with the development of Alzheimer's disease (AD), diabetic retinopathy (DR), age related macular degeneration (AMD), diabetic macular edema and bone disease where over-activation of the Wnt pathway plays a pathogenic role.<sup>341-343</sup> In AD, intracellular accumulation of clusterin has been reported to result in induced expression of DKK1, which eventually leads to production of toxic proteins detrimental to the cell survivability.<sup>344</sup> Further, DKK1 has been identified as a novel prognostic marker for a variety of tumors and its dysregulated expression has been observed in various malignant tissues such as hepatocellular carcinoma (HCC), pancreatic cancer, colorectal cancer, Wilms' tumor, breast cancer, lung and esophageal carcinomas suggesting a potential oncogenic and tumor suppressor function.<sup>345-350</sup>

#### **4.1.2 DKK1 as a potential risk factor in pseudoexfoliation**

Aberrant ECM deposits and elevated intraocular pressure (IOP) followed by glaucomatous optic nerve damage are the pathological hallmarks of PEX.<sup>351</sup> Emerging evidence suggest that the Wnt signaling pathway plays an essential role in regulating IOP in perfusion cultured human eyes and mouse eye and inhibition of the Wnt signaling pathway by DKK1 leads to increased IOP.<sup>352,353</sup> *In vivo* studies in mouse eyes have shown that inhibition of Wnt signaling by DKK1 results in change of cell adherens pathways that impact aqueous humor outflow, stiffen trabecular meshwork and thereby, resulting in an elevated IOP which is a pathological hallmark of PEX disease.<sup>354-356</sup> Therefore, evaluating DKK1 levels in circulation or ocular fluid could open up new

link with the development and progression of PEX disorder. Further, silencing of the canonical Wnt signaling has been reported to facilitate ECM deposition.<sup>357</sup> Clusterin; an extracellular chaperone has been reported as a probable risk factor in PEX as well as in AD pathogenesis.<sup>8,113,358</sup> Previous studies including dataset from our group reported a significant increase of clusterin protein in the aqueous humor of PEXG individuals<sup>8,85</sup> In AD, clusterin promotes aberrant Wnt signaling by inducing the expression of DKK1.<sup>344</sup> Since, DKK1 has been associated with AD which shares a similar etio-pathology with PEX; it is highly likely that DKK1 may play a decisive role in PEX pathogenesis. We speculated abnormal ECM deposits seen in PEX may be due to clusterin dependent DKK1 induction and deregulated Wnt signaling. In this study, we aimed to decipher the role of DKK1 by investigating its expression in anterior ocular segment of PEXS and PEXG. As PEX pathogenesis is very complex and still elusive; biomarkers for its clinical detection are limited. Identifying etiology and the risk factors associated with PEX and developing novel biomarkers for detection and prognosis of this disease is therefore crucial and important. Hence, an attempt was made to measure DKK1 concentration in plasma samples of PEX affected subjects which would help us to identify its potential role as a biomarker for predicting susceptibility for PEXS and PEXG. For a better understanding of the pathways involved, we also analyzed the expression of a few canonical and non-canonical Wnt targets at the mRNA and protein level in lens capsule tissues.

Following specific aims were put forth in this objective to address aforementioned lacunae:

1. To investigate the mRNA and protein expression of DKK1 in PEX affected anterior eye tissues.
2. To investigate the expression of canonical and non-canonical Wnt targets at the mRNA and protein level in lens capsule tissues.

3. To assess the circulating level of DKK1 in plasma of PEX and non-PEX control.

## **4.2 Materials and Methods**

### **4.2.1 Demographic and clinical characteristics of subjects**

Detailed information about study subjects' recruitment and inclusion or exclusion criteria followed for sample collection is mentioned in the materials and methods section 2.2.1 of chapter 2 (Page no. 28-29).

### **4.2.2 Enzyme-linked immunosorbent assay (ELISA)**

Plasma samples were acquired after informed consent from a total of 182 subjects including 59 patients with PEXS, 23 patients with PEXG and age-matched 100 non-PEX controls. Following the centrifugation of the samples at 3000 RPM for 10 min at 4°C, the plasma was separated from the freshly collected blood in EDTA vial and stored at -80°C until the assay was performed. Subjects were gender and age-matched among these groups. Demographic and clinical characteristics of subjects were shown in **Table 4.1**. Plasma levels of DKK1 were measured using a commercial Enzyme-linked immunosorbent assay (ELISA) kit (Human DKK1 DuoSet ELISA DY1906; R&D Systems, Minneapolis, MN, USA). It is a sandwich enzyme immunoassay that permits DKK1 measurements within a linear range of 62.5–4000 pg/ml. The assay allows sensitive and specific analysis of plasma DKK1 in study subjects. The procedures were performed according to the supplier's instructions. Capture antibody was diluted to a working concentration of 4.0µg/ml in 1x PBS and a 96-well microplate was coated with 100µl per well of the diluted capture antibody. The plate was sealed with a sealing film and incubated overnight at room temperature (RT). After 12 hours of incubation, each well was aspirated and washed with wash buffer (0.05% tween 20 in PBS) for a total of three washes. 300µl of blocking buffer (1% BSA in PBS) was added to each well and incubated for 1 hour. Meanwhile, seven

standards using 2-fold serial dilutions (4000 pg/ml-62.5 pg/ml) were prepared in reagent diluent (0.1% BSA, 0.05% Tween® 20 in Tris-buffered Saline {20 mM Trizma base, 150 mM NaCl}, pH 7.2-7.4). This was followed by washing each well thrice and 100µl of sample or standards in reagent diluent were added per well, covered with a sealing film and incubated for 2 hours at RT. Each well was washed 3-4 times and 100µl of detection antibody diluted in reagent diluent to a working concentration of 50ng/ml was added to the wells and incubated for 2 hours at RT. Further, the wells were washed 3-4 times and 100µl of Streptavidin-HRP (1:200 folds diluted) was added and incubated for 20 minutes at RT. This was followed by washing for three times and adding 100µl of substrate solution (tetramethylbenzidine or TMB substrate, Bangalore GeNei, India) to each well and incubating the plate in dark for 20 minutes at RT. The reaction was stopped by adding 50µl of stop reagent (2N sulphuric acid; H<sub>2</sub>SO<sub>4</sub>) into all wells. Absorbance of each well was measured immediately using a Varioskan Flash Multimode Reader (Thermo Scientific) set to 450 nm, with a reference wavelength at 570nm. All of the measurements were performed in duplicate for each sample, and the mean values were calculated.

**Table 4.1 Demographics, clinical and ocular characteristics of study subjects included for ELISA in plasma samples of Control, PEXS and PEXG.**

<b>Characteristics</b>	<b>Control (n=100)</b>	<b>PEX (n=82)</b>	<b>PEXS (n=59)</b>	<b>PEXG (n=23)</b>
<b>Age (years)</b>				
Mean ± SD	68.29 ± 8.64	70.43 ± 9.14	70.9 ± 9.28	69.52 ± 7.08
Median (Range)	69 (40-85)	71 (40-89)	71 (40-90)	70 (40-86)
p- value		<b>0.24</b>	<b>0.17</b>	<b>0.87</b>
<b>Gender, n (%)</b>				

Male	53 (53)	47 (57.3)	36 (61)	14 (60.8)
Female	47 (47)	35 (42.6)	23 (38)	9 (39.1)
p- value		<b>0.11</b>	<b>0.37</b>	<b>0.14</b>
<b>Intraocular pressure (IOP, mmHg)</b>				
Mean $\pm$ SD	14.06 $\pm$ 3.34	16.02 $\pm$ 4.14	15.55 $\pm$ 2.56	17.63 $\pm$ 6.41
Median (Range)	14.6 (7- 23)	14.8 (9-32)	15 (9- 23.1)	15.8 (8.5- 32)
p- value		<b>0.001</b>	<b>0.08</b>	<b>0.001</b>
<b>Systemic Hypertension, n (%)</b>		44 (53.65)	36 (61.01)	9 (39.13)

#### 4.2.3 Quantitative Real time-PCR (qRT- PCR)

Detailed steps followed for RNA extraction, cDNA synthesis and qRT-PCR were described in the materials and methods section 2.2.5-2.2.7 of Chapter 2 (Page no. 33-34). PrimerQuest Tool (IDT) was used to design gene specific primers overlapping exon-exon junction for the mRNA transcript of DKK1, Wnt5A, Rho-associated kinase 2 (ROCK2), Beta-Catenin (CTNNB1) and AXIN2 (Conductin). Nucleotide sequences of primers used are presented in the **Table 4.2**. GAPDH and ACTB mRNA expression was used as endogenous control for normalizing target gene expression. Comparative threshold cycle ( $\Delta\Delta C_t$ ) method was used to get the expression fold change for target gene and represented as fold difference in comparison to control.

**Table 4.2** List of oligos used in the study.

S. No.	Gene	Purpose	Sequence (5' $\rightarrow$ 3')
1	<i>DKK1</i> (NM_012242.3)	qRT-PCR	F: AGCACCTTGGATGGGTATTC R: CTGATGACCGGAGACAAACA
2	<i>WNT5a</i> (NM_003392.4)	qRT-PCR	F: CGGTCGCTCCGCTCG R: CAATGGACTTCTTCATGGCG

3	<i>ROCK2</i> (NM_004850.5)	qRT-PCR	F: AGATGGATGAAACAGGCATGG R: ACCAATCACATTCTCGCCCA
4	<i>CTNNB1</i> (NM_001904.4)	qRT-PCR	F: AGACGGAGGAAGGTCTGAGG R: TCCATCAAATCAGCTTGAGTAGC
5	<i>AXIN2</i> (NM_004655.4)	qRT-PCR	F: GCTGCGCTTTGATAAGGTC R: CCTCCTCTCTTTTACAGCAGG
6	<i>GAPDH</i> (NM_002046.5)	qRT-PCR	F: GGTGTGAACCATGAGAAGTATGA R: GAGTCCTTCCACGATACCAAAG
7	<i>ACTB</i> (NM_001101.3)	qRT-PCR	F: GCACAGAGCCTCGCCTT R: GTTGTGCGACGACGAGCG

#### 4.2.4 Immunostaining and immunofluorescence

For immunofluorescence labeling, lens capsules were obtained from subjects at the time of cataract surgery and stored at  $-80^{\circ}\text{C}$  until further use. Tissues were fixed in 4% paraformaldehyde for 20 minutes, three washes with 1XPBS were performed for 5 minute each followed by three PBST washes for 5 minutes each. Tissue samples were then kept in 10% blocking solution prepared in normal horse serum in PBST for 45 minutes and later incubated overnight at  $4^{\circ}\text{C}$  in primary polyclonal antibody against human DKK1 (sc-374574, Santa Cruz Biotechnology at 1:250) in blocking solution. After subsequent washing in PBST, the tissue was treated with Alexa-Fluor 488 Chicken anti-mouse IgG (A21200, Invitrogen) secondary antibody at 1:500 dilutions for two hours in dark at room temperature. Nuclear staining was done with DAPI (4,6-diamino-2-phenylindole; Sigma-Aldrich, 32670-5 MG-F) and lens capsule was mounted on the slide along with ProLong Gold antifade reagent (P36934, Invitrogen). Immunofluorescence recording was done in Olympus FV 3000 (Olympus, Japan) confocal laser scanning microscope. Images were further quantified in ImageJ and fluorescence intensity was plotted with respect to control.

#### **4.2.5 Immunoblotting**

Western blot analysis was performed with protein extracts of lens capsules, conjunctiva and aqueous humor from study subjects. The proteins were resolved on 12% SDS-PAGE and transferred to PVDF membranes (IPVH00010, Millipore-Merck). The membranes were blocked with 5% non-fat dry milk in TBST at room temperature for 1 hour to block nonspecific immunoreactivity. Subsequently, the membranes were incubated with the corresponding primary antibodies overnight at 4°C. Dickkopf-1 (sc-374574, Santa Cruz Biotechnology; 1:500), Wnt-5a (sc-365370, Santa Cruz Biotechnology; 1:250), Beta Catenin (Catalogue no., 712700, Invitrogen; 1:500), ROCK-2 (sc-398519, Santa Cruz Biotechnology; 1:250) were used as primary antibody and HRP conjugated Goat anti-rabbit IgG (621140380011730, Bangalore GeNei, India), and Goat anti-mouse IgG-HRP (621140680011730, Bangalore GeNei, India) each at 1:5000 dilution were used as secondary antibody. Equal loading was verified with GAPDH antibody (ABM22C5, Abgenex, India; 1:250). Detection was performed in a Fusion Solo S Chemi-Doc (Vilber Lourmat) using the Super Signal Femto kit. Signal intensity ratios relative to GAPDH were calculated for the normalization of protein expression level.

#### **4.2.6 Statistical analysis**

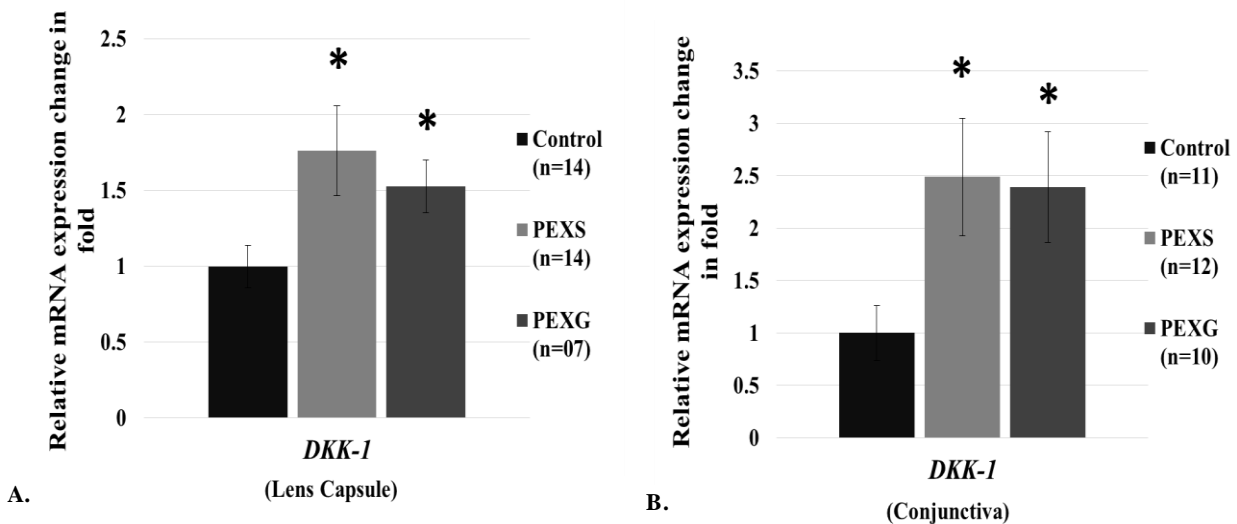
All experiments were performed at least three times independently statistical analysis was conducted with the SPSS software package (version 23.0; SPSS, Chicago, IL). All data were presented as mean  $\pm$  standard error of mean (SEM). Graphical representations for ELISA were performed with GraphPad Prism 7 (San Diego, CA, USA) software. All data obtained from the quantitative measurements were analyzed using Student's t-test or one-way ANOVA to determine statistical significance. Bonferroni's test was used for post hoc comparisons. For all

tests, a p-value <0.05 was considered statistically significant and indicated by asterisks in the figures.

### 4.3 Results

#### 4.3.1 Increased mRNA expression of DKK1 in lens capsule and conjunctiva of PEX affected tissues

To explore the comprehensive expression profile of DKK1 in anterior eye tissue of PEX we first analyzed its expression at mRNA level. Quantitative real-time PCR demonstrated mRNA expression of *DKK1* in human ocular tissues (lens capsule and conjunctiva) from PEX and non-PEX control eyes. As shown in **Figure 4.1**, a particularly pronounced expression of *DKK1* gene was examined in the lens capsule of PEXS (1.94 fold; p=0.02) and PEXG (2.11 fold; p=0.03) subjects compared to that of control. Similarly, *DKK1* expression was markedly increase in conjunctiva of PEXS (2.48 fold; p=0.04) and PEXG (2.39 fold; p=0.02) compared with control eyes without PEX (**Figure 4.1**). This suggests activation of DKK1 in anterior eye tissues of PEX that might lead to dysregulated Wnt signaling.



Study subjects (Lens capsule)	N (Female in %)	Gender Mean $\pm$ SEM	P-value	Age (in years) Mean $\pm$ SD	P-value	Manifestation	
						Unilateral	Bilateral
Control	14 (57%)	1.57 $\pm$ 0.14		70.28 $\pm$ 1.60		NA	NA
PEXS	14 (36%)	1.35 $\pm$ 0.13	0.27	72.07 $\pm$ 1.69	0.45	5	9
PEXG	7 (29%)	1.28 $\pm$ 0.18	0.23	74.14 $\pm$ 3.23	0.31	3	4

B.

Study subjects (Conjunctiva)	N (Female in %)	Gender Mean $\pm$ SEM	P-value	Age (in years) Mean $\pm$ SD	P-value	Manifestation	
						Unilateral	Bilateral
Control	11 (54%)	0.54 $\pm$ 0.15		67.09 $\pm$ 7.93		NA	NA
PEXS	12 (58%)	0.58 $\pm$ 0.14	0.86	67.41 $\pm$ 6.2	0.91	5	7
PEXG	10 (40%)	0.4 $\pm$ 0.16	0.52	69.7 $\pm$ 7.76	0.45	4	6

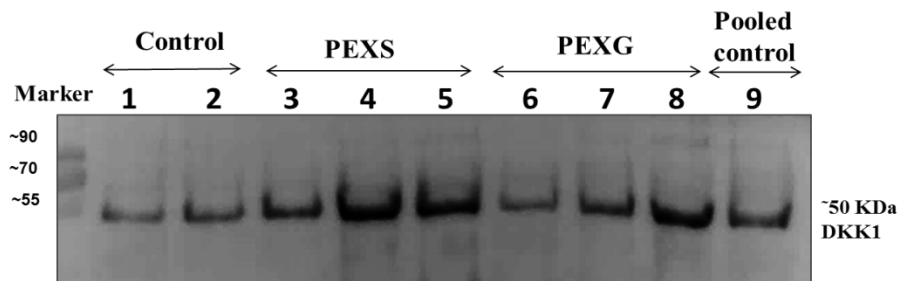
C.

**Figure 4.1 DKK1 mRNA expression in lens capsule and conjunctiva of PEX affected tissues and non PEX controls.** A. Increased mRNA expression of *DKK1* was observed in PEXS ( $p=0.02$ ) and PEXG ( $p=0.03$ ) affected individuals when compared with controls. While, in conjunctiva tissue, more than two-fold expression changes were observed for *DKK1* in PEXS ( $0.04$ ) and PEXG ( $p=0.02$ ) samples with respect to control subjects. “n” refers to sample size and bar plot is represented as mean  $\pm$  SEM. **B and C.** Demographics of the study subjects used for qRT-PCR using lens capsule and conjunctiva tissues respectively are shown. N=sample size. Student’s t-test was used to calculate statistical significance between groups. \*Represents  $P<0.05$ .

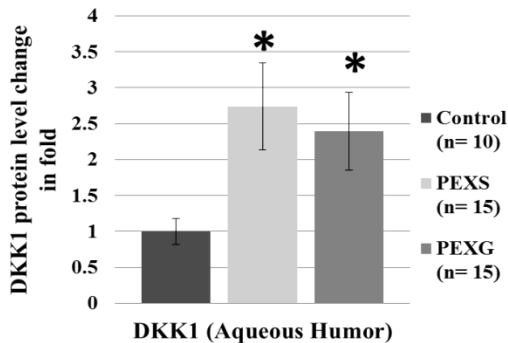
#### 4.3.2 Differential accumulation of DKK1 protein in anterior eye segment of PEX individuals

We further verified DKK1 protein expression in human ocular tissues by western blotting. Immunoblot analysis confirmed the elevated level of DKK1 in the aqueous humor (AH) of eyes from patients with PEXS and PEXG compared with those from control subjects. More than two-

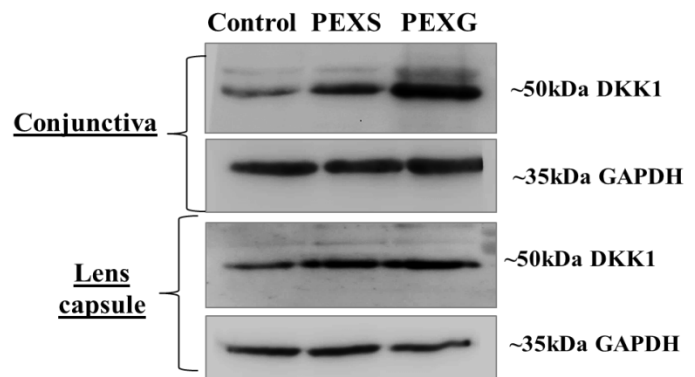
fold upregulation of DKK1 protein was observed in AH of PEXS (2.73 fold;  $p=0.01$ ) and PEXG (2.39 fold;  $p=0.02$ ) group (**Figure 4.2 A-B**) in comparison to control (n=10). Immunoblotting also showed the presence of DKK1 in tissue lysate of lens capsule and conjunctiva (**Figure 4.2C**). Similar to aqueous humor, the level of DKK1 was remarkably elevated in conjunctiva of PEXS (2.35 fold;  $p=0.04$ ) and PEXG (2.85 fold;  $p=0.02$ ) as well in lens capsule of PEXS (1.90 fold;  $p=0.02$ ) and PEXG (1.83 fold;  $p=0.01$ ) compared with their corresponding controls. A protein band of approximately 50 kDa, which is higher than the expected size of the secreted DKK1 protein, was detected in the AH, lens capsule, and conjunctiva protein lysates, which suggested post translational modifications in DKK1.



A. Aqueous humor



B.



C.

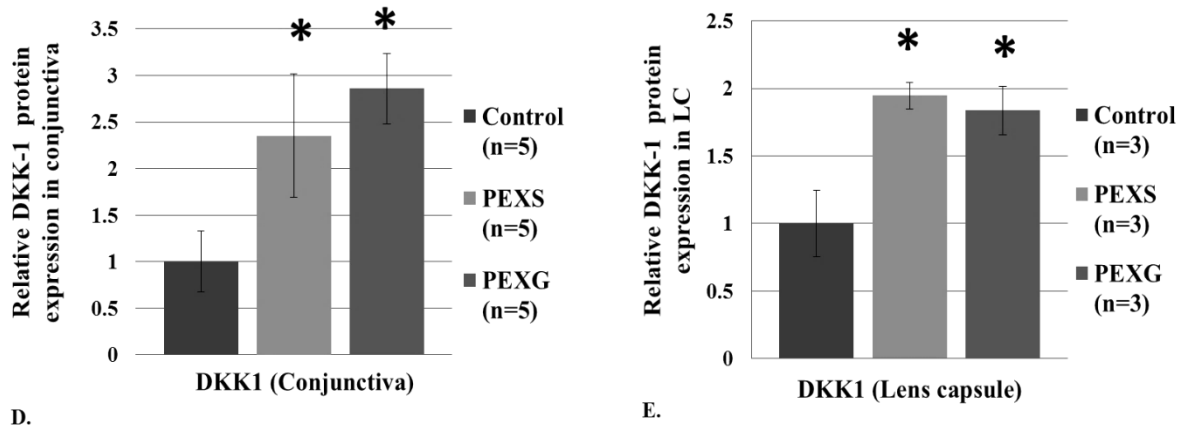


**Figure 4.2 Immunoblotting analysis to detect DKK1 protein level in PEX affected subjects versus control.** **A.** Representative western blot showing immunoreactive band for DKK1 in aqueous humor of control (lane 1 and 2), PEXS (lane 3, 4 and 5), PEXG (lane 6, 7 and 8) and pooled sample from ten controls (lane 9). **B.** In aqueous humor of PEXS ( $p=0.01$ ;  $n=15$ ) and PEXG ( $p=0.02$ ;  $n=15$ ) subjects increased DKK1 level was detected in comparison with controls ( $n=10$ ). **C.** Immunoblotting analysis revealed significant increase of DKK1 in tissue lysates of PEXS conjunctiva ( $p=0.04$ ;  $n=5$ ) and PEXG conjunctiva ( $p=0.02$ ;  $n=5$ ) with respect to control. Likewise, increased DKK1 level was observed in tissue lysates of lens capsule for PEXS ( $0.02$ ;  $n=3$ ) and PEXG ( $p=0.01$ ;  $n=3$ ) when compared with control ( $n=3$ ). Sample size denoted by ‘n’. **D-E.** Densitometry analysis was done to quantitate immunoblot result. Relative protein expression was normalized against GAPDH represented in bar plot. Age and gender matched study subjects recruited for experiments. Data are represented as mean  $\pm$  SEM. \* $P<0.05$ .

#### 4.3.3 Immunofluorescence analysis of DKK1 in lens capsule of study subjects

To assess the localization of DKK1 in lens capsule, tissue immunofluorescence staining was performed. Staining of complete sections of lens capsule showed the distribution and expression of DKK1 protein which was mostly distributed in both the cytoplasm and nucleus with a granular, speckle like appearance. In control tissue, the distribution was found mainly in the cytoplasm with granular appearance. While in PEXS, we observed DKK1 distribution in both the cytoplasm as well in nucleus and in PEXG tissue samples DKK1 was seen to aggregate inside

the nucleus, indicating DKK1's role in localizing to the nucleus for the regulation of specific target genes (**Figure 4.3A**).

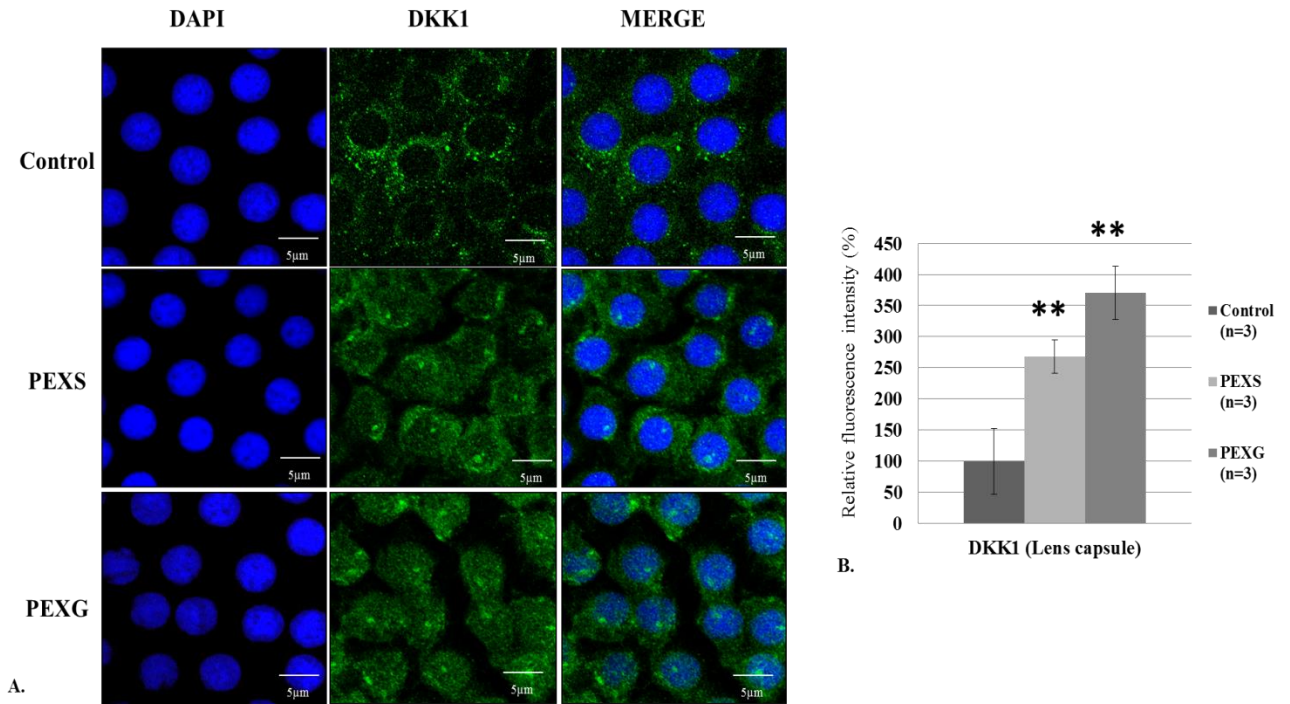


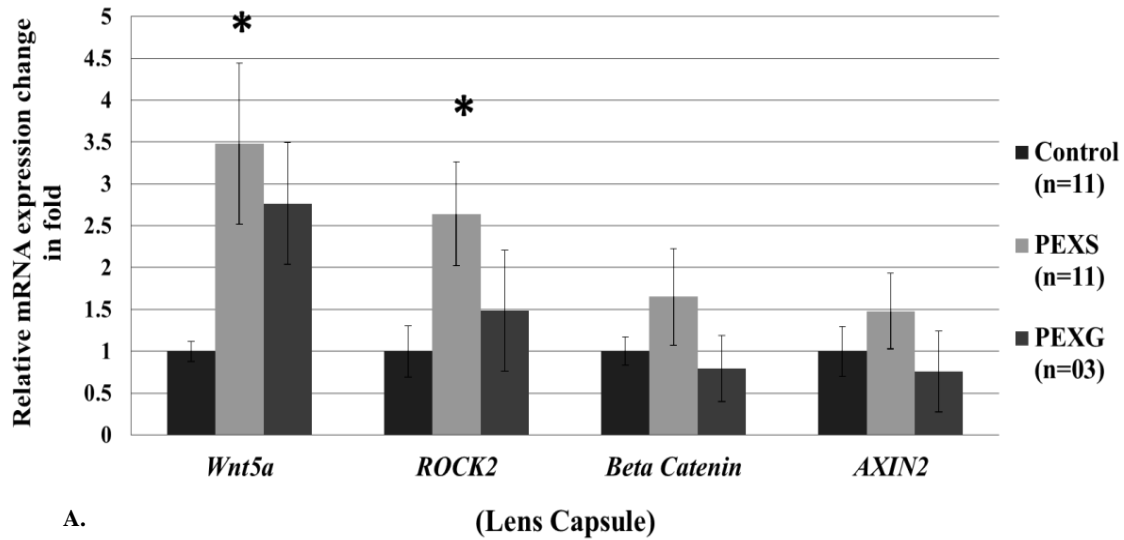
**Figure 4.3 Immunofluorescence image of control, PEXS and PEXG stained for DKK1. A.** Subcellular localization of DKK1 was detected in lens capsule of PEXS, PEXG and control. DKK1 stained with FITC-conjugated secondary antibody, was present in cytoplasm and nucleus of the cell appearing as fine-grained material in PEXS and PEXG study subjects, while in control DKK1 was mainly distributed in the cytoplasm **B.** The bar graph shows the relative fluorescence intensity of DKK1 expression where it was significantly increased in PEXS ( $p=0.002$ ;  $n=3$ ) and PEXG ( $p=0.008$ ;  $n=3$ ) affected tissues when compared with the control group. Age-gender matched study subjects recruited for the study. Sample size denoted by 'n'. Cell nucleus was stained with DAPI. Magnification- 600x, scale bar- 5µm. Data presented as mean  $\pm$  SEM, \*\* $P<0.01$ .

On comparing the relative fluorescent intensity we found significantly elevated expression of DKK1 in PEXS ( $p=0.002$ ) and PEXG ( $p=0.008$ ) when compared with control samples with observed nuclear aggregation (**Figure 4.3B**).

#### **4.3.4 Differential expression of genes involved in canonical and non-canonical Wnt pathways in lens capsule of PEX affected subjects and control**

With the present findings of elevated levels of a specific antagonist of classical Wnt signaling, DKK1, we investigated the key components of Wnt pathway in order to obtain a holistic view of the expression of other Wnt members in the context of PEX pathology. In order to clarify DKK1 role in activation of canonical or non-canonical Wnt pathway we further investigated the expression of genes involved in canonical and non-canonical Wnt targets to check which pathway is induced after elevated DKK1 expression. Of the canonical signaling, we checked mRNA expression of Wnt5a, Rho-associated coiled-coil containing protein kinase 2 (ROCK2),  $\beta$ -catenin (CATNNB) and Conductin (AXIN2) using qPCR assay.  $\beta$ -catenin is a transcriptional modulator of canonical Wnt signaling, and regulates the expression of genes involved in cell development and differentiation.<sup>359,360</sup> Another known Wnt target, AXIN2 is a specific indicator of the activated Wnt/ $\beta$ -catenin signaling, pathway activation and functions as a scaffolding protein in forming destruction complex.<sup>361,362</sup> Wnt5a is a key non-canonical Wnt ligand, and ROCK2, is a major component of Rho/ROCK signaling. Binding of Wnt5a mainly to its receptor subsequently triggers ROCK2 which helps in cellular proliferation, adhesion and maintenance of cytoskeleton.<sup>363-365</sup> Interestingly, the most distinctive changes in mRNA expression was shown by Wnt5a (3.58 fold; p=0.02) and ROCK2 (2.63 fold; p=0.03) in lens capsule of PEXS affected individuals while no significant differences were observed in PEXG for Wnt5a (2.76 fold; p=0.28) even after showing greater than two fold enhancement most likely due to limited samples. ROCK2 also failed to show significant differential expression in PEXG (1.87 fold; p=0.64) when compared with controls. On the other hand, canonical Wnt targets;  $\beta$ -catenin (1.65 fold; p=0.30), and AXIN2 (1.47fold; p=0.38) did not depict any significant differential

expression in either PEXS or PEXG cases with respect to control (**Figure 4.4**). Our finding at mRNA expression level suggest that upregulation of Wnt antagonist DKK1 leads to activation of non-canonical Wnt targets, Wnt5a and ROCK2 which might promote abnormal fibrillary deposition in anterior segment of PEXS individuals.



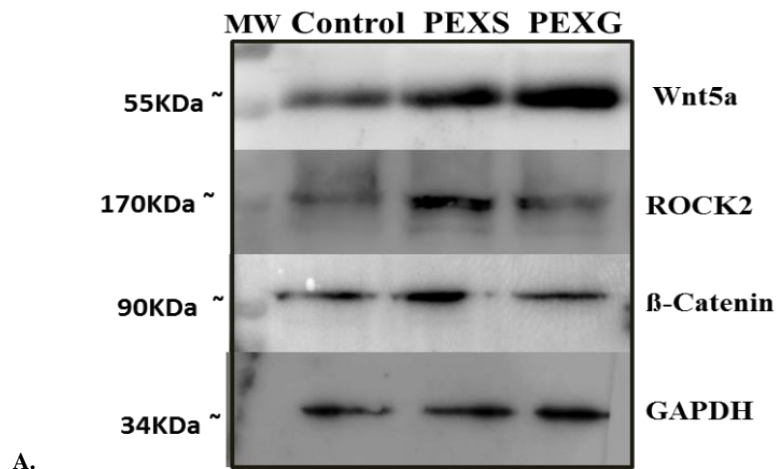
**B.**

Study subjects (Lens capsule)	N (Female in %)	Age (in years)	P-value	Gender	P-value
		Mean $\pm$ SD		Mean $\pm$ SEM	
<b>PEXS</b>	11 (57.1%)	71.07 $\pm$ 5.59	0.11	0.57 $\pm$ 0.14	0.46
<b>PEXG</b>	3 (33%)	74.0 $\pm$ 7.54	0.3	0.33 $\pm$ 0.3	0.81
<b>Control</b>	11 (42%)	68.00 $\pm$ 4.33		0.42 $\pm$ 0.14	

**Figure 4.4 mRNA expression of Wnt pathway genes in lens capsule of PEX affected tissues and non PEX controls.** Significantly increased mRNA expression of non-canonical Wnt ligands, Wnt5a and ROCK2 was observed in lens capsule of PEXS affected individuals (p=0.01 and p=0.03, respectively) with respect to controls while no significant difference was observed even though greater than two-fold increase of Wnt5a was seen in PEXG individuals due to large variance and small sample size. ROCK2 didn't show significant differences in PEXG. On the contrary, canonical Wnt targets Beta catenin and AXIN2 were not statistically different between the three study subjects (with p=0.24 and p=0.90

respectively) in PEXS and PEXG subjects with respect to controls. **B.** Demographics of the study subjects included in study. Bars are represented by mean  $\pm$  SEM. \* $P < 0.05$ .

We further validated our findings at protein level of those gene products that showed differential regulation at mRNA level in PEXS and PEXG tissues. Protein extracted from lens capsule were subjected for immunoblotting, and by immunoblot analysis we detected Wnt5a, Beta catenin and ROCK-2 in LC samples with an apparent molecular weight of 55, 90 and 162 kDa respectively (**Figure 4.5A**). Densitometry quantification of the three immunoreactive bands (**Figure 4.5B**) revealed that the levels of Wnt5a and ROCK-2 showed 1.7-fold, and 2.08-fold respectively, in LC samples from eyes with PEXS and 1.84 fold and 1.31 fold respectively in PEXG eyes when compared with non-PEX control eyes ( $n=3$  for each group). However, they failed to reach significance in the present samples size. In consistency with mRNA data, expression of Beta-catenin protein was insignificant in PEXS (1.12 fold;  $p=0.82$ ) and PEXG (0.86-fold,  $p=0.89$ ). **However, more samples are needed to validate these preliminary findings.**



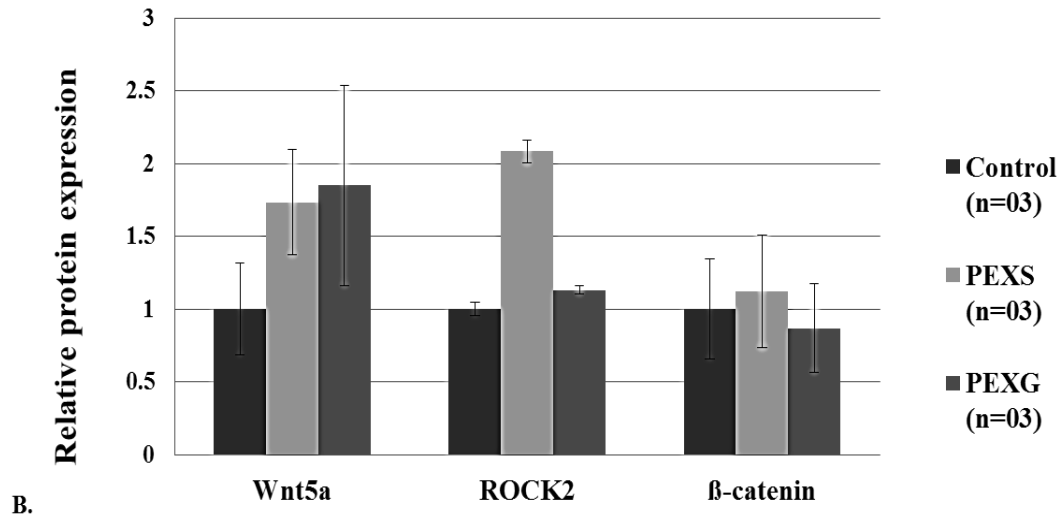


**Figure 4.5. Western blotting detection of Wnt genes in LC samples from patients with PEXS, PEXG and control.** A. Immunoblot analysis showed the protein level of Wnt5a, ROCK2 and Beta catenin where none of the genes significant variation in the level. Wnt5a showed moderate enrichment in PEXS (1.73 fold;  $p=0.32$ ) and PEXG (1.84 fold;  $p=0.28$ ), while ROCK-2 showed more than 2- fold increment in PEXS ( $p=0.16$ ) and nominal changes in PEXG (1.31 fold;  $p=0.20$ ), Beta- catenin failed to show any significant changes in either PEXS (1.12 fold;  $p=0.82$ ) and PEXG (0.86 fold;  $p=0.89$ ) B. Densitometry analysis quantified the intensities of specific immunoreactive bands. Data were normalized to GAPDH and are expressed as percentage of control. The data are expressed as the mean  $\pm$  SEM and are representative of results in three independent experiments ( $n=3$  for each group).

#### 4.3.5 Increased circulating level of DKK1 in plasma of pseudoexfoliation patients

As DKK1 has emerged as promising biomarker for numerous neurodegenerative diseases and cancers, we examined the relationship between DKK1 plasma level and the progression of PEX severity. DKK1 expression was assessed by ELISA which demonstrated the level of DKK1 in plasma of PEX and age-matched non-PEX control. We found that the DKK1 level was higher in PEX patients than in the control eyes (median 1144.0 pg/ml, range, 157.3 pg/ml -3824.0 pg/ml versus 615.9 pg/ml, 26.8pg/ml - 3260.0 pg/ml;  $P<0.0001$ ) (**Figure 4.6**).

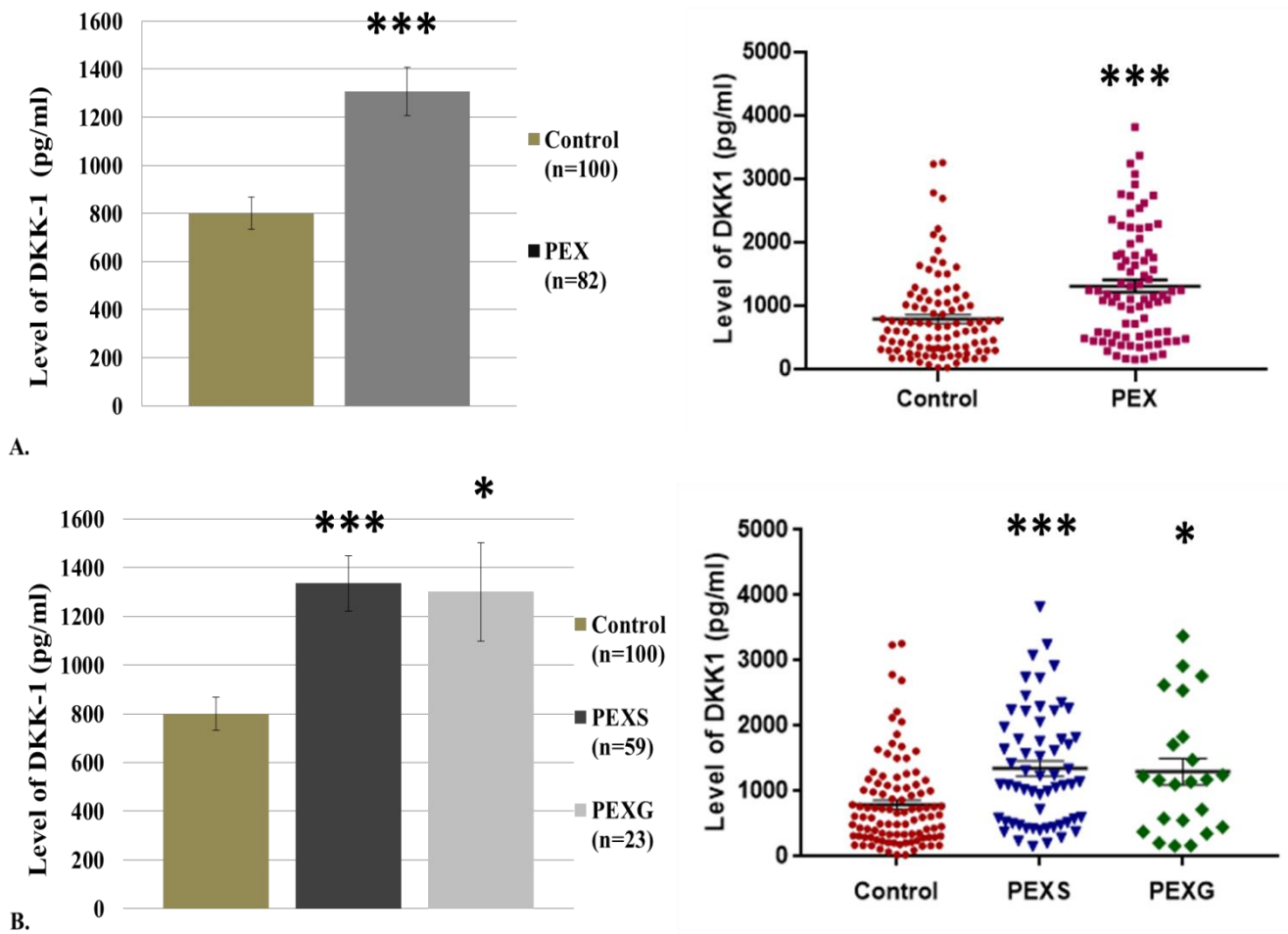


**Figure 4.6 ELISA of the DKK1 in plasma samples of PEX and control. A and B.** The Bar plot and column scatter plot depicting the levels of secreted DKK1 in plasma samples from PEX ( $1314.0 \pm 96.74$ ), PEXS ( $1335.2 \pm 113.3$ ) and PEXG ( $1301.3 \pm 228$ ) were higher than those from control samples ( $800.5 \pm 68.4$ ). In column scatter plot, each spot represents one patient. Middle lines represented the mean. Independent experiments were performed in duplicates. Sample size denoted by 'n'. The data are presented as mean  $\pm$  SE. \*\*\* $p < 0.0001$ , \*\* $p < 0.01$ . Unpaired t-test performed to compare two groups. One-way Anova and posthoc bonferroni multiple comparisons tests were done for comparing more than two groups.

There was a statistically significant difference of DKK1 levels in the plasma of PEX patients with respect to controls. Further, the PEX result was segregated into early syndrome (PEXS) and late advanced glaucoma (PEXG) stage as shown in **Figure 4.6**, the levels of DKK1 were

significantly higher in both PEXS (median: 1126.0pg/ml, range: 157.3pg/ml - 3824.0pg/ml, P=0.0001) and PEXG (1169.0pg/ml, 164.0pg/ml - 3377.0pg/ml, P=0.006) in comparison with those in non-PEX controls (615.9pg/ml, 25.6pg/ml-3260.0pg/ml). These findings demonstrated that enhanced circulating DKK1 levels might be linked with severity or progression of PEX.

#### **4.3.6 Potential of the circulating DKK1 levels to become a biomarker for detection of PEXS and PEXG**

Increased circulating level of DKK1 needs to be further evaluated in a specific manner for use as a predictive biomarker for two different stages of PEX disease. The receiver operating characteristics (ROC) curve analysis was performed to evaluate whether circulating DKK1 levels can be used as a biomarker for detection of PEX early and later stage. Total accuracy was measured by area under the ROC curve (AUC), and Youden index J was used to determine optimal cut-off value of DKK1. The AUC results were considered excellent at 0.9-1.0, good at 0.8-0.9, fair at 0.7-0.8, poor at 0.6-0.7, and failed at 0.5-0.6. (Lüdemann L. et al., 2006; Metz CE. 1978). Using the highest sensitivity and specificity combination, the optimal cutoff point was derived from ROC analysis. ROC curve for PEXS showed that the optimum diagnostic cutoff for DKK1 was 935.0pg/ml, with an AUC 0.70 (95% CI, 0.61–0.78; P < 0.001). This corresponds to a sensitivity of 66.1%, and specificity of 63.1% (**Figure 4.7**). These results suggested that the circulating DKK1 level has 70% chance for the detection of PEXS from control. While, ROC curve for PEXG has an AUC 0.65 (95% CI, 0.51-0.78, p<0.05) with optimum cut-off limit of 1103.4pg/mL, suggesting 65% probability of distinguishing PEXG from non-PEX controls with sensitivity 60.9% and 61% specificity (**Figure 4.7**). Overall, current findings indicated that plasma Dkk-1 might not be a potential biomarker in the prediction of clinical outcomes among

patients with PEXS or PEXG, but it still needed to be further checked in ocular fluid of affected tissues to validate or deny its potency as diagnostic biomarker.

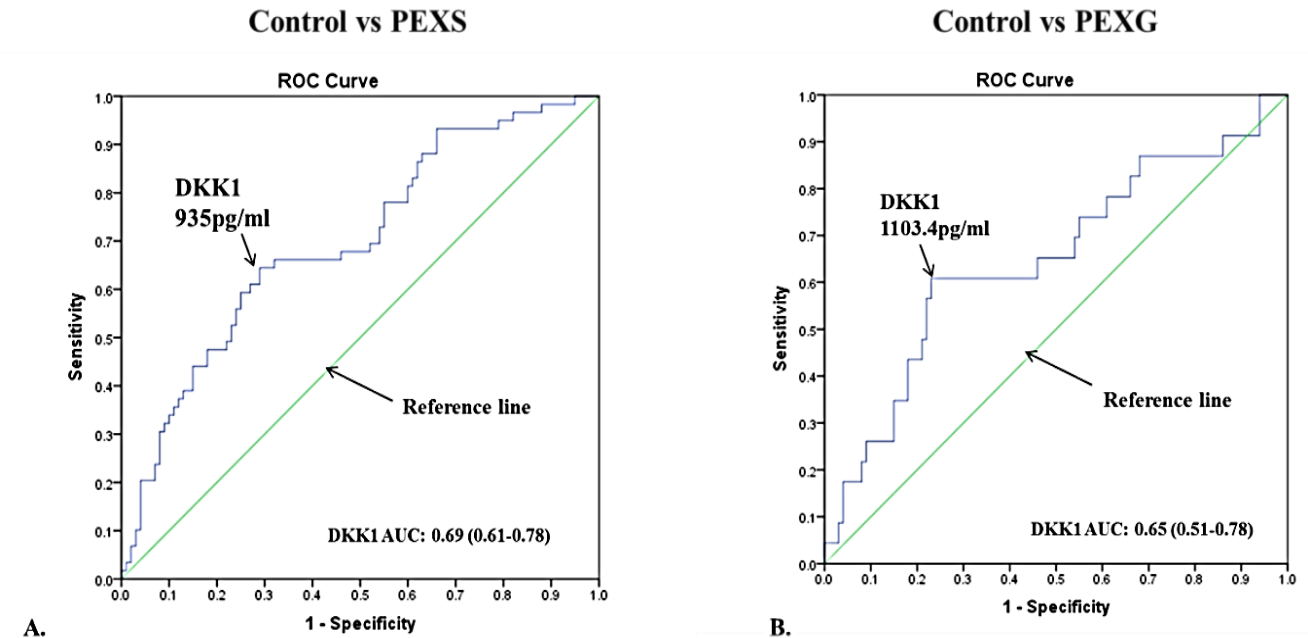


**Figure 4.7 Diagnostic outcomes for plasma DKK1 in the diagnosis of PEX.** A. ROC curve for DKK1, for all patients with PEXS versus all controls. Comparing PEXS patients with non-PEX controls, the best cutoff level of DKK1 was 935.0 pg/ml. The accuracy of DKK1 plasma levels in PEXS is at 66.1% sensitivity and 65%, specificity. B. ROC curves showed the optimum diagnostic cutoff for DKK1 in PEXG was 1103.4 pg/ml, sensitivity 60.9%, specificity 61%.

#### 4.4 Discussion

DKK1 is a secreted glycoprotein and acts as a negative modulator of the Wnt signaling that is implicated in multiple pathological and physiological processes.<sup>14,330,366</sup> DKK1 is expressed in numerous tissues and participates in diverse biological functions such as, apoptosis, growth suppression, bone formation depending on the cell types involved.<sup>327,367</sup> We hereby report significant upregulation of *DKK1* mRNA expression in lens capsule and conjunctiva tissues of PEXS and PEXG individuals compared to age matched non-PEX control. DKK1 protein levels,

as measured by western blotting, were significantly higher in aqueous humor of PEXS and PEXG individuals. This result was in line with the mRNA data. Furthermore, enhanced DKK1 expression in anterior eye tissues implicates dysregulation of Wnt signaling that could contribute to pathogenic aggregate formation in PEX. As Wnt signaling promotes the expression of genes involved in maintenance of extracellular matrix (ECM), repressed Wnt signaling would reduce the expression of ECM genes resulting in increased susceptibility to cytotoxicity. Further, PEXS and PEXG exhibited higher DKK1 levels, mainly in the nucleus. Although the mechanism of DKK1 translocation into nucleus is unknown, presence of DKK1 in nucleus of lens capsule tissue might suggest its role in transcriptional activation of target genes. Further investigation using nuclear markers such as Lamin B1 can make the data more conclusive. Recent study by Aguilera et al., has provided the evidence of DKK1 presence within nucleus of colorectal cancer (CRC) cells thus, establishing its gene regulatory function and a predictive biomarker for CRC.<sup>368</sup>

In addition to DKK1 other canonical and non-canonical Wnt targets responsible for Wnt signal transduction, AXIN2,  $\beta$ -catenin, -Wnt5a, and ROCK2 were detected in lens capsule tissues. The present findings revealed particularly enhanced expression of Wnt5a and ROCK2 in lens capsule of PEXS affected cases compared to control. Recent research attempted to create a mouse model by transient expression of Wnt5a in the mouse anterior segment via Adenovirus-mediated gene expression which recapitulates certain ocular manifestations of human PEXS suggesting a possible involvement of dysregulated Wnt signaling in PEX pathophysiology.<sup>369</sup> Emerging evidence have documented the role of ROCK2 protein in regulating IOP and ciliary muscles contractility, where treatment with ROCK2 inhibitors reduced the IOP in rabbit.<sup>364</sup> Thus, this finding led us to propose that there is an activation of non-canonical Wnt signaling in

lens capsule. Further studies need to be done to look for other intracellular components of non-canonical Wnt-pathway such as JNK (c-Jun N-Kinase) and transcription factor AP-1 to suggest their possible involvement in PEX pathology. In Alzheimer's disease, increased clusterin lead to induction of DKK1,<sup>344</sup> prompted us to speculate that increased DKK1 expression might be induced by increased clusterin in PEX which further triggers non-canonical Wnt/JNK signaling cascade by blocking the canonical Wnt pathway, as defined by the increase in c-Jun activity. Our findings in the current report indicate that elevated DKK1 leads to activation of Wnt5a inducible non-canonical Rho/ROCK pathway resulting in inhibition of Wnt signaling. However, further study is underway to understand the precise mechanism for elevated DKK1 induced ROCK2/Wnt5a activation in PEX pathogenesis.

In the current study, we also demonstrated that the DKK1 levels in the plasma of patients affected with PEX were significantly elevated when compared with the corresponding non-PEX subjects. This is the first study to provide evidence of circulating DKK1 levels in plasma of PEX patients. Altered circulating plasma level of DKK1 have been stated to be linked with various diseases such as multiple myeloma, rheumatoid arthritis, breast cancer, lung cancer, and esophageal cancer patients<sup>340,343,347,370,371</sup> thus, indicating its potential as a biomarker for disease prognosis. However, there is no documented study yet to associate circulating DKK1 levels with PEX. Current finding showed that enhanced circulating levels of DKK1 are associated with both PEXS and PEXG, implying that the higher DKK1 levels in the circulation are associated with the higher probability of PEX susceptibility. We also attempted to estimate the potency of circulating DKK1 level as a biomarker for PEX based on its optimal cut-off value as assessed by ROC analysis. Results revealed that DKK1 had a 70% probability of distinguishing PEXS from non-PEX controls and 65% (less than 70%) possibility of differentiating control samples from

PEXG affected subjects. This finding indicated that plasma level of DKK1 is a poor classifier for PEXS or PEXG. Further studies are directed to assess the DKK1 level in aqueous humor of study subjects to establish its correlation with disease severity more accurately. With its substantial high level in PEX anterior eye tissues it could serve as a prognostic marker for determining disease severity.

Based on the previous and present findings, we propose a model to explain DKK1 role in PEX pathogenesis (**Figure 4.8**). Clusterin has a preventive role on aggregate formation when the ratio of clusterin to substrate is high while within the sub-stoichiometric ratio/concentrations. However, at a later stage when the ratio of secretory clusterin (sCLU) protein to its substrate decreases, clusterin becomes cytotoxic as it is overwhelmed and accumulates along with the aggregates/substrate.<sup>372</sup> During chronic stress, deposition of extracellular aggregates in PEX leads to intracellular accumulation of clusterin. This leads to induced expression of DKK1, which inhibits the activation of classical Wnt pathway and leads to the increment of non-classical Wnt pathway proteins such as Wnt5a and ROCK2 which further trigger the upregulation of pro-apoptotic genes and induce apoptosis.

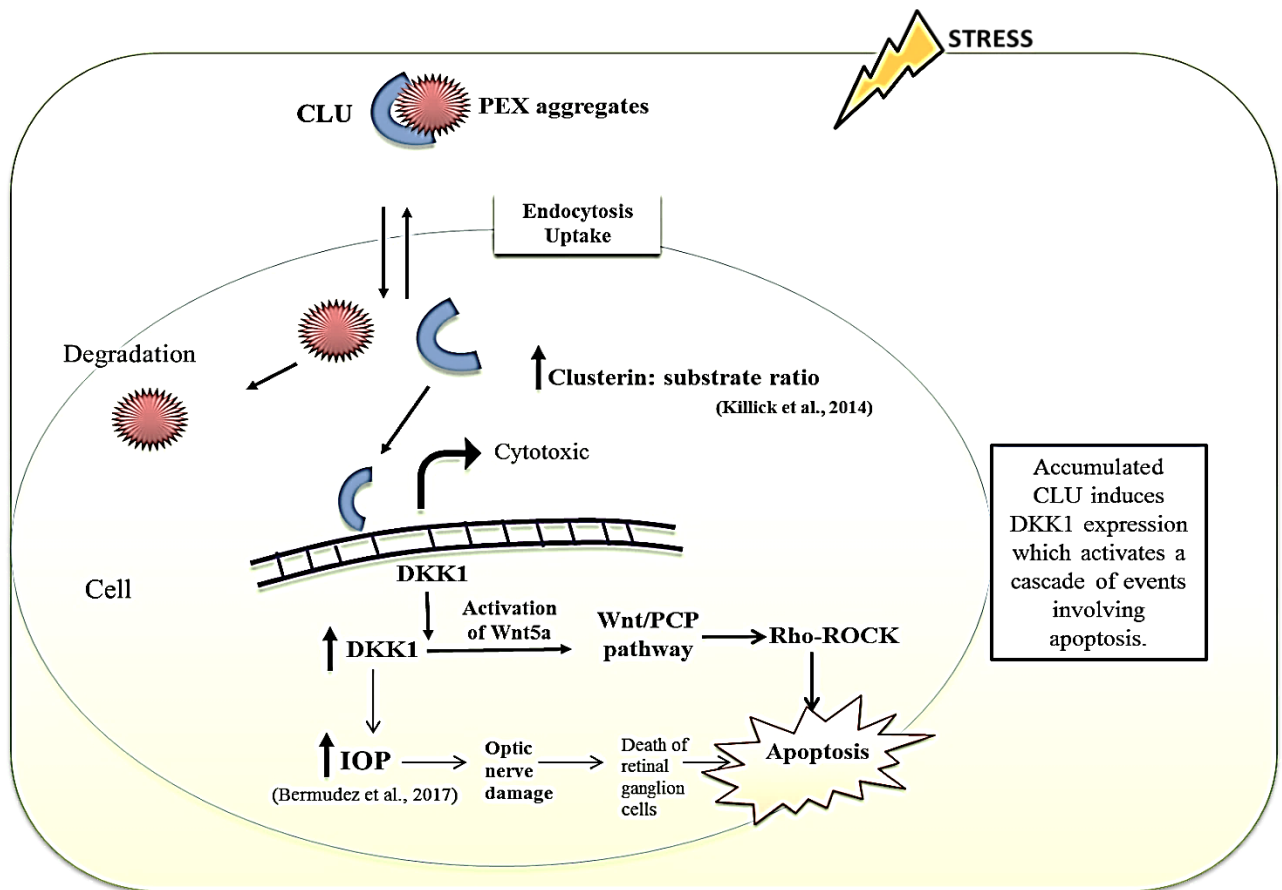


**Figure 4.8 Clusterin-dependent induction of DKK1 in PEX.** Increased intracellular accumulation of clusterin leads to increased expression of DKK1 in anterior eye segment of PEX affected subject. Increased expression of Wnt5a and ROCK2 suggest activation of non-canonical pathway which will further promote increased cell death.

#### 4.5 Conclusion

In conclusion, based on the expression analysis, findings from this study have identified that the elevated DKK1 expression and non-classical Wnt targets, Wnt5a and ROCK2 might be involved in the pathogenic process of PEX. Further investigation is required to elucidate their exact roles and to assess downstream targets of this aberrant Wnt signaling in PEX pathology.

# **CHAPTER 5**

*CACNA1A as a probable risk  
factor in the pathogenesis of  
PEX*

## 5.0 CACNA1A as a probable risk factor in the pathogenesis of PEX

### 5.1 Introduction

Genetic variation in *CACNA1A* (calcium channel, voltage dependent, P/Q type, alpha 1A subunit; Gene ID: 773) coding for a subunit of a  $\text{Ca}^{2+}$ -channel, has been identified as a risk factor for pseudoexfoliation (PEX). The following chapter is focused on finding *CACNA1A*'s role in the susceptibility of PEX pathology in Indian population. We also explored a mechanism by which *CACNA1A*'s intronic variant rs4926244 (hg38 chr19:g. 13264099 T>C) may affect PEX risk. *CACNA1A* encoded calcium channels are involved in a variety of calcium dependent processes including muscle contraction, neurotransmitter release and regulation of target gene expression.<sup>373–376</sup>

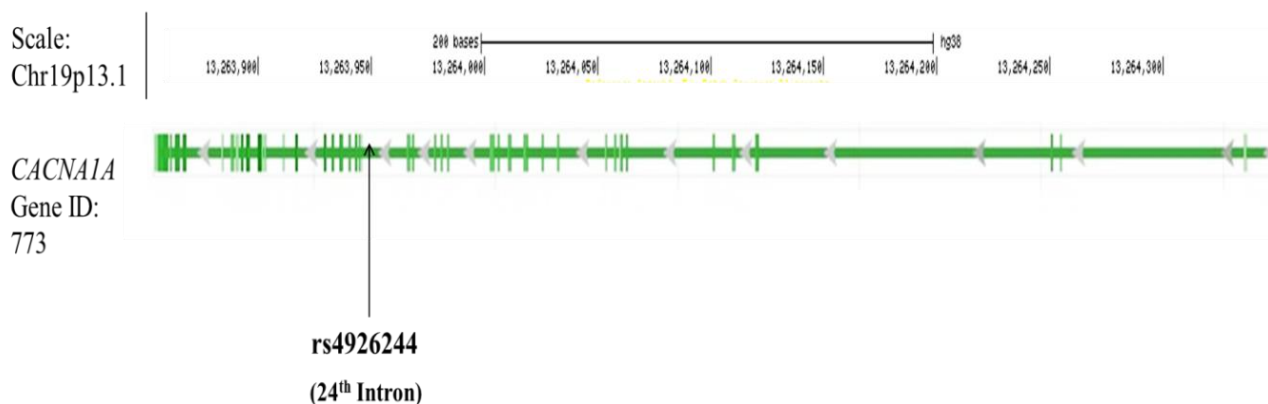


**Figure 5.1** The gene structure of *CACNA1A*. rs4926244 lies in the 24<sup>th</sup> intron. Gene structure is obtained from Genes, NCBI *Homo sapiens* Annotation Release 107, 2015-03-13.

#### 5.1.1 CACNA1A is a P/Q type voltage-sensitive calcium channel

*CACNA1A* belongs to calcium channel (CACN) gene family. *CACNA1A* gene encodes the alpha-1A subunit of a voltage-gated calcium channel called CaV2.1. CaV2.1 channels are multi-subunit complexes comprising of five subunits; a pore-forming subunit alpha 1 ( $\alpha_1$ ), intracellular beta ( $\beta$ ), accessory subunit- alpha2-delta ( $\alpha_2\delta$ ) and transmembrane gamma subunits (**Figure**

5.2).<sup>377</sup> The pore formed by the alpha-1A subunit ( $\alpha_1A$ ) facilitates the import of extracellular calcium ions and thus, this subunit is the main determinant of the channels' biochemical and physiochemical properties.<sup>377</sup> The  $\alpha_1A$  subunit is a tetra-domain transmembrane protein with cytoplasmic amino and carboxyl-terminus in distal region; the latter is involved in regulating channel activity and mediates protein-protein interactions.<sup>377-379</sup> Dysregulation of  $\alpha_1A$  C-terminus either due to mutation or proteolytic cleavage has led to severe functional consequences such as a toxic degeneration of Purkinje cells in homozygous mice expressing  $\alpha_1A$  subunit without C-terminus.<sup>380</sup>

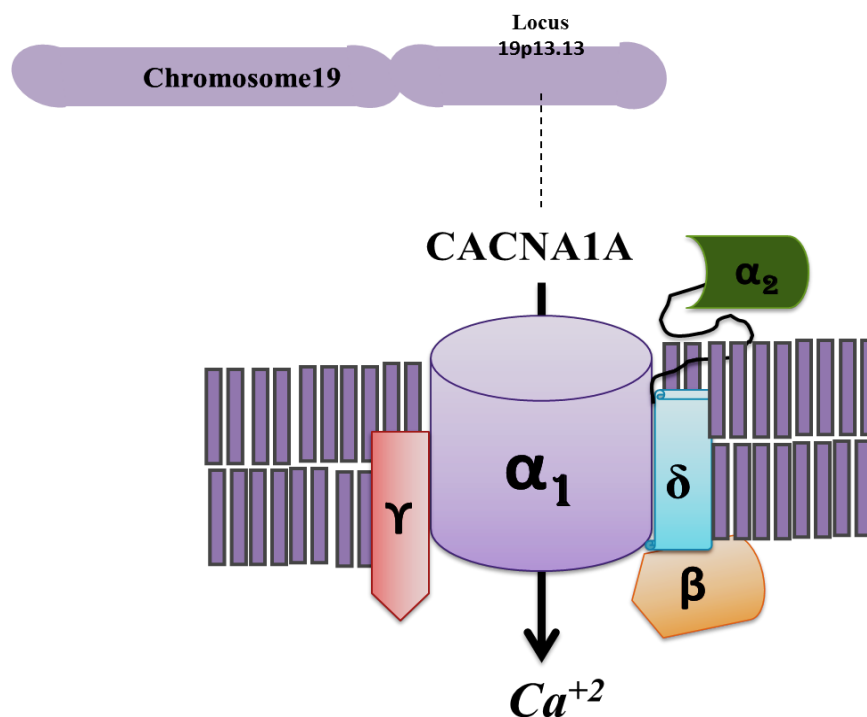


**Figure 5.2** Diagrammatic representation of the voltage gated calcium channel and its subunits.

### 5.1.2 Role of CACNA1A in various neurodegenerative disorders

Emerging evidence from previous studies has revealed that perturbed calcium channel plays a pivotal role in neurodegenerative processes (**Figure 5.3**). Altered calcium homeostasis resulting

in increased membrane permeability, overload of  $\text{Ca}^{2+}$ , release of pro-apoptotic factors etc. has been implicated in the pathogenesis of AD, PD, HD, and ALS.<sup>381,382</sup> In the late-onset AD, amyloid-beta ( $\text{A}\beta$ ) aggregates disrupt the calcium homeostasis by elevating an intracellular calcium concentration leading to apoptosis.<sup>382-384</sup> Mutations in  $\alpha 1\text{A}$  subunit of *CACNA1A* gene have been linked with various neurologic disorders such as spinocerebellar ataxia type 6 (SCA6) as well as familial and sporadic hemiplegic migraine and episodic ataxia type 2 (EA2).<sup>385,386</sup> Expansion of polyglutamine tracts in SCA6 alters  $\alpha 1\text{A}$  expression and results in cerebral dysfunction.<sup>387</sup>

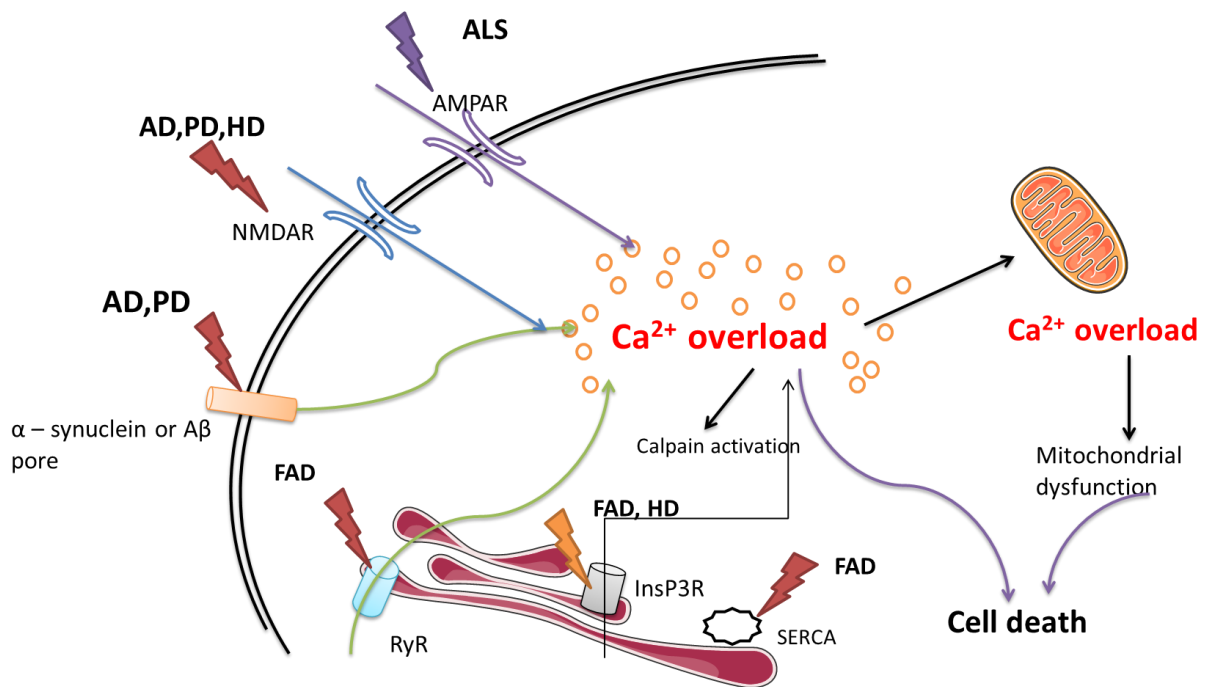


**Figure 5.3 Schematic representation of calcium channel disruption in neurodegenerative disorders.** Cytosolic calcium level is affected and calcium homeostasis is disrupted in neurodegenerative diseases such as Alzheimer's (AD), Huntington (HD), Parkinson's (PD) and Amyotrophic Lateral Sclerosis (ALS). Activities of cell surface calcium channels such as NMDAR (N-methyl-Daspartate receptor) and AMPAR ( $\alpha$ -amino-3-hydroxy-5-methyl-4-isoxazole propionic acid receptor) have been found to be deregulated in neurodegenerative disorders.  $\alpha$ -Synuclein of Lewy bodies in PD and  $\text{A}\beta$  peptides of senile

plaques in AD, can increase calcium channels permeability at the plasma membrane (Figure adapted from Marambaud *et. al.*, 2009).<sup>388</sup>

### **5.1.3 Potential role of CACNA1A as a risk factor in PEX progression**

Previous studies have documented the role of calcium in stabilizing fibrillin-1 in order to form stable aggregates.<sup>122</sup> Further, the presence of increased calcium concentration in aggregates of XFM fibrils has been demonstrated by electron microscopic studies in eyes affected with PEXS.<sup>121</sup> Hence, CACNA1A can play a critical role in changing cell surface calcium ions and in aggravation of disease condition (**Figure 5.4**). This idea prompted researchers to identify the role of calcium signalling in PEX affected subjects. GWAS detected significant association of a new genetic variant i.e. rs4926244 in *CACNA1A* gene that is linked with calcium signalling with PEX.<sup>9</sup> Blockade of the calcium ion channel by the drug verapamil results in a mechanical strain in human lamina cribrosa cells and thereby having a detrimental effect on ECM remodeling.<sup>18</sup> Besides, expression studies have found localization of CACNA1A in ocular tissues such as iris, ciliary body, lens epithelium, retina but not in XFM.<sup>9</sup> Based on these studies, it has been postulated that deregulated calcium ion concentrations due to mutation in *CACNA1A* gene may be one of the contributing factors in PEX pathogenesis, possibly by disrupting the function of proteins involved in ECM maintenance like LOXL1.

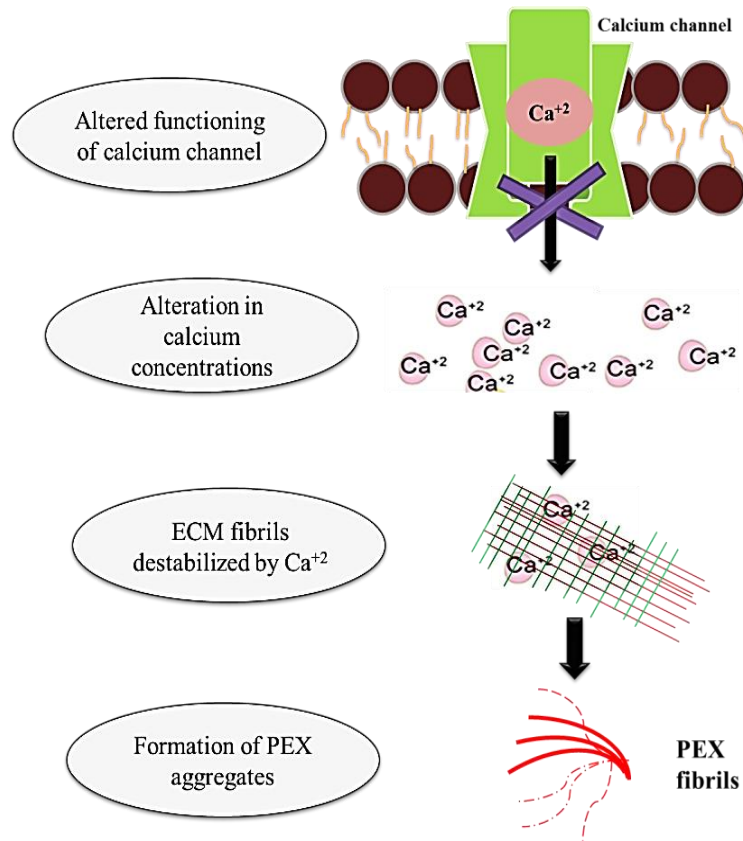


**Figure 5.4 Schematic illustrations for proposed role of CACNA1A in PEX pathogenesis.** The representative diagram depicts possible hypothesis of how mutation in *CACNA1A* gene contributes to PEX pathogenesis by altering calcium concentration, ECM dysfunction and increased formation of PEX aggregates.

The following study has been conducted to check the role of CACNA1A in the onset of PEX. Following specific aims were addressed in this chapter.

1. Genetic association of *CACNA1A* variants, rs4926244 in the pathogenesis of PEX in Indian population.
2. Status of *CACNA1A* mRNA expression in the anterior eye tissues of individuals affected with PEX.
3. To investigate the functional mechanism by which rs4926244 regulates CACNA1A expression.

4. To find the association of genetic variants linked with rs4926244 in the CACNA1A gene with PEX.

## 5.2 Materials and methods

### 5.2.1 Study subjects

Detailed information about study subjects' recruitment and inclusion or exclusion criteria followed for sample collection is mentioned in the materials and methods section 2.2.1 of Chapter 2 (page no. 28-29). Demographics of the study group are shown in **Table 5.1**.

**Table 5.1 Demographic of study subjects included for genotyping of CACNA1A variants. N=sample size.**

Study Subjects	N	Age(in years)		P-value	Gender		P-value
		Mean± SD	Range		Male	Female	
<b>PEX</b>	274	69.58 ± 5.57	45-92	0.13	188	86	0.32
<b>PEXS</b>	196	69.75 ± 8.90	50-85	0.10	129	67	0.78
<b>PEXG</b>	78	69.16 ± 7.72	45-92	0.6	59	19	0.07
Control	275	68.65 ± 10.15	50-90		177	98	

### 5.2.2 DNA extraction, PCR, elution and sequencing

Procedures followed for DNA extraction, PCR, elution and sequencing of targeted product is described in detail in materials and methods section 2.2.2-2.2.4 (Page no. 31-34). The primers were designed using Primer-BLAST. Both sequence details and annealing temperature of primers are shown in **Table 5.2**. PCR reactions were performed in 25µl volumes containing 10X reaction buffer (GeNet Bio, India), 1.5mM MgCl<sub>2</sub>, 0.5µM of each primer (IDT, USA), 1.0mM dNTP mix (GeNet, Bio, India), 50ng of genomic DNA, 0.3 unit of ExPrimeTaq DNA polymerase (GeNet Bio, India) and 2.5 mM of DMSO. The PCR products were subsequently eluted by gel elution kit (QIAquick Gel Extraction Kit, QIAGEN, Hilden) and sequenced unidirectionally using one of the previously mentioned primers (**Table 5.2**) with the help of

sequencing kit (Applied Biosystems, Austin, TX78744, USA). The automated sequencer 3130xl genetic analyzer from Applied Biosystems was used for sequencing and analysis was done using Sequencing analysis software v5.3 (Applied Biosystem) and BioEdit v7.1 (Freely available online at <http://www.mbio.ncsu.edu/bioedit/bioedit.html>).

**Table 5.2 List of oligos used in this study**

Primer	Purpose	Sequence (5'→3')	Annealing temperature T <sub>m</sub> (°C)
rs4926244	Genotyping	F: GTGGTATCAGTGGGCTCTTAAA R: GAATGGATGGCGGGATGTTA	56
rs4926246	Genotyping	F: GAGGACCGGGTAGTTCTGTG R: CCTTCCTTAACATCCCGCCA	54
rs121908212	Genotyping	F: CTACTCGCAAACAAAGAGAAAAGC R: AGTTCCTTAAAGAGCGTCAG	50
rs121908217	Genotyping	F: AGGTTATCATTGGGAGCATCTTCG R: GTTGAGGAGAGACGACCAG	57
CACNA1A (NM_001174080)	qRT-PCR	F: CTGCGGAGAACCACCATAAA R: AGAACCCACAGAGGCTATATCA	60
GAPDH (NM_002046.5)	qRT-PCR	F: GGTGTGAACCATGAGAAGTATGA R: GAGTCCTTCCACGATACCAAAG	60
rs4926244 (Intronic region)	Luciferase Assay	F: CTCCGGTACCCTGCATTGCTCCAAGGGTCT R: CACCTCGAGGGTGTCATGGCATCTCTGGG	62
CRISPR SgRNA pair 1	Genome editing	Sense: CACCGCATCTGAAAACAGCGGCACC Antisense: AAACGGTGCCGCTGTTTTTCAGATGC	–
CRISPR SgRNA pair 2	Genome editing	Sense: CACCGGAATGGATGGCGGGATGTTA Antisense: AAACTAACATCCCGCCATCCATTCC	–
CRISPR rs49KO	Genome editing	F: GTGGTATCAGTGGGCTCTTAAA R: GGGCTTGAGATATGTAGCCATAA	54

### 5.2.3 TaqMan SNP Genotyping Assay

Intronic SNP, rs4926246 in CACNA1A was genotyped in the PEXS, PEXG patients and control individuals using TaqMan SNP genotyping technology performed by Real-time PCR. In a

standard reaction of 5 $\mu$ l, 20ng of working DNA sample was dispensed on 384 well plates, along with 2.5 $\mu$ l TaqMan master mix (TaqMan assay for a single SNP), 1.87 $\mu$ l Nuclease Free Water (NFW) in each well. Reactions were run on a real-time PCR system (Quant studio 7 flex, Applied Biosystem) using a universal thermal cycling protocol with an initial denaturation step of 12 minutes at 95°C, 40 cycles of amplification for 15 seconds at 92°C and termination for 90 seconds at 60°C. After the run, the raw data was analyzed by Quant studio TaqMan genotyper software.

#### **5.2.4 Quantitative Real-Time PCR**

Procedures followed for RNA extraction, cDNA synthesis and RT-PCR is described in detail in materials and methods section 2.2.5-2.2.7 (Page no. 36-37). Gene specific primers were used for both *CACNA1A* and *GAPDH* which were designed using Primer-BLAST (**Table 5.2**). Comparative threshold cycle ( $\Delta\Delta$ Ct) method was used for normalization of target gene and change in expression was represented as fold difference.

#### **5.2.5 Cell culture**

HEK293 cells were grown in HiGlutaXL Dulbecco's Modified Eagle Medium, high glucose (DMEM) with 10% fetal bovine serum (FBS), 1x penicillin/streptomycin and 1x amphotericin B (HiMedia) while HLE B-3 cells cultured in DMEM/F12 (GIBCO) and supplemented with 10% inactivated FBS were grown at 37°C in a humidified environment of 5% CO<sub>2</sub>. Experiments for transient transfections were done in a 12 well plate with lipofectamine 2000 (Invitrogen, 64 Carlsbad, California).

#### **5.2.6 Dual Luciferase Reporter Assay**

For reporter assays, a luciferase reporter vector pGL4.23 (Promega, Madison, WI) with minimal promoter was used. The 118bp fragment surrounding rs4926244 was PCR-amplified from DNA of individuals homozygous for risk and non-risk alleles. Two restriction sites, KpnI and XhoI were added to the primers during amplification, and the resulting PCR products were double digested and cloned upstream of the minimal promoter region of pGL4.23 containing the firefly luciferase reporter. Five to six independent clones for each allele were isolated, verified by sequencing, and transfected in triplicate into HEK293 and HLE B-3 cell lines.

Approximately  $2 \times 10^5$  cells per well were seeded in 12-well plates. At 80% confluency, cells were co-transfected with luciferase constructs and internal control Renilla (phRL-TK; Promega) at a ratio of 100:1 using Lipofectamine 2000 (Invitrogen). At 48 hours post transfection, cells were lysed with passive lysis buffer (Promega), and luciferase activity was measured using the Dual-Luciferase Assay System (Promega). The ratios between firefly luciferase to Renilla luciferase provide normalized luciferase activity for each construct. Normalized luciferase values obtained for each group were plotted as percent relative luciferase activity in comparison to empty pGL4.23 vector. Data was obtained from three independent transfections and was reported as the fold change in mean  $\pm$ SE relative luciferase activity per allele.

### **5.2.7 CRISPR/Cas9 constructs preparation and genome editing**

Genome editing was done using CRISPR/Cas9 system. A pair of sgRNA was designed (<http://crispr.mit.edu/>) with a little off-target specificity to delete a 229 bp region around the SNP, rs4926244 (**Table 5.2**). Annealed oligonucleotides were phosphorylated and ligated into BbsI digested PX459 (Plasmid #62988; Addgene, Cambridge, Massachusetts). At 50% confluency, HEK293 cells were transfected with 2.5 $\mu$ g of each CRISPR construct (with sgRNA1 and sgRNA2) simultaneously using lipofectamine 2000 (Invitrogen, 64 Carlsbad, California).

Transfected cells were selected after 24 hours post-transfection in complete media supplemented with 2.5µg/µl puromycin. Single cell clones were then isolated and cultured by dilution cloning and subsequently genomic DNA was isolated using DNeasy Blood & Tissue Kit (Qiagen, Hilden, Germany) following manufacturer's instructions. Screening was done to find clones with homozygous deletion of genomic region containing rs4926244 by using a specific set of primers (**Table 5.2**) outside the targeted sites and subsequently confirmed by sequencing. Positive clones were used for subsequent experiments.

### **5.2.8 Statistical Analysis**

All the genetic analysis for the association such as, Hardy-Weinberg equilibrium, chi-square test and permutation analysis was done with IBM-SPSS and Haploview 4.2. Multiple comparisons were corrected by Bonferroni method. Online genetic power calculator OPENEPI (<http://web1.sph.emory.edu/users/cdckms/sample%20size%20%20grps%20cohort.htm>) was used to calculate statistical power of an association study. Group-wise results from qRT-PCR were analysed for statistical significance by Student's t-test. Data is presented as mean ± SE.

## **5.3 Results**

### **5.3.1 Genotypic association of risk variant SNP rs4926244 with pseudoexfoliation in Indian population**

Prior to association analysis, the raw data for the SNP was checked for Hardy Weinberg's equilibrium. Allelic and genotypic frequencies for rs4926244 are shown in the **Table 5.3** and **Table 5.4**, respectively. In the present sample size of 274 cases and 275 controls, rs4926244 failed to project an allelic association with PEX. The allele frequencies did not differ significantly between patients with PEX (p=0.37, OR-1.12 [0.86-1.46]), PEXS (p=0.51, OR-1.09 [0.82-1.46]), PEXG (p=0.41, OR-1.18 [0.79-1.76]) when compared with control subjects.

Current study has a very low statistical power of 7.73% and the samples required to achieve statistical significance with 80% genetic power are n>5680 cases and n>5663 controls. More samples need to be added to this study.

**Table 5.3 Allelic distribution of CACNA1A variant rs4926244 in PEX and control subjects.**

SNP	Allele	Allele count (frequency) in PEX (N=274)	Allele count (frequency) in Control subjects (N=275)	Chi sq. $\chi^2$	OR (95% CI)	P-value	P-value†
rs4926244	C	152 (0.271)	165 (0.30)	0.58	1.126 (0.867-1.463)	0.37	0.47
	T	397 (0.729)	385 (0.70)				
SNP	Allele	Allele count (frequency) in PEXS (N=196)	Allele count (frequency) in Control (N=275)	Chi sq.	OR (95% CI)	P-value	P-value
rs4926244	C	110 (0.281)	165 (0.30)	0.27	1.098 (0.825-1.462)	0.51	0.62
	T	282 (0.719)	385 (0.70)				
SNP	Allele	Allele count (frequency) in PEXG (N=78)	Allele count (frequency) in Control (N=275)	Chi sq.	OR (95% CI)	P-value	P-value
rs4926244	C	41 (0.266)	165 (0.30)	0.66	1.181 (0.790-1.764)	0.41	0.41
	T	113 (0.733)	385 (0.70)				

N= Sample size, OR: Odds ratio, CI: Confidence interval, †: P-value after permutation correction where N=10,000

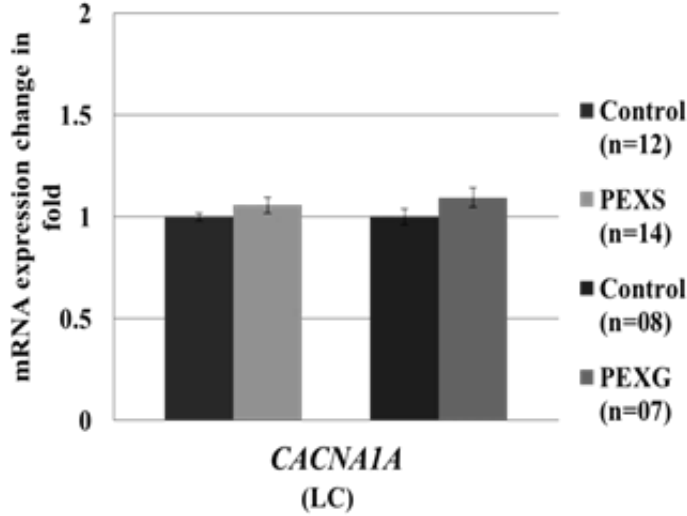
Further, association test for specific model of inheritance was analyzed which showed a significant genotypic association with higher frequency of the risk genotype ‘TT’ with PEX (p=0.02) and PEXS (p=0.03) but not with PEXG (p=0.33) compared to controls. However, no significant association under the dominant and recessive model was detected (Table 5.4).

**Table 5.4 Genotypic distribution of SNP rs4926244 in CACNA1A gene across PEX patients and controls.**

SNP	Genotype	Frequency in PEX (N=274)	Frequency in Control (N=275)	Genetic Model	$\chi^2$	OR (95% CI)	P-value
rs4926244	CC	0.1	0.08	Genotypic	7.02		<b>0.02</b>
	CT	0.33	0.44	Dominant	1.48	0.69 (0.39-1.24)	0.22
	TT	0.55	0.48	Recessive	1.29	1.36 (0.97-1.96)	0.06
SNP	Genotype	Frequency in PEXS (N=196)	Frequency in Control (N=275)	Genetic Model	$\chi^2$	OR (95% CI)	P-value
rs4926244	CC	0.11	0.08	Genotypic	6.71		<b>0.03</b>
	CT	0.32	0.44	Dominant	1..95	0.64 (0.34-1.19)	0.16
	TT	0.56	0.48	Recessive	2.65	1.35 (0.93-1.96)	0.1
SNP	Genotype	Frequency in PEXG (N=78)	Frequency in Control (N=275)	Genetic Model	$\chi^2$	OR (95% CI)	P-value
rs4926244	CC	0.09	0.08	Genotypic	2.2		0.33
	CT	0.36	0.44	Dominant	1.95	0.87 (0.35-2.12)	0.76
	TT	0.56	0.48	Recessive	1.71	1.40 (0.84-2.32)	0.19
N: Sample size, OR: Odds ratio, CI: Confidence interval, $\chi^2$ : Chi-square							

### 5.3.2 Reverse transcript expression analysis of CACNA1A in lens capsule of PEX affected patients

To further examine the role of *CACNA1A* in PEX pathogenesis, we performed mRNA expression analysis in lens capsule of PEXS, PEXG and control subjects. Quantitative real-time PCR detected no statistically significant differences in expression of *CACNA1A* in PEXS (1.1 fold; p=0.72) and PEXG (1.15 fold; p=0.61) individuals when compared to control (**Figure 5.5**).



A.

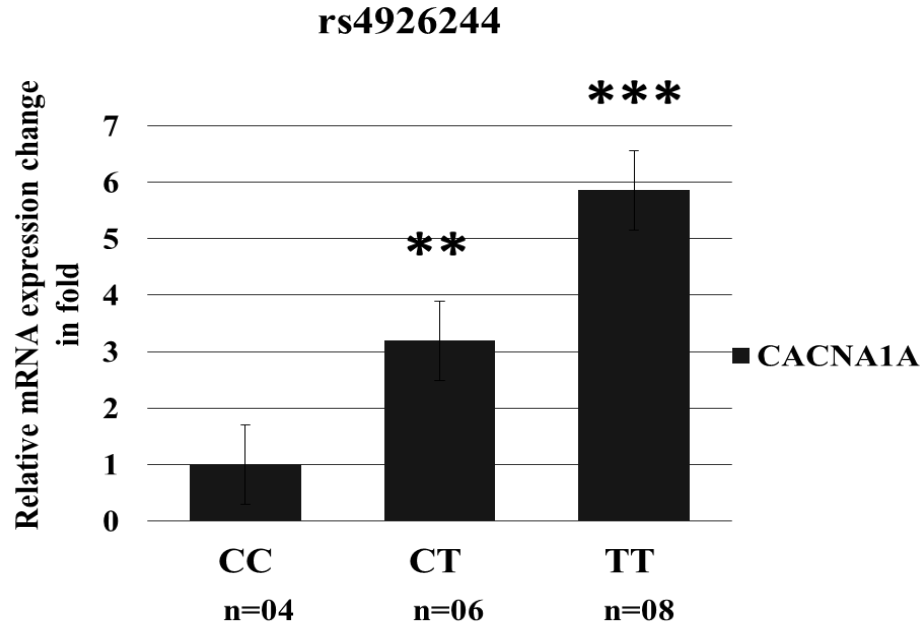
Study Subjects (Lens capsule)	N (females in %)	Age (in years) Mean± SD	P-value	Gender Mean± SEM	P-value
PEXS	14 (35.7%)	73.21 ± 5.57	0.12	0.35 ± 0.13	0.48
Control	12 (50%)	68.41 ± 8.90		0.5 ± 0.15	
PEXG	07 (40%)	69.5 ± 7.72	0.88	0.42 ± 0.20	0.84
Control	08 (37.5%)	70.25 ± 10.15		0.5 ± 0.16	

B.

**Figure 5.5 CACNA1A mRNA expression change in PEX affected subjects compared to control. A.** Real-time PCR showing the fold change of *CACNA1A* mRNA expression in the lens capsule of control, PEXS and PEXG individuals. There was no significant difference in expression of lens capsule tissues from control ( $1.04 \pm 0.02$ ), PEXS ( $1.1 \pm 0.04$ ,  $p=0.72$ ) and PEXG ( $1.15 \pm 0.05$ ,  $p=0.61$ ) individuals. **B.** Demographic of study subjects included for qRT-PCR for group wise comparison. Data are represented as Mean ± SEM, N=sample size, \* $P < 0.05$ .

In order to check for any genotype-based regulatory effect of the intronic variant, rs4926244 on *CACNA1A*, qRT-PCR data was reanalysed after grouping of  $\Delta\Delta C_t$  values according to genotype of rs4926244. Expression level of *CACNA1A* in the “CC” genotyped individuals was taken as base for comparing the expression level of “TT” genotyped individuals. Compared to “CC” genotyped individuals, mRNA expression of *CACNA1A* is higher in the risk genotype

“TT” individuals with a fold difference of 5.86 and was found to be statistically significant (p=0.0007, n=08). There was even a more than 3-fold increase in *CACNA1A* mRNA expression in individuals with genotype “CT” (p=0.005, n=06). **Figure 5.6** depicts the genotype wise comparison for the change in mRNA expression of *CACNA1A*.



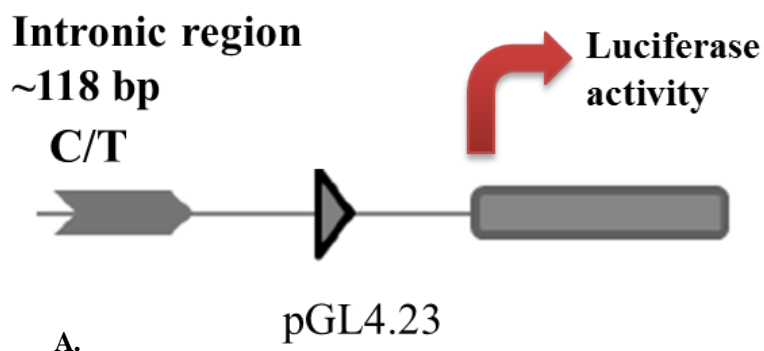
rs4926244 Genotypes	N (females in %)	Age (in years) Mean± SD	P-value	Gender Mean± SEM	P-value
CT	6 (50.0%)	67.83 ± 11.14		0.5 ± 0.22	
TT	8 (37%)	71.12 ± 9.68	0.57	0.37 ± 0.18	0.67
CC	4 (25%)	66.0±9.4	0.78	0.25 ± 0.2	0.48

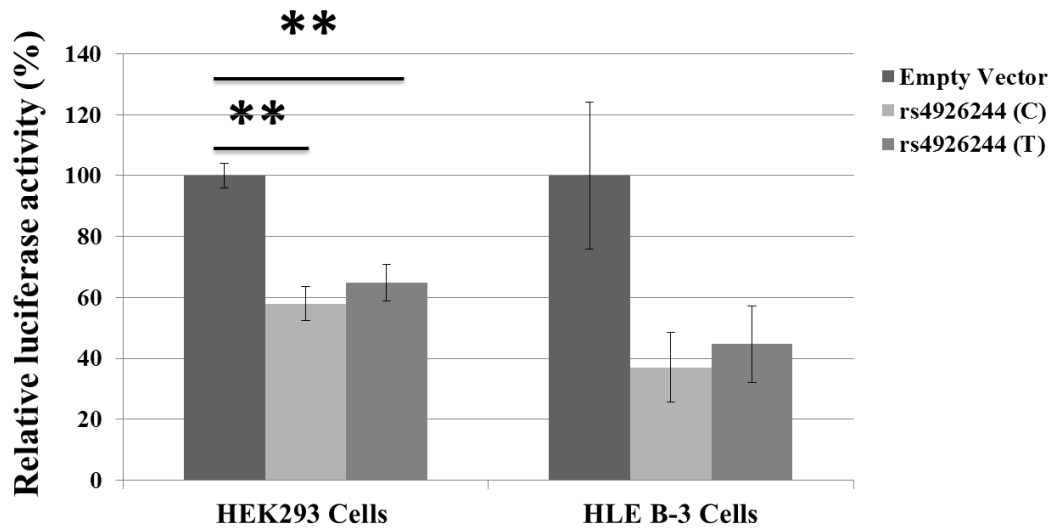
**Figure 5.6 rs4926244 genotype-based *CACNA1A* mRNA expression correlations.** **A.** *CACNA1A* mRNA expression was grouped according to rs4926244 genotypes by taking protective genotype “CC” as the reference genotype. Compared to genotype “CC” (1.00 fold) *CACNA1A* expression was found to be significantly upregulated in the risk genotype “TT” (5.89 fold; p=0.0007) as well as in the heterozygous genotype “CT” (3.19 fold; p=0.005) in the lens capsule. **B.** Demographic of study subjects included for

qRT-PCR using genotype-wise comparison. N= sample size. Data are represented as Mean  $\pm$  SEM, \*\*P<0.01; \*\*\*P<0.001.

### 5.3.3 Influence of rs4926244 locus on *CACNA1A* gene regulation

To determine a putative regulatory effect of this locus, *in vitro* luciferase assays were performed. We cloned a 118 bp genomic region surrounding the SNP rs4926244 (either ‘C’ or ‘T’ respectively) upstream to the minimal promoter of luciferase vector, pGL4.23 and checked its regulatory effect after transfecting them individually in both HEK293 and HLE B-3 cells. As shown in **Figure 5.7**, we observed statistically significant difference in luciferase activity between control empty vector and constructs with either allele ‘C’ (57.9%; p=0.003) or ‘T’ (64.8%; p=0.001) in HEK293 cells. Similarly, HLE B-3 cells showed comparable effect of the rs4926244 element on the reporter activity but no significant difference in luciferase activity were obtained with either allele ‘C’ (37.02%; p=0.07) or ‘T’ (44.68%; p=0.10) when compared to empty vector. Although the construct with ‘T’ allele showed slightly higher luciferase activity than the one with ‘C’ allele in both HEK293 and HLE B-3, the difference in luciferase activities was not significant. This suggests that rs4926244 resides in a regulatory region in *CACNA1A* and might play a role in its regulation but may not have an observable allele specific effect through luciferase assay.





B.

**Figure 5.7 Allelic effects on luciferase activity in HEK293 and HLE B-3 cells.** Normalized luciferase activity in HEK293 cells with constructs containing flanking region of rs4926244 compared to empty vector. There is a significant difference in reporter activity in HEK293 cells between control empty vector ( $100 \pm 4.00$ ) and “C” ( $57.9 \pm 5.47$ ) or “T” ( $64.8 \pm 5.94$ ) alleles with p-values of 0.003 and 0.001, respectively. However, there is no significant change in reporter activity on substituting allele “C” to allele “T” ( $p = 0.35$ ). Similarly, in HLE-B3, the difference between empty vector ( $100 \pm 24.49$ ) and “C” ( $37.7 \pm 11.36$ ;  $p=0.07$ ) or “T” ( $44.68 \pm 12.58$ ;  $p=0.10$ ) though showed similar trends as HEK293 but failed to reach significance. in HLE B-3 cells, there was no significant change in reporter activity on substituting allele “C” to allele “T” ( $p = 0.71$ ). Each experiment was independently replicated more than three times. \* $P < 0.05$ ; \*\* $P < 0.01$ .

### 5.3.4 *In vivo* effect of rs4926244 on CACNA1A gene expression

HEK293<sup>229/-</sup> cells was generated via CRISPR/Cas9 system in which 229 bp genomic region was deleted around rs4926244 in order to determine the effect of the rs4926244 locus on *CACNA1A* gene expression. As shown in the **Figure 5.4**, two sgRNA targeting sites were selected for genomic deletion. qRT-PCR revealed a significant decrease in *CACNA1A* expression (0.6 fold;  $p < 0.05$ ) in genome edited HEK293 cells compared to non-deleted cells confirming the regulatory effect of this locus on *CACNA1A* gene expression.

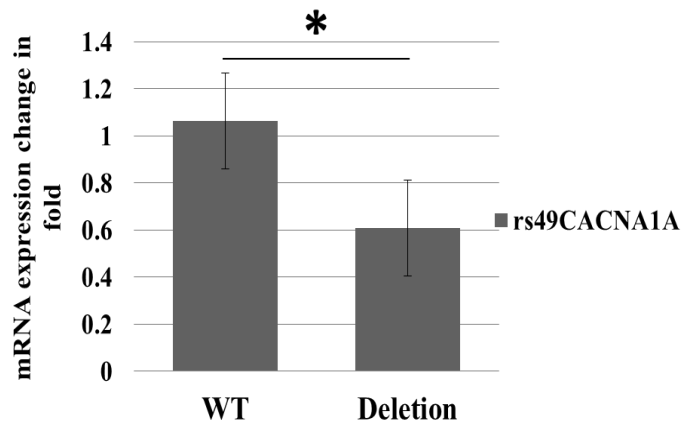
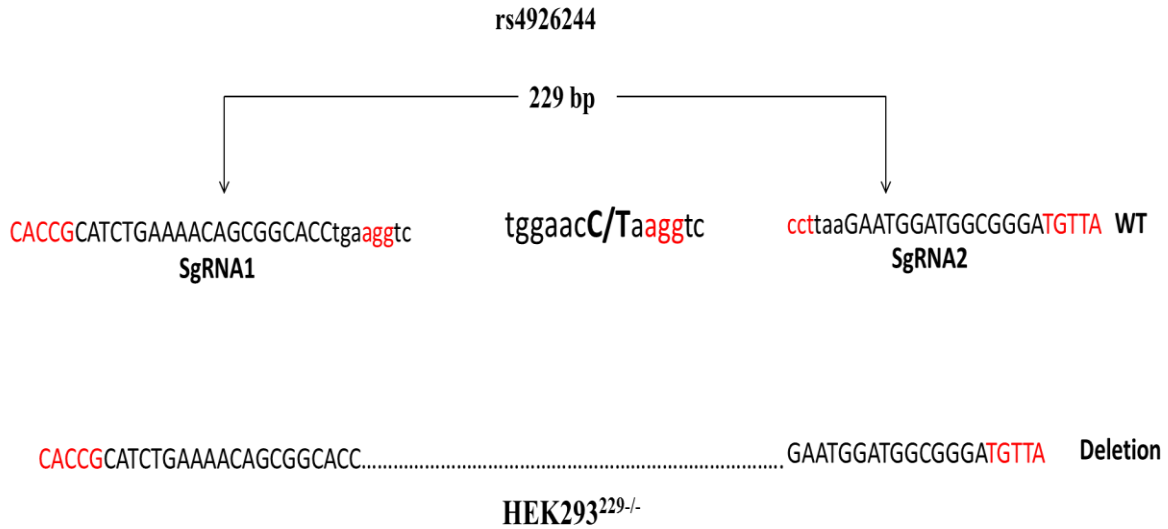


**Figure 5.8 *In vivo* effect of rs4926244 locus on CACNA1A expression.** **A.** A representative figure showing deletion of 229bp region around rs4926244. **B.** qRT-PCR assay for checking *CACNA1A* expression in control and knockout HEK293 cells. There is a significant downregulation of *CACNA1A* (0.6 fold;  $p=0.01$ ) in cells with deletion compared to that of non-deleted cells ( $1.24 \pm 0.2$ ). WT corresponds to wild type. Experiments were performed three times and values are represented as mean  $\pm$  SEM. Student's t-test was used to calculate statistical significance between groups, \* $P<0.05$

### 5.3.5 Genetic association of rs4926246, a tag SNP of r4926244 with pseudoexfoliation glaucoma

Tag SNPs were found through 1000 genome studies for rs4926244, and SNPs found to be in linkage disequilibrium (LD) with rs4926244 were shortlisted. The genetic association of one of the intronic variants, rs4926246:T>C (hg38 chr19:13264473 T>C) that was found to be in strong LD ( $D' = 1$ ,  $R^2 = 0.94$ ) with rs4926244 has been explored in this study (**Figure 5.9**).

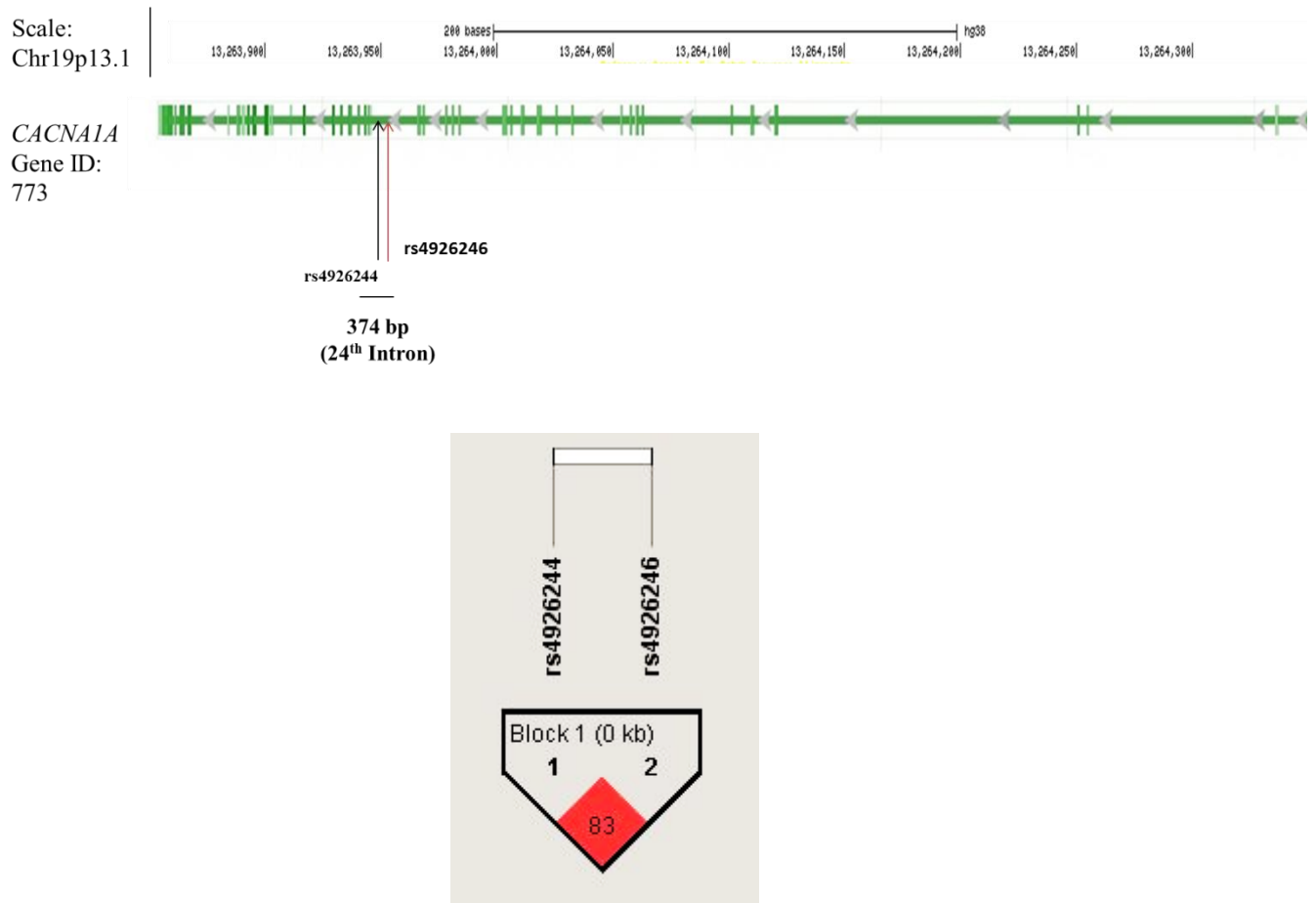


**Figure 5.9 LD block of rs4926244 and rs4926246.** The intronic SNP, rs4926246 found to be in Linkage disequilibrium and have a strong association with rs4926244. LD block obtained from Haploview 4.2.

In a case-control study (275 Control and 274 PEX) rs4926246 was genotyped through TaqMan SNP Genotyping Technology. The allele distribution and association results for rs4926246 are described in **Table 5.5**. We observed that intronic SNP, rs4926246 is significantly associated with PEXG in our population with “T” as the risk allele ( $p=0.04$ ) which confers a

modest risk of 1.51 (1.00–2.26) with increased chances of acquiring PEXG (Table 5.5). Its significance remains even after carrying out 10,000 permutations (p=0.048). The current study is at 40% power at  $\alpha = 0.05$  level significance. For the required genetic power (80%) more samples need to added for a stronger confirmation of its association with PEX.

**Table 5.5 Allelic distribution of CACNA1A variant rs4926246 in PEX, PEXS, PEXG and control subjects**

SNP	Allele	Allele count (frequency) in PEX (N=274)	Allele count (frequency) in Control subjects (N=275)	Chi sq. $\chi^2$	OR (95% CI)	P-value	P-value†
rs4926246	C	154 (0.280)	180 (0.332)	2.772	1.24 (0.96-1.61)	0.09	0.11
	T	394 (0.729)	370 (0.672)				
SNP	Allele	Allele count (frequency) in PEXS (N=196)	Allele count (frequency) in Control (N=275)	Chi sq.	OR (95% CI)	P-value	P-value†
rs4926246	C	116 (0.280)	180 (0.332)	1.042	1.17 (0.87-1.53)	0.3	0.33
	T	276 (0.704)	370 (0.672)				
SNP	Allele	Allele count (frequency) in PEXG (N=78)	Allele count (frequency) in Control (N=275)	Chi sq.	OR (95% CI)	P-value	P-value†
rs4926246	C	38 (0.243)	180 (0.332)	3.98	1.51 (1.00-2.26)	0.04	<b>0.04</b>
	T	118 (0.756)	370 (0.672)				

N: Sample size, OR: Odds ratio, CI: Confidence interval, †: P-value after permutation correction where N=10,000

However, the genotypic frequency of this SNP shows nominal association only with PEX (p=0.04), while PEXS (p=0.07) and PEXG (p=0.11) failed to project significant difference compared to control in genotypic model (Table 5.6). While Recessive model showed significant association of risk genotype TT with PEX (0.02) and PEXG (p=0.04). More samples need to be included in this study.

**Table 5.6 Genotype frequency of CACNA1A variant rs4926246 in PEX, PEXS, PEXG and control subjects**

SNP	Genotype	Frequency in PEX (N=274)	Frequency in Control (N=275)	Genetic Model	$\chi^2$	OR (95% CI)	P-value
rs4926246	CC	0.105	0.101	Genotypic	6.06	-	<b>0.04</b>
	CT	0.35	0.45	Dominant	0.02	0.95 (0.55-1.65)	0.87
	TT	0.543	0.447	Recessive	5.11	1.47 (1.05-2.06)	<b>0.02</b>
SNP	Genotype	Frequency in PEXS (N=196)	Frequency in Control (N=275)	Genetic Model	$\chi^2$	OR (95% CI)	P-value
rs4926246	CC	0.122	0.101	Genotypic	5.12	-	0.07
	CT	0.346	0.45	Dominant	0.49	0.81 (0.45-1.44)	0.48
	TT	0.539	0.447	Recessive	3.18	1.39 (0.96-2.01)	0.09
SNP	Genotype	Frequency in PEXG (N=78)	Frequency in Control (N=275)	Genetic Model	$\chi^2$	OR (95% CI)	P-value
rs4926246	CC	0.64	0.101	Genotypic	4.263	-	0.118
	CT	0.358	0.45	Dominant	1.165	1.65 (0.61-1.43)	0.31
	TT	0.576	0.447	Recessive	4.09	1.68 (1.01-2.80)	<b>0.04</b>

N: Sample size, OR: Odds ratio, CI: Confidence interval,  $\chi^2$ : Chi-square

Haplotype analysis as shown in **Table 5.7**, revealed “T-T” of rs4926244 and rs4926246, as the risk haplotype with a significant association both in PEX and in PEXG cases (p=0.02 and p=0.02, respectively). However, this frequency did not differ significantly after permutation correction (p=0.09 and p=0.08, respectively).

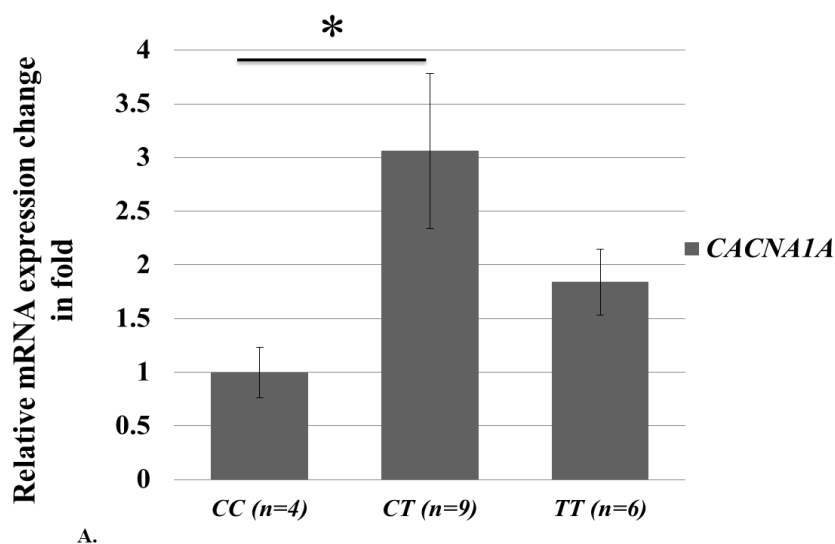
**Table 5.7 Haplotype association of the two variants rs4926244 and rs4926246 with study subjects.**

Frequency of haplotype combinations were compared between cases and controls.

Risk haplotype T-T (rs4926244-rs4926246)	Frequency	Chi sq. $\chi^2$	P-value	P-value†
PEX	0.694	4.846	0.02	0.09
PEXS	0.679	2.406	0.12	0.3
PEXG	0.728	5.162	0.02	0.08
Control	0.631			

†: p-value after permutation correction where n=10,000.

We then checked the regulatory effect of non-coding variants, rs4926246. After grouping of  $\Delta\Delta C_t$  values according to the genotype of rs4926246, we found an increase in CACNA1A mRNA level per “T” risk allele (**Figure 5.10A**). There was a more than half-fold increase in CACNA1A mRNA expression in individuals with genotype “TT” (n=06, p=0.05) compared to “CC” (n=4) genotype and this increases to three-fold in “CT” individuals (n=11, p=0.01). Demographic of study subjects included for q-RT PCR for genotype wise comparison of rs4926246 is shown in **Table 5.10B**. (**Confirmation with more samples is necessary to validate this initial preliminary finding**).



rs4926246 Genotypes	N (females in %)	Age(in years)	P-value	Gender	P-value
		Mean± SD		Mean± SEM	
CT	9 (55.5%)	69.88 ± 9.34	0.39	0.55 ± 0.17	0.35
TT	6 (33.3%)	71.12 ± 9.68	0.15	0.33 ± 0.21	0.8
CC	4 (25%)	64.0 ± 11.1		0.25 ± 0.2	

B.

Figure 5.10. rs4926246 genotype wise comparison of *CACNA1A* mRNA expression. (A) *CACNA1A* mRNA expression is grouped according to genotype of rs4926246 by taking protective genotype “CC” as the reference genotype. There was a significant difference of *CACNA1A* expression between genotype “CC” ( $1.08 \pm 0.23$ ) versus “CT” ( $3.06 \pm 0.72$ ,  $p=0.01$ ) but failed to reach significance when compared “CC” versus “TT” ( $1.84 \pm 0.30$ ,  $p=0.05$ ). (B) Demographic of study subjects included for q-RT PCR for genotype wise comparison. n=sample size. \* $P<0.05$ .

## 5.4 Discussion

*CACNA1A* codes for the alpha-1 A, pore-forming subunit for the voltage gated, calcium channel, important for regulating calcium ion entry, mediating release of hormones and neurotransmitters, gene transcription, muscle contraction and it majorly participates in maintaining the physiological and biochemical properties of the channel.<sup>377,389–391</sup> GWAS conducted by a Japanese group (involving multi-institutional collaborations across the globe including south Indian samples) followed by two-stage replication studies identified a novel variant residing in *CACNA1A* gene involved in calcium signaling.<sup>9</sup> Disease associated SNP rs4926244 is located in the intronic region of *CACNA1A* and showed a consistent association of minor allele “C” with PEXS in multiple populations. However, in the present study, the allelic association was not found involving samples from 274 cases and 275 controls. As can be noted from Aung et al, samples provided from India  $n > 1000$  cases and  $n > 3000$  controls, showed a significance ( $p$ -value= 0.006) which is moderate as compared to other ethnic groups included in the study.<sup>9,318</sup>

Interestingly, we found a strong genotypic association of “TT” genotype with PEXS in our study population. This shows that the risk allele homozygosity incurred higher risk of acquiring the disease. This also explains that PEX patients and control cohort show distinct distribution of genotypes such that individual with genotype “TT” have a higher susceptibility to the disease. Hence, the alleles per se are not associated but maybe a particular genotype can incur sufficient risk in acquiring the disease. This suggests that common variant (rs4926244) may contribute to modest PEX risk but larger datasets are required to confirm these findings, besides yet unknown causal variants of *CACNA1A* might contribute to the genetic risk of PEX.

Bioinformatics analysis suggests risk allele of *CACNA1A* may decrease its expression in peripheral blood cells.<sup>9</sup> Besides, reduced expression level of *CACNA1A* mRNA was reported in ocular tissues (cornea, iris, ciliary body and choroid) of PEXS patients compared with control tissues.<sup>392,393</sup> In our study, genotype correlated expression analysis revealed an association of risk genotype “TT” of rs4926244 with increased *CACNA1A* expression levels in lens capsule of study subjects; however, no significant difference could be established in mRNA expression on comparing only PEXS and PEXG affected tissues with control. We then carried out studies to check for functional significance of the genomic region surrounding rs4926244 by luciferase reporter assays *in vitro*. We found that rs4926244 resides in a regulatory region and observed that the locus has an effect on *CACNA1A* expression after deletion of the genomic region by CRISPR/Cas9. Deletion of the locus surrounding rs4926244 resulted in downregulation of *CACNA1A* mRNA expression, implicating the locus might have a regulatory effect on the gene expression.

Extending the work to tag SNP of rs4926244, we identified a novel association of an intronic SNP rs4926246 (located ~374 bp upstream of rs4926244) with PEXG individuals. Both

the SNPs are non-coding variant located in 24<sup>th</sup> intron. Here, we found a significant association of the common variant, rs4926246 (T>C) with allele “T” as the risk factor for PEXG which has not been reported before. This result suggests that the interplay of genetic variants may influence the P/Q type calcium channel function in PEX pathogenesis. Polymorphism in CACNA1A has been implicated in many neurologic disorders such as episodic ataxia 2, SCA6 and migraine.<sup>394–</sup>

<sup>396</sup> Overall, this study supports the involvement of genetic variation at rs4926246 in a genetic risk of PEXG and suggests CACNA1A as a contributing factor in the pathogenesis of PEX. Additional genetic studies with large cohorts attaining sufficient power are required to fully elucidate the role of the *CACNA1A* genes in the development of PEXS and PEXG. Moreover, to understand its functional significance allele-specific effects needs to be studied.

## 5.5 Conclusion

In nutshell, the current study demonstrates the association of CACNA1A polymorphic marker rs4926244 with PEX and PEXS only at genotypic level, whereas *de novo* variant, rs4926246 in linkage disequilibrium with rs4926244 was found to be significantly associated with PEXG with the T allele as a risk allele in PEXG patients. Further investigation is required to identify the mechanisms underlying the involvement of CACNA1A polymorphic variants in PEX susceptibility and more functional studies are warranted to understand the role of CACNA1A in the pathology of PEX.

# **CHAPTER 6**

## *Discussion*

## 6.0 Discussion

Proteopathies are a group of human diseases that arise due to non-native or abnormal conformational changes in the proteins. Destabilizing mutations and stress are major causes of these changes, which cause the misfolded proteins to aggregate and form intra- or extra-cellular deposits.<sup>397</sup> The cellular proteostasis network, which consists of molecular chaperones, ubiquitin-proteasomal pathway (UPP), and autophagy keeps the protein misfolding and toxic accumulation under check by breaking down the proteins into polypeptide chains.<sup>243,245,246,398</sup> When this proteostasis network is impaired, the unwanted and misfolded proteins accumulate as aggregates in various parts of the body. Therefore, in neurodegenerative disorders, such as Alzheimer's disease (AD)<sup>399</sup>, Parkinson's disease (PD)<sup>400</sup>, Prion disease, and polyglutamine diseases<sup>243,247</sup>, impaired proteostasis and aberrant accumulation of misfolded proteins in different parts of the body is noted. Pseudoexfoliation is an age-related proteinopathy characterized by aggregation of extracellular matrix (ECM) material in both ocular and extra-ocular tissues, which suggests that aberrant ECM synthesis or impaired degradation may contribute to disease pathogenesis.<sup>401</sup> Interestingly, clinical features observed in PEX individuals, such as deposition of fibrillar materials, age associated severity and neurodegeneration also resemble other age-related neurodegenerative disorders. Apart from an impaired proteostasis network, altered Wnt signaling has also been reported to be involved in ECM deposition.<sup>16,17</sup> At genetic level, numerous genes have been associated as risk factors with PEX. Recently, polymorphism in *CACNA1A* has been genetically associated with PEX though the functional studies remain unknown.<sup>9,318</sup> The current study highlights the role of proteostasis components, Wnt signaling genes and calcium channel subunit, *CACNA1A* in PEX pathology.

### 6.1 HSP70 in the pathogenesis of pseudoexfoliation

Stress induced HSP70 is the most conserved cytosolic chaperone. HSP70 is expressed as a response to a range of stress stimuli, including reactive oxygen species and DNA damage, and plays a key role in maintaining cell integrity and viability.<sup>205,206</sup> Transcriptional activation of HSP70 is dependent on the binding of heat shock factors on heat shock element of *HSP70* gene.<sup>402</sup> However, in current study both the mRNA and protein expression of HSP70 were significantly downregulated in lens capsule of PEXS patients despite the upregulation of its transcriptional regulators, PARP1 and HSF1. Decreased expression of HSP70 has been reported previously in the retina of R6/2, R6/1 and R7E spinocerebral ataxia type 7 (SCA7) mice which was attributed to an impairment at the level of gene expression or protein turnover<sup>403,404</sup> Another study has reported chromatin modification that prevents binding of heat shock regulators on HSP70 thereby reducing its expression.<sup>222,405</sup> We suspected the role of epigenetic modification in modulating the level of HSP70 expression.

### **6.1.1 Aberrant epigenetic alterations of HSP70 in PEXS**

Epigenetic aberrations have been linked with many eye diseases, including glaucoma,<sup>11</sup> age-related macular degeneration (ARMD),<sup>12</sup> uveal melanoma,<sup>406</sup> cataract,<sup>407</sup> and diabetic retinopathy<sup>408</sup> but reports on epigenetic modifications in PEX are scarce. In the study presented here, we revealed for the first time that CpG island in the exon of Hsp70 is hypermethylated in lens capsule of PEXS patients, resulting in a substantial reduction in the level of HSP70 expression. We also observed elevated expression of *de novo* methyltransferase DNMT3A in PEXS eyes, implicating that HSP70 expression is regulated in methylation dependent manner and it may be preferentially methylated by DNMT3A. Further, treating lens epithelial cells with 5-aza-dC, a demethylating agent, restored this downregulation effect of DNA hypermethylation.

Thus, the hypermethylation of the HSP70 coincides with its diminished expression suggesting that these methylation events could contribute to PEX risk or pathogenesis.

## **6.2 Dysregulated expression of genes involved in ER-UPR pathway**

Excessive production and accumulation of fibrillar materials in PEX is an indicative of proteostasis imbalance. We examined the expression status of a set of crucial UPR genes in PEX affected anterior eye tissues through Custom RT<sup>2</sup> profiler PCR arrays. Increased ER stress markers *SYVN1*, *EIF2AK*, *DNAJB11*, *CASP12*, *HSPA5*, *HSPD1* and *CANX* were identified in the lens capsule of PEX individuals compared to age-matched controls, of which relative expression of synoviolin1 (*SYVN1*), an E3 ligase protein, and calnexin, an ER localized chaperone was markedly increased and showed significant upregulation in the lens capsule of PEX subjects as compared with controls. Further assessment of *SYVN1* using immunohistochemistry and western blot exhibited an increased expression in the lens capsule of PEXS and PEXG affected tissues while *CANX* was seen to be upregulated only in lens capsule of PEXG individuals which implicates activation of UPR genes in diseased individuals. Hence, activation of UPR is taken as an indicator that ER function is disturbed in PEX pathological process under investigation. Though earlier studies have documented evidence for perturbation in cytoprotective mechanisms including cellular stress response, and antioxidant defense in anterior segment tissue of PEX eyes.<sup>199</sup> we revealed a new set of candidate genes involved in PEX pathogenesis in our study.

### **6.2.1 Impaired proteasome and increased apoptotic cell death in the lens capsule of PEX affected subjects**

Additionally, we found significant amount of ubiquitinated proteins in cases than in controls suggesting that reduced protein degradation may lead to overall accumulation of aberrant proteins with age in lens capsule of PEXS affected subjects. Subsequently, we found decreased

expression of two key proteasome subunits, PSMD1 and PMSA5 which is in concordance with a significant decrease of the chymotrypsin-like proteasome activity in the lens capsule of PEXS individuals in comparison to age-matched control. This confirmed a dysfunctional proteasomal system, which could indicate failed retro-translocation of misfolded ER proteins and a hampered ERAD mechanism in PEXS individuals. Besides impaired UPS, the role of autophagy impairment in the pathogenesis of PEXS has been recently examined by Andrew Want et al. showing that Tenon's cells from PEXS patients exhibited impaired relocation of lysosomes to the perinuclear area upon induction of autophagy and also had a reduced rate of autophagosome clearance.<sup>158</sup> When proteasome activity is inhibited, elevated ER stress can lead to the activation of apoptosis pathways including the activation of caspase-12 (CASP12) and DDIT3.<sup>267,281</sup> PEX individuals showed higher levels of ER-stress markers (including CASP12), which implies that they may also be more sensitive to apoptosis. In agreement with this hypothesis, PEXS subjects showed increased number of apoptotic cell death in the lens capsule of PEXS and PEXG which in turn might mediate ER-stress mediated cell death. Altogether, our study suggests reduced protein degradation and proteasome activity resulting in increased apoptosis in the PEX affected tissues might lead to proteostasis impairment which consequent into fibrillar protein deposition in the extracellular space.

### **6.3 Elevated expression of DKK1, a potent Wnt antagonist in the anterior eye tissues of PEX**

In Alzheimer's disease, increased clusterin led to induction of Dickkopf-1 (DKK1)<sup>344</sup> which tempted us to hypothesize that increased DKK1 expression might be induced by increased clusterin in PEX which further triggers non-canonical Wnt signaling cascade. Our findings in the current report demonstrate a comprehensive expression profile of DKK1 in the anterior eye

segment of PEX subjects which showed pronounced increase at both mRNA and protein levels in anterior eye tissues of PEXS and PEXG individuals compared to non-PEX control. The secreted glycoprotein DKK1, an antagonist of the Wnt signaling pathway, has been implicated in many neurodegenerative diseases such as Alzheimer's disease.<sup>409</sup> A very recent attempt was made to create a mouse model by transient expression of Wnt5a in the mouse anterior eye segment via Adenovirus-mediated gene expression which recapitulates certain ocular manifestations of human PEXS suggesting a possible involvement of dysregulated Wnt signaling in its pathophysiology.<sup>369</sup> Furthermore, our study revealed an enhanced circulating level of DKK1 is associated with PEX susceptibility. In addition to DKK1, Wnt5a, and ROCK responsible for non-canonical Wnt signal transduction also showed an increased expression in PEXS affected cases compared to that of control in our analysis.

#### **6.4 Genetic variants in CACNA1A as a risk factor in PEX pathogenesis**

Recently, Aung et al. discovered genetic association between an intronic variant, rs4926244 in the gene, Calcium voltage-gated channel subunit- $\alpha$ 1A (CACNA1A).<sup>9</sup> Genotypic association of rs4926244 was found with PEXS in a case-control study with 196 cases and 275 control in an Indian population with the frequency of risk genotype 'TT' being significantly higher in PEXS individuals. Genotype-specific expression analysis revealed significant increase in expression of CACNA1A by the risk genotype 'TT'. On further functional analysis, we found a significant difference in luciferase expression between control empty vector and constructs with either allele at rs4926244 in HEK293 cells, though we did not find allele specific regulatory activity, which suggest a regulatory effect of the genomic region surrounding the variants rather than the SNP itself.

We speculated a presence of unknown causal variants in *CACNA1A* that could contribute to the genetic risk of PEX. This led us to genotype an intronic variant, rs4926246 which was in strong LD with rs4926244. rs4926246 showed a significant association with PEXG individuals with the 'T' allele conferring a risk effect of 1.5. This study confirmed a novel association of the variant, rs4926246 in *CACNA1A* with PEXG individuals indicating a genetic contribution of *CACNA1A* in PEX pathogenesis in Indian population.

## **6.5 Conclusion**

Overall findings from the present study reveal a decreased expression of cytosolic chaperone, HSP70 which corresponds to the *de novo* DNA hypermethylation in its first exon. We further reported dysregulation in ER related stress marker implicating an impaired UPR pathway in individuals affected with PEX. Our study is the first to demonstrate that the plasma level of DKK1 is significantly elevated in patients with PEX compared with control subjects, subsequently its increased expression has been observed in affected tissue that provides a novel insight into disease pathogenesis. We also conducted a case-control study to identify putative risk variants in *CACNA1A* gene, coding for a subunit of a Calcium channel essential for pre- and postsynaptic signaling. Genotypic association of rs4926244 in *CACNA1A* gene substantiates its role as risk factor for pseudoexfoliation (PEX) syndrome in Indian cohort. We also found a novel variant of *CACNA1A*, rs4926246 to be genetically associated with PEXG in our study population. In summation, this study provides insight into perturbed cytoprotective mechanisms and regulatory roles of candidate genes in PEX pathogenesis.

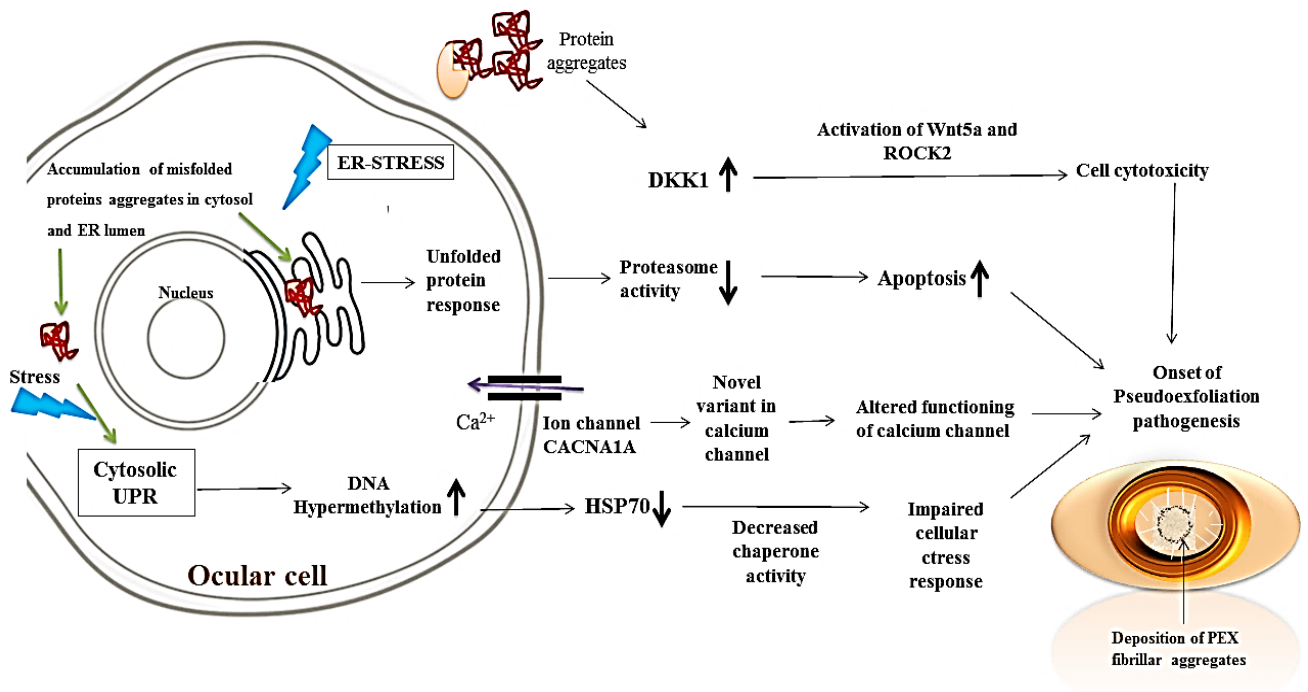


**Figure 6.1 Factors contributing to pseudoexfoliation pathogenesis.** The present study unraveled the role of components involved in maintenance of proteostasis network, Wnt signaling and calcium channel that might be derailed during PEX pathogenesis. Presence of fibrillar aggregates in PEX indicates impaired proteostasis, which activates a signaling cascade to restore protein homeostasis. We demonstrate increased DNA hypermethylation leading to decreased expression of HSP70, a stress-response chaperone in PEXS affected lens capsule tissues. Following this we found increased expression of endoplasmic reticulum related stress markers indicating unfolded protein response activation in lens capsule of PEX individuals. Reduced proteasome activity and proteasome subunit expression were also observed in PEX subjects implying impaired proteasome function which ultimately led to cell death in lens capsules. In addition, increased expression of Wnt antagonist, DKK1 in the anterior eye tissue suggests increased cytotoxicity. We also found reduced CACNA1A expression on deletion of locus surrounding rs4926244 region suggesting altered functioning of calcium channel. These findings provide evidence that proteostasis imbalance contribute significantly to abnormal XFM formation and aggregation.

## 6.6 Key findings from the study

- HSP70, major cytosolic chaperone is significantly downregulated in the lens capsule of PEXS individuals than in PEXG individuals compared to control.

- Reduced HSP70 expression corresponds to DNA hypermethylation of CpG island of *HSP70* gene.
- Hypermethylation of the exon of *HSP70* gene has a functional regulatory effect implicated in the transcriptional regulation.
- Treatment with a DNMT inhibitor, 5-aza-deoxycytidine (5-Aza DC) restored HSP70 expression in HLE B-3 cell line.
- Increased expression of ER-stress markers, Synoviolin1 and Calnexin, suggests UPR activation in PEX.
- Reduced chymotrypsin-like proteasome activity and decreased proteasome subunits (PSMD1 and PSMA5) expression indicate impaired proteasome function.
- Cells in the lens capsules of PEXS and PEXG individuals showed higher apoptotic rate.
- DKK1 expression was found to be significantly upregulated in the anterior eye tissues of PEXS and PEXG subjects than in those of control individuals.
- This is the first study to demonstrate circulating level of DKK1 in the plasma of PEX affected subjects.
- CACNA1A major susceptibility variant, rs4926244 is associated with PEXS at genotypic level.
- A novel variant, rs4926246 in CACNA1A is found to be significantly associated with PEXG in our study population.

### **6.7 Methods standardized during the course of this project in the laboratory**

- Bisulfite sequencing for checking DNA methylation
- Protein extraction from lens capsule to check protein level via immunoblotting
- *In vitro* methylation and demethylation assay to validate methylation status of gene

- TUNEL assay to check apoptotic activity in eye tissue
- Proteasome-Glo<sup>TM</sup> based assay to check proteasome activity in tissue lysates
- Sandwich ELISA assay to look for prognostic marker in plasma of affected subjects

### **6.8 Future Prospective**

- Additional elaborate studies need to be carried out to focus on the effect of locus specific DNA methylation on the role of transcription factors regulating the expression of *HSP70*.
- To determine the role of specific histone modifications in HSP70 regulation.
- Detailed role of genes, SYVN1 and CANX in the progression of PEX warrants further research.
- *In vitro* experiments such as TCF/LEF reporter assay need to be performed to determine whether DKK1 is involved in the beta-catenin dependent or independent pathway.
- Further studies are needed to find more regulatory SNPs within the *CACNA1A* gene in association with PEX.
- Functional effects of *CACNA1A* associated polymorphisms with PEX need to be explored.

# **CHAPTER 7**

## *References*

1. Ritch, R. & Schlötzer-Schrehardt, U. Exfoliation syndrome. *Surv. Ophthalmol.* **45**, 265–315 (2001).
2. Schlötzer-Schrehardt, U. & Naumann, G. O. H. Ocular and Systemic Pseudoexfoliation Syndrome. *Am. J. Ophthalmol.* **141**, (2006).
3. Mitchell, P., Jie Jin Wang & Smith, W. Association of pseudoexfoliation syndrome with increased vascular risk. *Am. J. Ophthalmol.* **124**, 685–687 (1997).
4. Naumann, G. O. H., Schlötzer-Schrehardt, U. & Küchle, M. Pseudoexfoliation syndrome for the comprehensive ophthalmologist: Intraocular and systemic manifestations. *Ophthalmology* **105**, 951–968 (1998).
5. Schumacher, S., Schlötzer-Schrehardt, U., Martus, P., Lang, W. & Naumann, G. Pseudoexfoliation syndrome and aneurysms of the abdominal aorta. *Lancet* (2001). doi:10.1016/S0140-6736(00)03645-X
6. Arvind, H. *et al.* Pseudoexfoliation in south India. *Br. J. Ophthalmol.* **87**, 1321–1323 (2003).
7. Jonas, J. B. *et al.* Pseudoexfoliation: Normative Data and Associations. The Central India Eye and Medical Study. *PLoS One* **8**, (2013).
8. Padhy, B. *et al.* Role of an extracellular chaperone, Clusterin in the pathogenesis of Pseudoexfoliation Syndrome and Pseudoexfoliation Glaucoma. *Exp. Eye Res.* **127**, 69–76 (2014).
9. Aung, T. *et al.* A common variant mapping to CACNA1A is associated with susceptibility to exfoliation syndrome. *Nat. Genet.* **47**, 387–392 (2015).
10. Young, J. C., Barral, J. M. & Hartl, F. U. More than folding: Localized functions of cytosolic chaperones. *Trends in Biochemical Sciences* (2003). doi:10.1016/j.tibs.2003.08.009
11. Wiggs, J. L. The cell and molecular biology of complex forms of glaucoma: Updates on genetic, environmental, and epigenetic risk factors. *Investig. Ophthalmol. Vis. Sci.* **53**, 2467–2469 (2012).
12. Hunter, A. *et al.* DNA methylation is associated with altered gene expression in AMD. *Invest. Ophthalmol. Vis. Sci.* **53**, 2089–2105 (2012).
13. McCarthy, N. Retinoblastoma: Epigenetic outcome. *Nature Reviews Cancer* **12**, 80 (2012).
14. Niehrs, C. Function and biological roles of the Dickkopf family of Wnt modulators. *Oncogene* **25**, 7469–7481 (2006).
15. Mao, W., Rubin, J. S., Anoruo, N., Wordinger, R. J. & Clark, A. F. SFRP1 promoter methylation and expression in human trabecular meshwork cells. *Exp. Eye Res.* **97**, 130–136 (2012).

16. Bermudez, J. Y. *et al.* A comparison of gene expression profiles between glucocorticoid responder and non-responder bovine trabecular meshwork cells using RNA sequencing. *PLoS One* **12**, 1–20 (2017).
17. Bermudez, J. Y. Exploring Trabecular Meshwork Molecular Pathogenic Mechanisms In Primary Open Angle Glaucoma And Glucocorticoid Induced Glaucoma. (2016).
18. Quill, B. *et al.* Calcium channel blockade reduces mechanical strain-induced extracellular matrix gene response in lamina cribrosa cells. *Br. J. Ophthalmol.* **99**, 1009–1014 (2015).
19. Schlotzer-Schrehardt, U. & Naumann, G. O. H. Trabecular meshwork in pseudoexfoliation syndrome with and without open-angle glaucoma: A morphometric, ultrastructural study. *Investig. Ophthalmol. Vis. Sci.* **36**, 1750–1764 (1995).
20. Ritch, R. Exfoliation syndrome and occludable angles. *Trans. Am. Ophthalmol. Soc.* **92**, 845–944 (1994).
21. Heijl, A., Bengtsson, B., Hyman, L. & Leske, M. C. Natural History of Open-Angle Glaucoma. *Ophthalmology* **116**, 2271–2276 (2009).
22. Davis, R. E. & Schuman, J. S. Pseudoexfoliation syndrome: don't brush it off. **97**, 2013–2015 (2013).
23. Andrikopoulos, G. K. *et al.* Pseudoexfoliation syndrome prevalence in Greek patients with cataract and its association to glaucoma and coronary artery disease. *Eye* **23**, 442–447 (2009).
24. Citirik, M., Acaroglu, G., Batman, C., Yildiran, L. & Zilelioglu, O. A possible link between the pseudoexfoliation syndrome and coronary artery disease. *Eye* **21**, 11–15 (2007).
25. Demir, N. *et al.* Assessment of myocardial ischaemia using tissue Doppler imaging in pseudoexfoliation syndrome. *Eye* **25**, 1177–1180 (2011).
26. Wang, W., He, M., Zhou, M. & Zhang, X. Ocular Pseudoexfoliation Syndrome and Vascular Disease: A Systematic Review and Meta-Analysis. *PLoS One* **9**, e92767 (2014).
27. Repo, L. P., Suhonen, M. T., Teräsvirta, M. E. & Koivisto, K. J. Color Doppler Imaging of the Ophthalmic Artery Blood Flow Spectra of Patients Who Have Had a Transient Ischemic Attack: Correlations with Generalized Iris Translucence and Pseudoexfoliation Syndrome. *Ophthalmology* **102**, 1199–1205 (1995).
28. Ritland, J., Egge, K., Lydersen, S., Juul, R. & Semb, S. Exfoliative glaucoma and primary open-angle glaucoma: associations with death causes and comorbidity. *Acta Ophthalmol Scand* **82**, (2004).
29. Yuksel, N., Anik, Y., Altintas, O., Onur, I. & Caglar, Y. Magnetic resonance imaging of the brain in patients with pseudoexfoliation syndrome and glaucoma. *Ophthalmologica*

- 220, (2006).
30. Katsi, V., Pavlidis, A., Kallistratos, M., Fitsios, A. & Bratsas, A. Cardiovascular Repercussions of the Pseudoexfoliation Syndrome. *N Am J Med Sci* **5**, (2013).
  31. Roedl, J. B. *et al.* Vitamin deficiency and hyperhomocysteinemia in pseudoexfoliation glaucoma. *J. Neural Transm.* **114**, 571–575 (2007).
  32. Wirostko, B. M. *et al.* Risk for exfoliation syndrome in women with pelvic organ prolapse: A Utah Project on Exfoliation Syndrome (UPEXS) study. *JAMA Ophthalmol.* **134**, 1255–1262 (2016).
  33. Andrikopoulos, G. K. Pseudoexfoliation syndrome and cardiovascular diseases. *World J. Cardiol.* **6**, 847 (2014).
  34. Lindberg, J. G. Clinical investigations on depigmentation of the pupillary border and translucency of the iris in cases of senile cataract and in normal eyes in elderly persons. *Acta Ophthalmol. Suppl. (Oxf. ).* **190**, 1–96 (1989).
  35. Helsinki, J. L.-, University, F. H. & 1917, undefined. Clinical studies of depigmentation of the pupillary margin and transillumination of the iris in cases of senile cataract and also in normal eyes in the aged.
  36. Vogt, A. A new slit lamp image of the pupil area: light blue pupil hem felt with skin formation on the front lens capsule. *Klin Mon. Gaz.* (1925).
  37. Dvorak-Theobald, G. Pseudo-exfoliation of the lens capsule. Relation to ‘true’ exfoliation of the lens capsule as reported in the literature and role in the production of glaucoma capsulocuticulare. *Am. J. Ophthalmol.* **37**, 1–12 (1954).
  38. Supplementum, O. S.-A. ophthalmologica. & 1956, undefined. On the so-called senile exfoliation of the anterior lens capsule; a clinical and anatomical study. *ncbi.nlm.nih.gov*
  39. Hirvelä, H., Luukinen, H. & Laatikainen, L. Prevalence and Risk Factors of Lens Opacities in the Elderly in Finland: A Population-based Study. *Ophthalmology* (1995). doi:10.1016/S0161-6420(95)31072-X
  40. Arnarsson, Á. M. Epidemiology of exfoliation syndrome in the Reykjavik eye study. *Acta Ophthalmol.* **87**, 1–17 (2009).
  41. Arnarsson, A., Damji, K. F., Sverrisson, T., Sasaki, H. & Jonasson, F. Pseudoexfoliation in the Reykjavik Eye Study: Prevalence and related ophthalmological variables. *Acta Ophthalmol. Scand.* (2007). doi:10.1111/j.1600-0420.2007.01051.x
  42. Forsius, H. EXFOLIATION SYNDROME IN VARIOUS ETHNIC POPULATIONS. *Acta Ophthalmol.* **66**, 71–85 (1988).
  43. Mitchell, P. The Relationship Between Glaucoma and Pseudoexfoliation. *Arch. Ophthalmol.* (1999). doi:10.1001/archoph.117.10.1319
  44. Cashwell, L. F. & Shields, M. B. EXFOLIATION SYNDROME IN THE

- SOUTHEASTERN UNITED STATES I. PREVALENCE IN OPEN-ANGLE GLAUCOMA AND NON-GLAUCOMA POPULATIONS. *Acta Ophthalmol.* (1988). doi:10.1111/j.1755-3768.1988.tb02637.x
45. AASVED, H. THE GEOGRAPHICAL DISTRIBUTION OF FIBRILLOPATHIA EPITHELIOCAPSULARIS: so-called senil exfoliation or Pseudoexfoliation of the anterior lens capsule. *Acta Ophthalmol.* (1969). doi:10.1111/j.1755-3768.1969.tb08170.x
  46. McCarty, C. A. & Taylor, H. R. Pseudoexfoliation syndrome in Australian adults. *Am. J. Ophthalmol.* **129**, 629–633 (2000).
  47. Rotchford, A. P., Kirwan, J. F., Johnson, G. J. & Roux, P. Exfoliation syndrome in black South Africans. *Arch. Ophthalmol.* (2003). doi:10.1001/archophth.121.6.863
  48. Young, A. L., Tang, W. W. T. & Lam, D. S. C. The prevalence of pseudoexfoliation syndrome in Chinese people. *Br. J. Ophthalmol.* **88**, 193–195 (2004).
  49. Miyazaki, M. *et al.* The prevalence of pseudoexfoliation syndrome in a Japanese population: The hisayama study. *J. Glaucoma* **14**, 482–484 (2005).
  50. Ball, S. F. EXFOLIATION SYNDROME PREVALENCE IN THE GLAUCOMA POPULATION OF SOUTH LOUISIANA. *Acta Ophthalmol.* (1988). doi:10.1111/j.1755-3768.1988.tb02636.x
  51. Cashwell, L. F. & Shields, M. B. Exfoliation syndrome. Prevalence in a southeastern United States population. *Arch. Ophthalmol.* (1988). doi:10.1001/archophth.1988.01060130361021
  52. Krishnadas, R. *et al.* Pseudoexfoliation in a rural population of southern India: The Aravind Comprehensive Eye Survey. *Am. J. Ophthalmol.* (2003). doi:10.1016/S0002-9394(02)02271-7
  53. Thomas, R., Nirmalan, P. K. & Krishnaiah, S. Pseudoexfoliation in Southern India: The Andhra Pradesh eye disease study. *Investig. Ophthalmol. Vis. Sci.* (2005). doi:10.1167/iovs.04-1062
  54. Vijaya, L. *et al.* Six-year incidence and baseline risk factors for pseudoexfoliation in a south Indian population: The chennai eye disease incidence study. *Ophthalmology* **122**, 1158–1164 (2015).
  55. Kanthan, G. L., Mitchell, P., Burlutsky, G., Rochtchina, E. & Wang, J. J. Pseudoexfoliation syndrome and the long-term incidence of cataract and cataract surgery: The blue mountains eye study. *Am. J. Ophthalmol.* **155**, 83-88.e1 (2013).
  56. Ritch, R. & Schlötzer-Schrehardt, U. Exfoliation syndrome. *Surv. Ophthalmol.* **45**, 265–315 (2001).
  57. Tarkkanen, A., Voipio, H. & Koivusalo, P. FAMILY STUDY OF PSEUDOEXFOLIATION AND GLAUCOMA. *Acta Ophthalmol.* (1965). doi:10.1111/j.1755-3768.1965.tb00338.x

58. Hiller, R., Sperduto, R. D. & Krueger, D. E. Pseudoexfoliation, Intraocular Pressure, and Senile Lens Changes in a Population-Based Survey. *Arch. Ophthalmol.* (1982). doi:10.1001/archophth.1982.01030040058007
59. Ekström, C. Elevated intraocular pressure and pseudoexfoliation of the lens capsule as risk factors for chronic open-angle glaucoma: A population-based five-year follow-up study. *Acta Ophthalmol.* (1993). doi:10.1111/j.1755-3768.1993.tb04989.x
60. Ekström, C. & Kilander, L. Pseudoexfoliation and Alzheimer's disease: A population-based 30-year follow-up study. *Acta Ophthalmol.* **92**, 355–358 (2014).
61. Arnarsson, A., Sasaki, H. & Jonasson, F. Twelve-year incidence of exfoliation syndrome in the Reykjavik Eye Study. *Acta Ophthalmol.* (2013). doi:10.1111/j.1755-3768.2011.02334.x
62. Yalaz, M. *et al.* The frequency of pseudoexfoliation syndrome in the Eastern Mediterranean area of Turkey. *Acta Ophthalmol.* (1992). doi:10.1111/j.1755-3768.1992.tb04125.x
63. Kozobolis, V. P., Papatzanaki, M., Vlachonikolis, I. G., Pallikaris, I. G. & Tsambarlakis, I. G. Epidemiology of pseudoexfoliation in the island of Crete (Greece). *Acta Ophthalmol. Scand.* (1997). doi:10.1111/j.1600-0420.1997.tb00640.x
64. Colin, J., Gall, G. Le, Jeune, B. Le & Cambrai, M. D. THE PREVALENCE OF EXFOLIATION SYNDROME IN DIFFERENT AREAS OF FRANCE. *Acta Ophthalmol.* (1988). doi:10.1111/j.1755-3768.1988.tb02634.x
65. Miyazaki, M. *et al.* The prevalence of pseudoexfoliation syndrome in a Japanese population: The hisayama study. *J. Glaucoma* **14**, 482–484 (2005).
66. Arvind, H. *et al.* Pseudoexfoliation in south India. *Br. J. Ophthalmol.* (2003). doi:10.1136/bjo.87.11.1321
67. McCarty, C. A. & Taylor, H. R. Pseudoexfoliation syndrome in Australian adults. *Am. J. Ophthalmol.* (2000). doi:10.1016/S0002-9394(99)00466-3
68. Stefanidou, M., Petroustos, G. & Psilas, K. The frequency of Pseudoexfoliation in a region of Greece (Epirus). *Acta Ophthalmol.* (1990). doi:10.1111/j.1755-3768.1990.tb01927.x
69. Schlötzer-Schrehardt, U., Kuchle, M., Jünemann, A. & Naumann, G. O. H. Relevance of the pseudoexfoliation syndrome for the glaucomas. *Ophthalmologie* **99**, 683–690 (2002).
70. Ringvold, A. Epidemiology of the pseudo-exfoliation syndrome. A review. *Acta Ophthalmologica Scandinavica* **77**, 371–375 (1999).
71. Arnarsson, A., Damji, K. F., Sverrisson, T., Sasaki, H. & Jonasson, F. Pseudoexfoliation in the Reykjavik Eye Study: Prevalence and related ophthalmological variables. *Acta Ophthalmol. Scand.* **85**, 822–827 (2007).

72. Ovodenko, B. *et al.* Proteomic analysis of exfoliation deposits. *Investig. Ophthalmol. Vis. Sci.* (2007). doi:10.1167/iovs.06-0411
73. Schlotzer-schrehardt, U., Mark, K. Von Der, Sakai, L. Y. & Naumann, G. O. H. Increased Extracellular Deposition of Fibrillin-Containing Fibrils in Pseudoexfoliation Syndrome. **38**, 970–984 (1997).
74. Schlötzer-Schrehardt, U. *et al.* LOXL1 deficiency in the lamina cribrosa as candidate susceptibility factor for a pseudoexfoliation-specific risk of glaucoma. *Ophthalmology* (2012). doi:10.1016/j.optha.2012.03.015
75. Sharma, S. *et al.* Novel protein constituents of pathological ocular pseudoexfoliation syndrome deposits identified with mass spectrometry. *Mol. Vis.* (2018).
76. Padhy, B., Kapuganti, R. S., Hayat, B., Mohanty, P. P. & Alone, D. P. De novo variants in an extracellular matrix protein coding gene, fibulin-5 (FBLN5) are associated with pseudoexfoliation. *Eur. J. Hum. Genet.* **5**, (2019).
77. Liu, X. *et al.* Elastic fiber homeostasis requires lysyl oxidase-like 1 protein. *Nat. Genet.* **36**, 178–182 (2004).
78. Schlotzer-Schrehardt, U. Genetics and genomics of pseudoexfoliation syndrome/glaucoma. *Middle East Afr. J. Ophthalmol.* **18**, 30–36 (2011).
79. Schlötzer-Schrehardt, U., Lommatzsch, J., Küchle, M., Konstas, A. G. P. & Naumann, G. O. H. Matrix metalloproteinases and their inhibitors in aqueous humor of patients with pseudoexfoliation syndrome/glaucoma and primary open-angle glaucoma. *Investig. Ophthalmol. Vis. Sci.* **44**, 1117–1125 (2003).
80. Bradley, J. M. B. *et al.* Effect of matrix metalloproteinases activity on outflow in perfused human organ culture. *Investig. Ophthalmol. Vis. Sci.* (1998).
81. Sahay, P. *et al.* Functional activity of matrix metalloproteinases 2 and 9 in tears of patients with glaucoma. *Investig. Ophthalmol. Vis. Sci.* (2017). doi:10.1167/iovs.17-21723
82. Konstas, A. G., Marshall, G. E. & Lee, W. R. Immunogold localisation of laminin in normal and exfoliative iris. *Br. J. Ophthalmol.* (1990). doi:10.1136/bjo.74.8.450
83. Zenkel, M., Kruse, F. E., Jünemann, A. G., Naumann, G. O. H. & Schlötzer-Schrehardt, U. Clusterin deficiency in eyes with pseudoexfoliation syndrome may be implicated in the aggregation and deposition of pseudoexfoliative material. *Investig. Ophthalmol. Vis. Sci.* (2006). doi:10.1167/iovs.05-1580
84. Schlötzer-Schrehardt, U. *et al.* Selective upregulation of the A3 adenosine receptor in eyes with pseudoexfoliation syndrome and glaucoma. *Investig. Ophthalmol. Vis. Sci.* **46**, 2023–2034 (2005).
85. Zenkel, M. *et al.* Differential gene expression in pseudoexfoliation syndrome. *Investig. Ophthalmol. Vis. Sci.* **46**, 3742–3752 (2005).

86. Lemmelä, S. *et al.* Association of LOXL1 gene with Finnish exfoliation syndrome patients. *J. Hum. Genet.* (2009). doi:10.1038/jhg.2009.28
87. Thorleifsson, G. *et al.* Common sequence variants in the LOXL1 gene confer susceptibility to exfoliation glaucoma. *Science (80-. ).* **317**, 1397–1400 (2007).
88. Abu-Amero, K. K. *et al.* Analysis of LOXL1 polymorphisms in a Saudi Arabian population with pseudoexfoliation glaucoma. *Mol. Vis.* (2010).
89. Schlötzer-Schrehardt, U. *et al.* Genotype-correlated expression of lysyl oxidase-like 1 in ocular tissues of patients with pseudoexfoliation syndrome/glaucoma and normal patients. *Am. J. Pathol.* **173**, 1724–1735 (2008).
90. Hewitt, A. W. *et al.* Ancestral LOXL1 variants are associated with pseudoexfoliation in Caucasian Australians but with markedly lower penetrance than in Nordic people. *Hum. Mol. Genet.* (2008). doi:10.1093/hmg/ddm342
91. Lee, K. Y. C. *et al.* Association of LOXL1 polymorphisms with pseudoexfoliation in the Chinese. *Mol. Vis.* (2009).
92. Ozaki, M. *et al.* Association of LOXL1 gene polymorphisms with pseudoexfoliation in the Japanese. *Investig. Ophthalmol. Vis. Sci.* (2008). doi:10.1167/iovs.08-1805
93. Ramprasad, V. L. *et al.* Association of non-synonymous single nucleotide polymorphisms in the LOXL1 gene with pseudoexfoliation syndrome in India. *Mol. Vis.* (2008).
94. Park, D. Y., Won, H. H., Cho, H. kyung & Kee, C. Evaluation of lysyl oxidase-like 1 gene polymorphisms in pseudoexfoliation syndrome in a Korean population. *Mol. Vis.* **19**, 448–453 (2013).
95. Guadarrama-Vallejo, D., Miranda-Duarte, A. & Zenteno, J. C. The T allele of lysyl oxidase-like 1 rs41435250 is a novel risk factor for pseudoexfoliation syndrome and pseudoexfoliation glaucoma independently and through intragenic epistatic interaction. *Mol. Vis.* **19**, 1937–1944 (2013).
96. Micheal, S. *et al.* Role of lysyl oxidase-like 1 gene polymorphisms in Pakistani patients with pseudoexfoliative glaucoma. *Mol. Vis.* (2012).
97. Malukiewicz, G. *et al.* Analysis of LOXL1 single nucleotide polymorphisms in Polish population with pseudoexfoliation syndrome. *Acta Ophthalmol.* (2011). doi:10.1111/j.1755-3768.2010.02083.x
98. Challa, P. *et al.* Analysis of LOXL1 polymorphisms in a United States population with pseudoexfoliation glaucoma. *Mol. Vis.* (2008).
99. Fan, B. J. *et al.* DNA sequence variants in the LOXL1 gene are associated with pseudoexfoliation glaucoma in a U.S. clinic-based population with broad ethnic diversity. *BMC Med. Genet.* (2008). doi:10.1186/1471-2350-9-5

100. G, T., KP, M. & P, S. Common sequence variants in the LOXL1 gene confer susceptibility to exfoliation glaucoma. *Science (80-. )*. **317**, 1397–1400
101. Ramprasad, V. L. *et al.* Association of non-synonymous single nucleotide polymorphisms in the LOXL1 gene with pseudoexfoliation syndrome in India. *Mol. Vis.* **14**, 318–322 (2008).
102. P, C., S, S. & Y, L. Analysis of LOXL1 polymorphisms in a United States population with pseudoexfoliation glaucoma. *Mol Vis* **14**, 146–149
103. Pasutto, F. *et al.* Pseudoexfoliation syndrome-associated genetic variants affect transcription factor binding and alternative splicing of LOXL1. *Nat. Commun.* (2017). doi:10.1038/ncomms15466
104. Hayashi, H., Gotoh, N., Ueda, Y., Nakanishi, H. & Yoshimura, N. Lysyl Oxidase-like 1 Polymorphisms and Exfoliation Syndrome in the Japanese Population. *Am. J. Ophthalmol.* (2008). doi:10.1016/j.ajo.2007.10.023
105. Chen, L. *et al.* Evaluation of LOXL1 polymorphisms in exfoliation syndrome in a Chinese population. *Mol. Vis.* (2009).
106. Williams SEI *et al.* Major LOXL1 risk allele is reversed in exfoliation glaucoma in a black South African population. *Mol. Vis.* (2010).
107. Anastasopoulos, E. *et al.* Association of LOXL1 polymorphisms with pseudoexfoliation, glaucoma, intraocular pressure, and systemic diseases in a Greek population. The Thessaloniki eye study. *Investig. Ophthalmol. Vis. Sci.* (2014). doi:10.1167/iovs.14-13991
108. Malukiewicz, G., Lesiewska-Junk, H., Linkowska, K., Grzybowski, T. & Kaźmierczak, K. Analysis of CNTNAP2 polymorphisms in Polish population with pseudoexfoliation syndrome. *Acta Ophthalmol.* **90**, 2011–2012 (2012).
109. Sharma, S. *et al.* Identification of LOXL1 protein and Apolipoprotein E as components of surgically isolated pseudoexfoliation material by direct mass spectrometry. *Exp. Eye Res.* (2009). doi:10.1016/j.exer.2009.05.001
110. Berner, D. *et al.* The protective variant rs7173049 at LOXL1 locus impacts on retinoic acid signaling pathway in pseudoexfoliation syndrome. *Hum. Mol. Genet.* **28**, 2531–2548 (2019).
111. Wilson, M. R. & Easterbrook-Smith, S. B. Clusterin is a secreted mammalian chaperone. *Trends in Biochemical Sciences* **25**, 95–98 (2000).
112. Burdon, K. P. *et al.* Genetic analysis of the clusterin gene in pseudoexfoliation syndrome. *Mol. Vis.* (2008).
113. Krumbiegel, M. *et al.* Exploring functional candidate genes for genetic association in German patients with pseudoexfoliation syndrome and pseudoexfoliation glaucoma. *Investig. Ophthalmol. Vis. Sci.* **50**, 2796–2801 (2009).

114. Padhy, B., Hayat, B., Nanda, G. G., Mohanty, P. P. & Alone, D. P. Pseudoexfoliation and Alzheimer's associated CLU risk variant, rs2279590, lies within an enhancer element and regulates CLU, EPHX2 and PTK2B gene expression. *Hum. Mol. Genet.* **26**, 4519–4529 (2017).
115. Poliak, S. *et al.* Caspr2, a new member of the Neurexin superfamily, is localized at the juxtaparanodes of myelinated axons and associates with K<sup>+</sup> channels. *Neuron* (1999). doi:10.1016/S0896-6273(00)81049-1
116. Poliak, S. & Peles, E. The local differentiation of myelinated axons at nodes of ranvier. *Nature Reviews Neuroscience* (2003). doi:10.1038/nrn1253
117. Krumbiegel, M. *et al.* Genome-wide association study with DNA pooling identifies variants at CNTNAP2 associated with pseudoexfoliation syndrome. *Eur. J. Hum. Genet.* (2011). doi:10.1038/ejhg.2010.144
118. Shimizu, A. *et al.* Evaluation of CNTNAP2 gene polymorphisms for exfoliation syndrome in Japanese. *Mol. Vis.* **18**, 1395–1401 (2012).
119. Krumbiegel, M., Pasutto, F. & Reis, A. Genome-wide association study with DNA pooling identifies variants at CNTNAP2 associated with pseudoexfoliation syndrome Materials and methods Study populations GPFrontend and GPGraphics Individual genotyping. 1–9 (2014).
120. Schlötzer-Schrehardt, U., Dorfler, S. & Naumann, G. O. H. Immunohistochemical localization of basement membrane components in pseudoexfoliation material of the Lens capsule. *Curr. Eye Res.* (1992). doi:10.3109/02713689209001788
121. Schlötzer-Schrehardt, U., Körtje, K. H. & Erb, C. Energy-filtering transmission electron microscopy (EFTEM) in the elemental analysis of pseudoexfoliative material. *Curr. Eye Res.* **22**, 154–162 (2001).
122. Reinhardt, D. P., Ono, R. N. & Sakai, L. Y. Calcium stabilizes fibrillin-1 against proteolytic degradation. *J. Biol. Chem.* **272**, 1231–1236 (1997).
123. Zenkel, M. *et al.* Differential gene expression in pseudoexfoliation syndrome. *Investig. Ophthalmol. Vis. Sci.* (2005). doi:10.1167/iovs.05-0249
124. Elhawry, E., Kamthan, G., Dong, C. Q. & Danias, J. Pseudoexfoliation syndrome, a systemic disorder with ocular manifestations. *Human Genomics* (2012). doi:10.1186/1479-7364-6-22
125. Pfeffer, K. Biological functions of tumor necrosis factor cytokines and their receptors. *Cytokine and Growth Factor Reviews* (2003). doi:10.1016/S1359-6101(03)00022-4
126. Wajant, H. & Siegmund, D. TNFR1 and TNFR2 in the control of the life and death balance of macrophages. *Frontiers in Cell and Developmental Biology* (2019). doi:10.3389/fcell.2019.00091
127. Khan, M. I. *et al.* Association of tumor necrosis factor alpha gene polymorphism G-

- 308A with pseudoexfoliative glaucoma in the Pakistani population. *Mol. Vis.* (2009).
128. Razeghinejad, M. R., Rahat, F. & Kamali-Sarvestani, E. Association of TNFA -308 G/A and TNFRI +36 A/G gene polymorphisms with glaucoma. *Ophthalmic Res.* (2009). doi:10.1159/000226108
  129. Tekeli, O., Turacli, M. E., Egin, Y., Akar, N. & Elhan, A. H. Tumor necrosis factor alpha-308 gene polymorphism and pseudoexfoliation glaucoma. *Mol. Vis.* **14**, 1815–8 (2008).
  130. Mossböck, G. *et al.* TNF- $\alpha$  promoter polymorphisms and primary open-angle glaucoma. *Eye* (2006). doi:10.1038/sj.eye.6702078
  131. Damji, K. F. *et al.* Is pseudoexfoliation syndrome inherited? A review of genetic and nongenetic factors and a new observation. *Ophthalmic Genet.* (1998). doi:10.1076/opge.19.4.175.2310
  132. Resnikoff, S., Filliard, G. & Dell'Aquila, B. Climatic droplet keratopathy, exfoliation syndrome, and cataract. *Br. J. Ophthalmol.* (1991). doi:10.1136/bjo.75.12.734
  133. Lee, R. K. The molecular pathophysiology of pseudoexfoliation glaucoma. *Curr. Opin. Ophthalmol.* **19**, 95–101 (2008).
  134. Stein, J. D. *et al.* Geographic and climatic factors associated with exfoliation syndrome. *Arch. Ophthalmol.* (2011). doi:10.1001/archophthalmol.2011.191
  135. Pasquale, L. R. *et al.* Solar Exposure and Residential Geographic History in Relation to Exfoliation Syndrome in the United States and Israel Critical revision of the manuscript for important intellectual content: Pasquale. *JAMA Ophthalmol* (2014). doi:10.1001/jamaophthalmol.2014.3326
  136. Kang, J. H., Wiggs, J. L. & Pasquale, L. R. Relation between time spent outdoors and exfoliation glaucoma or exfoliation glaucoma suspect. *Am. J. Ophthalmol.* (2014). doi:10.1016/j.ajo.2014.05.015
  137. Pasquale, L. R., Wiggs, J. L., Willett, W. C. & Kang, J. H. The relationship between caffeine and coffee consumption and exfoliation glaucoma or glaucoma suspect: A prospective study in two cohorts. *Investigative Ophthalmology and Visual Science* (2012). doi:10.1167/iovs.12-10085
  138. Nita, M. & Grzybowski, A. The Role of the Reactive Oxygen Species and Oxidative Stress in the Pathomechanism of the Age-Related Ocular Diseases and Other Pathologies of the Anterior and Posterior Eye Segments in Adults. *Oxidative Medicine and Cellular Longevity* (2016). doi:10.1155/2016/3164734
  139. Schlötzer-Schrehardt, U. Oxidativer stress beim pseudoexfoliationsglaukom. *Klinische Monatsblätter für Augenheilkunde* (2010). doi:10.1055/s-0028-1109977
  140. Strzalka-Mrozik, B. *et al.* Quantitative analysis of SOD2, ALDH1A1 and MGST1 messenger ribonucleic acid in anterior lens epithelium of patients with pseudoexfoliation

- syndrome. *Mol. Vis.* **19**, 1341–1349 (2013).
141. Gartaganis, S. P. *et al.* Glutathione and lipid peroxide changes in pseudoexfoliation syndrome. *Curr. Eye Res.* **30**, 647–651 (2005).
  142. Ferreira, S. M., Lerner, S. F., Brunzini, R., Evelson, P. A. & Llesuy, S. F. Oxidative stress markers in aqueous humor of glaucoma patients. *Am. J. Ophthalmol.* **137**, 62–69 (2004).
  143. Zoric, L., Miric, D., Milenkovic, S., Jovanovic, P. & Trajkovic, G. Pseudoexfoliation syndrome and its antioxidative protection deficiency as risk factors for age-related cataract. *Eur. J. Ophthalmol.* (2006). doi:10.1177/112067210601600212
  144. Kondkar, A. A. *et al.* Increased plasma levels of 8-hydroxy-2'-deoxyguanosine (8-OHdG) in patients with pseudoexfoliation glaucoma. *J. Ophthalmol.* (2019). doi:10.1155/2019/8319563
  145. Yağci, R. *et al.* Oxidative stress and protein oxidation in pseudoexfoliation syndrome. *Curr. Eye Res.* **31**, 1029–1032 (2006).
  146. Gartaganis, S. P., Patsoukis, N. E., Nikolopoulos, D. K. & Georgiou, C. D. Evidence for oxidative stress in lens epithelial cells in pseudoexfoliation syndrome. *Eye* (2007). doi:10.1038/sj.eye.6702596
  147. Yaz, Y. A. *et al.* Role of oxidative stress in pseudoexfoliation syndrome and pseudoexfoliation glaucoma. *Turkish J. Ophthalmol.* **49**, 61–67 (2019).
  148. Yaz, Y. A. *et al.* Role of oxidative stress in pseudoexfoliation syndrome and pseudoexfoliation glaucoma. *Turkish J. Ophthalmol.* (2019). doi:10.4274/tjo.galenos.2018.10734
  149. Seina, J. *et al.* Exfoliation syndrome: New genetic and pathophysiologic insights. *Current Opinion in Ophthalmology* **24**, 167–174 (2013).
  150. Brustolin, S., Giugliani, R. & Félix, T. M. Genetics of homocysteine metabolism and associated disorders. *Brazilian Journal of Medical and Biological Research* (2010). doi:10.1590/s0100-879x2009007500021
  151. Vessani, R. M., Ritch, R., Liebmann, J. M. & Jofe, M. Plasma homocysteine is elevated in patients with exfoliation syndrome. *Am. J. Ophthalmol.* **136**, 41–46 (2003).
  152. Roedl, J. B. *et al.* Homocysteine in tear fluid of patients with pseudoexfoliation glaucoma. *J. Glaucoma* **16**, 234–239 (2007).
  153. Tranchina, L. *et al.* Levels of plasma homocysteine in pseudoexfoliation glaucoma. *Graefe's Arch. Clin. Exp. Ophthalmol.* **249**, 443–448 (2011).
  154. Leibovitch, I. *et al.* Hyperhomocystinemia in pseudoexfoliation glaucoma. *J. Glaucoma* **12**, 36–39 (2003).
  155. Fan, B. J. *et al.* Lack of association of polymorphisms in homocysteine metabolism

- genes with pseudoexfoliation syndrome and glaucoma. *Mol. Vis.* (2008).
156. Koliakos, G. G. *et al.* Transforming and insulin-like growth factors in the aqueous humour of patients with exfoliation syndrome. *Graefe's Arch. Clin. Exp. Ophthalmol.* **239**, 482–487 (2001).
  157. Zenkel, M., Lewczuk, P., Junemann, A., Kruse, F. & Naumann, G. Proinflammatory cytokines are involved in the initiation of the abnormal matrix process in pseudoexfoliation syndrome/glaucoma. *Am J Pathol* **176**, (2010).
  158. Want, A. *et al.* Autophagy and mitochondrial dysfunction in tenon fibroblasts from exfoliation glaucoma patients. *PLoS One* **11**, 1–21 (2016).
  159. Bernstein, A. M., Ritch, R. & Wolosin, J. M. Exfoliation Syndrome: A Disease of Autophagy and LOXL1 Proteopathy. *J. Glaucoma* **27**, S44–S53 (2018).
  160. Wolosin, J. M., Ritch, R. & Bernstein, A. M. Is Autophagy Dysfunction a Key to Exfoliation Glaucoma? *J Glaucoma* **27**, 197–201 (2018).
  161. Zenkel, M. *et al.* Proinflammatory cytokines are involved in the initiation of the abnormal matrix process in pseudoexfoliation syndrome/glaucoma. *Am. J. Pathol.* **176**, 2868–2879 (2010).
  162. Yildirim, Z., Yildirim, F., Uçgun, N. I. & Sepici-Dinçel, A. The role of the cytokines in the pathogenesis of pseudoexfoliation syndrome. *Int. J. Ophthalmol.* **6**, 50–53 (2013).
  163. Chono, I. *et al.* High interleukin-8 level in aqueous humor is associated with poor prognosis in eyes with open angle glaucoma and neovascular glaucoma. *Sci. Rep.* **8**, 1–11 (2018).
  164. Türkyilmaz, K. *et al.* Serum YKL-40 levels as a novel marker of inflammation and endothelial dysfunction in patients with pseudoexfoliation syndrome. *Eye* **27**, 854–859 (2013).
  165. Gonen, T., Guzel, S. & Keskinbora, K. H. YKL-40 is a local marker for inflammation in patients with pseudoexfoliation syndrome. *Eye* **33**, 772–776 (2019).
  166. Dickson, D. H. & Ramsay, M. S. Fibrilloglucosaminoglycan (pseudoexfoliation). A clinical and electron microscope study. *Can. J. Ophthalmol.* (1975).
  167. Drolsum, L., Haaskjold, E. & Davanger, M. Results and complications after extracapsular cataract extraction in eyes with pseudoexfoliation syndrome. *Acta Ophthalmol.* (1993). doi:10.1111/j.1755-3768.1993.tb08598.x
  168. Ringvold, A. Electron microscopy of the wall of iris vessels in eyes with and without exfoliation syndrome (pseudoexfoliation of the lens capsule). *Virchows Arch. Abteilung A Pathol. Anat.* (1969). doi:10.1007/BF00548526
  169. Harnisch, J. P., Barrach, H. J., Hassell, J. R. & Sinha, P. K. Identification of a basement membrane proteoglycan in exfoliation material. *Albr. von Graefes Arch. für Klin. und*

- Exp. Ophthalmol.* (1981). doi:10.1007/BF00407666
170. Ringvold, A. *et al.* The Middle-Norway eye-screening study: I. Epidemiology of the pseudo-exfoliation syndrome. *Acta Ophthalmol.* (1988). doi:10.1111/j.1755-3768.1988.tb04056.x
  171. Konstas, A. G. P., Stewart, W. C., Stroman, G. A. & Sine, C. S. Clinical presentation and initial treatment patterns in patients with exfoliation glaucoma versus primary open-angle glaucoma. *Ophthalmic Surg. Lasers* (1997). doi:10.3928/1542-8877-19970201-05
  172. Konstas, A. G. P. *et al.* Exfoliation syndrome in a 17-year-old girl. *Arch. Ophthalmol.* (1997). doi:10.1001/archoph.1997.01100160233014
  173. Kuchle, M. & Naumann, G. O. H. Occurrence of pseudoexfoliation following penetrating keratoplasty for keratoconus. *Br. J. Ophthalmol.* (1992). doi:10.1136/bjo.76.2.98
  174. Sampaolesi, R., Casiraghi, J. & Geria, R. The occurrence of exfoliation syndrome after penetrating keratoplasty: a report of three cases. (1995).
  175. Liu, X. *et al.* Elastic fiber homeostasis requires lysyl oxidase-like 1 protein. *Nat. Genet.* (2004). doi:10.1038/ng1297
  176. Djordjevic-Jocic, J. *et al.* Transforming growth factor  $\beta$ 1, matrix metalloproteinase-2 and its tissue inhibitor in patients with pseudoexfoliation glaucoma/syndrome. *Vojnosanit. Pregl. Med. Pharm. J. Serbia* (2012). doi:10.2298/vsp1203231d
  177. Hauser, M. A. *et al.* Genetic variants and cellular stressors associated with exfoliation syndrome modulate promoter activity of a lncRNA within the LOXL1 locus. *Hum. Mol. Genet.* **24**, 6552–6563 (2015).
  178. scmitt 2020 lox1l as1 - Google Scholar. Available at: [https://scholar.google.com/scholar?hl=en&as\\_sdt=0%2C5&q=scmitt+2020+lox1l+as1&btnG=#d=gs\\_cit&u=%2Fscholar%3Fq%3Dinfo%3AGLQcOsAFqnYJ%3Ascholar.google.com%2F%26output%3Dcite%26scirp%3D0%26hl%3Den](https://scholar.google.com/scholar?hl=en&as_sdt=0%2C5&q=scmitt+2020+lox1l+as1&btnG=#d=gs_cit&u=%2Fscholar%3Fq%3Dinfo%3AGLQcOsAFqnYJ%3Ascholar.google.com%2F%26output%3Dcite%26scirp%3D0%26hl%3Den). (Accessed: 23rd February 2020)
  179. Powers, E. T. & Balch, W. E. Diversity in the origins of proteostasis networks—a driver for protein function in evolution. *Nat. Rev. Mol. Cell Biol.* **14**, 237–248 (2013).
  180. Broadley, S. A. & Hartl, F. U. The role of molecular chaperones in human misfolding diseases. *FEBS Lett.* **583**, 2647–2653 (2009).
  181. Hartl, F. U., Bracher, A. & Hayer-Hartl, M. Molecular chaperones in protein folding and proteostasis. *Nature* **475**, 324–332 (2011).
  182. Trinklein, N. D., Murray, J. I., Hartman, S. J., Botstein, D. & Myers, R. M. The Role of Heat Shock Transcription Factor 1 in the Genome-wide Regulation of the Mammalian Heat Shock Response. *Mol. Biol. Cell* (2004). doi:10.1091/mbc.E03-10-0738

183. Haynes, C. M. & Ron, D. The mitochondrial UPR - Protecting organelle protein homeostasis. *Journal of Cell Science* (2010). doi:10.1242/jcs.075119
184. Lecomte, S. *et al.* Unraveling Complex Interplay between Heat Shock Factor 1 and 2 Splicing Isoforms. *PLoS One* **8**, (2013).
185. Zou, J., Guo, Y., Guettouche, T., Smith, D. F. & Voellmy, R. Repression of heat shock transcription factor HSF1 activation by HSP90 (HSP90 complex) that forms a stress-sensitive complex with HSF1. *Cell* (1998). doi:10.1016/S0092-8674(00)81588-3
186. Anckar, J. & Sistonen, L. of Stress and Developmental Pathways. *Shock* (2007).
187. Mosser, D. D. & Morimoto, R. I. Molecular chaperones and the stress of oncogenesis. *Oncogene* (2004). doi:10.1038/sj.onc.1207529
188. Powers, M. V. & Workman, P. Inhibitors of the heat shock response: Biology and pharmacology. *FEBS Letters* (2007). doi:10.1016/j.febslet.2007.05.040
189. Åkerfelt, M., Morimoto, R. I. & Sistonen, L. Heat shock factors: Integrators of cell stress, development and lifespan. *Nat. Rev. Mol. Cell Biol.* **11**, 545–555 (2010).
190. Morimoto, R. I. Proteotoxic stress and inducible chaperone networks in neurodegenerative disease and aging. *Genes and Development* (2008). doi:10.1101/gad.1657108
191. Batista-Nascimento, L., Neef, D. W., Liu, P. C. C., Rodrigues-Pousada, C. & Thiele, D. J. Deciphering human heat shock transcription factor 1 regulation via post-translational modification in yeast. *PLoS One* (2011). doi:10.1371/journal.pone.0015976
192. KAKIMURA, J.-I. *et al.* Microglial activation and amyloid- $\beta$  clearance induced by exogenous heat-shock proteins. *FASEB J.* (2002). doi:10.1096/fj.01-0530fje
193. Dickey, C. A. *et al.* The high-affinity HSP90-CHIP complex recognizes and selectively degrades phosphorylated tau client proteins. *J. Clin. Invest.* (2007). doi:10.1172/JCI29715
194. Hay, D. G. *et al.* Progressive decrease in chaperone protein levels in a mouse model of Huntington's disease and induction of stress proteins as a therapeutic approach. *Hum. Mol. Genet.* (2004). doi:10.1093/hmg/ddh144
195. Yamanaka, T. *et al.* Mutant Huntingtin reduces HSP70 expression through the sequestration of NF-Y transcription factor. *EMBO J.* (2008). doi:10.1038/emboj.2008.23
196. Gao, X. C. *et al.* Co-chaperone HSP110a dually regulates the proteasomal degradation of ataxin-3. *PLoS One* (2011). doi:10.1371/journal.pone.0019763
197. Baldo, B. *et al.* A screen for enhancers of clearance identifies huntingtin as a heat shock protein 90 (Hsp90) client protein. *J. Biol. Chem.* **287**, 1406–1414 (2012).
198. Ernst, J. T. *et al.* Identification of novel HSP90 $\alpha/\beta$  isoform selective inhibitors using structure-based drug design. demonstration of potential utility in treating CNS disorders

- such as huntington's disease. *J. Med. Chem.* (2014). doi:10.1021/jm500042s
199. Zenkel, M., Kruse, F. E., Naumann, G. O. H. & Schlötzer-Schrehardt, U. Impaired cytoprotective mechanisms in eyes with pseudoexfoliation syndrome/glaucoma. *Investig. Ophthalmol. Vis. Sci.* **48**, 5558–5566 (2007).
  200. Hayat, B., Padhy, B., Mohanty, P. P. & Alone, D. P. Altered unfolded protein response and proteasome impairment in pseudoexfoliation pathogenesis. *Exp. Eye Res.* **181**, 197–207 (2019).
  201. Rüdiger, S., Buchberger, A. & Bukau, B. Interaction of Hsp70 chaperones with substrates. *Nature Structural Biology* (1997). doi:10.1038/nsb0597-342
  202. Hartl, F. U., Bracher, A. & Hayer-hartl, M. Molecular chaperones in protein folding and proteostasis. (2011). doi:10.1038/nature10317
  203. Redgrove, K. A. *et al.* The Molecular Chaperone HSPA2 Plays a Key Role in Regulating the Expression of Sperm Surface Receptors That Mediate Sperm-Egg Recognition. *PLoS One* (2012). doi:10.1371/journal.pone.0050851
  204. Nixon, B. *et al.* The role of the molecular chaperone heat shock protein A2 (HSPA2) in regulating human sperm-egg recognition. in *Asian Journal of Andrology* (2015). doi:10.4103/1008-682X.151395
  205. Kiang, J. G. & Tsokos, G. C. Heat shock protein 70 kDa: Molecular biology, biochemistry, and physiology. *Pharmacology and Therapeutics* **80**, 183–201 (1998).
  206. Lixia, S. *et al.* Effects of 1.8 GHz radiofrequency field on DNA damage and expression of heat shock protein 70 in human lens epithelial cells. *Mutat. Res. - Fundam. Mol. Mech. Mutagen.* **602**, 135–142 (2006).
  207. McLean, P. J., Klucken, J., Shin, Y. & Hyman, B. T. Geldanamycin induces Hsp70 and prevents  $\alpha$ -synuclein aggregation and toxicity in vitro. *Biochem. Biophys. Res. Commun.* (2004). doi:10.1016/j.bbrc.2004.07.021
  208. Bagchi, M., Katar, M. & Maisel, H. Heat shock proteins of adult and embryonic human ocular lenses. *J. Cell. Biochem.* (2002). doi:10.1002/jcb.10023
  209. Dean, D. O., Kent, C. R. & Tytell, M. Constitutive and inducible heat shock protein 70 immunoreactivity in the normal rat eye. *Investig. Ophthalmol. Vis. Sci.* (1999).
  210. Niforou, K., Cheimonidou, C. & Trougakos, I. P. Molecular chaperones and proteostasis regulation during redox imbalance. *Redox Biol.* **2**, 323–332 (2014).
  211. Saibil, H. Chaperone machines for protein folding, unfolding and disaggregation. *Nature Reviews Molecular Cell Biology* (2013). doi:10.1038/nrm3658
  212. Whitesell, L. & Lindquist, S. L. HSP90 and the chaperoning of cancer. *Nature Reviews Cancer* (2005). doi:10.1038/nrc1716
  213. Cheng, C.-F. *et al.* Transforming Growth Factor (TGF)-Stimulated Secretion of

- HSP90 : Using the Receptor LRP-1/CD91 To Promote Human Skin Cell Migration against a TGF -Rich Environment during Wound Healing. *Mol. Cell. Biol.* (2008). doi:10.1128/mcb.01287-07
214. Ahsan, A. *et al.* Wild-type EGFR is stabilized by direct interaction with HSP90 in cancer cells and tumors. *Neoplasia (United States)* (2012). doi:10.1593/neo.12986
  215. Friedman, J. A. *et al.* HSP90 inhibitor SNX5422/2112 targets the dysregulated signal and transcription factor network and malignant phenotype of head and neck squamous cell carcinoma. *Transl. Oncol.* (2013). doi:10.1593/tlo.13292
  216. Misso, G. *et al.* Pharmacological inhibition of HSP90 and ras activity as a new strategy in the treatment of HNSCC. *J. Cell. Physiol.* (2013). doi:10.1002/jcp.24112
  217. Bock, C. *et al.* BiQ Analyzer: Visualization and quality control for DNA methylation data from bisulfite sequencing. *Bioinformatics* (2005). doi:10.1093/bioinformatics/bti652
  218. Zenkel, M., Kruse, F. E., Naumann, G. O. H. & Schlötzer-Schrehardt, U. Impaired cytoprotective mechanisms in eyes with pseudoexfoliation syndrome/glaucoma. *Investig. Ophthalmol. Vis. Sci.* **48**, 5558–5566 (2007).
  219. Mathelier, A. *et al.* JASPAR 2016: A major expansion and update of the open-access database of transcription factor binding profiles. *Nucleic Acids Res.* **44**, D110–D115 (2016).
  220. Kon, M. *et al.* Chaperone-mediated autophagy is required for tumor growth. *Sci. Transl. Med.* (2011). doi:10.1126/scitranslmed.3003182
  221. Mayer, M. P. & Bukau, B. Hsp70 chaperones: Cellular functions and molecular mechanism. *Cell. Mol. Life Sci.* **62**, 670–684 (2005).
  222. Mathur, S. K. *et al.* Deficient induction of human hsp70 heat shock gene transcription in Y79 retinoblastoma cells despite activation of heat shock factor 1. *Proc. Natl. Acad. Sci. U. S. A.* **91**, 8695–8699 (1994).
  223. Deaton, A. M. & Bird, A. CpG islands and the regulation of transcription. *Genes Dev.* **25**, 1010–1022 (2011).
  224. Feltus, F. A., Lee, E. K., Costello, J. F., Plass, C. & Vertino, P. M. Predicting aberrant CpG island methylation. *Proc. Natl. Acad. Sci. U. S. A.* (2003). doi:10.1073/pnas.2037852100
  225. Costello, J. F. *et al.* Aberrant CpG-island methylation has non-random and tumour-type-specific patterns. *Nat. Genet.* (2000). doi:10.1038/72785
  226. Zhou, P., Luo, Y., Liu, X., Fan, L. & Lu, Y. Down-regulation and CpG island hypermethylation of CRYAA in age-related nuclear cataract. *FASEB J.* **26**, 4897–4902 (2012).

227. Palsamy, P., Ayaki, M., Elanchezian, R. & Shinohara, T. Promoter demethylation of Keap1 gene in human diabetic cataractous lenses. *Biochem. Biophys. Res. Commun.* **423**, 542–548 (2012).
228. Ye, H. *et al.* LOXL1 hypermethylation in pseudoexfoliation syndrome in the uighur population. *Investig. Ophthalmol. Vis. Sci.* **56**, 5838–5843 (2015).
229. Okano, M., Bell, D. W., Haber, D. A. & Li, E. DNA methyltransferases Dnmt3a and Dnmt3b are essential for de novo methylation and mammalian development. *Cell* **99**, 247–257 (1999).
230. Venugopal, R. & Jaiswal, A. K. Nrf2 and Nrf1 in association with Jun proteins regulate antioxidant response element-mediated expression and coordinated induction of genes encoding detoxifying enzymes. *Oncogene* **17**, 3145–3156 (1998).
231. Izumi, H. *et al.* p300/CBP-associated factor (P/CAF) interacts with nuclear respiratory factor-1 to regulate the UDP-N-acetyl- $\alpha$ -D-galactosamine: polypeptide N-acetylgalactosaminyltransferase-3 gene. *Biochem. J* **373**, (2003).
232. Gui, Y. *et al.* Frequent mutations of chromatin remodeling genes in transitional cell carcinoma of the bladder. *Nat. Genet.* **43**, 875–878 (2011).
233. Zhang, Z. Phosphorylation of Kruppel-like factor 5 (KLF5/IKLF) at the CBP interaction region enhances its transactivation function. *Nucleic Acids Res.* **31**, 2196–2208 (2003).
234. Wang, G. L. & Semenza, G. L. General involvement of hypoxia-inducible factor 1 in transcriptional response to hypoxia. *Proc. Natl. Acad. Sci. U. S. A.* **90**, 4304–4308 (1993).
235. Zhou, P., Lu, Y. & Sun, X. H. Effects of a novel DNA methyltransferase inhibitor Zebularine on human lens epithelial cells. *Mol. Vis.* **18**, 22–28 (2012).
236. Laurenzana, A. *et al.* Inhibition of DNA methyltransferase activates tumor necrosis factor  $\alpha$ -induced monocytic differentiation in acute myeloid leukemia cells. *Cancer Res.* **69**, 55–64 (2009).
237. Tabolacci, E. *et al.* Genome-wide methylation analysis demonstrates that 5-aza-2-deoxycytidine treatment does not cause random DNA demethylation in fragile X syndrome cells. *Epigenetics Chromatin* **9**, 12 (2016).
238. Juttermann, R., Li, E. & Jaenisch, R. Toxicity of 5-aza-2'-deoxycytidine to mammalian cells is mediated primarily by covalent trapping of DNA methyltransferase rather than DNA demethylation. *Proc. Natl. Acad. Sci. U. S. A.* **91**, 11797–11801 (1994).
239. Jones, P. A. & Taylor, S. M. Cellular differentiation, cytidine analogs and DNA methylation. *Cell* **20**, 85–93 (1980).
240. Kostova, Z. & Wolf, D. H. For whom the bell tolls: Protein quality control of the endoplasmic reticulum and the ubiquitin-proteasome connection. *EMBO Journal* (2003). doi:10.1093/emboj/cdg227

241. McCracken, A. A. & Brodsky, J. L. Evolving questions and paradigm shifts in endoplasmic-reticulum-associated degradation (ERAD). *BioEssays* (2003). doi:10.1002/bies.10320
242. Vernia, S., Rubio, T., Heredia, M., Rodríguez de Córdoba, S. & Sanz, P. Increased endoplasmic reticulum stress and decreased proteasomal function in Lafora disease models lacking the phosphatase laforin. *PLoS One* **4**, (2009).
243. Ciechanover, A. & Kwon, Y. T. a. Degradation of misfolded proteins in neurodegenerative diseases: therapeutic targets and strategies. *Exp. Mol. Med.* **47**, e147 (2015).
244. Rubinsztein, D. C. The roles of intracellular protein-degradation pathways in neurodegeneration. *Nature* (2006). doi:10.1038/nature05291
245. Zhao, Y. *et al.* Autophagy is induced by UVA and promotes removal of oxidized phospholipids and protein aggregates in epidermal keratinocytes. *J. Invest. Dermatol.* (2013). doi:10.1038/jid.2013.26
246. Lim, J. & Yue, Z. Neuronal Aggregates: Formation, Clearance, and Spreading. *Developmental Cell* (2015). doi:10.1016/j.devcel.2015.02.002
247. Zheng, C., Geetha, T. & Babu, J. R. Failure of ubiquitin proteasome system: Risk for neurodegenerative diseases. *Neurodegenerative Diseases* (2014). doi:10.1159/000367694
248. Anholt, R. R. H. & Carbone, M. A. A molecular mechanism for glaucoma: Endoplasmic reticulum stress and the unfolded protein response. *Trends in Molecular Medicine* (2013). doi:10.1016/j.molmed.2013.06.005
249. Li, J., Wang, J. J., Yu, Q., Wang, M. & Zhang, S. X. Endoplasmic reticulum stress is implicated in retinal inflammation and diabetic retinopathy. *FEBS Lett.* (2009). doi:10.1016/j.febslet.2009.04.007
250. Doudevski, I. *et al.* Clusterin and complement activation in exfoliation glaucoma. *Investig. Ophthalmol. Vis. Sci.* (2014). doi:10.1167/iovs.13-12941
251. Urra, H., Dufey, E., Lisbona, F., Rojas-Rivera, D. & Hetz, C. When ER stress reaches a dead end. *Biochimica et Biophysica Acta - Molecular Cell Research* (2013). doi:10.1016/j.bbamcr.2013.07.024
252. Majumder, M. *et al.* A Novel Feedback Loop Regulates the Response to Endoplasmic Reticulum Stress via the Cooperation of Cytoplasmic Splicing and mRNA Translation. *Mol. Cell. Biol.* (2012). doi:10.1128/mcb.06665-11
253. Takayanagi, S., Fukuda, R., Takeuchi, Y., Tsukada, S. & Yoshida, K. Gene regulatory network of unfolded protein response genes in endoplasmic reticulum stress. *Cell Stress and Chaperones* (2013). doi:10.1007/s12192-012-0351-5
254. Ron, D. & Walter, P. Signal integration in the endoplasmic reticulum unfolded protein

- response. *Nature Reviews Molecular Cell Biology* (2007). doi:10.1038/nrm2199
255. Harding, H. P. *et al.* An integrated stress response regulates amino acid metabolism and resistance to oxidative stress. *Mol. Cell* (2003). doi:10.1016/S1097-2765(03)00105-9
256. Halliday, M. & Mallucci, G. R. Targeting the unfolded protein response in neurodegeneration: A new approach to therapy. *Neuropharmacology* (2014). doi:10.1016/j.neuropharm.2013.08.034
257. Hershko, A. & Ciechanover, A. THE UBIQUITIN SYSTEM. *Annu. Rev. Biochem.* (1998). doi:10.1146/annurev.biochem.67.1.425
258. Kleiger, G. & Mayor, T. Perilous journey: A tour of the ubiquitin-proteasome system. *Trends in Cell Biology* (2014). doi:10.1016/j.tcb.2013.12.003
259. Pickart, C. M. Mechanisms Underlying Ubiquitination. *Annu. Rev. Biochem.* (2001). doi:10.1146/annurev.biochem.70.1.503
260. Bhattacharyya, S., Yu, H., Mim, C. & Matouschek, A. Regulated protein turnover: Snapshots of the proteasome in action. *Nature Reviews Molecular Cell Biology* (2014). doi:10.1038/nrm3741
261. Tanaka, K. The proteasome: Overview of structure and functions. *Proceedings of the Japan Academy Series B: Physical and Biological Sciences* (2009). doi:10.2183/pjab.85.12
262. Dev, K. K., Hofele, K., Barbieri, S., Buchman, V. L. & Van Der Putten, H. Part II:  $\alpha$ -synuclein and its molecular pathophysiological role in neurodegenerative disease. *Neuropharmacology* (2003). doi:10.1016/S0028-3908(03)00140-0
263. DE VRIJ, F. M. S. *et al.* Mutant ubiquitin expressed in Alzheimer's disease causes neuronal death 1. *FASEB J.* (2001). doi:10.1096/fj.01-0438com
264. Campello, L., Esteve-Rudd, J., Cuenca, N. & Martín-Nieto, J. The ubiquitin-proteasome system in retinal health and disease. *Molecular neurobiology* (2013). doi:10.1007/s12035-012-8391-5
265. Magnoni, R. *et al.* Late onset motoneuron disorder caused by mitochondrial Hsp60 chaperone deficiency in mice. *Neurobiol. Dis.* (2013). doi:10.1016/j.nbd.2013.02.012
266. Hoshino, T. *et al.* Endoplasmic reticulum chaperones inhibit the production of amyloid- $\beta$  peptides. *Biochem. J.* (2007). doi:10.1042/BJ20061318
267. Ito, Y. *et al.* Involvement of CHOP, an ER-stress apoptotic mediator, in both human sporadic ALS and ALS model mice. *Neurobiol. Dis.* (2009). doi:10.1016/j.nbd.2009.08.013
268. Hoozemans, J. J. M. *et al.* The unfolded protein response is activated in pretangle neurons in alzheimer's disease hippocampus. *Am. J. Pathol.* (2009). doi:10.2353/ajpath.2009.080814

269. Reinhardt, S. *et al.* Unfolded protein response signaling by transcription factor XBP-1 regulates ADAM10 and is affected in Alzheimer's disease. *FASEB J.* (2014). doi:10.1096/fj.13-234864
270. Valdés, P. *et al.* Control of dopaminergic neuron survival by the unfolded protein response transcription factor XBP1. *Proc. Natl. Acad. Sci. U. S. A.* (2014). doi:10.1073/pnas.1321845111
271. Vidal, R. L. *et al.* Targeting the UPR transcription factor XBP1 protects against Huntington's disease through the regulation of FoxO1 and autophagy. *Hum. Mol. Genet.* (2012). doi:10.1093/hmg/dd5040
272. Carbone, M. A. *et al.* Genes of the unfolded protein response pathway harbor risk alleles for primary open angle glaucoma. *PLoS One* **6**, 1–5 (2011).
273. Lee, H. *et al.* IRE1 plays an essential role in ER stress-mediated aggregation of mutant huntingtin via the inhibition of autophagy flux. *Hum. Mol. Genet.* (2012). doi:10.1093/hmg/ddr445
274. Stutzbach, L. D. *et al.* The unfolded protein response is activated in disease-affected brain regions in progressive supranuclear palsy and Alzheimer's disease. *Acta Neuropathol. Commun.* (2014). doi:10.1186/2051-5960-1-31
275. Matus, S., Valenzuela, V., Medinas, D. B. & Hetz, C. ER dysfunction and protein folding stress in ALS. *International Journal of Cell Biology* (2013). doi:10.1155/2013/674751
276. Hashida, K. *et al.* ATF6alpha Promotes Astroglial Activation and Neuronal Survival in a Chronic Mouse Model of Parkinson's Disease. *PLoS One* (2012). doi:10.1371/journal.pone.0047950
277. Genereux, J. C. *et al.* Unfolded protein response-induced ER dj3 secretion links ER stress to extracellular proteostasis. *EMBO J.* (2015). doi:10.15252/embj.201488896
278. Chung, J. Y. *et al.* Elevated TRAF2/6 expression in Parkinson's disease is caused by the loss of Parkin E3 ligase activity. *Lab. Invest.* (2013). doi:10.1038/labinvest.2013.60
279. Boyce, M. *et al.* A selective inhibitor of eIF2 $\alpha$  dephosphorylation protects cells from ER stress. *Science* (80-. ). (2005). doi:10.1126/science.1101902
280. Scheper, W. & Hoozemans, J. J. M. The unfolded protein response in neurodegenerative diseases: a neuropathological perspective. *Acta Neuropathol.* **130**, 315–331 (2015).
281. Hetz, C., Russelakis-Carneiro, M., Maundrell, K., Castilla, J. & Soto, C. Caspase-12 and endoplasmic reticulum stress mediate neurotoxicity of pathological prion protein. *EMBO J.* (2003). doi:10.1093/emboj/cdg537
282. Nakagawa, T. *et al.* Caspase-12 mediates endoplasmic-reticulum-specific apoptosis and cytotoxicity by amyloid- $\beta$ . *Nature* (2000). doi:10.1038/47513

283. Gorbatyuk, M. S. *et al.* Glucose regulated protein 78 diminishes  $\alpha$ -synuclein neurotoxicity in a rat model of parkinson disease. *Mol. Ther.* (2012). doi:10.1038/mt.2012.28
284. Roussel, B. D. *et al.* Endoplasmic reticulum dysfunction in neurological disease. *The Lancet Neurology* (2013). doi:10.1016/S1474-4422(12)70238-7
285. Taguchi, J. *et al.* Different expression of calreticulin and immunoglobulin binding protein in Alzheimer's disease brain. *Acta Neuropathol.* (2000). doi:10.1007/s004019900165
286. Omura, T., Kaneko, M., Okuma, Y., Matsubara, K. & Nomura, Y. Endoplasmic reticulum stress and Parkinson's disease: The role of HRD1 in averting apoptosis in neurodegenerative disease. *Oxidative Medicine and Cellular Longevity* (2013). doi:10.1155/2013/239854
287. Conway, M., Nafar, F., Straka, T. & Mearow, K. Modulation of amyloid- $\beta$  protein precursor expression by HspB1. *J. Alzheimer's Dis.* (2014). doi:10.3233/JAD-140348
288. Kuo, Y., Ren, S., Lao, U., Edgar, B. A. & Wang, T. Suppression of polyglutamine protein toxicity by co-expression of a heat-shock protein 40 and a heat-shock protein 110. *Cell Death Dis.* (2013). doi:10.1038/cddis.2013.351
289. Baig, S. *et al.* Clusterin mRNA and protein in Alzheimer's disease. *J. Alzheimer's Dis.* (2012). doi:10.3233/JAD-2011-110473
290. Van Leeuwen, F. W., Hol, E. M. & Fischer, D. F. Frameshift proteins in Alzheimer's disease and in other conformational disorders: Time for the ubiquitin-proteasome system. *Journal of Alzheimer's Disease* (2006). doi:10.3233/jad-2006-9s336
291. Ciechanover, A. & Brundin, P. The ubiquitin proteasome system in neurodegenerative diseases: Sometimes the chicken, sometimes the egg. *Neuron* (2003). doi:10.1016/S0896-6273(03)00606-8
292. Doyle, K. M. *et al.* Unfolded proteins and endoplasmic reticulum stress in neurodegenerative disorders. *Journal of Cellular and Molecular Medicine* (2011). doi:10.1111/j.1582-4934.2011.01374.x
293. Hetz, C. Protein homeostasis networks in neurodegeneration : A look to the ER Protein misfolding and ER stress.
294. Valastyan, J. S. & Lindquist, S. Mechanisms of protein-folding diseases at a glance. *DMM Dis. Model. Mech.* (2014). doi:10.1242/dmm.013474
295. Hetz, C. The unfolded protein response: Controlling cell fate decisions under ER stress and beyond. *Nature Reviews Molecular Cell Biology* (2012). doi:10.1038/nrm3270
296. Ross, C. A. & Poirier, M. A. Protein aggregation and neurodegenerative disease. *Nat. Med.* **10**, S10 (2004).

297. Aboobakar, I. F., Johnson, W. M., Stamer, W. D., Hauser, M. A. & Allingham, R. R. Major review: Exfoliation syndrome; advances in disease genetics, molecular biology, and epidemiology. *Exp. Eye Res.* **154**, 88–103 (2017).
298. Yam, G. H. F., Gaplovska-Kysela, K., Zuber, C. & Roth, J. Aggregated myocilin induces Russell bodies and causes apoptosis: Implications for the pathogenesis of myocilin-caused primary open-angle glaucoma. *Am. J. Pathol.* (2007). doi:10.2353/ajpath.2007.060806
299. Teixeira, P. F., Cerca, F., Santos, S. D. & Saraiva, M. J. Endoplasmic reticulum stress associated with extracellular aggregates: Evidence from transthyretin deposition in familial amyloid polyneuropathy. *J. Biol. Chem.* (2006). doi:10.1074/jbc.M602302200
300. Lee, A. S. The ER chaperone and signaling regulator GRP78/BiP as a monitor of endoplasmic reticulum stress. *Methods* (2005). doi:10.1016/j.ymeth.2004.10.010
301. Wang, M., Wey, S., Zhang, Y., Ye, R. & Lee, A. S. Role of the unfolded protein response regulator GRP78/BiP in development, cancer, and neurological disorders. *Antioxidants and Redox Signaling* (2009). doi:10.1089/ars.2009.2485
302. Park, K. W. *et al.* The Endoplasmic Reticulum Chaperone GRP78/BiP Modulates Prion Propagation in vitro and in vivo. *Sci. Rep.* (2017). doi:10.1038/srep44723
303. Zhu, G. & Lee, A. S. Role of the unfolded protein response, GRP78 and GRP94 in organ homeostasis. *J. Cell. Physiol.* (2015). doi:10.1002/jcp.24923
304. Carvalho, P., Goder, V. & Rapoport, T. A. Distinct Ubiquitin-Ligase Complexes Define Convergent Pathways for the Degradation of ER Proteins. *Cell* (2006). doi:10.1016/j.cell.2006.05.043
305. Denic, V., Quan, E. M. & Weissman, J. S. A Luminal Surveillance Complex that Selects Misfolded Glycoproteins for ER-Associated Degradation. *Cell* (2006). doi:10.1016/j.cell.2006.05.045
306. Rao, R. V. & Bredesen, D. E. Misfolded proteins, endoplasmic reticulum stress and neurodegeneration. *Current Opinion in Cell Biology* (2004). doi:10.1016/j.ceb.2004.09.012
307. Kaneko, M., Ishiguro, M., Niinuma, Y., Uesugi, M. & Nomura, Y. Human HRD1 protects against ER stress-induced apoptosis through ER-associated degradation. *FEBS Lett.* (2002). doi:10.1016/S0014-5793(02)03660-8
308. Stahon, K. E. *et al.* Age-related changes in axonal and mitochondrial ultrastructure and function in white matter. *J. Neurosci.* (2016). doi:10.1523/JNEUROSCI.1316-16.2016
309. Gagnon, E. *et al.* Endoplasmic reticulum-mediated phagocytosis is a mechanism of entry into macrophages. *Cell* (2002). doi:10.1016/S0092-8674(02)00797-3
310. Shang, F., Gong, X., Palmer, H. J., Nowell, T. R. & Taylor, A. Age-related decline in ubiquitin conjugation in response to oxidative stress in the lens. *Exp. Eye Res.* (1997).

doi:10.1006/exer.1996.0176

311. Ciechanover, A. Proteolysis: From the lysosome to ubiquitin and the proteasome. *Nature Reviews Molecular Cell Biology* (2005). doi:10.1038/nrm1552
312. Finley, D. Recognition and Processing of Ubiquitin-Protein Conjugates by the Proteasome. *Annu. Rev. Biochem.* (2009). doi:10.1146/annurev.biochem.78.081507.101607
313. Pickart, C. M. & Cohen, R. E. Proteasomes and their kin: Proteases in the machine age. *Nature Reviews Molecular Cell Biology* (2004). doi:10.1038/nrm1336
314. Baumeister, W., Walz, J., Zühl, F. & Seemüller, E. The proteasome: Paradigm of a self-compartmentalizing protease. *Cell* (1998). doi:10.1016/S0092-8674(00)80929-0
315. Coux, O., Tanaka, K. & Goldberg, A. L. Structure and Functions of the 20S and 26S Proteasomes. *Annu. Rev. Biochem.* (1996). doi:10.1146/annurev.bi.65.070196.004101
316. Murata, S., Yashiroda, H. & Tanaka, K. Molecular mechanisms of proteasome assembly. *Nature Reviews Molecular Cell Biology* (2009). doi:10.1038/nrm2630
317. Arlt, A. *et al.* Increased proteasome subunit protein expression and proteasome activity in colon cancer relate to an enhanced activation of nuclear factor E2-related factor 2 (Nrf2). *Oncogene* (2009). doi:10.1038/onc.2009.264
318. Aung, T. *et al.* Genetic association study of exfoliation syndrome identifies a protective rare variant at LOXL1 and five new susceptibility loci. *Nat. Genet.* **49**, 993–1004 (2017).
319. Küchle, M., Nguyen, N. X., Hannappel, E. & Naumann, G. O. H. The blood-aqueous barrier in eyes with pseudoexfoliation syndrome. *Ophthalmic Res.* (1995). doi:10.1159/000267859
320. Luthra, S. *et al.* Activation of caspase-8 and caspase-12 pathways by 7-ketocholesterol in human retinal pigment epithelial cells. *Investig. Ophthalmol. Vis. Sci.* **47**, 5569–5575 (2006).
321. Can Demirdöğen, B., Ceylan, O. M., Işıkoğlu, S., Mumcuoğlu, T. & Erel, Ö. Evaluation of oxidative stress and paraoxonase phenotypes in pseudoexfoliation syndrome and pseudoexfoliation glaucoma. *Clin. Lab.* **60**, 79–86 (2014).
322. Oltulu, P. & Oltulu, R. The Association of Cataract and Lens Epithelial Cell Apoptosis in Patients with Pseudoexfoliation Syndrome. *Curr. Eye Res.* **43**, 300–303 (2018).
323. Shi, L. S., Huang, G., Yu, B. & Wen, X. Q. Clinical significance and prognostic value of serum Dickkopf-1 concentrations in patients with lung cancer. *Clin. Chem.* (2009). doi:10.1373/clinchem.2009.125641
324. MacDonald, B. T., Tamai, K. & He, X. Wnt/beta-catenin signaling: component MacDonald BT, Tamai K & He X (2009) Wnt/beta-catenin signaling: components, mechanisms, and diseases. *Dev. Cell* 17: 9–26s, mechanisms, and diseases.

- Dev. Cell* (2009). doi:10.1016/j.devcel.2009.06.016
325. Zhu, W. *et al.* IGFBP-4 is an inhibitor of canonical Wnt signalling required for cardiogenesis. *Nature* (2008). doi:10.1038/nature07027
326. Klaus, A. & Birchmeier, W. Wnt signalling and its impact on development and cancer. *Nature Reviews Cancer* (2008). doi:10.1038/nrc2389
327. Pinzone, J. J. *et al.* The role of Dickkopf-1 in bone development, homeostasis, and disease. (2009). doi:10.1182/blood-2008-03
328. Mao, B. *et al.* Kremen proteins are Dickkopf receptors that regulate Wnt/ $\beta$ -catenin signalling. *Nature* (2002). doi:10.1038/nature756
329. Aravind, L. & Koonin, E. V. A colipase fold in the carboxy-terminal domain of the Wnt antagonists - The Dickkopfs [1]. *Current Biology* (1998). doi:10.1016/s0960-9822(98)70309-4
330. Glinka, A. *et al.* Dickkopf-1 is a member of a new family of secreted proteins and functions in head induction. *Nature* (1998). doi:10.1038/34848
331. Tsuji, T., Miyazaki, M., Sakaguchi, M., Inoue, Y. & Namba, M. A REIC gene shows down-regulation in human immortalized cells and human tumor-derived cell lines. *Biochem. Biophys. Res. Commun.* (2000). doi:10.1006/bbrc.1999.2067
332. Hoang, B. H. *et al.* Dickkopf 3 Inhibits Invasion and Motility of Saos-2 Osteosarcoma Cells by Modulating the Wnt- $\beta$ -Catenin Pathway. *Cancer Res.* (2004). doi:10.1158/0008-5472.CAN-03-1952
333. Abarzua, F. *et al.* Adenovirus-mediated overexpression of REIC/Dkk-3 selectively induces apoptosis in human prostate cancer cells through activation of c-Jun-NH 2-kinase. *Cancer Res.* (2005). doi:10.1158/0008-5472.CAN-05-0829
334. Fedi, P. *et al.* Isolation and biochemical characterization of the human Dkk-1 homologue, a novel inhibitor of mammalian Wnt signaling. *J. Biol. Chem.* (1999). doi:10.1074/jbc.274.27.19465
335. Krupnik, V. E. *et al.* Functional and structural diversity of the human Dickkopf gene family. *Gene* **238**, 301–313 (1999).
336. Semenov, M. V. *et al.* Head inducer dickkopf-1 is a ligand for Wnt coreceptor LRP6. *Curr. Biol.* (2001). doi:10.1016/S0960-9822(01)00290-1
337. Semenov, M., Tamai, K. & He, X. SOST is a ligand for LRP5/LRP6 and a Wnt signaling inhibitor. *J. Biol. Chem.* (2005). doi:10.1074/jbc.M504308200
338. Li, X. *et al.* Sclerostin binds to LRP5/6 and antagonizes canonical Wnt signaling. *J. Biol. Chem.* **280**, 19883–19887 (2005).
339. Zhao, D.-M. *et al.* Constitutive Activation of Wnt Signaling Favors Generation of Memory CD8 T Cells. *J. Immunol.* (2010). doi:10.4049/jimmunol.0901199

340. Voorzanger-Rousselot, N., Journe, F., Doriath, V., Body, J.-J. & Garnero, P. Assessment of circulating Dickkopf-1 with a new two-site immunoassay in healthy subjects and women with breast cancer and bone metastases. *Calcif. Tissue Int.* **84**, 348–54 (2009).
341. Qiu, F. *et al.* Decreased Circulating Levels of Dickkopf-1 in Patients with Exudative Age-related Macular Degeneration. *Sci. Rep.* **7**, 1–9 (2017).
342. Qiu, F. *et al.* Plasma and vitreous fluid levels of Dickkopf-1 in patients with diabetic retinopathy. *Eye* **28**, 402–409 (2014).
343. Lane, N. E., Nevitt, M. C., Lui, L. Y., De Leon, P. & Corr, M. Wnt signaling antagonists are potential prognostic biomarkers for the progression of radiographic hip osteoarthritis in elderly Caucasian women. *Arthritis Rheum.* (2007). doi:10.1002/art.22867
344. Killick, R. *et al.* Clusterin regulates  $\beta$ -amyloid toxicity via Dickkopf-1-driven induction of the wnt-PCP-JNK pathway. *Mol. Psychiatry* **19**, 88–98 (2014).
345. Tao, Y. M., Liu, Z. & Liu, H. L. Dickkopf-1 (DKK1) promotes invasion and metastasis of hepatocellular carcinoma. *Dig. Liver Dis.* (2013). doi:10.1016/j.dld.2012.10.020
346. Forget, M. A. *et al.* The Wnt pathway regulator DKK1 is preferentially expressed in hormone-resistant breast tumours and in some common cancer types. *Br. J. Cancer* (2007). doi:10.1038/sj.bjc.6603579
347. Yamabuki, T. *et al.* Dickkopf-1 as a novel serologic and prognostic biomarker for lung and esophageal carcinomas. *Cancer Res.* **67**, 2517–2525 (2007).
348. Takahashi, N. *et al.* Dickkopf-1 is overexpressed in human pancreatic ductal adenocarcinoma cells and is involved in invasive growth. *Int. J. Cancer* (2010). doi:10.1002/ijc.24865
349. Makino, T. *et al.* Dickkopf-1 expression as a marker for predicting clinical outcome in esophageal squamous cell carcinoma. *Ann. Surg. Oncol.* (2009). doi:10.1245/s10434-009-0476-7
350. Patil, M. A. *et al.* An integrated data analysis approach to characterize genes highly expressed in hepatocellular carcinoma. *Oncogene* (2005). doi:10.1038/sj.onc.1208479
351. Gottanka, J., Flügel-Koch, C., Martus, P., Johnson, D. H. & Lütjen-Drecoll, E. Correlation of pseudoexfoliative material and optic nerve damage in pseudoexfoliation syndrome. *Investig. Ophthalmol. Vis. Sci.* (1997).
352. Mao, W. *et al.* Existence of the canonical wnt signaling pathway in the human trabecular meshwork. *Investig. Ophthalmol. Vis. Sci.* (2012). doi:10.1167/iovs.12-9664
353. Wang, W. H. *et al.* Increased expression of the WNT antagonist sFRP-1 in glaucoma elevates intraocular pressure. *J. Clin. Invest.* **118**, 1056–1064 (2008).
354. Raghunathan, V. K. *et al.* Dexamethasone stiffens trabecular meshwork, trabecular meshwork cells, and matrix. *Investig. Ophthalmol. Vis. Sci.* (2015). doi:10.1167/iovs.15-

355. Morgan, J. T., Raghunathan, V. K., Chang, Y. R., Murphy, C. J. & Russell, P. The intrinsic stiffness of human trabecular meshwork cells increases with senescence. *Oncotarget* (2015). doi:10.18632/oncotarget.3798
356. Mao, W. *et al.* Existence of the canonical wnt signaling pathway in the human trabecular meshwork. *Investig. Ophthalmol. Vis. Sci.* **53**, 7043–7051 (2012).
357. Villarreal, G. *et al.* Canonical Wnt signaling regulates extracellular matrix expression in the trabecular meshwork. *Investig. Ophthalmol. Vis. Sci.* **55**, 7433–7440 (2014).
358. Burdon, K. P. *et al.* Genetic analysis of the clusterin gene in pseudoexfoliation syndrome. *Mol. Vis.* **14**, 1727–1736 (2008).
359. Behrens, J. *et al.* Functional interaction of  $\beta$ -catenin with the transcription factor LEF- 1. *Nature* (1996). doi:10.1038/382638a0
360. Shang, S., Hua, F. & Hu, Z. W. The regulation of  $\beta$ -catenin activity and function in cancer: Therapeutic opportunities. *Oncotarget* **8**, 33972–33989 (2017).
361. Jho, E. -h. *et al.* Wnt/ -Catenin/Tcf Signaling Induces the Transcription of Axin2, a Negative Regulator of the Signaling Pathway. *Mol. Cell. Biol.* **22**, 1172–1183 (2002).
362. Behrens, J. *et al.* Functional interaction of an axin homolog, conductin, with  $\beta$ -catenin, APC, and GSK3 $\beta$ . *Science (80-. )*. **280**, 596–599 (1998).
363. Grumolato, L. *et al.* Canonical and noncanonical Wnts use a common mechanism to activate completely unrelated coreceptors. *Genes Dev.* **24**, 2517–2530 (2010).
364. Waki, M., Yoshida, Y., Oka, T. & Azuma, M. Reduction of intraocular pressure by topical administration of an inhibitor of the Rho-associated protein kinase. *Curr. Eye Res.* (2001). doi:10.1076/ceyr.22.6.470.5489
365. Wei, L., Surma, M., Shi, S., Lambert-Cheatham, N. & Shi, J. Novel Insights into the Roles of Rho Kinase in Cancer. *Archivum Immunologiae et Therapiae Experimentalis* **64**, 259–278 (2016).
366. Niida, A. *et al.* DKK1, a negative regulator of Wnt signaling, is a target of the  $\beta$ -catenin/TCF pathway. *Oncogene* **23**, 8520–8526 (2004).
367. Lee, A. Y. *et al.* Dickkopf-1 antagonizes Wnt signaling independent of  $\beta$ -catenin in human mesothelioma. *Biochem. Biophys. Res. Commun.* (2004). doi:10.1016/j.bbrc.2004.09.001
368. Aguilera, Ó. *et al.* Nuclear DICKKOPF-1 as a biomarker of chemoresistance and poor clinical outcome in colorectal cancer. *Oncotarget* **6**, 5903–5917 (2015).
369. Yuan, Y. *et al.* Transient expression of Wnt5a elicits ocular features of pseudoexfoliation syndrome in mice. *PLoS One* **14**, 1–16 (2019).

370. Kaiser, M. *et al.* Serum concentrations of DKK-1 correlate with the extent of bone disease in patients with multiple myeloma. *Eur. J. Haematol.* (2008). doi:10.1111/j.1600-0609.2008.01065.x
371. Shi, L. S., Huang, G., Yu, B. & Wen, X. Q. Clinical significance and prognostic value of serum Dickkopf-1 concentrations in patients with lung cancer. *Clin. Chem.* **55**, 1656–1664 (2009).
372. Yerbury, J. J. *et al.* The extracellular chaperone clusterin influences amyloid formation and toxicity by interacting with prefibrillar structures. *FASEB J.* (2007). doi:10.1096/fj.06-7986com
373. Diriong, S. *et al.* Chromosomal localization of the human genes for  $\alpha 1a$ ,  $\alpha 1b$ , and  $\alpha 1e$  voltage-dependent  $Ca^{2+}$  channel subunits. *Genomics* **30**, 605–609 (1995).
374. Dunlap, K., Luebke, J. I. & Turner, T. J. Exocytotic  $Ca^{2+}$  channels in mammalian central neurons. *Trends in Neurosciences* **18**, 89–98 (1995).
375. calcium, W. C.-C. & 1998, undefined. Structure and function of neuronal  $Ca^{2+}$  channels and their role in neurotransmitter release. *Elsevier*
376. Heyes, S. *et al.* Genetic disruption of voltage-gated calcium channels in psychiatric and neurological disorders. *Progress in Neurobiology* **134**, 36–54 (2015).
377. Catterall, W. A. S TRUCTURE AND R EGULATION OF V OLTAGE -G ATED  $Ca^{2+}$  C HANNELS. (2000).
378. Walker, D. & De Waard, M. Subunit interaction sites in voltage-dependent  $Ca^{2+}$  channels: role in channel function. *Trends Neurosci.* **21**, 148–54 (1998).
379. Catterall, W. A. Voltage-gated calcium channels. *Cold Spring Harb. Perspect. Biol.* **3**, 1–23 (2011).
380. Fletcher, C., Lutz, C., Cell, T. O.- & 1996, undefined. Absence epilepsy in tottering mutant mice is associated with calcium channel defects. *Elsevier*
381. Dawson, T. M. & Dawson, V. L. Molecular Pathways of Neurodegeneration in Parkinson's Disease. *Science* **302**, 819–822 (2003).
382. Mattson, M. P. Pathways towards and away from Alzheimer's disease. *Nature* (2004). doi:10.1038/nature02621
383. Mattson, M. P. Excitotoxic and excitoprotective mechanisms: Abundant targets for the prevention and treatment of neurodegenerative disorders. *NeuroMolecular Medicine* **3**, 65–94 (2003).
384. Keller, J. N., Quo, Q., Holtsberg, F. W., Bruce-Keller, A. J. & Mattson, M. P. Increased sensitivity to mitochondrial toxin-induced apoptosis in neural cells expressing mutant presenilin-1 is linked to perturbed calcium homeostasis and enhanced oxyradical production. *J. Neurosci.* (1998). doi:10.1523/jneurosci.18-12-04439.1998

385. Pietrobon, D. Ca<sub>v</sub>2.1 channelopathies. 375–393 (2010). doi:10.1007/s00424-010-0802-8
386. Neurol, P. Novel frameshift mutation in the CACNA1A gene causing a mixed phenotype of episodic ataxia and familiar hemiplegic migraine. *19*, 3–4 (2017).
387. Kordasiewicz, H. B., Thompson, R. M., Clark, H. B. & Gomez, C. M. C-termini of P/Q-type Ca<sub>v</sub>2.1 channel  $\alpha$ 1A subunits translocate to nuclei and promote polyglutamine-mediated toxicity. *15*, 1587–1599 (2006).
388. Marambaud, P., Dreses-Werringloer, U. & Vingtdeux, V. Calcium signaling in neurodegeneration. *Molecular Neurodegeneration* (2009). doi:10.1186/1750-1326-4-20
389. Simen, A. A. & Miller, R. J. Structural features determining differential receptor regulation of neuronal Ca channels. *J. Neurosci.* (1998). doi:10.1523/jneurosci.18-10-03689.1998
390. Randall, A. & Tsien, R. W. Pharmacological dissection of multiple types of Ca<sup>2+</sup> channel currents in rat cerebellar granule neurons. *J. Neurosci.* (1995). doi:10.1523/jneurosci.15-04-02995.1995
391. Rettig, J. *et al.* Alteration of Ca<sup>2+</sup> dependence of neurotransmitter release by disruption of Ca<sup>2+</sup> channel/syntaxin interaction. *J. Neurosci.* **17**, 6647–6656 (1997).
392. Schlötzer-Schrehardt, U. Molecular Biology of Exfoliation Syndrome. (2018). doi:10.1097/IJG.0000000000000903
393. Expression of CACNA1A in Patients with Pseudoexfoliation Syndrome | Scinapse. Available at: <https://scinapse.io/papers/2568691528>. (Accessed: 22nd February 2020)
394. Gerola, S. *et al.* CACNA1A gene non-synonymous single nucleotide polymorphisms and common migraine in Italy: A case-control association study with a micro-array technology. *Clinical Chemistry and Laboratory Medicine* **47**, 783–785 (2009).
395. Zhuchenko, O. *et al.* Autosomal dominant cerebellar ataxia (SCA6) associated with small polyglutamine expansions in the  $\alpha$ (1A)-voltage-dependent calcium channel. *Nature Genetics* **15**, 62–69 (1997).
396. Spacey, S. D., Hildebrand, M. E., Materek, L. A., Bird, T. D. & Snutch, T. P. Functional implications of a novel EA2 mutation in the P/Q-type calcium channel. *Ann. Neurol.* **56**, 213–220 (2004).
397. Brockwell, D. J. & Radford, S. E. Intermediates: ubiquitous species on folding energy landscapes? *Current Opinion in Structural Biology* **17**, 30–37 (2007).
398. Bukau, B., Weissman, J. & Horwich, A. Molecular Chaperones and Protein Quality Control. *Cell* (2006). doi:10.1016/j.cell.2006.04.014
399. Taylor, J. P., Hardy, J. & Fischbeck, K. H. Toxic proteins in neurodegenerative disease. *Science* (2002). doi:10.1126/science.1067122

400. Cooper, A. A. *et al.*  $\alpha$ -synuclein blocks ER-Golgi traffic and Rab1 rescues neuron loss in Parkinson's models. *Science* (80-. ). (2006). doi:10.1126/science.1129462
401. Aboobakar, I. F., Johnson, W. M., Stamer, W. D., Hauser, M. A. & Allingham, R. R. Major review: Exfoliation syndrome; advances in disease genetics, molecular biology, and epidemiology. *Experimental Eye Research* **154**, 88–103 (2017).
402. Abravaya, K. & Biology, C. Attenuation of the heat shock response in HeLa cells is mediated by the release of bound heat shock transcription factor and is modulated by changes in growth and in heat shock temperatures. 2117–2127 (1991).
403. Merienne, K., Helmlinger, D., Perkin, G. R., Devys, D. & Trottier, Y. Polyglutamine expansion induces a protein-damaging stress connecting heat shock protein 70 to the JNK pathway. *J. Biol. Chem.* **278**, 16957–16967 (2003).
404. Helmlinger, D. *et al.* Disease Progression Despite Early Loss of Polyglutamine Protein Expression in SCA7 Mouse Model. *J. Neurosci.* **24**, 1881–1887 (2004).
405. Gómez, A. V. *et al.* Characterizing HSF1 binding and post-translational modifications of hsp70 promoter in cultured cortical neurons: Implications in the heat-shock response. *PLoS One* **10**, 1–11 (2015).
406. Rajaii, F. *et al.* The demethylating agent 5-Aza reduces the growth, invasiveness, and clonogenicity of uveal and cutaneous melanoma. *Investig. Ophthalmol. Vis. Sci.* (2014). doi:10.1167/iovs.14-13933
407. Chen, J. *et al.* Aberrant Epigenetic Alterations of Glutathione-S-Transferase P1 in Age-Related Nuclear Cataract. *Curr. Eye Res.* **42**, 402–410 (2017).
408. Zhong, Q. & Kowluru, R. A. Epigenetic changes in mitochondrial superoxide dismutase in the retina and the development of diabetic retinopathy. *Diabetes* (2011). doi:10.2337/db10-0133
409. Vallée, A. & Lecarpentier, Y. Alzheimer disease: Crosstalk between the canonical Wnt/beta-catenin pathway and PPARs alpha and gamma. *Frontiers in Neuroscience* **10**, (2016).

## List of Abbreviations

5-Aza-dC	5-aza-2'-deoxycytidine
AD	Alzheimer's disease
AH	Aqueous humour
ALS	Amyotrophic lateral sclerosis
ARMD	Age-related macular degeneration
BIRC6	Baculoviral IAP repeat containing 6
CACNA1A	Calcium voltage-gated channel subunit alpha1 A
CANX	Calnexin
CDKN2B-AS	Cyclin dependent kinase 2-beta- antisense RNA
CDS	Coding DNA sequence
CGI	CpG island
CLU	Clusterin
CNTNAP2	Contactin associated protein-like 2
CONJ	Conjunctiva
CRISPR-Cas9	Clustered regularly interspaced short palindromic repeat- associated protein-9 nuclease
DAPI	4',6-diamidino-2-phenylindole
DKK1	Dickopff-1
DNaseI	Deoxyribonuclease I
DNMTs	DNA methyltransferases
ECM	Extracellular matrix
ENCODE	Encyclopedia of DNA elements

ERAD	Endoplasmic reticulum associated degradation
GWAS	Genome-wide association study
HD	Huntington's disease
HEK293	Human embryonic kidney 293 cell
HLE B-3	Human lens epithelial B-3 cell
HG	Human genome
HS	Heat shock
HSE	Heat shock element
HSF1	Heat shock factor-1
HSF2	Heat shock factor-2
HSF4	Heat shock factor-4
HSFs	Heat shock factors
HSPs	Heat shock proteins
HSP70	Heat shock protein 70
HSP90	Heat shock protein 90
HSR	Heat shock response
IOP	Intraocular pressure
KO	Knockout
LC	Lens capsule
LOXL1	Lysyl oxidase like-1
MMPs	Matrix metalloproteinases
mRNA	Messenger RNA
nCLU	Nuclear clusterin

PBK	PDZ binding kinase
PEX	Pseudoexfoliation
PEXG	Pseudoexfoliation glaucoma
PEXS	Pseudoexfoliation syndorme
PD	Parkinson's disease
PN	Proteostasis network
PSMD1	Proteasome 26S subunit, non-ATPase1
PSMA5	Proteasome subunit alpha type-5
qRT-PCR	Quantitative real time PCR
sCLU	Secretory clusterin
siRNA	Small interfering RNA
SNP	Single nucleotide polymorphism
SYNV	Synoviolin-1
TRIM35	Tripartite motif-containing 35
TSS	Transcription start site
TUNEL	Terminal deoxynucleotidyl transferase dUTP nick end labeling
UBA	Ubiquitin-like modifier activating enzyme-1
UBB	Ubiquitin B
UBE2J1	Ubiquitin conjugating enzyme E2J1
UCHL1	Ubiquitin C-terminal hydrolase-1
UCSC	University of California, Santa Cruz
UPR	Unfolded protein response
UPS	Ubiquitin proteasome system

UTR	Untranslated region
XFM	Exfoliative material

## Thesis Highlight

**Name of the Student:** Bushra Hayat

**Name of the CI/OCC:** National Institute of Science Education and Research

**Enrolment No.:** LIFE11201404001

**Thesis Title:** Dissecting the role of genes involved in proteostasis maintenance and Wnt signaling in pseudoexfoliation pathogenesis

**Discipline:** Life Sciences

**Sub-Area of Discipline:** Molecular Genetics and epigenetics

**Date of Viva Voce:** 5<sup>th</sup> June, 2020

Pseudoexfoliation (PEX; OMIM: 177650) is an age-dependent systemic disorder, clinically manifested by the gradual deposition of whitish fibrillar proteinaceous materials known as exfoliative material (XFM) in the ocular and non-ocular tissues. Deposition of these fibrils in ocular tissues leads to an increased intraocular pressure (IOP) which subsequently results in the death of optic nerve head cells (ONH) and gradually contributes to blindness. Early syndrome form of PEX is referred as pseudoexfoliation syndrome (PEXS) and later severe stage is known as pseudoexfoliation glaucoma (PEXG). The disease manifests its pathophysiology through the combination of various factors mainly the interaction of chronic stress conditions and genetic predisposition in an ageing individual. Through this study we aim to understand the components of proteostasis network, status of Wnt antagonist and variant in calcium channel. The major findings from the present study are depicted in the **Fig. 1**.

Findings from the present study unraveled DNA hypermethylation leading to decreased expression of HSP70, a stress-response chaperone implicating impaired cellular stress in PEXS affected lens capsule tissues. Following this increased expression of endoplasmic reticulum (ER) related stress markers such as synoviolin1 and calnexin indicating unfolded protein response activation in lens capsule of PEX individuals. Subsequently, reduced proteasome

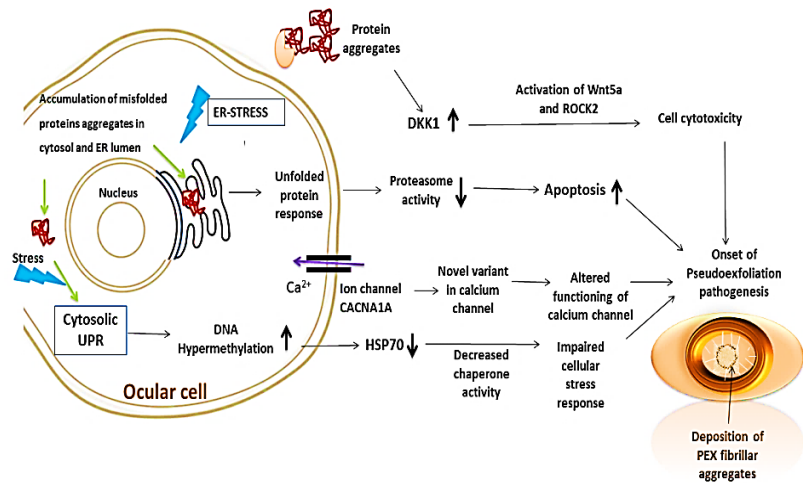


**Fig. 1.** Impaired cellular stress response, altered Wnt antagonist expression and further, association of novel genetic variant in CACNA1A gene leads to deposition of PEX fibrils.

activity and proteasome subunit expression were also observed in PEX subjects implying impaired proteasome function which ultimately led to increased cell death in lens capsules of PEX affected cases. In addition, increased expression of Wnt antagonist, Dickkopf-1 (DKK1) in the anterior eye tissue suggests increased cytotoxicity. We also found reduced CACNA1A expression on deletion of locus surrounding rs4926244 region and genetic association of *de novo* variant, rs4926246 with PEXG suggesting altered functioning of calcium channel. These findings provide evidence that proteostasis imbalance contribute significantly to abnormal XFM formation and aggregation. In nutshell, this study yield insights into perturbed cytoprotective mechanisms and illuminates the role of novel candidate genes as risk factor in PEX pathogenesis.